

UniS



University of Surrey

APPLICATION OF ANGULAR RATE
GYROSCOPES AS SENSORS
IN ELECTRICAL ORTHOSES
FOR FOOT DROP CORRECTION

By

Salim Ghoussayni

Centre for Biomedical Engineering

School of Engineering

University of Surrey

Guildford, Surrey

Presented as part of the requirements for the degree of
Doctor of Philosophy

© Salim Ghoussayni 2004

Abstract

Functional Electrical Stimulation (FES) is the application of electrical stimulation to neural pathways or muscles in order to achieve an effective muscle contraction with the aim of restoring lost or impaired function. In 1961 Liberson introduced the use of electrical stimulation for foot drop correction, a common condition following a cerebrovascular accident or stroke. Despite growing evidence on the beneficial use of FES for foot drop, and more than 40 years on from Liberson's work, FES systems for foot drop have not gained wide-spread use, and the basic design remains unchanged. It was the aim of this work to investigate the use of alternative sensors and the development of a sensor system that will improve the reliability, ease of use, and cosmetic aspects of a FES foot drop correction system.

The proposed method is a novel approach of using a single gyroscope placed at the anterior aspect of the shank to obtain feedback for a FES foot drop correction system. Previous work carried out in the Centre for Biomedical Engineering had demonstrated the potential of the angular velocity gyroscope (Gyro) as an alternative sensor to foot switches. It is believed that the replacement of the heel switch with the gyroscopic sensor would offer several advantages, which could improve system reliability and function. The Gyro is a small and lightweight sensor - with potential for further miniaturisation and implantation - which can be easily donned and doffed - positioning is not very critical - with minimal encumbrance to the patient. The nature of the Gyro contributes to its high reliability and long lifetime during which there is little or no deterioration in its performance.

The first part of the project involved the development of an automated reference method for gait event detection that can be used to assess the accuracy of the new gyroscope-based sensor. A kinematic-based approach was adopted and the new method was validated using data from 12 subjects. The new algorithm based method was compared to times given by visual inspection and force platforms. Ninety percent of all timings given by the algorithm were within one frame (16.7 ms) when compared to visual inspection. The new method for gait event detection required a thorough understanding of 3D co-

ordinate data processing. As part of this, an investigation was undertaken to analyse the frequency content of gait kinematic data and the means for noise reduction in the first and higher derivatives of motion data.

Hardware and software were then developed in order to perform gait event detection using the gyroscope signal. The sensor was housed within a small and easy to don and doff package. Software was implemented on a portable microcontroller based unit that can be worn by the patient at the waist. The sensor system was evaluated by two groups: able-bodied subjects (n=5) and patients with foot drop (n=3).

Data collected from these two studies were used to evaluate and compare the performance of the new sensor to that of the commonly used foot switch using the reference kinematic system. The overall accuracy of the gyroscope sensor system was 96 % in the able-bodied trials and 94 % in the patient trials, where accuracy is the percentage of time where the sensor detects the correct phase as determined by the reference system. The results suggest the practicability of the new sensor system to control the timing of the stimulation.

Further testing of the new sensor system is needed to establish its reliability when walking outside the laboratory, and over different terrains. Additional testing by a patient group with a larger size and more varied pathological causes for foot drop would be necessary prior to clinical use of a system based on the Gyro sensor. The design or modification of an existing stimulator to integrate the control unit is also suggested as a follow-up from this study. The shank location of the sensor in the proximity of the stimulation electrodes over the peroneal nerve would allow the design of a self-contained unit that would integrate the stimulator, electrodes, sensor, and control unit. It is believed that this would offer a significant advancement to the current technology.

Nomenclature

AP	Action Potential
B/F	Barefoot
CP	Cerebral Palsy
CVA	Cerebrovascular Accident
Diff	Difference
ES	Electrical Stimulation
FES	Functional Electrical Stimulation
FSR	Force Sensitive Resistor foot switch
Gyro	Gyroscope sensor system
HC	Heel Contact
HR	Heel Rise
ISCI	Incomplete Spinal Cord Injury
MCS	Motion Capture System
MS	Multiple Sclerosis
Ref	Reference kinematic gait event detection system
SCI	Spinal Cord Injury
SNR	Signal to Noise Ratio
STDEV	Standard Deviation
Stim	Stimulation
TA	Tibialis Anterior muscle
TBI	Traumatic Brain Injury
TC	Toe Contact
TO	Toe Off
UMNL	Upper Motor Neuron Lesion

Acknowledgements

I would like to acknowledge the help and contribution of the following people and organisations:

First and foremost, I would like to thank my supervisor *Dr David Ewins* for his continuous support, advice, encouragement, guidance, and endless patience. This thesis and work would not have been possible without his help.

I would like to thank the *School of Engineering* at the *University of Surrey* for the financial support towards the cost of my studies, and for the various opportunities I have been given during my time here.

I would like to thank the *Lebanese National Council for Scientific Research*, its president and board of administration, secretary general, and the fellowships programme for the financial support they provided during my studies.

I would like to thank friends, colleagues and staff at the *Centre for Biomedical Engineering*, both current and past. My experiences with them have made this place feel a lot nicer especially through the sad and difficult times.

I am also very grateful to all the patients and subjects who took part in my experimental studies, and their willingness to offer their help and time generously.

I would also like to thank my friends who have been extremely patient and great listeners and supporters throughout the duration of my PhD.

Finally, I would like to thank my family for all the encouragement they have provided me with throughout the years, and for their ever-growing support. I would like to express my sincere appreciation for all their efforts and help. I am forever indebted to them.

Table of Contents

Abstract	i
Nomenclature	iii
Acknowledgements	iv
Table of Contents	v
List of Tables	ix
List of Figures	x
List of Conference Presentations & Publications	xiv
Chapter 1: Introduction	1
1.1 Electrical orthoses.....	1
1.2 Need for current work.....	1
1.3 Aims of research.....	2
1.4 Hypothesis and statement of objective	2
1.5 Previous work with rate gyroscopes at the University of Surrey	3
1.6 Overview of thesis	3
Chapter 2: The foot drop condition	5
2.1 Foot drop.....	5
2.2 Underlying pathology and causes.....	5
2.2.1 <i>Upper motor neuron lesion</i>	6
2.2.2 <i>Peripheral nerve damage and neuropathies</i>	6
2.2.3 <i>Other causes of foot drop</i>	7
2.3 Epidemiology.....	7
2.4 Symptoms and gait deviations in foot drop	8
2.5 Treatment options	11
Chapter 3: Functional electrical stimulation: literature review and discussion	13
3.1 FES: History and principles of operation	13
3.1.1 <i>History</i>	13
3.1.2 <i>Physiological principles</i>	14

3.1.3	<i>Limitations and challenges facing the general use of FES</i>	18
3.2	FES systems for the correction of foot drop.....	19
3.2.1	<i>Liberson and after</i>	20
3.2.2	<i>Evidence of the benefit of FES in foot drop</i>	26
3.2.3	<i>FES systems for foot drop correction</i>	30
3.2.4	<i>Who is suitable for FES correction of foot drop</i>	31
3.2.5	<i>Comparison of FES to other interventions</i>	32
3.3	Sensor technology and algorithms used in FES systems.....	33
3.4	Issues and potentials	44
3.4.1	<i>Why do patients reject the stimulator?</i>	44
3.4.2	<i>Solutions</i>	45
3.4.3	<i>Issues with sensor technology</i>	46
Chapter 4:	Development of a reference method for gait event detection	49
4.1	Requirements and objectives: outline specification	49
4.2	Available methods for gait event detection	50
4.2.1	<i>Introduction to gait event detection methods</i>	52
4.2.2	<i>Overview of gait event detection methods</i>	52
4.3	Kinematic-based techniques	54
4.3.1	<i>Reasons for this choice</i>	54
4.3.2	<i>Literature</i>	55
4.3.3	<i>Limitations</i>	57
4.4	Proposed method	59
4.4.1	<i>From Visual Inspection to Automation</i>	59
4.4.2	<i>Criteria selection</i>	60
4.4.3	<i>Practical issues with implementation</i>	62
4.4.4	<i>Development of method</i>	62
4.4.5	<i>Pilot study</i>	69
4.5	Formal experimental assessment	76
4.5.1	<i>Results and discussion</i>	78
4.6	Pathological gait case study.....	88
4.7	Conclusions	89
Chapter 5:	Choice of cut-off frequency for the filtering of gait kinematic data	91

5.1 Choice of cut-off frequency.....	91
5.2 Differentiation magnifies noise	92
5.3 Reported techniques for the filtering of kinematic signals.....	93
5.4 More on the residual analysis method	97
5.5 Study plan and methods.....	98
5.5.1 <i>Data analysis</i>	99
5.5.2 <i>Results</i>	101
5.6 Discussion.....	107
5.6.1 <i>Comments on the residual analysis method</i>	108
5.7 Conclusions	109
Chapter 6: Theory and methods for the Gyro sensor system.....	112
6.1 Theory.....	112
6.1.1 <i>Shank behaviour during a gait cycle</i>	113
6.1.2 <i>Development of detection algorithms</i>	115
6.1.3 <i>Experimental approach: hardware and software description</i>	116
6.2 Assessment of sensor performance: study design	130
6.2.1 <i>Equipment and data collection</i>	131
6.2.2 <i>Protocols</i>	134
6.3 Data analysis and presentation	138
6.3.1 <i>Power analysis</i>	139
Chapter 7: Evaluation of the Gyro sensor system: results and discussions	141
7.1 Results of the evaluation.....	141
7.1.1 <i>Study A</i>	142
7.1.2 <i>Study B</i>	145
7.1.3 <i>Detection accuracy</i>	148
7.1.4 <i>Statistical analysis results</i>	149
7.1.5 <i>Reliability of the system</i>	150
7.2 Discussion.....	151
7.2.1 <i>Detection accuracy in able-bodied subjects</i>	151
7.2.2 <i>Detection accuracy in patients</i>	153
7.2.3 <i>Detection accuracy and reliability</i>	154
7.2.4 <i>Agreement between methods</i>	155

Chapter 8: Summary and conclusions	157
8.1 Kinematic-based gait event detection.....	157
8.2 The choice of cut-off frequency for kinematic data analysis	158
8.3 Development of the Gyro sensor system for use in FES foot drop correction.....	159
8.4 Other conclusions drawn from this work	160
8.5 Limitations of the study	162
Chapter 9: Future work	163
9.1 Gyro sensor system and FES for foot drop.....	163
9.2 Gait event detection and kinematic algorithms	165
References.....	167
Bibliography	178
Appendices.....	179
Appendix A: MATLAB code used for gait event detection.....	A1-A39
Appendix B: Assembly language code running on the PIC	B1-B17
Appendix C: Data sheets.....	C1-C4
Appendix D: Manufacturer details.....	D1-D2
Appendix E: Contents of the compact disc.....	E1-E2

List of Tables

Table 4-1: The mean, standard deviation and 95% confidence interval limit of marker sagittal velocities (in mm/s) for 4 subjects standing (STDEV = standard deviation).....	67
Table 4-2: Percentage distribution of the visual and algorithm differences (% occurrence of difference). 1 frame = 16.7 ms.....	76
Table 4-3: Table showing subject data details with average and standard deviation.	77
Table 4-4: Descriptive statistics of the walking speed and gait cycle duration of the 12 subjects. b/f: barefoot, -n: normal, -s: slow, STDEV: standard deviation.....	78
Table 4-5: Results of the statistical significance tests of the differences in the gait event detection by the 3 methods. F: force estimates, V: visual estimates, A: algorithm estimates YES: statistically significant difference ($p < 0.05$), NOT: not statistically significant ($p > 0.05$).	86
Table 4-6: Results of the statistical significance tests of the differences in the gait interval estimation by the 3 methods.	86
Table 5-1: Detailed data of subjects who took part in this study.....	98
Table 5-2: The FC99 and FC95 values for the 7 markers for different speeds and footwear.	104
Table 5-3: The FC1 values for the 7 markers for different speeds and footwear.	105
Table 6-1: Details of other gyroscope sensors available on the market.....	117
Table 6-2: Table showing the device parts list	123
Table 6-3: Heel state detection algorithm description. (n1 to n8 = algorithm parameters – n = consecutive count condition – V and V-1 are the values of angular rate in current frame and previous frames respectively).....	127
Table 6-4: Subject data for study A participants.....	137
Table 6-5: Subject data for the 3 patients who took part in Study B.	138
Table 7-1: Normalised and raw average of absolute timing differences for both systems.....	144
Table 7-2: Performance percentage accuracy of both sensor systems for all three conditions in both data sets.	148
Table 7-3: Overall performance percentage accuracy for both sensor systems in the two data sets.....	149
Table 7-4: Statistical analysis results, with * indicating statistical significance at the $p < 0.05$ level.....	149
Table 7-5: Statistical analysis results, with * indicating statistical significance at the $p < 0.05$ level.....	150
Table 7-6: Description of detection errors by both systems in study A.....	151
Table 7-7: Description of detection errors by both systems in Study B	151

List of Figures

Figure 2-1: Figure showing the different phases of a gait cycle and the defining start and end events for each phase (IC = initial contact, TV = tibia vertical, TO = toe off, HR = heel rise, FA = feet adjacent, L = left, R = right).	9
Figure 2-2: Normal range of ankle motion during 1 gait cycle (left) and normal mean intensity of EMG (as % of maximum manual muscle test) during free walking (right). The light grey area in the TA plot represents EMG activity seen in some normal subjects. (Perry 1992).....	10
Figure 3-1: The effect of increasing current amplitude on the muscle force response measured by torque (Baker et al. 1993).	16
Figure 3-2: Electrically induced tetany by applied stimuli at different frequencies (pps = pulses per second) (Baker et al. 1993).	17
Figure 3-3: Arrangement of the foot drop stimulator used by Liberson. S is the stimulator, E1 and E2 are the electrodes, and K is the foot switch. (Liberson et al. 1961).	20
Figure 3-4: Patient walk without stimulation (top) and with stimulation (bottom) (Liberson et al. 1961).	27
Figure 3-5: The gait phase detection sensor designed by Pappas et al. and made into a stand-alone system (Pappas et al. 2001).	40
Figure 3-6: Schematic of EEG-based controller for a hand grasp neuroprosthesis (Lauer et al. 2000).	43
Figure 4-1: Figure showing the marker placement used in this study	61
Figure 4-2: A plot of the heel marker velocities in both progression and vertical directions versus time. X =progression direction; Z=vertical direction; Vel=velocity; H=heel; F=filtered (Sampling rate 240 Hz).....	64
Figure 4-3: A plot of the heel and toe sagittal velocities during swing to stance period. Z = vertical co-ordinate; Vels = velocity; HC = heel contact, TC = toe contact. (healthy subject, self-selected normal walking speed).....	66
Figure 4-4: Plot of the sagittal velocities of the heel and toe markers and the times of detected events shown. HC=Heel contact; TC=Toe contact; HR=Heel rise; TO=Toe-off.....	68
Figure 4-5: The MATLAB® graphical user interface used for processing the 3D marker data and gait event detection.	69
Figure 4-6: Foot placement across the two force platforms (FP) in a clean trial and an image capture of the video recordings.	70
Figure 4-7: Screenshot of Q Trac View used for display of marker trajectories and visual inspection (Trajectories of sacral, heel, and toe markers in red, green, and yellow respectively).	72
Figure 4-8: Average of differences between the force, visual, and algorithm methods. 1 error bar = 1 standard deviation; Diffs = Difference; 1 frame = 16.7 ms.	73

Figure 4-9: Average of absolute differences between the force, visual, and algorithm methods. 1 error bar = 1 standard deviation; Diffs = Difference; 1 frame = 16.7 ms.	74
Figure 4-10: Average of differences between the visual and algorithm methods. 1 error bar = 1 standard deviation; Diffs = Difference; 1 frame = 16.7 ms.	75
Figure 4-11: Average of absolute differences between the force, visual, and algorithm methods. 1 error bar = 1 standard deviation; Diffs = Difference; 1 frame = 16.7 ms.	75
Figure 4-12: Average of differences between force (f), visual (v), and algorithm (a) determination of gait event times (normal and slow velocity).	79
Figure 4-13: Average of absolute differences between force (f), visual (v), and algorithm (a) determination of gait event times (normal and slow velocity).	80
Figure 4-14: Normalised average of absolute differences between force (f), visual (v), and algorithm (a) determination of gait event times (normal and slow velocity).	81
Figure 4-15: Percentage distribution for the differences in the estimated gait event times between visual inspection and the algorithm (All events, both footwear and velocities).	82
Figure 4-16: Normalised average interval durations as determined by the 3 methods for the normal speed trials (HC-TC: Heel contact to toe contact, TC-HR: Toe contact to heel rise, HR-TO: Heel rise to toe off).	83
Figure 4-17: Normalised average interval durations as determined by the 3 methods for the slow speed trials (HC-TC: Heel contact to toe contact, TC-HR: Toe contact to heel rise, HR-TO: Heel rise to toe off).	83
Figure 4-18: Agreement test regression plots of the V/A differences in determining the 4 gait event timings (Normalised data).	84
Figure 4-19: Agreement test regression plots of the V/A differences in determining the durations of the 3 gait intervals (Normalised data).	85
Figure 4-20: Bland and Altman plot for the V/A differences in determining HC in the b/f-n condition (Normalised data).	87
Figure 4-21: Percentage frequency distribution for the V/A absolute differences in estimating the gait events.	88
Figure 5-1: A representative plot of residual between filtered and unfiltered data vs. filter cut-off frequency (Winter 1990).	101
Figure 5-2: Cumulative power spectrum in the progression component of the motion signals of different lower limb markers (data from 1 representative trial of 1 subject).	102
Figure 5-3: Cumulative power spectrum in the medial-lateral component of the motion signals of different lower limb markers (data from 1 representative trial of 1 subject).	102
Figure 5-4: Cumulative power spectrum in the vertical component of the motion signals of different lower limb markers (data from 1 representative trial of 1 subject).	103

Figure 5-5: The residuals in the X components of the 7 markers. Data averaged from the 30 barefoot normal speed walking trials.	106
Figure 5-6: The residuals in the Y components of the 7 markers. Data averaged from the 30 barefoot normal speed walking trials.	106
Figure 5-7: The residuals in the Z components of the 7 markers. Data averaged from the 30 barefoot normal speed walking trials.	107
Figure 6-1: The shank angular rate (random scale) for a representative gait cycle (0 to 100%) with the tibialis anterior active period (in red). (LR = loading response; TS = terminal stance; PS = pre-swing).	112
Figure 6-2: Typical stimulator output envelope. Stimulation is started after heel rise with a rising edge ramp (A) and stopped after heel contact with a falling edge ramp (B). An extension to the stimulation time (C) can be applied after heel contact for a better control of plantarflexion.	113
Figure 6-3: An illustration of a single gait cycle showing the position of the right leg at 40 ms intervals. (Whittle 1996).	114
Figure 6-4: A typical gait cycle shank angular rate and foot switch recording (HC heel contact, FF foot flat, HR heel rise, TO toe off).	115
Figure 6-5: A block diagram describing the main components in the experimental set-up used.	116
Figure 6-6: The principle of the Coriolis force (left), and the metallic triangular prism vibrator used in the GYROSTAR® from Murata (right). (Murata).	120
Figure 6-7: Schematic circuit diagram of the microcontroller unit.	122
Figure 6-8: The microcontroller-based unit with labelled buttons and connectors.	124
Figure 6-9: Initialisation subroutine.	125
Figure 6-10: Interrupt service subroutine.	126
Figure 6-11: Serial communication subroutine.	126
Figure 6-12: Heel state detection subroutine.	129
Figure 6-13: LabVIEW front panel for serial communication between the PC and the microcontroller unit.	130
Figure 6-14: Diagram showing the different components of the experimental set-up. ..	131
Figure 6-15: Front panel and user interface (top) and data display (bottom) of the LabVIEW code used for data collection.	132
Figure 6-16: A schematic of the motion capture system with the cameras and measurement volume.	133
Figure 6-17: Force sensitive resistor technology (Interlink Electronics).	134
Figure 6-18: ODFS single channel foot drop stimulator (Salisbury District Hospital, UK)	134
Figure 6-19: Two of the subjects who took part in the study (surface electrodes, Gyro, markers and connecting wires in these frontal and side views).	137
Figure 7-1: Normalised detection times of heel contact and rise as given by the Gyro, FSR, and reference system.	142

Figure 7-2: Average of event timing differences between the Gyro/FSR and reference system..... 143

Figure 7-3: Average of absolute event timing differences between the Gyro/FSR and reference system..... 143

Figure 7-4: Scatter plot for Gyro and FSR differences from the reference times (raw data)..... 144

Figure 7-5: Percentage frequency distribution of Gyro/FSR differences (raw data and x 10 ms)..... 145

Figure 7-6: Normalised detection times of heel contact and rise as given by the Gyro, FSR, and Reference system 146

Figure 7-7: Average of absolute event timing differences between the Gyro/FSR and reference system..... 146

Figure 7-8: Scatter plot for Gyro and FSR differences from reference times (raw data-all conditions)..... 147

Figure 7-9: Percentage Frequency distribution of Gyro/FSR differences (raw data and x 10 ms)..... 148

Figure 7-10: Bias plot for HC detection comparison between the Gyro vs Ref (left) and FSR vs Ref (right). 155

Figure 7-11: Bias plot for HR detection comparison between the Gyro vs Ref (left) and FSR vs Ref (right). 156

Figure 8-1: Schematic showing the evolution in the design of FES foot drop correction systems.....161

List of Conference Presentations & Publications

Ghoussayni, S., J. Henty, D. Wood and D. Ewins (2001). The use of a gyroscope in FES foot-drop correction systems. 7th Vienna International Workshop on Functional Electrostimulation, Vienna, Austria.

Ghoussayni, S., J. Henty, D. Wood and D. Ewins (2002). The use of the gyroscope as a sensor in FES foot-drop correction systems. Poceedings of the 1st annual conference of FESnet, University of Strathclyde, Glasgow.

Ghoussayni, S., C. Stevens, S. Durham and D. Ewins (2002). Gait event detection: A comparison of force platform, visual inspection, and kinematic algorithm based methods. Gait and Clinical Movement Analysis Society Seventh Annual Meeting, Chattanooga, Tennessee.

Ghoussayni, S., P. Catalfamo, D. Moser and D. Ewins (2004). Experience in the use of a single gyroscope as a sensor for FES foot drop correction systems. 9th Annual Conference of the International Functional Electrical Stimulation Society, Bournemouth, UK.

Ghoussayni, S., C. Stevens, S. Durham and D. Ewins (2003). "Assessment and validation of a simple automated method for the detection of gait events and intervals." Gait and Posture **20**(3): 266-272.

Ghoussayni, S. and D. Ewins (2004). "The use of a single gyroscope for gait event detection and control of a FES foot drop correction system." Medical Engineering & Physics. **Submitted for publication.**

Chapter 1: Introduction

This dissertation describes the work done towards the development of a novel sensor system for an electrical orthosis. The orthosis considered is a single channel electrical stimulator used by patients suffering from foot drop. The main purpose of this chapter is to introduce the undertaken work, and to report on the need for it. The aims and objectives of the research are then given. The chapter ends with an overview of the whole report.

1.1 Electrical orthoses

An orthosis is often described as an artificial external device, for example a brace or a splint, which may be powered or unpowered, and which is worn to assist or restrict motion in order to aid or correct the function of the limb(s) it is attached to. The term electrical orthosis usually refers to any orthosis that fulfils its function using electrical pulses applied to the neural pathways or muscles. This is in contrast to mechanical, passive or active orthoses, which perform their function by means of mechanical principles with or without electronic or electric power. Electrical orthoses where electrical stimulation is used in conjunction with some mechanical bracing are commonly referred to as hybrid orthoses.

1.2 Need for current work

More than 40 years ago, Liberson *et al.*, 1961 pioneered the application of electrical stimulation for the functional correction of foot drop. Since then many researchers have been involved in the development of Functional Electrical Stimulation (FES) systems or electrical orthoses for foot drop correction and various other applications. Work in this field focused on improving different aspects of the system and encompassed many attempts at developing an optimal system. FES foot drop stimulators typically employ a physical sensor (usually a foot switch) as a feedback source controlling the timing of stimulation to the peroneal nerve. In addition, the body of evidence on the effectiveness of FES use in the correction of foot drop has grown significantly since then.

Liberson's original work effectively created a new field of research into clinical applications of electrical stimulation. In the case of foot drop correction, and more than 40 years later, current FES systems have not gained wide clinical use. This is disappointing

when consideration is given to the potential number of patients who could benefit from FES, together with the effectiveness of this technique. To date, sufficient evidence has been reported on the beneficial use of FES for foot drop correction. However, one of the main factors that continue to hinder the wide use of these systems is the available technology, and in particular, the lack of a reliable and easy to use system in the clinical setting and the everyday life of the patient.

1.3 Aims of research

The objectives of this project fall within the boundaries of working towards a totally self-contained device with the surface stimulator, sensor, and electrodes part of one unit to be worn on the shank. After reviewing current systems and issues facing FES use for foot drop, it became evident that the development of such a device would be a significant contribution to FES users and use. Having the sensor in the controller unit or stimulator at the shank will reduce donning and doffing time, reduce the need for wires, and improve cosmetic aspects. Eliminating the need for a foot switch would also improve the reliability of the system by avoiding some of the commonly faced problems linked to the usage of foot switches.

Such a development is believed to offer the following:

- Reduces the donning and doffing time, and ease of use by the patient
- Improves the cosmetic effects of the system

The development of the new sensor system is also expected to:

- Provide an accurate and reliable sensor system for triggering
- Provide sufficient information that offer the potential of additional feedback
- Overcome a number of limitations associated with the use of foot switches
- Have the potential for miniaturisation and implantation

1.4 Hypothesis and statement of objective

The overall hypothesis for the area of research into which this current work falls is that “a new sensor system that can be worn at the shank will allow for the development and subsequent use of a self-contained stimulator device, that will benefit patients suffering from foot drop and improve on the practicality and reliability of existing systems”. The work undertaken in this PhD addressed one particular part within this area. The specific

hypothesis for the current work is that “ a rate gyroscope worn at the shank may be used for gait event detection and the control of a foot drop stimulator”.

The objective of this work was to design, test, and validate a sensor system that meets the second hypothesis and therefore support the first hypothesis.

1.5 Previous work with rate gyroscopes at the University of Surrey

Previous work at the Centre for Biomedical Engineering investigated the use of rate gyroscopes as possible sensors for foot drop FES systems. Henty *et al.*, 1999 demonstrated the feasibility of using a single gyroscopic sensor placed on the foot as a signal source for the triggering of a foot drop correction system. The gyroscope was successfully used to detect four gait events and provided accurate timings when compared to foot switches and visually determined times from 3D recordings of foot kinematics (Henty 2004). Pilot tests undertaken as part of a MSc project demonstrated the feasibility of using a single gyroscopic sensor placed on the shank as a signal source for controlling a foot drop FES system (Ghoussayni 2000). This evidence served as the basis for further work into the development and implementation of the new sensor system.

1.6 Overview of thesis

After this introductory chapter, the second chapter deals with the pathological condition of foot drop and its management. The third chapter focuses in more detail on the application of FES in the correction of foot drop. FES is first introduced and its principles of operation explained. A historical review of FES systems and the sensor technology that have been used for foot drop correction since 1961 is then made. The study of this application emphasizes the need for the current work. The requirements for achieving the aims are then stated. These included the availability of a reference method for gait event detection that can be used in the assessment of the new sensor system.

Chapter 4 is concerned with the development of a reference gold standard method for gait event detection. A summary of existing methods is presented. The summary highlights the need for the development of a new approach. The adopted kinematic-based approach is described and the results from an experimental study for its assessment and validation are presented.

Chapter 5 describes the techniques that were used in the treatment of the 3D co-ordinate data prior to using them for gait event detection. The chapter's main focus is the choice of cut-off frequency for low-pass filtering the data before differentiation. An experimental study that was completed is described and the results from this study are used to justify the choice made.

Chapter 6 describes the development of the new sensor system utilising a gyroscope as the feedback sensor and a microcontroller based unit for the detection of gait events and stimulation control. Chapter 7 presents the results from a study assessing the new sensor system. A discussion of the results is given in the second part of the chapter. Chapter 8 presents the conclusions from this work. The conclusions are made in 3 sections referring to the reference method for gait event detection, the choice of cut-off frequency, and the new sensor system. The final chapter identifies key areas for future work.

Chapter 2: The foot drop condition

The main objective of this chapter is to introduce and describe the pathological condition of foot drop, a common problem following an upper motor neuron lesion (UMNL). The chapter presents the underlying pathological causes of this condition as well as key epidemiological data followed by a description of the main symptoms and gait deviations observed in this group of patients. A variety of treatment options are available for the correction of foot drop. One of these is the use of functional electrotherapy or functional electrical stimulation as it is more commonly referred to. A brief summary of FES and other treatment options used in the correction of foot drop is then given.

2.1 Foot drop

“Foot drop”, “dropped foot”, “footdrop”, and “drop foot” all refer to a condition that involves the inability to dorsiflex the foot or ankle during the swing phase of gait. The first use of the term and reported occurrence are not clear, however the biblical story in the Book of Genesis of Jacob limping after a long night of wrestling can be argued to be the first written report of foot drop.

2.2 Underlying pathology and causes

Foot drop can be attributed to a variety of causes that result in the inability to dorsiflex the foot (forefoot) and ankle (hindfoot). The main muscle responsible for dorsiflexion is the tibialis anterior (TA), in addition to the extensor hallucis longus, extensor digitorum longus, and peroneus tertius. The contraction of these muscles is used to lift the foot and clear the ground during swing and to provide (in combination with the plantar flexors) a controlled plantar flexion at heel strike avoiding foot slap. The neural input for the dorsiflexors comes from the deep peroneal nerve. The peroneal nerve together with the tibial nerve constitute the sciatic nerve which has nerve fibres from branches of the ventral rami of spinal nerves L4-S3. The sciatic nerve divides into the tibial and peroneal nerve between the mid thigh level and the knee posteriorly. The peroneal nerve crosses laterally and passes over near the head of the fibula, where it becomes subcutaneous. It then enters the anterior compartment of the leg and branches into a superficial and deep part.

Any source of interference with the neural input to these muscles or direct injury to the muscles themselves can effectively lead to a disruption of the normal mechanisms and a possible foot drop. Increased tone and activity in the plantar flexors (antagonist) muscles can also prevent dorsiflexion and cause foot drop. The causes of foot drop can then be categorised according to the source of malfunction, whether it is neural, muscular, or anatomical. The causes might overlap and the problem can be the result of a combination of causes. Among those causes we identify:

2.2.1 Upper motor neuron lesion

By definition, an upper motor neuron lesion is any pathology that affects the neurons of the motor cortex or their axons, including those in the corticospinal pathways. Possible causes of UMNL are stroke (cerebrovascular accidents or CVA), spinal cord injury (SCI), multiple sclerosis (MS), cerebral palsy (CP), and traumatic head or brain injury. Stroke patients are the most commonly treated patient group for the correction of foot drop using FES (Swain *et al.* 2001). A stroke can be the result of either an ischaemic attack or a subarachnoid haemorrhage, with variable effects on the patient depending on the extent of damage and area of brain affected. Common outcomes of stroke are hemiplegia, a weakness or paralysis on one side of the body, and hemiparesis, partial hemiplegia. Loss of control over the movement of limbs, spasticity (an increased tone), and paralysis contribute to the observed mobility losses and gait deviations, including foot drop.

2.2.2 Peripheral nerve damage and neuropathies

Peripheral nerves connect the central nervous system (brain + spinal cord) to sensory receptors, muscles and glands in peripheral parts of the body. These nerves are two types: cranial, arising from the brain, and spinal, emerging from the spinal cord. Pathologies that affect the function of the peripheral neural input to the dorsiflexors are known to cause foot drop. Some examples of these are mononeuropathies of the deep and common peroneal, and sciatic nerves. These conditions can be separated into three categories: generalised, localised and common peroneal neuropathies. Motor neuronopathy, hereditary motor and sensory neuropathy (HMSN), and mononeuritis multiplex are examples of generalised conditions, while L4/L5 radiculopathy (most often caused by a disc herniation at the L4-5 interspace), lumbosacral plexopathy, and sciatic neuropathy (buttock injection) are examples of the localised neuropathies. A common peroneal neuropathy can be the result of trauma at the fibular head, forcible stretch, external

compression (casts), prolonged immobility (anaesthesia), occupational (e.g. gardening), and habitual leg crossing.

Other conditions and causes that may lead to peripheral neuropathy are diabetes, alcohol, and Guillain-Barre syndrome.

2.2.3 Other causes of foot drop

What follows is a list of conditions that can be quoted as possible causes of foot drop:

- Leprosy neuritis resulting in peroneal nerve palsy.
- Trauma to the muscles or nerve as a result of the lack of proprioception and protective sensation.
- Total knee arthroplasty or proximal tibial osteotomy are also possible causes of peroneal palsy.
- Correction of severe valgus or flexion deformity are suggested to cause stretch of peroneal nerve and lead to palsy.
- Anterior compartment syndromes (of the leg) due to fracture or acute traumas. Other forms of compartment syndromes also exist and can be the result of strenuous activity and acute exercise.
- Brain tumours (Baysefer *et al.* 1998).
- Bilateral foot-drop has also been reported in a patient with anorexia nervosa (Kershenbaum *et al.* 1997).
- Transverse myelitis (Waters *et al.* 1975).
- Charcot-Marie-Tooth disease (Vinci *et al.* 2003).

2.3 Epidemiology

The majority of patients in the UK treated by FES for the correction of foot drop are stroke patients followed by MS (Swain *et al.* 2001). This section presents some statistical data on the prevalence and incidence of these two conditions and some of the other causes of foot drop.

The annual incidence of a first stroke in England and Wales is estimated at about 100,000 (1 in 500), with people above the age of 55 accounting for 90% of the total. It is also estimated that a third of those having a first stroke will die within one year, a third will make good recovery, while a third are left with varying disabilities. The prevalence of

stroke is estimated at 12000 per million, and 300000 living with disabilities as a result of a stroke (Westcott 2000). A conservative estimate of patients suffering from a foot drop as a result of the stroke is 20% (Burrige *et al.* 1997). Swain *et al.*, 1996 estimated that 12,800 foot drop patients per year are suitable for treatment by FES in the UK. Similar estimates are given by other authors on the percentage of stroke survivors suffering from foot drop. A 10-20% figure is quoted by Lyons *et al.*, 2002. Merletti *et al.*, 1979 suggested that 15% of the ambulatory hemiparetic population are suitable for using FES foot drop correction systems. Using this estimate, and assuming that a patient will use the system for an average 5 years and the current stroke to other pathologies ratio of treated patients, Burrige (2001) estimated that 29000 patients in the UK can potentially benefit from FES for the correction of foot drop.

MS is the most common neurological disorder among young adults and affects around 85,000 people in the UK (about 1 in 2000) (Graham 2000). Prevalence estimates for MS are 2000/million, CP 3000/million (affects about 1 in 500 children), SCI 800/million, and 20000/million for head injuries (about 1 million treated for head trauma in the UK) (Lyons *et al.* 2002).

According to Bajd *et al.*, 1999 peroneal nerve stimulation can be useful in at least 10% of ISCI patients to augment dorsiflexion, knee, and hip flexion in a total lower limb flexion reflex pattern.

2.4 Symptoms and gait deviations in foot drop

This section presents the main observations related to the mobility dysfunction in patients suffering from foot drop. The main focus is the changes seen in the general gait pattern of these subjects, although a wide inter-subject variability exists. The underlying causes of the observed patterns are discussed, which are often a reflection of the compensation mechanisms utilised by the patient to alleviate the effects of the foot drop.

A brief overview of the 'normal' gait cycle and its phases is essential for the following discussion. Walking is a rather complex motion that occurs as a result of several systems acting together in order to achieve the final aim of moving the body from point A to B in a safe and efficient way, adapting to changing extrinsic factors, such as the environment, and intrinsic factors such as fatigue. The sequence of events whereby the body achieves

bipedal locomotion is repetitive and each cycle is called a gait cycle. This sequence of events can be viewed in light of foot to floor contact. During walking 3 phases can be identified, two of these with a single limb in contact with the floor, and one phase with both limbs being in contact with the ground. A gait cycle is defined as the sequence of events between two consecutive occurrences of the same event, usually initial foot contact with the floor by the same limb. Considering each side of the body separately, the limb can be seen to be either in contact with the ground, stance phase, or not, swing phase. The stance phases of the two limbs overlap in a period of bilateral support or double stance. The existence of this overlap period is what differentiates walking from running. A complete cycle can be divided into several phases where the functional requirements of the limb vary between weight-bearing and limb advancement (Figure 2-1). Seven phases are commonly referred to: loading response (LR), mid stance (MSt), terminal stance (TSt), pre-swing (PSw), initial swing (ISw), mid swing (MSw), and terminal swing (TSw) (Whittle 1996). This number is increased to eight when initial contact (IC) is considered as one phase (Perry 1992).

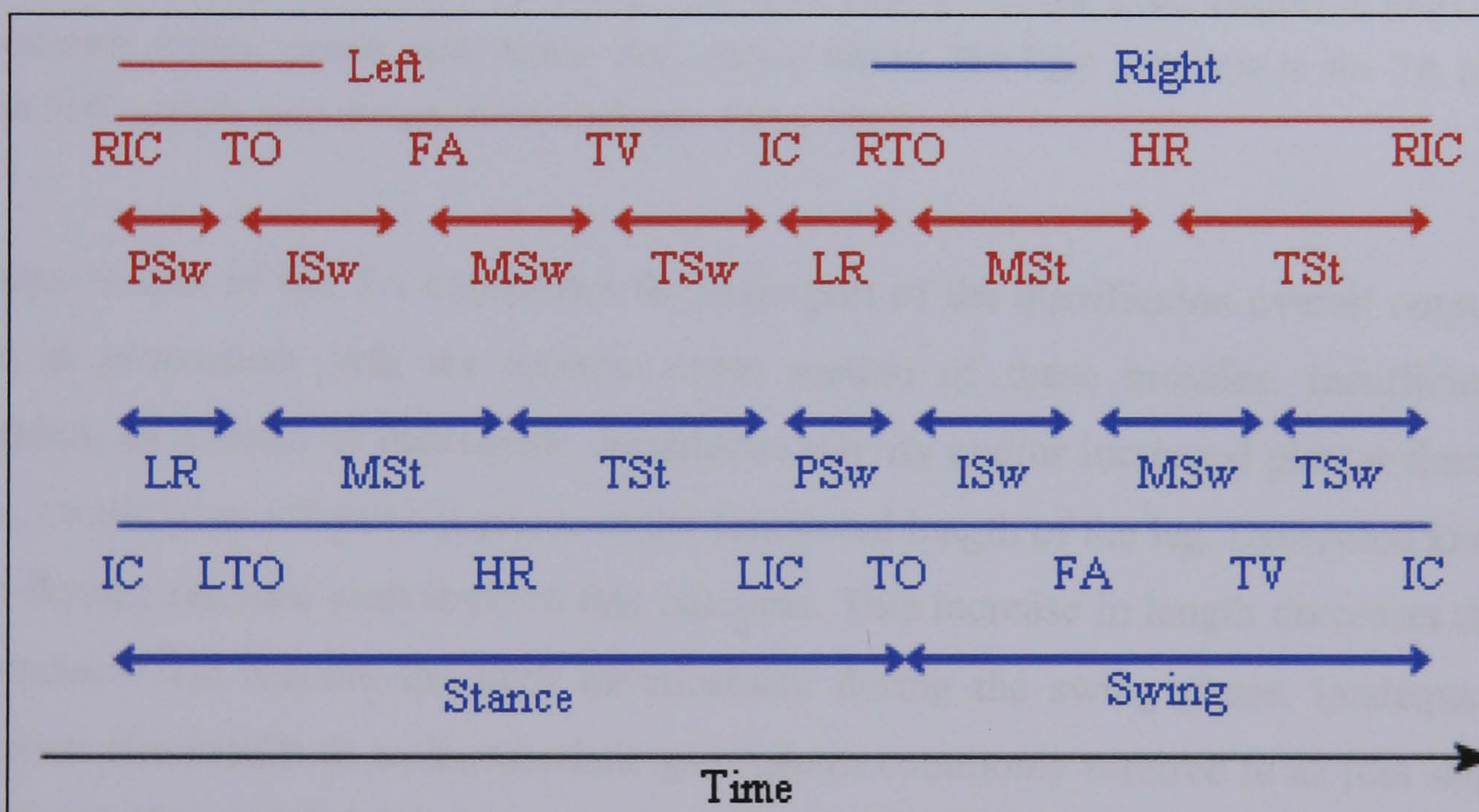


Figure 2-1: Figure showing the different phases of a gait cycle and the defining start and end events for each phase (IC = initial contact, TV = tibia vertical, TO = toe off, HR = heel rise, FA = feet adjacent, L = left, R = right).

The ankle motion during the above phases alternates between dorsiflexion and plantar flexion, with an average total range of motion of 30° (Perry 1992). The dorsiflexors are mainly active during the swing phase and the plantar flexors during the stance phase.

Some dorsiflexor activity is present during LR, the first part of the stance phase, providing an eccentric contraction and gradual lowering of the forefoot to the floor. The detailed electromyographic (EMG) record of the dorsiflexor activity during a gait cycle can be seen in Figure 2-2.

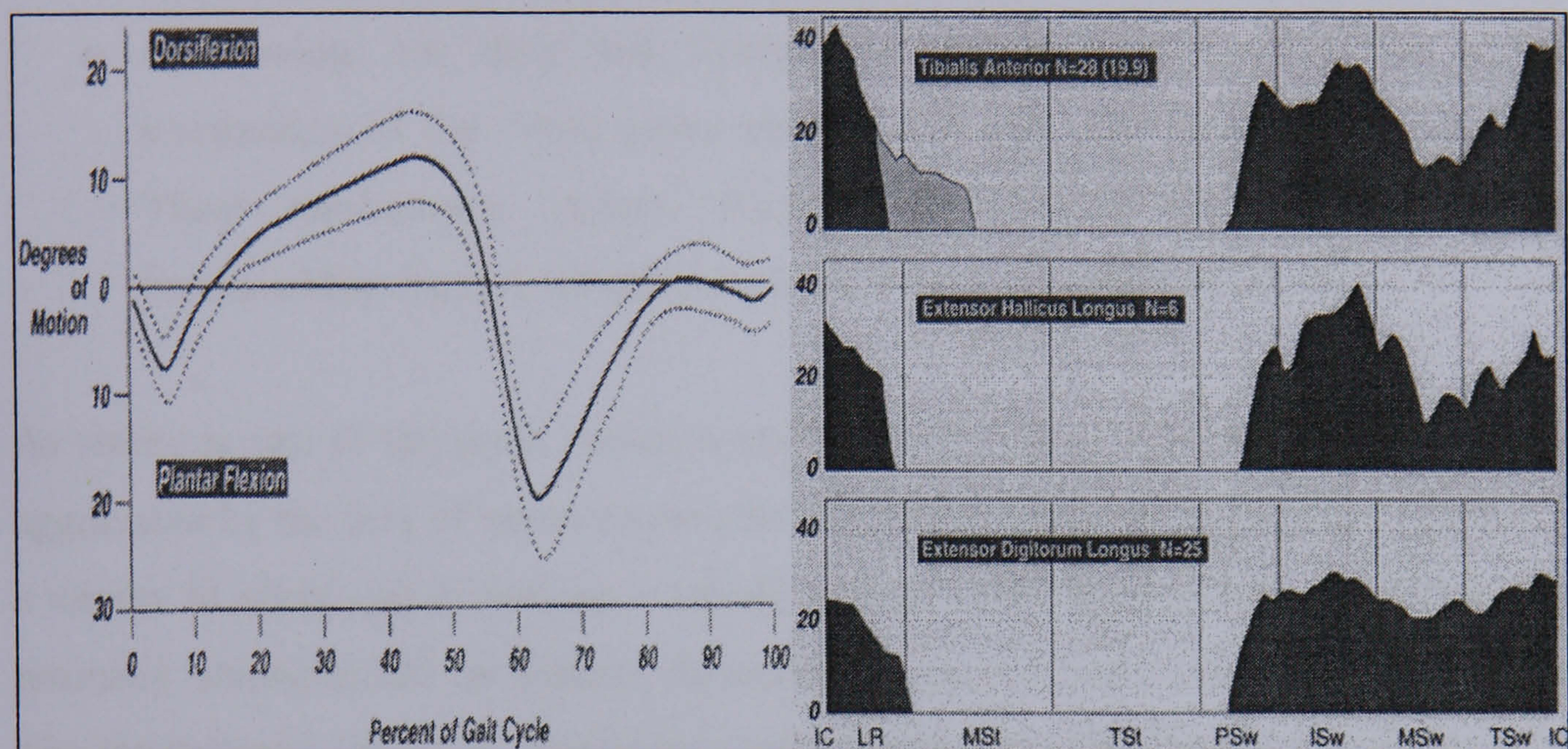


Figure 2-2: Normal range of ankle motion during 1 gait cycle (left) and normal mean intensity of EMG (as % of maximum manual muscle test) during free walking (right). The light grey area in the TA plot represents EMG activity seen in some normal subjects. (Perry 1992).

The torque output of the TA constitutes the main part of the dorsiflexion overall output. This is in proportion with the relative cross section of these muscles. Insufficient dorsiflexion, as a result of inadequate dorsiflexor activity and/or increased plantar flexor activity, results in an effective increase in the functional length of the leg. Decreased knee and hip flexion can also contribute to this outcome. This increase in length decreases the foot clearance and hinders the limb advancement during the swing phase. Inadequate dorsiflexion also results in a characteristic gait pattern commonly referred to as foot slap. This refers to the sound the foot makes as a result of an instantaneous and uncontrolled foot to floor contact following heel contact. The presence of foot drop often becomes very clear during the mid swing phase, made apparent by the presence of toe drag or the complete absence of, or minimal, foot clearance.

Some of the common observations in foot drop specific to each one of the gait phases are outlined below:

- Initial contact: limited toe clearance at heel contact, or the contact with the floor is made with a flat foot, or a toe-heel contact.
- Loading response: foot slap and a reduced heel rocker.
- Mid stance: the presence of excessive plantar flexion reduces tibial advancement and progression, resulting in a shortened step length on the contralateral limb.
- Mid swing: toe drag and limited foot clearance that results in premature termination of the swing phase unless a compensatory mechanism is employed. These mechanisms include circumduction, hip hiking, steppage, vaulting, increased hip flexion, lateral trunk lean, or a combination of these.

As stroke is one of the most common causes of foot drop, the presence of foot drop is aggravated by the lack of control over other muscle groups as a result of the UMNL. Thus a variety of other gait deviations is usually present affecting the subject walking and are normally characterised by kinetic, kinematic, temporal and muscle activation patterns. The number and extent of deviations seen are related to the degree of severity of brain damage. Winters *et al.*, 1987 identified 4 groups of patients (I to IV) in order of severity among 46 patients who had spastic hemiplegia. However, such attempts of classifying the degrees of severity are not usually used in common practice due to the overlap between groups of subjects and lack of clear cut differences.

In terms of the spatial, temporal and kinetic outcomes, common observations are reduced walking speed, increased stance phase duration and reduced step length of the unaffected side, decreased stance phase time, reduced weight-bearing, and increased swing phase time on the affected side (Craig *et al.* 1995).

2.5 Treatment options

The underlying pathology and the resulting deficits are two critical factors in determining the therapy given to the patient with foot drop. The patient's needs, age, and levels of activity are also main determinants of the type of intervention chosen with the ultimate goal of improving their independence and reintegration into society.

As the majority of involved subjects are stroke patients, focus will be made on the management of the stroke patient. The overall management and care of patients after stroke involves a variety of specialist therapists and clinicians who deal with the different

types of disabilities and lost or impaired functions. Both the time course and extent of recovery are patient dependent, although generalisations are sometimes made in an attempt to quantify or define recovery stages. The rehabilitation of walking is mainly done by physiotherapists who attempt to help the patient regain the ability to walk through physical and strengthening exercises, Bobath training, motor learning approach, massage, biofeedback therapy, and active and passive range of motion practice. Strength training being one area of debate among therapists with some therapists discouraging its use because they believe that it will exacerbate abnormalities of movement control (Edwards 1996). Traditional techniques focus on means of inhibiting spasticity and the use of reflex patterns to assist mobility. More recent approaches utilise the knowledge about neural plasticity and motor learning (Teasell *et al.* 2004).

During later stages, the presence of a chronic mobility dysfunction after the period of recovery, such as foot drop, can be treated by a group of interventions that includes surgery, use of orthotics or walking aids, botulinum neurotoxin injections, and therapeutic electrical stimulation. One alternative orthotic treatment approach introduced by Liberson *et al.* in 1961 was the use of electrotherapy. The efficacy of this treatment was very obvious in Liberson's study. Over four decades later, electrical stimulation for the correction of foot drop has not gained very wide use nor has it realised its potential. Many reasons contribute to this, however with the advances in both technology and our understanding of motor control, FES systems are becoming more commonly used. One main element facilitating this is the increase in the body of evidence supporting the effectiveness of FES, and to a certain degree its superiority, in the treatment of foot drop.

The use of FES for foot drop correction is the focus of the next chapter. The chapter also presents a historical review of all FES systems and the sensor technology that have been used for foot drop correction since 1961. This review highlights and further emphasizes the need for the current work.

Chapter 3: Functional electrical stimulation: literature review and discussion

The aim of this chapter is to provide an introduction to the field of Functional Electrical Stimulation (FES) with special emphasis on the application of FES in the correction of foot drop. The focus in the first section is on FES history and principles of operation. This is followed by a summary of the main limitations facing the use of FES. The second section provides a review of the systems that have been used for the correction of foot drop since 1961. The review highlights the major advances in the field since Liberson first introduced his transistorised electrical stimulator in 1961. This section also presents the evidence on the beneficial use of FES for foot drop. The third section describes the sensor systems and technology that have been used for stimulation triggering and control. This is followed by a discussion of the issues and limitations with the current technology and the potential for further development, in particular in the area of sensor systems and gait event detection for FES control. The current work can be seen within the context of overcoming some of those limitations and improving on current technology.

3.1 FES: History and principles of operation

Before proceeding to discuss the use of FES systems in the correction of foot drop, it is at this point considered important to give a brief historical overview and to highlight some of the main principles of operation for electrical stimulation and its interaction with the neuromuscular system.

3.1.1 History

Electrical Stimulation (ES), a technique in which electrical pulses are applied to the human body for a clinical purpose, dates back more than 2000 years. The very early applications (400 BC) utilised the electric pulses from a torpedo fish to treat headaches by applying the fish topically to the head, asthma and haemorrhoids. Other ancient methods of generating the electric currents utilised shocks from amber after being rubbed (Baker *et al.* 1993).

The developments in the understanding of electricity and its generation and interaction with the human body were accompanied by improvements in the understanding of human physiology and the neuromuscular system. Reports of electricity being used for the treatment of patients date back to the 18th and 19th centuries, in which work was undertaken by scientists and physicians like Franklin, Kratzenstein, and Duchenne who is labelled as the ‘father of electrotherapy’ (McNeal 1977). The first half of the 20th century saw the succession of events and developments leading to the use of cardiac pacemakers. In 1961 Liberson *et al.* introduced the concept of functional electrotherapy and described the use of electrical stimulation in the clinical treatment of hemiplegic patients. Since then, the scope of applications of ES has been continually expanding. Some examples of ES applications are cardiac pacemakers, pain relief methods, muscle re-strengthening, micturition and urinary continence control, phrenic nerve stimulators, defibrillators, cochlear implants, pressure ulcer treatment methods, electroejaculation procedures, and neuroprosthetic and orthotic applications. Hambrecht *et al.*, 1977, and 1992 and McNeal 1977 are three good references for a more detailed account of the history of electrical stimulation.

Electrical stimulation applications can be classified into different categories, one of which is Functional Electrical Stimulation. One definition of FES is the application of electrical stimulation to neural pathways or muscles in order to achieve an effective muscle contraction with the aim of restoring a lost or impaired function. Some examples of FES systems are those used to achieve or aid standing and walking function, hand grasping, breathing, and bladder function. At this point in time, FES can be used as an almost routine therapy for a selected group of patients including stroke, multiple sclerosis, incomplete spinal cord injured, and cerebral palsy patients. The following discussion is restricted primarily to the stimulation of innervated muscle.

3.1.2 Physiological principles

Locomotion is made possible by the multiple interactions that take place between different systems and sub-systems of the human body. These include higher brain centres, spinal cord, central pattern generators, peripheral sensory systems, vision, and muscular and skeletal systems. Communication between the central (command) and peripheral (actuators and sensors) parts is a very critical element for the initiation, maintenance, and

termination of movement. This is achieved by the neuron, the basic unit of the nervous system. Nerves using a nerve impulse carry both motor and sensory signals originating in either other neurons or in sensory organs. This nerve impulse is the message unit used by the nervous system to communicate and activate muscles. The signal carried by the neurons is based on an electrochemical process known as the action potential (AP), which is often referred to as an “all or none” phenomenon. The AP is effectively an electrical event characterized by a brief change in the resting membrane potential, which is the outcome of membrane permeability characteristics and the presence of ion pumps. Both nerve and muscle cells alter their permeability characteristics causing a change in resting membrane potential that is utilised for AP and contraction propagation. An AP is triggered by an adequate stimulus that can be mechanical, chemical or electrical in nature.

The application of an external electric current through two ‘poles’ creates an electric field, to which the cell and its extra cellular environment are subjected. The presence of this field affects the cellular membrane potential by altering the distribution of the charged ions in the extra cellular fluid. This migration of ionic charges towards the oppositely charged pole results in a depolarisation of cellular membrane nearer to the cathode. Several factors affect whether a certain current will be sufficient to produce an AP. These include the parameters of the electric current itself as well as the impedance characteristics of the tissue between the electrode and nerve interface.

In the artificial electrical stimulation of nerves, several observations can be made which are related to the stimulation parameters:

Thresholds: the amplitude or the duration of the current pulses should be equal to or higher than the threshold of excitability. The relationship between the current amplitude and duration is reciprocal, meaning that a higher duration is needed when a lower current is used in order to cause stimulation and vice versa. Increasing either the duration or amplitude of the stimulus will affect the strength of the resulting muscle contraction as a result of an increase in the number of activated motor units. An increasing amplitude will increase the muscle output, up to a supra-maximal level where additional increases in current amplitude result in no increase in the force output (Figure 3-1). This is commonly used to vary the strength of the contraction from a threshold to a near maximal level.

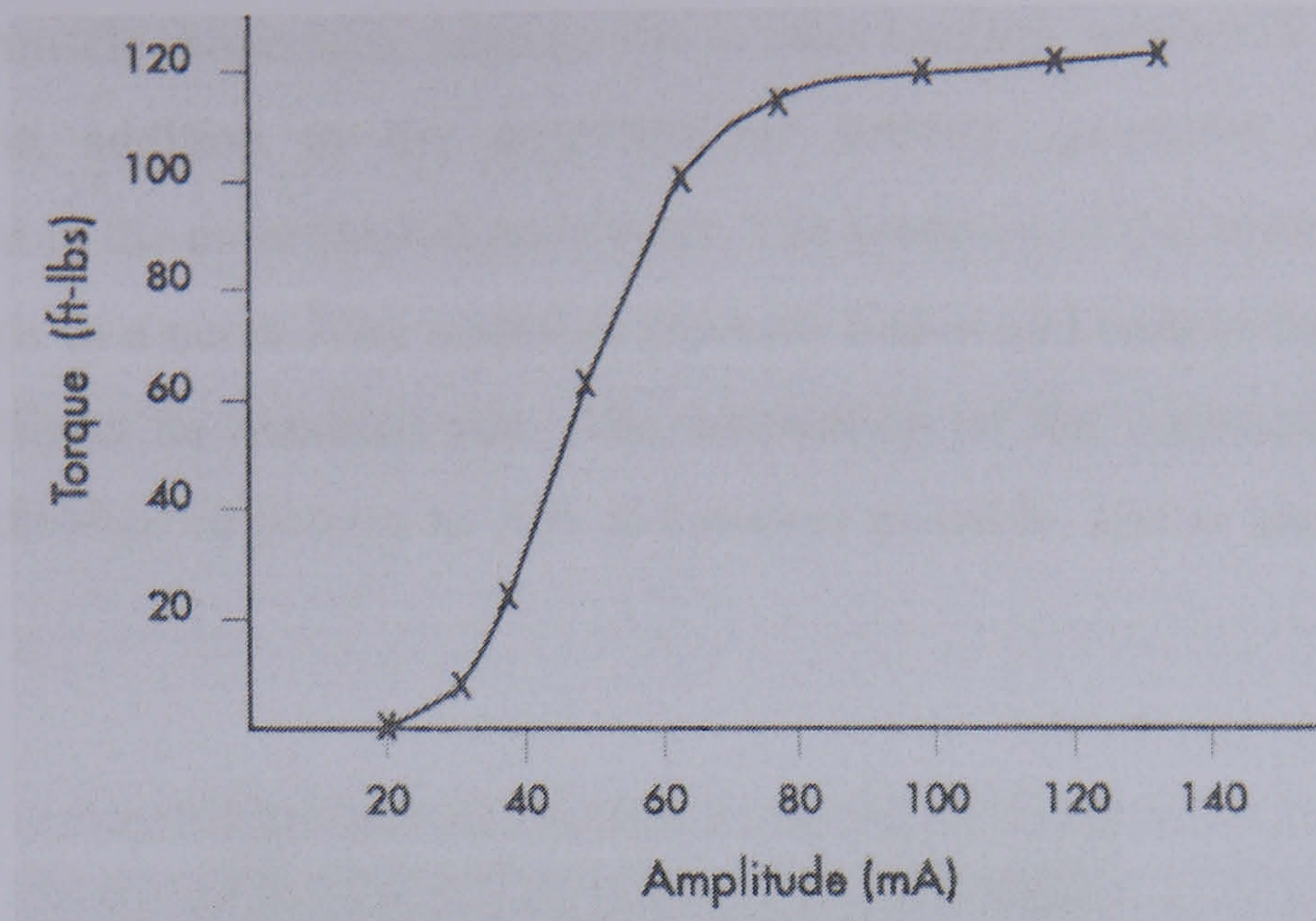


Figure 3-1: The effect of increasing current amplitude on the muscle force response measured by torque (Baker *et al.* 1993).

The time it takes the current amplitude to reach its maximum value (rise time) is also of importance in terms of the response due to a capability of the excitable membrane to 'accommodate' to slow rising current amplitudes. The combination of pulse amplitude, duration, and rise time is what determines whether an AP and a contraction will occur.

Recruitment order: In a voluntary contraction, the recruitment of motor neurons, and consequently motor units in each muscle, is achieved asynchronously (A motor unit being one motor nerve plus all of the muscle fibres that it innervates). The small motor neurons innervating slow-fatiguing motor units are generally recruited first followed by the larger motor neurons and motor units, which fatigue more rapidly. The diameter of the motor neuron is inversely proportional to its excitability threshold and hence under the effect of an external current, larger motor neurons are excited first in an almost reverse order to the normal physiological case. In addition the resulting excitation is also synchronous, and is dictated by the frequency of the external stimulus. Smaller motor neurons exhibiting a higher threshold of excitability, innervating smaller and slower fatiguing motor neurons units, are only recruited when higher pulse intensities are used.

Frequency: the frequency at which the neuron fires APs under the effect of the electric stimulus is dependent on the frequency rate of the applied stimulus. The resultant motor response of the muscles will also depend on this rate. In the normal physiological case of

limb and trunk muscle movement, neurons fire at rates ranging between 5 and 25 APs per second. This, in addition to the asynchronous activity, generates smooth muscle contractions seen in the co-ordinated movement. The presence of the absolute and relative refractory periods in a nerve fibre response prevents fusion and summation of the neuron AP firing and limits its maximal rate. The summation of the contractile force of the muscle fibre individual responses to APs is however possible, and is known as “tetany” (Figure 3-2).

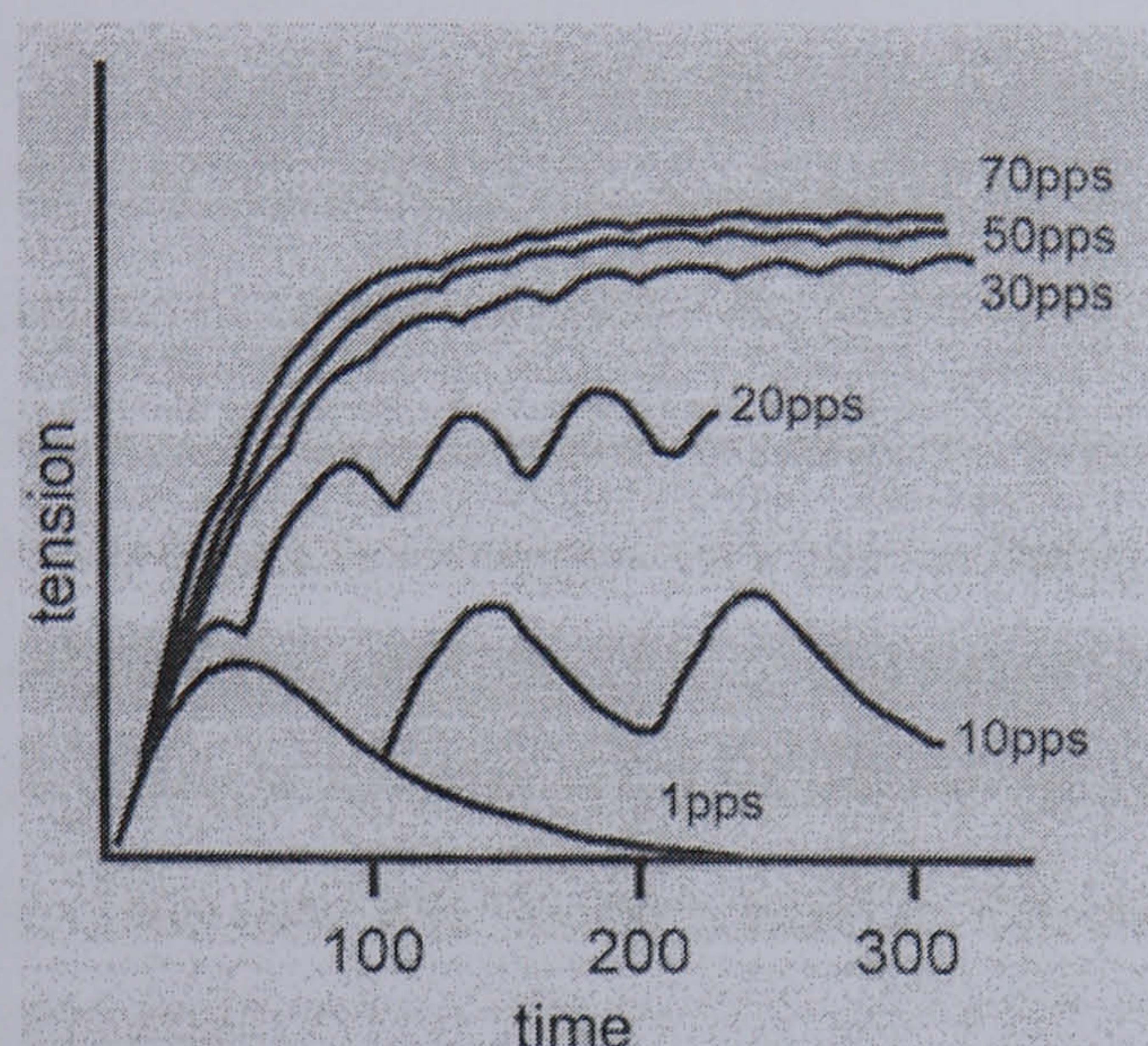


Figure 3-2: Electrically induced tetany by applied stimuli at different frequencies (pps = pulses per second) (Baker *et al.* 1993).

In order to achieve the same objective of smooth contractions using electrical stimulation, higher rates are required due to the synchronous activity of the activated motor neurons and motor units. This higher rate requires a higher energy output from the stimulator and causes a more rapid neuromuscular fatigue.

Waveform shape: different shape waveforms can be used to cause depolarisation of nerve fibres. These can be classified into monophasic and biphasic currents. The biphasic waveform in turn can be either symmetrical or asymmetrical. The asymmetrical biphasic waveform can be also split into charge balanced or unbalanced. The most prominent concern of the use of these different types of waveforms is their effect on charge transfer and ion flow. Constant DC current or galvanic stimulation is also used in certain applications of ES, where neuromuscular stimulation for restoration of movement is not the main objective.

Other factors: the type and size of the electrodes are two parameters that can affect the quality of the resulting movement, the specificity of response, and skin response. Current density and the impedance of the tissue-electrode interface are affected by the choice of electrode. The stimulus can be applied using either surface electrodes (transcutaneously) or implanted electrodes (percutaneously or subcutaneously), with a variety of available electrode designs in each case. The required stimulus energy is lowered when the electrode is implanted closer to the nerve fibre. Ramping the stimulation output, either up or down, is used to optimise the muscle contraction output while minimising discomfort. A gradually rising stimulus can minimise the discomfort of the stimulus by avoiding a sudden onset of a contraction. Another parameter that can affect the stimulation outcome is the source of the stimulus current. Stimulators can be designed to provide either a constant voltage or current. Impedance changes will cause changes in the stimulus current if a constant voltage stimulator is used. However, if a constant current stimulator is used, there exists a risk of skin damage as a result of increased current density with a partial removal of an electrode. This can also be the case if the electrode skin contact for example is limited to small areas.

In the case of foot drop, for the stimulation to be effective, the above parameters and choices should be optimized to produce a repeatable, effective, and smooth muscle contraction with minimal or no patient discomfort, skin irritation, and with minimal energy costs on the stimulator (Bowman *et al.* 1985).

3.1.3 Limitations and challenges facing the general use of FES

Some of the limitations and challenges faced when using FES are pain or discomfort due to the sensation of the stimulation, obtaining the optimal muscle contraction and ankle joint movement in the case of foot drop, reproducibility of the muscle contraction, muscle fatigue, and selectivity. Finding the right electrode positions in surface stimulators, particularly foot drop stimulators, is often reported as one of the main issues that patients and therapists face, and leading to longer times in setting up the stimulator (Liberson *et al.* 1961; Takebe *et al.* 1975; Stanic *et al.* 1978; Granat *et al.* 1996; Taylor *et al.* 1999). Prolonged donning times are also more of an issue with multichannel stimulators.

The main challenge however lies in developing a system that is capable of adapting to a changing environment and a dynamic neuromuscular system. A reliable system with the above capability is likely to have a complex control strategy with substantial feedback. Designing such a system and yet having an end-product that is simple and easy to use is one challenge that faces anyone working in the field, and is yet to be fully solved.

3.2 FES systems for the correction of foot drop

The first use of an electrical stimulator for the functional correction of foot drop was by Liberson *et al.* in 1961. This section presents the developments that have occurred since, and the evidence reported in the literature related to the use of FES for foot drop correction. The importance of presenting a historical review of this type lies in highlighting the areas where a scope for improvement exists and is most needed. By giving this review, the need for this current work is made more evident.

A typical FES foot drop system consists of a single channel device stimulating the peroneal nerve in order to induce ankle dorsiflexion, and knee and hip flexion during the swing phase of the gait cycle. The stimulation of the peroneal nerve leads to both direct and indirect stimulation of muscles. The direct stimulation is the result of depolarising motoneurons controlling the dorsiflexors. The stimulation of sensory nerves could lead to the stimulation of the flexion withdrawal reflex and results in flexion at the hip, knee and ankle joints. Electrical pulses can be applied using surface electrodes placed near the head of the fibula over the peroneal nerve. The system employs a sensor system that controls the timing of the stimulation. This sensor is usually a footswitch placed under the heel. Stimulation starts once the heel rises off the ground and ends when the heel makes contact with the ground during the swing to stance transition. The stimulator is usually worn either in a pocket or attached to a belt. Two leads are used to connect it to the electrodes and the foot switch (Figure 3-3).

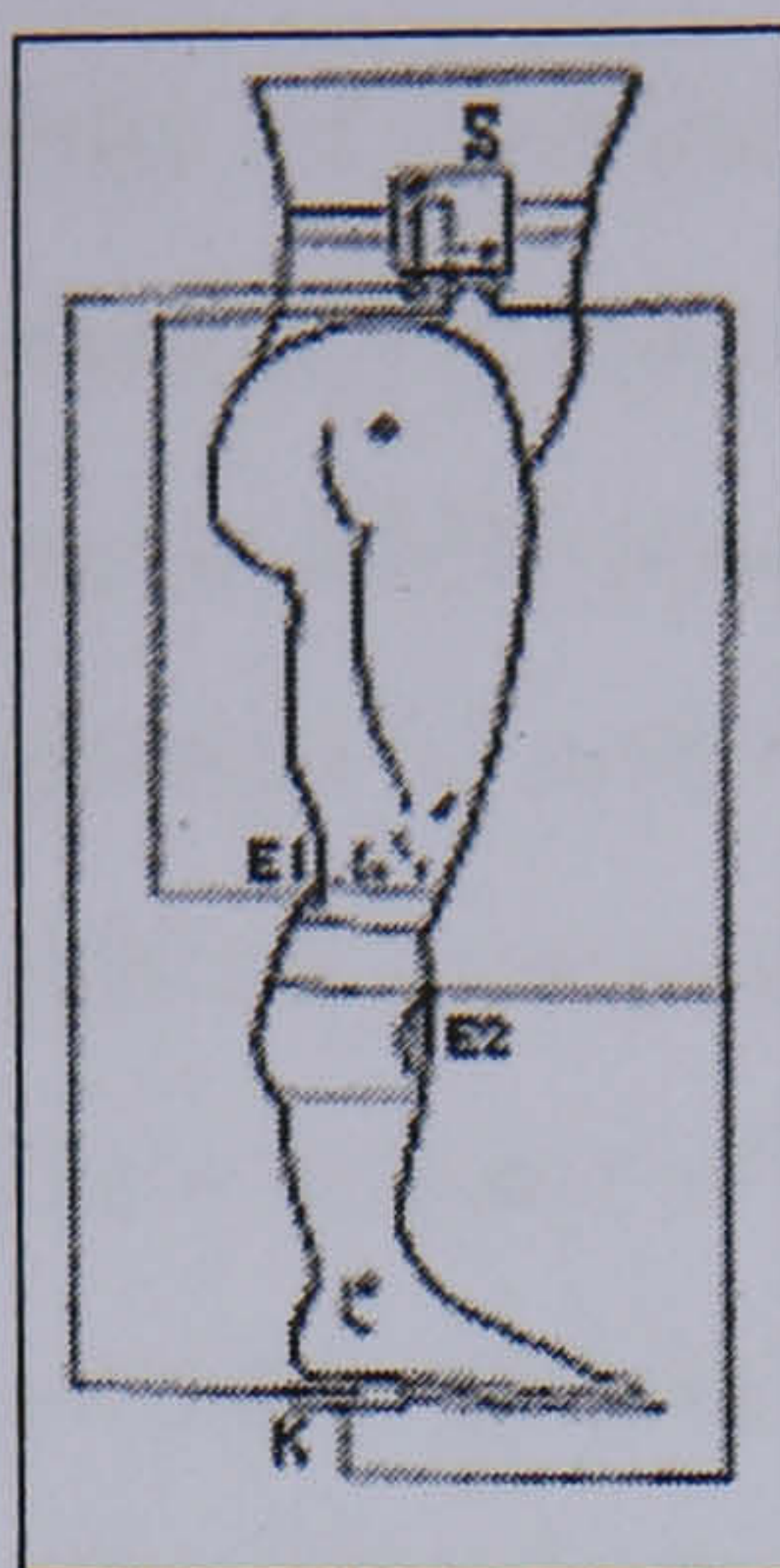


Figure 3-3: Arrangement of the foot drop stimulator used by Liberson. S is the stimulator, E1 and E2 are the electrodes, and K is the foot switch. (Liberson *et al.* 1961).

3.2.1 Liberson and after

The first stimulator described by Liberson *et al.*, 1961 (Figure 3-3) was transistorized and connected to the surface electrodes and foot switch using wires. The active electrode was an EEG-type electrode specially constructed with elastic material taking into account its point of application behind the head of the fibula and the difficulty in finding the correct location. The stimulator was the size of a cigarette to a cigar box (dimensions not specified) and was placed at the belt of the patient. The switch was an “open-close” mechanical type electrical switch, and when pressure was applied it closed a part of the circuit with a shunt and prevented the current from being applied to the peroneal nerve. Opening the switch resulted in the current flowing through the electrodes.

In 1962, Moe *et al.* described the stimulator that they used. The principle of operation was similar to that used by Liberson. It was transistorized and to be worn on the belt and weighed less than 0.2 kg. An elastic cuff held the electrodes in place, which were disposable and kept moist with a non-irritating electro-conductive wetting agent. A foot switch was used to time the stimulation, which had an adjustable intensity between 20 and 80 V and a fixed frequency at 58 Hz. Both Moe’s and Liberson’s designs relied on a foot switch and surface electrodes with wires connecting these to the stimulator worn on a belt. This dependence on a foot switch and the use of wires and multiple attachment sites would affect both the reliability of the system and reduce the practicality of using the system by patients.

Vodovnik *et al.*, 1965 at the University of Ljubljana, described the use of a foot drop stimulator, which they called FPS, functional peroneal splint, which could be triggered by a manual hand switch, a foot switch, or an EMG sensor. The pulse width used was 300 μ s applied at an adjustable frequency between 30 and 60 Hz, values that were selected as a result of a series of comfort tests of different stimulation parameters. Later developments by the same group of researchers led to a number of other stimulators called PO-8, FEPA (Functional Electronic Peroneal Apparatus), and MICORFES (Vodovnik *et al.* 1965 as referred to by Lyons *et al.* 2002). Vodovnik selected a set of stimulation parameters that maximised comfort to the patient, but the practicality of the system was still hindered by the use of surface electrodes, a footswitch or push button. The researchers encountered problems when using EMG for stimulation triggering as a result of cross-talk between electrodes.

Later developments considered implantation in order to improve some aspects of the system, in particular issues related to electrode positioning and ease of use. The group at Rancho Los Amigos National Rehabilitation Medical Center reported on a single channel implantable system, the Neuromuscular Assist, which was made commercial (Waters *et al.* 1975). The initial system, which was reported on in 1969, went through 2 revisions in 1970 and 1971. Waters described the performance of the system in 16 subjects who had the implant and reported good results. The system was composed of 3 modules, an external stimulator unit, a foot switch and transmitter, and an implanted receiver and electrode wrapped around the peroneal nerve. Only a small percentage of patients were candidates for this peroneal Neuromuscular Assist, and the system encountered frequent equipment failure of mechanical nature. The system also depended on an insole switch and hence the limitations pertaining to that use, which will be discussed later in this chapter.

Around the same time, researchers in Ljubljana reported on their design of an implanted foot drop stimulator (Jeglic *et al.* 1970). The system consisted of 3 elements too, with an external stimulator and control unit with a RF transmitter. The foot switch had a wireless connection with the unit. A RF receiver combined with the bipolar electrode was implanted during a surgical procedure. The report, however, did not include any clinical results of the performance of this system. The use of a RF link is believed to be an improvement on earlier designs as it eliminates the need for wires to connect the switch to

the stimulator. The implantation approach taken in this and other earlier and later systems, improved certain aspects of the use of FES, however, does not address the needs of the patient who requires FES use temporarily or for short periods, when the risks associated with invasive procedures are considered.

Multi-channel stimulation was proposed by Kralj and his group in 1971. 3 channels of stimulation allowed the stimulation of 2 additional muscle groups to the dorsiflexors. The system was triggered by one foot switch linked to the bulky control unit (weight 1.2 kg) using a wireless connection. The extra channels provided the possibility to further control and improve the patient gait, however using one sensor input for this made optimizing the timing of stimulation neither easy nor quick to achieve (Kralj *et al.* 1971). Later developments by the same group led to two 6-channel stimulators, one analogue and one digital, which were both controlled by foot switches. Both stimulators were aimed as an improvement on the initial system, as they allowed more reliable detection of events and easier setting of stimulation sequences (Stanic *et al.* 1978; Strojnik *et al.* 1979). The use of multi-channel stimulation and the advantages gained in control of multiple muscle groups are compromised by the increased difficulty in setting up the system and impracticality in being used by the patient at home.

In 1975, Takebe *et al.* reported on the performance results of a commercially available foot drop stimulator made by Philips. The system was a single channel stimulator carried by the subject and consisted of a stimulator box, two electrodes and an air filled rubber insole placed under the front part of the unaffected foot. Air pressure changes caused by the varying weight placed on the foot were used to time the stimulation. Four selected case reports provided some insights into the use of the system but no formal evaluation was conducted. In addition only 3 patients continued using the stimulator out of the 9 carefully selected patients mainly due to pain and discomfort and difficulty in locating correct electrode sites. This fact likely reflected a poor acceptance of the technology by the patients for the reasons mentioned above and possibly others to do with the practicality of using the system. Although no experimental assessments have been made of the insole switch, using the contra lateral foot is expected to make the timing of the stimulation less optimal.

The advance in electronics technology led to the inevitable development of microcontroller-based stimulators. Bogataj *et al.*, 1984 described a 6-channel microprocessor based stimulator. The stimulator could be used for foot drop correction and had arrays of switches that allowed setting the stimulation sequence for each channel. A foot switch controlled the timing of stimulation and the microprocessor-based stimulator could measure and record some gait parameters, such as number of steps taken, mean stride time, and mean heel-on time.

Since then, several stimulators have been developed that included both surface or implantable, single and multichannel systems. The majority of these were designed with one specific application in mind, however some of the multichannel stimulators could be used for more than one application (Marsolais 1986; Meadows 1987; Philips 1989; James 1991; in Ilic *et al.*, 1994). The “Footlifter” (or KDC 2000), a commercial device from Elmetect (Elmetec, Denmark), is a 1-channel underknee surface stimulator and weighs less than 100 grams. This device was again triggered by a heel “wedge” with built-in contacts and hence affected by the limitations of that sensor approach (Pedersen *et al.*, 1986 as referred to by Lyons *et al.* 2002). IPPO, the commercial name of an underknee implantable stimulator, was developed by Strojnik *et al.* in 1987 as an improvement on the earlier version of stimulator developed by the researchers at Ljubljana with a simpler surgical procedure and improved reliability (Jeglic *et al.* 1970). The use of the system by 20 subjects gave beneficial results as measured by the ankle joint movement.

Another example of a later system is a 2-channel implantable stimulator, which can provide stimulation for 2 degrees of freedom around the ankle joint, *i.e.* dorsiflexion – plantar flexion, and inversion – eversion. An external controller unit controlled the stimulator, and a separate external programmer module could be used to set the stimulator. Both the programmer and controller unit were microcontroller based, and the stimulator was powered by an RF link (Kelih *et al.* 1988). This system was expected to overcome some of the problems faced when using a single channel implanted stimulator such as that described by Waters. The second channel was used to effect a more natural inversion-eversion movement.

The development of the most common foot drop stimulator in the UK in current use took place between 1989 and 1995. The group at Salisbury District Hospital, UK developed

and tested a single channel surface stimulator, named ODFS (Odstock Dropped Foot Stimulator). The stimulator, worn on the belt or inside the pocket, is linked to the electrodes using wires and triggered by a foot switch placed inside the shoe. Miniature potentiometers can be used to adjust the stimulation parameters such as the amplitude and ramps (Burridge *et al.* 1997).

Another surface but 2-channel stimulator was also developed in the early nineties by Malezic *et al.* (1992), which was microcontroller based, and foot switch controlled. The stimulator system was composed of 2 components, a stimulator unit, and a programmer and stride analyser unit. The stimulation sequences and durations could be adapted in real time based on previous stride times using linear and weighted extrapolation computations. The system was also capable of data logging and recording gait temporal parameters.

The FEO- KM25 is another example of a functional electrical orthosis developed in 1992 by a group of researchers in Brazil. The system is similar to other foot drop correction systems in that it has 1 channel of stimulation and is controlled by a switch placed in an insole. The stimulus frequency can be set between 10 and 90 Hz, with 0.2 to 0.6 ms pulse width, 0 to 100 V intensity and powered by a 9 V battery (Junqueira *et al.* 1998).

A totally self-contained device, made commercial by NeuroMotion (Edmonton, Canada), incorporates a 1-channel surface stimulator and a tilt sensor that measures the shank angle and triggers the stimulation. The microcontroller-based device straps onto the lower leg below the knee and uses surface electrodes to stimulate the peroneal nerve (Wieler *et al.* 1996). The use of a tilt sensor as a replacement of the foot switch allowed the integration of the sensor, electrodes and stimulator into a single unit. This approach of bringing the sensor, electrodes, and stimulator together is an improvement on other systems, however, the use of the tilt sensor and stimulation timing algorithms have been criticized on the basis of accurate performance (Pappas *et al.* 2001). This is expected as a result of the use of simple thresholds for the detection of gait events. False detections can result from non-walking activities such as sit to stand transfers.

Compustim 10B, a versatile portable and microcontroller-based 2-channel stimulator, was developed by Michael. The stimulation parameters and sequences can be easily adjusted and set using a PC and user-friendly control panels (using the LabVIEW environment)

linked to the stimulator by a serial interface. Digital and analogue inputs allowed the use of additional and alternative sensors to the foot switch as demonstrated by the author's use of ultrasonic sensors for foot elevation measurement and a closed-loop control approach (Michael 1996).

Lyons *et al.* reported on their microcontroller-based 2-channel surface stimulator, "The University of Limerick Drop Foot Stimulator" (Lyons *et al.* 1997; O'Keeffe *et al.* 2002). A Visual Basic interface was used in this case to set the control parameters, and digital and analogue inputs provided the user with the flexibility in the choice of sensors. A similar 4-channel neuroprosthesis was developed by Popovic *et al.* (1998) and aimed at assisting and restoring walking in the ISCI patient and stroke subjects. The system "ETHZ-ParaCare" could be controlled by a hand push button or a foot switch. The same group of researchers developed a gyroscope and force sensitive resistors-based gait phase identification sensor for the control of the microcontroller-based stimulator.

The group at Salisbury District Hospital developed a 2-channel version of the ODFS, which permitted the correction of bilateral foot drop or the stimulation of an additional muscle group in addition to the peroneal nerve stimulation used for foot drop correction. The O2CHS surface stimulator can be controlled by one or two foot switches (Taylor *et al.* 1999).

Researchers at the University of Twente (Enschede, The Netherlands) developed a dual channel implantable stimulator which is controlled by an external control unit and triggered by a foot switch. The system (produced by Finetech Medical Ltd.) uses bipolar epineural electrodes and allows for the control of both inversion-eversion and dorsiflexion and plantar flexion (Holsheimer *et al.* 1993; Holsheimer *et al.* 2000). Initial tests by 2 subjects are promising and showed walking speed improvement (Kenny *et al.* 2002). A similar implantable and 2-channel system controlled by a foot switch was developed at Aalborg University (Haugland *et al.* 2000). The electrode is a 12-polar nerve cuff implanted above the knee and allows for the stimulation of both dorsiflexors and everters/inverters groups. The system is fitted in a two-stage surgical procedure.

Compex Motion (manufactured by Compex SA) is another more recent development by Popovic *et al.* (2001). This system, which is a further development and expansion of the

ETHZ-ParaCare portable FES system, is a 4-channel stimulator, microcontroller-based, and with 2 input channels. The stimulation parameters and sequences can be set using a graphical user interface and a “drag-and-drop” technique, and stored on readily exchangeable memory chip-cards.

More than 40 years after the work of Liberson, the most commonly and currently used stimulator for foot drop correction in the UK is the ODFS made by Salisbury District Hospital. This system follows very similar principles to Liberson’s stimulator with the stimulator worn on the belt or placed inside the patient’s pocket, with two leads connecting it to the foot switch and surface electrodes. The foot switch is based on a force sensitive resistor and controls the timing of stimulation. Both the number of commercially available stimulators and number of subjects using them are relatively limited. This number is estimated to be less than 14000 over the period of 40 years (Lyons *et al.* 2002). Attempts at optimising the performance of these systems have resulted in a variety of designs for multi-channel implantable or surface stimulators. Although this work has improved certain aspects (e.g. higher specificity in controlling muscle groups through implantable devices), many designs are hampered by excessive set-up times or limited suitability among patients.

This review of existing systems highlighted some of the issues faced by researchers and clinicians involved in this field and the approaches that were adopted in order to address these problems. The last section in this chapter summarises both of these and offers some potential solutions to those outstanding issues with FES systems for foot drop correction.

3.2.2 Evidence of the benefit of FES in foot drop

This section presents a summary of the main evidence of FES benefits to foot drop patients. Most reports on FES work referred to the benefits of FES using either subjective observations or more objective measures. Relatively few studies followed formal and controlled protocols to study the benefits of FES. The benefits observed could in turn be split into two types: orthotic and therapeutic effects. This summary will include the reported gains in the earlier studies, and the results of the relatively more recent controlled and major studies.

The studies described in this section used a variety of outcome measures in order to evaluate the effect of FES for foot drop patients. These are:

- Walking speed and other gait temporal spatial parameters
- Energy cost of walking such as oxygen consumption and physiological cost index (PCI)
- Gait parameters including joint kinematics and range of motion (ROM), kinetics including the ground reaction forces and centre of pressure calculations, and EMG studies

In addition to the above measures, questionnaires and indices such as the Barthel index were used in order to assess the effect of FES on other aspects of the patient's function and quality of life. There is an overall agreement on the use of walking speed as an outcome measure for assessing the effect of the foot drop stimulator. This is partly due to the relatively easy ways of measuring this parameter. It can be argued that walking speed is not the most suitable measure, as the benefits to a patient might not be manifested in an increase of walking speed, but more importantly in the total distance that can be walked. Walking speed, however, is a relatively appropriate measure of the orthotic effect of the stimulator, particularly when it is combined with a reduction in the energy cost of walking.

In Liberson's study, the author reported considerable gait improvement in all seven hemiplegic subjects who took part in his trial. This was mainly seen in the increased dorsiflexion of the affected foot (Figure 3-4).

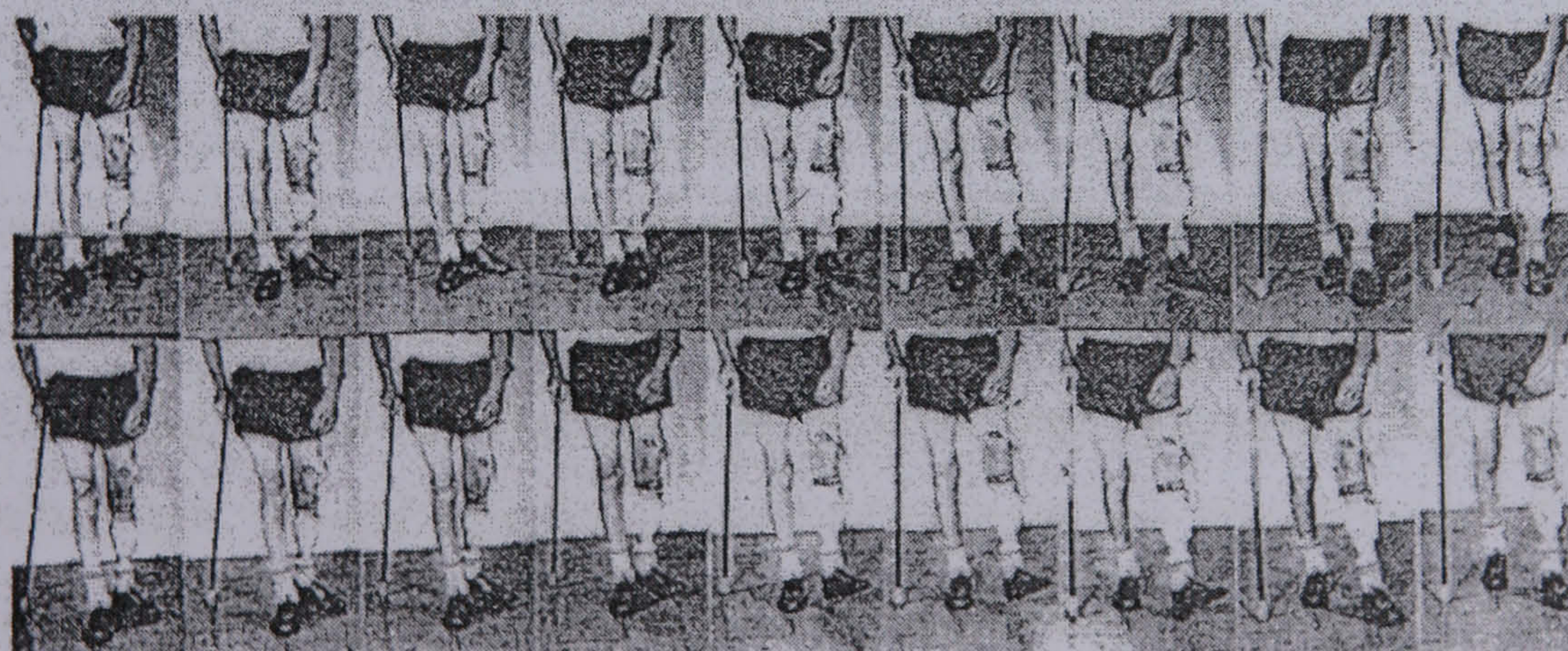


Figure 3-4: Patient walk without stimulation (top) and with stimulation (bottom) (Liberson *et al.* 1961).

A carry over effect was also observed in some patients as seen by an improvement in their spontaneous dorsiflexion even after discontinuing the use of the stimulator (Liberson *et al.* 1961). The study by Moe and Post in 1962 reported the results in 3 of their patients and stated that similar results were seen in a number of other patients in the test program. Improved walking, including up and down stairs, reduced fatigue, improved voluntary contraction and/or ability to walk longer distances were reported in the 3 cases included in the study (Moe *et al.* 1962). 13 out of the 16 subjects, who took part in the trials by Waters and his group, benefited by improved stride length, gait velocity, and cadence. An increase from 0.55 to 0.71 m/s was seen as a result of the use of the implanted stimulator (Waters *et al.* 1975).

Only 3 out of the 9 patients, who took part in the study by Takebe *et al.*, 1975 tolerated the sensation. The 1st case was reported to have improved muscle force but no remarkable improvement in the gait pattern. Case 2 experienced an increase in ankle ROM as a result of the stimulation, while case 3 showed an increase in voluntary EMG.

Stanic *et al.*, 1978 used both qualitative and quantitative gait analysis using goniometers in order to monitor the changes in 11 patients who participated in their study. They reported that the applied surface multichannel stimulation reduced or even completely corrected most of the typical gait deviations of hemiplegic patients. Merletti *et al.*, 1979 observed beneficial orthotic effects in 76% of the cases when they considered a sample of 50 hemiplegic subjects. In a subgroup of these patients, oxygen consumption was slightly reduced and they also noted an improvement in motivation. He concluded as a result of this experience that FES appears to be useful in 15% of the total ambulatory hemiparetic population.

In a later study and follow-up by Waters *et al.* in 1985, 7 out of the 16 subjects continued to use the device for an average of 11.6 years (10.1 to 12.3 years). The reasons for removing the implanted device from the rest varied between inconvenience and difficulty in use, malfunction, wound infection, nerve damage, or the development of complete paraplegia. One subject refused to use orthoses and preferred walking with the foot drop uncorrected.

In a different study by Malezic *et al.*, 1992 a group of 21 hemiplegic subjects used two-channel stimulation, the authors noted a mean decrease in stride time of 0.22 s, a mean increase in stride length of 5.9 cm, and an average increase in walking speed of 0.05 m/s (17.9%) in the stroke subgroup of the subjects. The traumatic brain injury subgroup showed similar results, but with a greater increase in walking speed (24.4%). Significant improvements were also seen in 10 out of 19 subjects using a 1-channel implantable stimulator (Kljajic *et al.* 1993). The gait parameters considered by Kljajic were quality of ankle movement, EMG responses, ground reaction forces point of application, centre of pressure, and joint angles. The remaining 9 subjects did not respond in a similar way as a result of excessive eversion in the movement following stimulation, and consequently required electrode re-implantation.

The effect of peroneal nerve stimulation in ISCI subjects was assessed by Stein *et al.*, 1993. 10 ISCI subjects (level C2 to T10) were studied, while using a variety of stimulators in terms of number of channels and surface or implantable types. Gait (video, goniometers, heel and toe switches) and Oxygen consumption studies were done. Speed increased in all subjects (mean of 4m/min which can be significant for very slow walkers), while the swing phase duration and proportion of total cycle time decreased. A modest decrease in Oxygen consumption was also noted.

Granat *et al.*, 1996 performed one of the few studies where the benefits of FES were assessed against a controlled set of results. The results of this ABA crossover study lasting for 11 weeks were reported for a group of 16 subjects. The outcome measures were speed, temporal gait parameters, symmetry, heel strike, foot inversion during stance, and the Barthel index. Subjects were tested while walking over carpet, linoleum, and uneven ground. The authors reported an overall orthotic improvement in particular in terms of heel strike and inversion.

The group at Salisbury District Hospital reported the results from a randomised controlled trial with 32 subjects split into treatment and control groups (Burrige *et al.* 1997). The treatment group received physiotherapy together with FES, while the control group received physiotherapy alone. The intervention was the functional use of the ODFS single channel stimulator. Walking was statistically improved by the ODFS when considering the walking speed and PCI with a mean increase of 20.5% (5.2% for control) in walking

speed and a reduction of 24.9% (1% for control) in PCI. In another study by the same group, 107 current users and 53 past users took part in a questionnaire that assessed their perceptions of the ODFS. The reasons given by patients for using the ODFS (current users) were reduced effort, reduced risk of tripping, increased walking distance, increased confidence, increased walking speed, increased independence, ability to walk on uneven ground, no longer needed ankle foot orthosis (AFO), improved fitness with the use of ODFS, no longer need assistance when walking, improved walking without ODFS if used periodically, and no longer needed walking stick (Taylor *et al.* 1999).

In a multicentre evaluation of the effect of FES systems for walking, Wieler *et al.*, 1999 assessed 40 subjects (31 ISCI, 8 stroke, 1 head injury) distributed in 4 centres in Canada. Walking speed, cycle time, and stride length were monitored and acceptance of the systems was assessed by a questionnaire. Stimulation was done with 1 to 4 channels using one of these three systems: Unistim, Walkaide, or Quadstim. The stride length increased over 20%, but with no significant changes in cycle time. Both training and orthotic effects were seen in walking speed with an average total improvement at 45%, with the patients who initially had slower walking speeds benefiting more from the stimulation. The responses to the questionnaire were overall very positive.

Data from a number of studies assessing the orthotic effect of FES on the improvement of walking in stroke patients with foot drop were pooled and used to measure the improvement in walking speed (Kottink *et al.* 2004). An average improvement of 0.13 m/s (0.07-0.2) or 38% (22.18-53.8) was calculated, and described as a positive orthotic effect of FES on walking speed.

One more recent study assessed the efficacy of FES in improving walking ability for people with MS (Swain *et al.* 2000). The study reports the changes in speed and PCI after 4 and ½ months and after 3 years. In the first case, a total orthotic effect was observed with 16% increase in speed and 20% reduction in PCI, while a 36% increase in speed and 29% reduction in PCI were seen in the 3-year follow-up group.

3.2.3 FES systems for foot drop correction

In the UK the ODFS has become the most commonly used stimulator for the correction of foot drop, after being recommended by the South and South West Regional Health

Authority Development and Evaluation Committee as a “treatment” for use within the National Health Service. Over 1000 systems have been provided for subjects suffering from foot drop as a result of CVA, MS, ISCI, CP, and TBI. Lyons *et al.*, 2002 estimates the total number of manufactured FES systems for foot drop correction at less than 14000 over the period 1961 to 2001. Past and current systems include the FEPA-10, PO-8, IPPO, and MICROFES (Jozef Stefan Institute, Slovenia), KDC-2000A or Footlifter (Elmetec, Denmark), ODFS (Salisbury District Hospital, UK), the Neuro-Muscular Assist (Medtronic Inc., USA), and Walkaide (NeuroMotion, Canada).

Other stimulators that were either reported in the literature or available for purchase are the FEO KM25 (Junqueira *et al.* 1998), and the Akita system (Matsunaga *et al.* 2000). The existence of several models and stimulators, in combination with the limited number of stimulators that are used by patients further highlights the fact that there still exists some need for a stimulator system that is both reliable and practical to use from the patient perspective.

3.2.4 Who is suitable for FES correction of foot drop

Careful selection of patients is important for the successful application of any clinical intervention. The unavailability of clear and well-defined patient selection criteria has been partly responsible for the lack of wide-spread success and hence use of FES for foot drop correction. Sufficient cognition, motivation and dexterity, enough “gadget tolerance”, ability to tolerate the discomfort of the stimulation, intact peroneal nerve and dorsiflexor muscles, intact skin and peripheral circulation are all referred to in the selection of subjects for clinical and research studies and are directly relevant for the choice of patients to use FES (Takebe *et al.* 1975; Waters *et al.* 1975; Stanic *et al.* 1978; Burridge 2001). A key factor for the suitability of FES for the correction of foot drop is the presence of an intact peripheral nerve and dorsiflexor muscles, allowing the stimulation of the nerve and consequently an effective muscle contraction. In the ISCI patient population, Bajd *et al.*, 1999 identified a group of patients who are candidates for the use of a peroneal stimulator, as those patients with inadequate voluntary ankle dorsiflexion, but with sufficiently strong knee extensors.

The presence of lower motor neuron disease, ankle joint contractures, muscular disease, and excessive spasticity have all been described as either possible contraindications or

exclusion criteria for subjects. Pregnancy, hypertension, presence of malignant tumours, cardiac pacemaker users, and poor skin condition are situations where either FES should not be used or extra care given if used (Baker *et al.* 1993).

3.2.5 Comparison of FES to other interventions

A number of studies have presented a comparison between FES and other interventions, particularly AFO's and physiotherapy, and reported some advantages in the use of FES. Although many of these findings are true under the conditions of the trials performed, care must be taken when presenting FES as a better replacement of other treatment methods. A more reasonable and possibly beneficial approach is to view FES as both an alternative and complimentary method that might be superior in the case of some patient groups and not others. With this in mind, some of the reports and findings of studies comparing FES to other methods are presented in this section.

FES was compared to and found to be superior to other treatment options such as the use of mechanical orthoses (Bogataj *et al.* 1993; Granat *et al.* 1996) and physical therapy. In both studies a preference for FES was found. According to Kralj A. 1989, FES assisted walking requires less energy and is more aesthetic than walking with passive mechanical orthosis. The conventional correction of foot drop using AFO often lacks effectiveness and comfort, and prevents passive motion. Teasell *et al.*, 2003 presented a review of major reported evidence – mainly randomised controlled trials – assessing the efficacy of FES and other treatment techniques currently in clinical use, including strength training, use of AFO, treadmill training, partial body-weight support, biofeedback training, for the gait retraining of stroke survivors. The authors concluded that there is moderate evidence that FES and gait retraining result in improvements in hemiplegic gait. Similar conclusions were reached regarding the use of strength training, combined AFO use and posterior tibial nerve deinnervation, and biofeedback training as adjunctive therapy. This is in comparison to conflicting or limited evidence on the benefits of treadmill training and partial body-weight support when compared to conventional therapy.

The fact that FES utilises the remaining mechanisms in the patient might be the reason behind the therapeutic effects seen in some patients. It also allows both active and passive range of motion of the ankle joint. The active correction of gait encourages relearning and prevents or slows muscle tissue atrophy and degeneration. It has also been reported that

the effect of stimulation can help maintain denervated fibres in a vital state, improve vascular and lymphatic circulation, increase muscular strength, and re-educate movement (Liberson *et al.* 1961; Moe *et al.* 1962; Bogataj *et al.* 1993; Granat *et al.* 1996; Mann *et al.* 2000).

3.3 Sensor technology and algorithms used in FES systems

This section presents a review of FES systems used for foot drop correction, but from the perspective of the different sensors used with such systems. Some of these sensors were used as part of past systems that were either applied in clinical settings or did not leave the research laboratories. Other sensors are currently used in some of these systems or being researched as possible sensors for use in future FES systems. In the first system, designed by Liberson *et al.*, 1961 a mechanical open-close type of electrical switch was used. Since then researchers have attempted to improve on the reliability and functionality of the system as a whole and the sensor in particular. The main reasons behind such attempts are to overcome some of the limitations that were inherent to the system as a result of the use of the foot switch, in addition to some of the commonly reported difficulties with the use of stimulators or causes of rejecting them. For example, the use of the foot switch presented some obstacles to further development of the systems such as implantation and miniaturisation.

The variety of sensors used for such purposes consists of both artificial and natural sensors and includes:

- Foot switches, both the open-close mechanical type and force sensitive resistor based (Liberson *et al.* 1961; Moe *et al.* 1962; Waters *et al.* 1975; Stanic *et al.* 1978; Strojnik *et al.* 1979; Malezic *et al.* 1992; Burridge *et al.* 1997)
- Push buttons and hand switches (Vodovnik 1965, as referred to by Lyons 2002)
- Accelerometers (Willemsen *et al.* 1990; Ando *et al.* 1990; Mansfield *et al.* 2003)
- Tilt sensors (Dai *et al.* 1996)
- Goniometers (Sweeney *et al.* 1999)
- Gyroscopes (Henty *et al.* 1998; Ghoussayni 2000)
- Ultrasonic sensors for the measurement of foot elevation (Michael 1996)
- Combination of the above sensors (Pappas *et al.* 2001; Veltink *et al.* 2003)

- EMG (Vodovnik *et al.* 1965; Kershaw *et al.* 1993; Graupe 1983 as referred to by Pappas 2001)
- Electroneurogram (ENG) (Popovic *et al.* 1993; Haugland *et al.* 1995; Hansen *et al.* 2003)

Some other authors reported sensors that were used to obtain temporal parameters of gait but not as part of FES systems. Pinzur *et al.*, 1984 used an ultrasonic transmitter and receiver system which continuously monitored the inter-ankle distance, by mounting transmitter and receivers at both medial malleoli. The times of toe off and initial contact were then derived from the inter-ankle distance recordings. Aminian *et al.*, 1999 used a uni-axial accelerometer to measure the tangential component of the thigh acceleration in the sagittal plane. Toe-off and heel strike are identified as local minima in the acceleration signal.

The work in this area has focused on either overcoming a number of limitations with the commonly used foot switches or on further improvement and development of the systems in terms of their reliability and functionality. These issues will become more evident in the following section, after summarising the main principles and sensors investigated in the control and triggering of FES systems for foot drop correction.

The underlying principle and technology of the foot switch are fairly simple. The open-close mechanical type foot switch is used as an electrical switch that triggers and ends the stimulation sequences during gait. The force sensitive resistor (FSR)-based foot switch operates in a similar manner; with the resistance changes in the switch reflecting the applied forces and timing the stimulation. Foot switches with a transmitter enabling a radio link with the controller unit or stimulator have been utilised as early as the Rancho Los Amigos Hospital system and systems designed by the researchers at Ljubljana in the 1970s. This radio link-based design never got sufficiently practical, reliable, and cost attractive to be a widely marketable solution (Kralj *et al.* 1995). A different foot switch was reported by Takebe and used in the Philips foot drop stimulator. This switch is based on an air filled rubber insole that uses air pressure to transduce foot to ground contact (Takebe *et al.* 1975).

Push buttons or hand switches as they are commonly referred to are also used sometimes to control the timing of the stimulation, by the patient (or clinician) to control the stimulation. The patient often learns and improves their ability to time the stimulation by pressing the switch at the right time.

Willemsen *et al.*, 1990 used four accelerometers attached to a bracket that is in turn attached to the lower leg between the knee and ankle joints using Velcro straps. The signals from the 4 accelerometers were used to calculate the equivalent ankle joint acceleration. This acceleration is in turn used by a state-space controller to automatically detect 5 phases of walking, which are: stance, push-off, swing down, swing up, and heel strike. One of the four hemiplegic subjects used to test the method showed large disturbances in the acceleration signal during the swing phase and as a result his data were not used in the analysis of performance. For the remaining 3 subjects, only 3 errors were reported for a total of 106 steps. The author reported that similar detection was achieved using a single accelerometer placed below the knee, with slightly higher errors in the detection of heel strike.

In a study by Williamson *et al.*, 2000 the subject wore a calf strap with 3 accelerometers arranged in a cluster and mounted on a rigid platform and secured with an elasticated calf strap. One accelerometer was oriented in the vertical direction approximately along the tibial axis. The other two were mounted orthogonal to the tibial axis and with approximately 70 degrees between their detection axes. An instrumented shoe insole was used to determine the gait phases by recording the force beneath the heel, lateral, and medial metatarsal heads. A supervised machine learning program (Rough SetsTM) was used to discern the 5 gait phases (as determined by the shoe insole) from the sampled accelerometer recordings. The Rough Sets program constructed a sequence of IF THEN rules from 5 strides of data looking at the accelerometer amplitude and its first derivative and the 5 gait phases (Loading response, mid-stance, terminal stance, pre-swing, and swing). These rules were then applied to the remaining strides to predict the gait phases from accelerometer data recorded from 3 able-bodied subjects walking along an oval path and one figure of eight path. Two heuristic rules were then applied to the output of the rule-based controller in order to prevent “jitter” around the transitions between the phases and to eliminate the errors associated with high sampling rates of the inputs. The gait

detection accuracy was greater than 80%, with the errors in detection being either a late or early detection of a transition.

In a more detailed study on the detection of gait events and phases using accelerometers, Williamson reported on the performance of two commercially available supervised machine learning programs (Adaptive Logic Networks (ALNs) and Rough Sets (RS)) and compared these to a hand-crafted dual-threshold algorithm (the one described by Dai *et al.*). FSR-based foot switches were used to provide the reference signals of gait phase from the foot-floor contact patterns (Williamson *et al.* 2000). A postdetector filter was used to improve the accuracy of the RS and ALN detectors' accuracy. This filter was effectively, an IF THEN rule applied to each 3 samples to avoid erroneous transitions back and forth between phases. 3 able-bodied subjects walked along an oval path and a figure eight path to test the detection ability of the 3 adopted approaches. The accuracy of swing/stance detection ranged within 94-97 %, 87-94 %, and 87-95 % for the RS, ALN, and the handcrafted methods respectively.

Ando *et al.*, 2000 described the use of a bi-axial accelerometer mounted on the thigh to provide the timing of swing and stance phases of gait. An inductive learning algorithm was used to detect the phases from the vertical and forward acceleration signals on a personal computer post collection. The neural network was trained using a target signal derived from a heel switch. Data from 50 gait cycles from 5 healthy subjects and one stroke patient were used to test the system. The author quotes 60 ms and 80 ms as the maximum differences found between the 2 systems in the timing of the swing phase for the able-bodied and stroke subjects respectively. The author also reported sporadic stimulation spikes occurring during stance when using the accelerometer-based system. Though this study showed some encouraging results, more thorough testing protocols for the system would be essential prior to its clinical use.

An accelerometer was also used by another study in order to detect heel contact events for use as a sensor in FES assisted walking (Mansfield *et al.* 2003). The accelerometer was placed on the trunk and changes in the slope of the anterior-posterior horizontal acceleration signal were used to indicate the occurrence of heel contact. This approach was tested by 4 able-bodied subjects and evaluated against timings obtained using a force sensitive resistor-based foot switch. It was found that a 150 ms delay existed between heel

contact as identified by the foot switch and the negative to positive change in acceleration. Though the evaluation showed relatively high accuracies (between 98.2 and 99.8%) of the accelerometer sensor in detecting heel contact, the sensor ability for detecting heel rise – important event for FES triggering – was not described. In addition, the performance of the used algorithm deteriorated when hemiplegic walking was simulated and no discussion is made with regard to its performance to postural sway or noise.

Dai *et al.*, 1996 utilised a magneto-resistive tilt sensor to measure the absolute angular displacement of the shank in order to detect the foot contact events required for timing the stimulation of the peroneal nerve. The stimulation is turned on when the tilt signal rises above an ON threshold, and is turned off either if the tilt falls below a second level or a preset maximum period of stimulation is exceeded. This system was tested with a stroke subject and the detection compared to that given by foot switches placed in the shoe insole. A prototype FES device with the tilt sensor and control unit was designed for further clinical trials, and the early results from such trials were reported to be encouraging. The device was later produced under the name “Walkaide” and made commercial by Neuromotion (Edmonton, Canada) (Stein 1998). Dai refers to an alternative approach used by Bowker and Heath for the control of peroneal stimulation using a magneto transducer to monitor the angular velocity of the knee (Bowker *et al.* 1995). The reliability of the algorithm and approach is not sufficient as step initiation can be falsely identified when non-walking movements produce limb inclinations in the range of walking.

In a different approach by Sweeney and Lyons, 1999 the subject’s shank and thigh inclinations along with their first and second derivatives comprised the system inputs, and a technique called ‘subtractive clustering’ was used to identify the relationships between leg segment inclination values and the occurrence of gait events. Sensor inputs were used in a finite state approach to trigger transitions between the states according to a set of rules. Test results of the performance of the system with drop foot subjects were presented. The advantages of using finite state control in neural prostheses are that it is intuitive and powerful, overcomes problems related to fluctuations in individual sensor values, and provides a scope for fine control of movement subject to the constraints of FES as an actuating technique. The use of inductive learning for example in finite state control is capable of identifying relationships between gait sensor values and gait state

transitions that might not be apparent to the human expert. This and other similar approaches are often limited by their cumbersome nature due to the use of multiple external sensors.

Mourselas and Granat reported on the use of a miniature stimulator that incorporated a fuzzy logic controller in an embedded processor for the closed-loop control of the stimulator (Mourselas *et al.* 2000). A simple resistive goniometer and a FSR placed under the heel, measuring the ankle flexion angle and heel-ground contact, were used as the inputs to the fuzzy controller. The system was evaluated by 3 subjects within the laboratory and by 2 subjects outside the laboratory, and was found to perform better than the open-loop system after their comparison. The need for multiple sensors and at different locations is expected to reduce both the practicality and cosmetic aspects of the system.

Ng and Chizeck also tested fuzzy controllers for the classification of gait events in paraplegics (Ng *et al.* 1997). Joint angle goniometer measurements at the hip, knee, and ankle joints were used in combination with a fuzzy model identification method to detect 5 gait phases. The system suffered from a number of errors. Improving the method's practicality and accuracy were the subject of the study by Skelly and Chizeck, 2001. An instrumented shoe insole with 4 FSRs was used to replace the goniometers as the source signal for the controller. The real time detection of gait events was used to evaluate the quality of past gait cycles and modify the stimulation patterns for the next gait cycle to improve the quality of gait. Thus the event detection is not used to trigger the stimulation but as part of a cycle-to-cycle controller for the stimulation.

Machine learning was suggested even in earlier work as a method for the automatic detection of gait events and gait phase classification. In an earlier study, Kirkwood *et al.*, 1989 described an automatic method for the classification of different gait phases using the artificial intelligence approach of inductive learning. The technique presented also allowed for the quantitative assessment of the importance of different sensors, as opposed to the intuitive assessment by the researcher. Combined measurements from goniometers and instrumented shoe insoles were used as inputs to the inductive learning-based controller. The detection accuracy of the system was between 70% and 97%. In addition

to the relatively low detection accuracy, this approach suffers from the same practicality limitations of the previous two approaches.

Tong and Granat presented a study that evaluated the reliability of artificial intelligence systems in FES controllers. The two ISCI patients recruited for this study used AFO's and crutches to assist their walking. FES applied to the peroneal nerve was used to elicit the flexion withdrawal reflex and the timing was controlled by a hand switch placed on the crutch. Ten force sensors placed under the foot (FSR's) and on the crutch tip (strain gauge based) and 22 virtual artificial sensors including goniometers, accelerometers, gyroscopes, and inclinometers (signals obtained from 3D motion analysis recordings and body models) were used in order to obtain the inputs to the neural network using various sets of sensors each time. Different sensor combinations were used including one-sensor, two-sensor, and three-sensor sets to provide the feedback information to the controller. The desired output was the hand switch. The systems using 3-sensor sets were still reliable after 6 months with an average accuracy of about 91%. The authors concluded that 2 or 3 sensors were sufficient to generate a reliable FES controller for ISCI patients using neural networks. The authors reported that the performance of the neural network control system declined significantly after few months if using only one sensor as an input. This is expected as the gait pattern of the subject is altered slightly. The reliability was improved when using two or three sensors (Tong *et al.* 1999). However, in this current work, we opted for the use of one sensor for various reasons including practicality, ease of use, and cost. The approach taken in this work is not expected to suffer from the same declining performance issues due to the non-dependence of the algorithms on a neural network set of rules. The algorithms developed in this study utilised the input from one sensor and the algorithm rules were designed to accommodate moderate changes in the gait pattern without significant decline in the accuracy of the system.

In a series of papers, Pappas *et al.* described a novel gait phase detection system and reported on its performance in the detection of gait phases (Pappas *et al.* 2001). The system relies on 3 FSR-based foot switches, and a gyroscopic sensor used to measure the forces exerted by the foot and the foot's angular velocity. The foot switches were placed under the heel, first and fourth metatarsal heads and attached to a 3 mm insole. The gyroscope was attached to the posterior aspect (heel) of the shoe with its sensing axis oriented perpendicular to the sagittal plane to measure the angular rotation of the foot in

that plane. The sensor divided the gait cycle into 4 phases stance, heel-off, swing, and heel-strike, which formed 4 distinct states. A set of seven different transitions between these states were allowed and governed by a set of rules. An experimental study was undertaken to evaluate the sensor system as tested by ten healthy subjects and 6 adults with various gait deviations. The study was split into 4 parts: part 1 the sensor was evaluated using a reference gait phase signal from a Vicon motion analysis system; In part 2 the performance of the system was tested on a variety of walking tasks such as walking on level ground, walking on slopes, walking on irregular surfaces, and climbing stairs; Part 3 tested the sensor and its ability in avoiding false detections in a variety of non-walking tasks such as standing up and sitting down from a chair, bending down while standing, turning while standing up by foot sliding; In part 4 the system was tested over a range of walking speeds between 0.5 to 13 km/h. The sensor successfully detected the gait phases for both groups of subjects when walking on level ground, irregular surfaces and slopes in 99 % of the cases. The sensor was reported to correlate well with the reference signal in all trials, except for a systematic delay ranging between 35 ms to 70 ms in the detection of the 4 phases. This was accounted for as a consequence of the 2 systems using different aspects of the events for the detection, such as weight acceptance as opposed to initial contact for the detection of heel strike. The sensor system was integrated into a shoe insole as a stand-alone system. Despite the high accuracy of this sensor system, a foot drop stimulator using this sensor will be dependent upon multiple sensors, which are used in a shoe insole. The need for wires and different shoe insole sizes will affect the cosmetic aspects and practical use of the system, in addition to the cost of the sensor system. Barefoot use of the stimulator is also an issue.

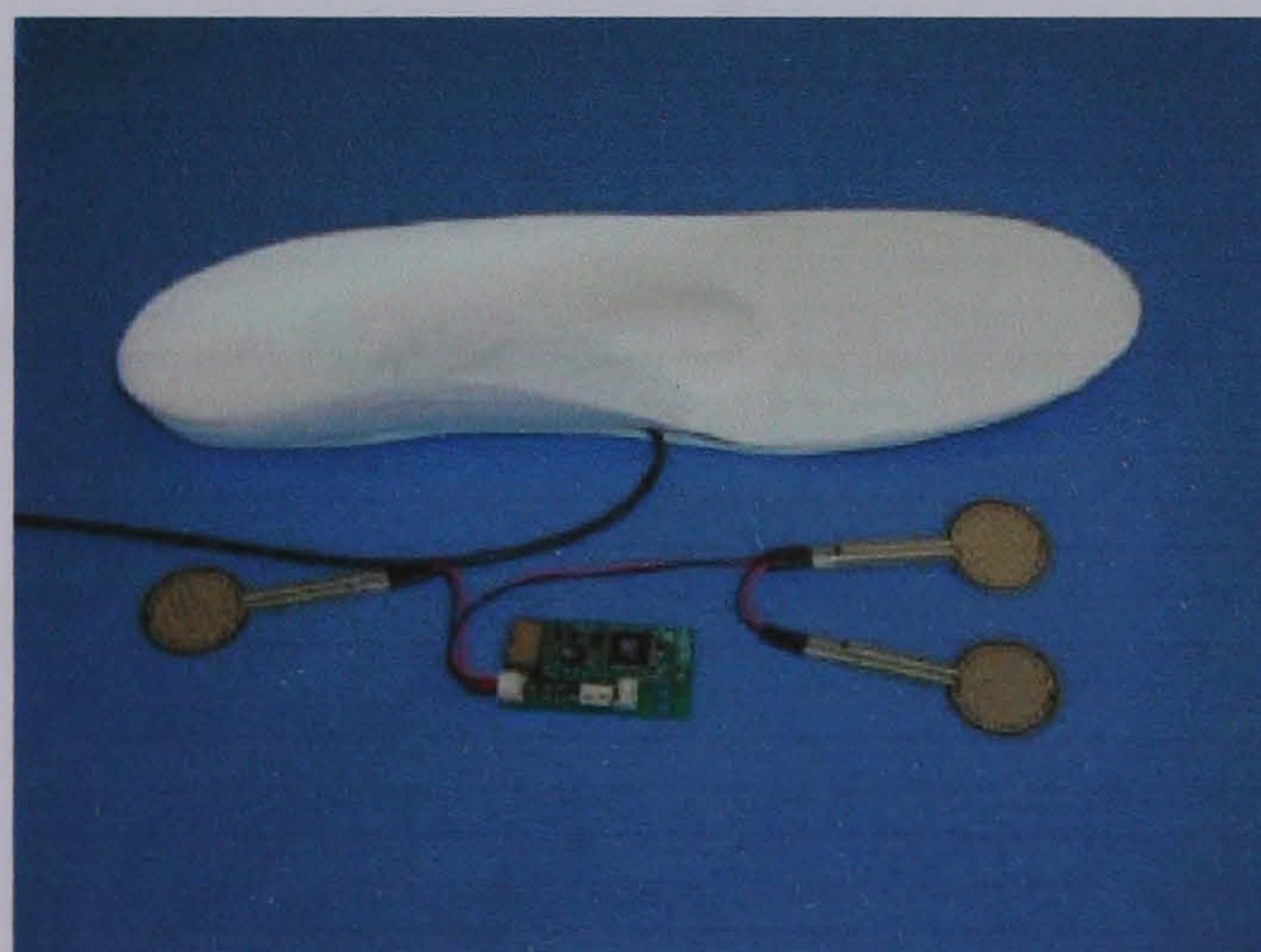


Figure 3-5: The gait phase detection sensor designed by Pappas *et al.* and made into a stand-alone system (Pappas *et al.* 2001).

As an alternative to the use of artificial sensors to obtain feedback signals, researchers have investigated the use of signals from the natural body sensors, for example ENG.

The latest paper by a group of researchers exploring this approach, reported on a real time implementation of a FES system for foot drop correction, with the timing of stimulation derived from ENG recordings of the sural nerve, a peripheral sensory nerve (Haugland *et al.* 1995; Kostov *et al.* 1995; Kostov *et al.* 1999; Hansen *et al.* 2000; Hansen *et al.* 2002; Hansen *et al.* 2003). An Adaptive Logic Network (ALN) was used to generate the timings of stimulation from its ENG input. One subject suffering from foot drop was implanted with a stimulator and 2 cuff electrodes on the sural nerve (for recording ENG) and on the peroneal nerve. The sural nerve contains mainly cutaneous sensory nerve fibres originating from the lateral side of the heel, foot sole, and the fifth digit, and hence the ENG recorded represents the mechanical activity on the foot sole. The ENG signal was amplified and wirelessly transmitted to signal conditioning hardware carried by the subject in a backpack. The responses of 2 FSRs placed under the heel, and fifth metatarsal were added followed by a hysteresis threshold and provided the target signal to be used in the training of the ALN. Data was transmitted using a cable to a stationary computer in the lab for processing. Adaptive restrictive rules were applied to the output of the ALN in order to optimise its performance (Kostov *et al.* 1999). The subject performed a combination of walking on level ground and up and down a 5-step staircase. The tasks were repeated each time with the first data set used for training the ALN and the second test used to test the detection system. This was repeated on multiple occasions on a period covering 392 days. The system was able to detect all the events of heel strike and foot lift-off in plain walking, but with some errors, both missing events and false detections occurring while walking over stairs and in transitions between walking and standing. The tests showed that the training of the ALN should be done with data from tasks that will be performed by the subject in his normal daily activities. For this system to be practical however, the ALN should have a successful detection after being trained once without the need for multiple training.

Hansen *et al.*, 2003 recently reported on the feasibility of using the peroneal nerve recordings for deriving stimulation timing in a foot drop correction system. ENG recordings from cuff electrodes placed on the peroneal nerve were used in two subjects

for the detection of stimulation timing and examined for the presence of proprioceptive information. In a similar way to the previously described study, ALNs were trained and used to predict the timing. FSRs were also placed under the heel and lateral metatarsal to generate the target signal for both training and performance comparison purposes. Ankle angular data were also recorded using a goniometer for peroneal ENG proprioceptive content examination. The detection of stimulation timing from the ENG was dependent on the SNR, with an overall performance of 92.5% for 1 subject and 73.4% for the other. Proprioceptive information in the peroneal ENG was very weak, with very poor correlation with the ankle angular data. A switching circuit was described which would allow the use of the same electrode for both stimulation and recording. This study showed the possibility of extracting stimulation timing from recorded peroneal ENG. It also demonstrated in a separate part the possibility of using the same electrode for stimulation and recording.

In a different study, Strange and Hoffer demonstrated the possibility of using ENG recordings from the median, ulnar and/or radial nerves to detect the paw contact and lift-off in 7 cats. Threshold detection was used to extract features and bursts in neural activity that were correlated to contact and lift-off events. The study suggested that the ENG signals could be used as feedback and timing control in FES state controllers.

The use of the electromyogram (EMG) for the control of FES systems is another possibility and is an approach of interest to researchers. Vodovnik *et al.* suggested this approach as early as the year 1965, and has since been applied in both lower and upper limb control of FES systems (Kershaw *et al.* 1993; Saxena *et al.* 1995; Frigo *et al.* 2000; Popovic *et al.* 2001). The EMG can be recorded from muscles that the subject has some residual or full voluntary control over. The EMG signal, after the appropriate processing, can then be used as an input for a comparator and used as a trigger by applying a single threshold. An alternative is to use multiple thresholds and use the EMG to modulate the stimulus output signals. A common challenge faced by anyone using this approach for FES control is the presence of a stimulation artefact when recording the EMG. The use of blanking circuitry and appropriate filtering can help eliminate the stimulation artefact and associated noise. In a paper by Jones *et al.* (2002) EMG triggering of a programmable stimulator for foot drop correction system is briefly described. Unfortunately, the paper

does not provide enough details on the approach used or the reliability and use of the actual device with EMG triggering.

The use of EEG in FES control is another attractive approach that was investigated by several researchers (Lauer *et al.* 1999; Juul *et al.* 2000; Wolpaw *et al.* 2000). Lauer *et al.* investigated the feasibility of using the EEG signals as a brain computer interface to control a FES system for hand grasp (Figure 3-6). Two able-bodied subjects and one neuroprosthesis user were able to move a cursor to targets on a computer screen with more than 90% accuracy rate after 6 months of training, through training to control the amplitude of the beta rhythm. The neuroprosthesis user was able to control his prosthesis and manipulate several objects using the EEG signal. Two main issues related to the quality and usefulness of the EEG signal face this approach. These are the effect of cortical plasticity on the signals as a result of changes in the somatomotor area representations. Stimulus artefact is also an issue as the stimulation of the forearm affects the EEG signal recorded by scalp electrodes.

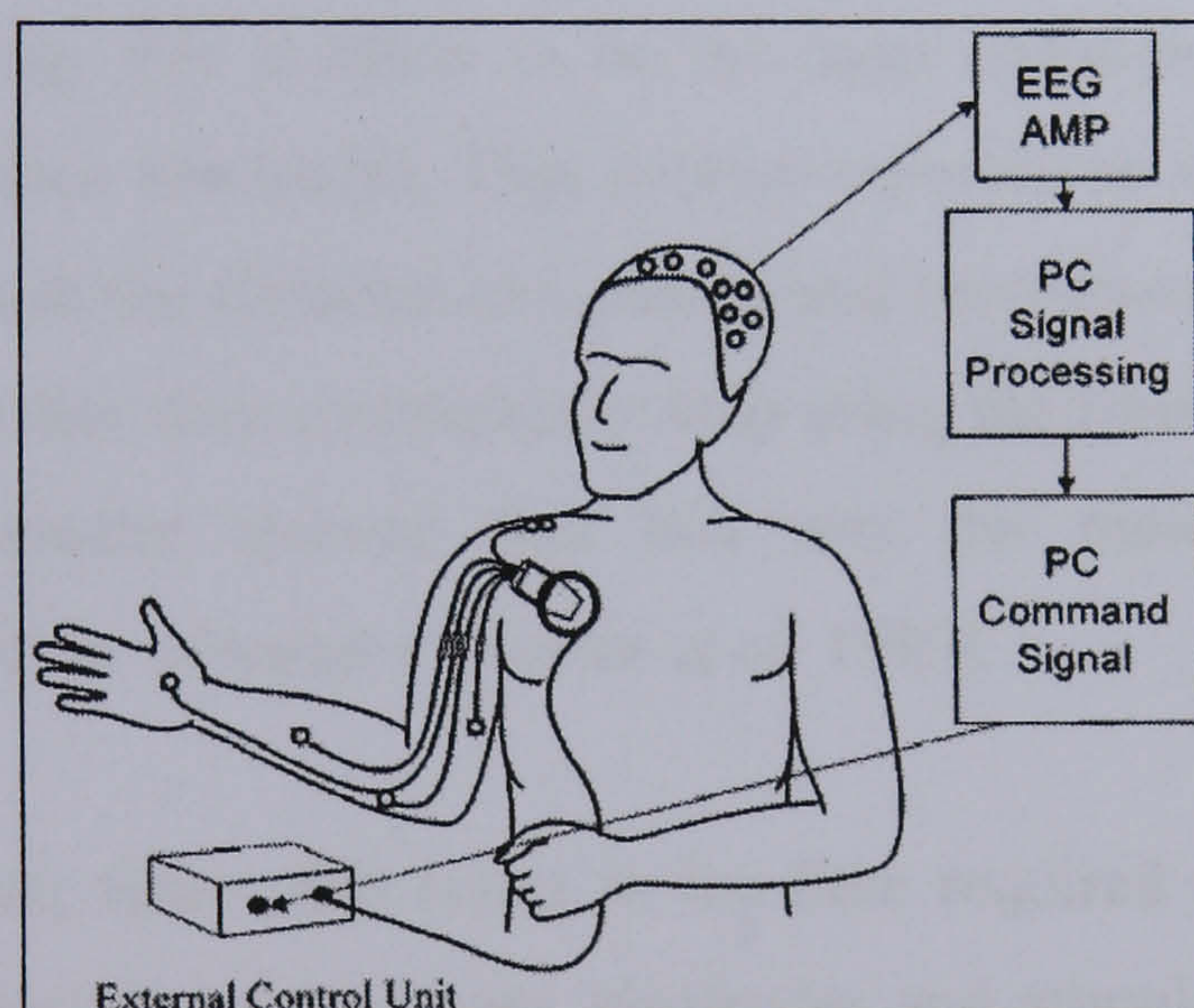


Figure 3-6: Schematic of EEG-based controller for a hand grasp neuroprosthesis (Lauer *et al.* 2000).

In the study by Juul *et al.*, 2000 it was showed that the rate of torque development during the preparation of foot movement could be retrieved from movement related potentials recorded from the brain motor cortex. Such information could be useful in the design of feed-forward controllers for FES walking aids. The author speculated that the availability of information on certain properties of the movement before it is activated would make it possible to rapidly adapt the stimulation to changing environments.

3.4 Issues and potentials

This section highlights some of the issues with the existing technologies and attempts at identifying some useful trends and needs for the future.

3.4.1 Why do patients reject the stimulator?

Many studies related to FES and foot drop correction refer to a variety of causes behind the acceptance and rejection of stimulators by the patient. This section will highlight the ones most commonly referred to, which are:

- **Discomfort due to sensation:** this is an issue with surface stimulation due to the presence of sensory nerve endings beneath the skin. In the first paper by Liberson, 1 out of the 7 subjects treated could not use the stimulator due to discomfort. This sensation was also reported by long term users of the ODFS as one of the causes for rejection (Taylor et al. 1999). Takebe reported that 4 out of the 6 subjects in his study could not use the stimulator as a result of the sensation being too strong.
- **Electrode positioning:** this is likely to be the most common reason for rejecting a stimulator with surface electrodes. This is often reported as a difficulty in setting up the stimulator by both the clinician and patient and sometimes becomes a major issue for the patient such that they consequently stop using the stimulator. Responses to the IMPULSE questionnaire showed that this was the most common reason for discontinuing use of the stimulator (Taylor *et al.* 1999).
- **Donning and doffing times:** this refers to the time required to set up the stimulator with the wires connecting the sensors, electrodes and stimulator unit. This becomes more of an issue with multichannel stimulation and can be prolonged as a result of the previous problem.
- **Skin problems:** allergy or irritation can stop the patient from benefiting from a stimulator that uses surface electrodes. However, this problem can be minimised with proper care of the electrodes and the skin and sound education to the patient on the use of the electrodes and system.

- Problems with foot switches: breakage or damage to the commonly used foot switches and the wires and connectors used are often reported as a reason for rejecting the stimulator. This was found to be the second most common problem in the IMPULSE questionnaire (Taylor *et al.* 1999).
- Problems with equipment: some patients report problems as a result of the equipment being too much bother to use, too difficult to use or unreliable (Taylor *et al.* 1999).
- Others: Liberson estimates that only 10% of hemiplegics might be able to use the stimulator outside hospital due to psychological factors. Takebe reported that one subject faced problems when encountering stairs and hence stopped the use of the stimulator. In the study by Taylor *et al.* (1999) on patients' perceptions of the ODFS, two further reasons for discontinuing use of the stimulator were that the system was being cosmetically unacceptable to the user, or that walking was not improved by the system.

3.4.2 Solutions

Researchers have attempted to minimise the effects of the issues discussed in the previous section. Discomfort can be minimised by the appropriate setting of the stimulus intensity and pulse duration. Liberson suggested asynchronous stimulation of different parts of the muscle, denervation of skin under electrode, and secondary interruption of tetanising current as possible solutions.

Implanting the electrodes can minimise or eliminate the sensation problem in addition to avoiding any skin reactions. Implantation will further reduce the time needed for donning and doffing the system and the time and effort required to find the right positions for the electrodes. The use of steerable electrodes is another approach to minimise on the electrode positioning issue with surface stimulators. By using a symmetrical biphasic stimulation waveform, hypoallergenic electrodes, improved skin and electrode care, and better patient education, the problem of skin irritation and allergy can be significantly reduced. With these solutions, however, one is left with the issues related to the sensor used for the stimulator, which are discussed in the following section.

3.4.3 Issues with sensor technology

After reviewing the literature on FES sensors and systems, a set of issues relevant to the existing technology can be identified. Those related to the use of the foot switch will be summarised first, as this has been the sensor of choice in many foot drop correction systems. The use of foot switches and wires for their connection was reported as a cause of mechanical failure. It was also reported as one of the common reasons for patients to stop using their stimulator. The potential of foot switches for further development (size, handling, implantability) is limited. They also limit the subject's ability to walk barefoot and may respond differently over different terrains and when wearing different types of foot wear. The continuous substantial loading and forces applied during walking limits their lifetime to a relatively short one (few months in a many cases). Another issue is the limited usefulness of the foot switch when negotiating stairs, as the heel might not come in contact with the floor while ascending. The stimulation is applied generally when the load is removed from the foot switch irrelevant of the context, so stimulation may occur as a result of leg sliding and weight shifting. The switch is generally placed under the heel and the stimulation started after the heel comes off the ground with a slight delay or ramping up. This delay or ramp time is fixed which is not optimal for changing walking speed, where a more dynamic delay would be more suitable. The same applies for the delay or ramp down used before terminating the stimulation at heel contact. Ankle plantar flexion tone or ankle plantar flexion contractures in some patients may require the switch to be moved to a position under the metatarsal head, which may make the timing even less optimal. Contractures can also cause loading responses on the foot switches during the swing phase. In addition foot switches do not provide any information about the leg or foot during the swing phase of gait.

The other commonly used trigger source is the hand switch or push button. The most obvious limitation of this approach is that it requires the subject's uninterrupted and continuous attention and imposes a conscious burden. An additional constraint is that with the push-button the subject can only indicate a limited number of gait events. This fact diminishes the practicality of using such a system long term.

For these reasons researchers have been actively investigating the use of alternative and better suited sensors or the addition of multiple sensors to improve the functioning of the

system. However, those attempts are yet to result in a system that is both reliable and easy to use with wide clinical application.

In addition, the review provides some insight into understanding what could be a useful system for regular use in the correction of foot drop. It is hence believed that two approaches will be sufficient to cover the majority of foot drop population who can benefit from FES. These two approaches will require future work into evolving the available technology and current systems to:

- Fully implantable systems: Patients requiring permanent orthotic treatment can be considered for an implantable system: For example, 2 channels to control eversion/inversion in addition to dorsiflexion. Further work into the use of biosignals (natural sensors) to control stimulation, or the development of artificial implantable sensors will make such systems fully implantable.
- Totally self-contained external systems: Surface stimulators can be a more reversible and less risky intervention for patients who might not need the stimulator long term. The development of a totally self-contained device, which is simple to use, easy to don and doff, reliable, and cosmetically acceptable will solve almost all the issues and challenges facing the users of current systems as highlighted by the above review.

This chapter reviewed the application of FES for foot drop correction, and sensor technology used in these systems. The review resulted in highlighting a number of limitations in the current technology, in addition to defining future trends for development and further work in the field. This was achieved with two main objectives in mind. First, the practicality and ease of use of the system by both the patient and the therapist involved. Second, the reliability of the sensor system and hence of the accurate timing of stimulation and increased benefits to the subject.

The proposed sensor system, which is the subject of this current work, is a suggested means to addressing the needs for the above two approaches. This will allow for the implementation of a totally self-contained device with the surface stimulator, sensor, and electrodes part of one unit to be worn on the shank. As can be seen from section 1.5,

previous work at the University of Surrey has encouraged further investigations into a gyroscope based sensor system. In addition to meeting the criteria for the above two approaches and overcoming the issues discussed in section 3.4.3, the new sensor system has to reliably and accurately control the timing of stimulation. Reliability is defined as the ability of the sensor system to detect the same event in the cycle on repeated and successive trials. Accurate detection is defined as the sensor system's ability to detect the event time with respect to an accepted reference (gold standard).

The appropriate timing of the stimulation is a result of the correct identification of the relevant gait events and phases. In order to evaluate the performance of the new sensor system, a gold standard technique for gait event detection is needed. The process of developing such a method will be the subject of the next chapter.

Chapter 4: Development of a reference method for gait event detection

This chapter describes the work undertaken for the development of an automated reference method for gait event detection. This was considered necessary as it would allow an effective comparison to be made between the existing sensor and the new sensor approach. Any differences between the two sensors could then be judged in light of a third accurate reference system. It is also believed that a gold standard method would enable a better understanding of the foot switch and the events used for stimulation. The gold standard would shed light on the question of whether the stimulation timing as a result of the foot switch use is the same as the timings of gait events. Such knowledge would contribute to our understanding of the currently used foot drop stimulator.

The chapter starts by looking at the requirements for any method to be used as a reference method. Then, a brief review of the available methods for gait event detection is given. The focus is then made on the methods that were relevant to the experimental set-up used in this work. The case is made for the choice of kinematic-based methods as the most suitable approach for this application. A review of published work on gait event detection using kinematic data is then given. The existing techniques are shown to be either not relevant for this project or not sufficiently automated or objective. A new method is proposed and its application described. This is then evaluated in a pilot study and further evaluation done in a full study. The chapter ends with a discussion of the results and a conclusion on the usefulness of the new method.

4.1 Requirements and objectives: outline specification

The need and use of a reference method for gait event detection in our study are the main factors in defining the requirements for such a method. The main objective is the evaluation of the Gyro sensor system and comparing it to the foot switch when used for triggering a single channel foot drop stimulator. The performance of a foot drop stimulator is determined by the accuracy and reliability in detecting heel rise and contact, and hence the main requirement for a reference method is detecting these two events. The ability to detect additional events, for example foot flat or toe off, can be useful if an

additional stimulation channel is to be used, for example if a different muscle group needs to be stimulated at different times during the gait cycle. As a result it was decided that it will be useful for the new method to provide detection times for foot flat and toe off in addition to heel contact and heel rise.

Key additional requirements can be summarised as follows:

- The outcomes should be unaffected and independent of the person or rater performing the detection.
- The technique should be automated in order to minimise analysis time and cost. This is particularly important when large data sets are to be analysed.
- The time resolution of the technique should be high enough in order to detect event timings that enable an acceptable comparison of detection times given by the Gyro sensor system and foot switches. It was decided that a resolution of 25 ms or a higher resolution would be acceptable for the purpose of this study. This decision is mainly the result of the commonly used stimulation frequency of 40 Hz. Although no experimental studies were made in order to investigate the effect of slightly delaying or starting the stimulation earlier on the gait of the patient, it is believed that one or even two stimulation pulses (25 – 50 ms) difference should not have any significant effects.

4.2 Available methods for gait event detection

There are various methods available for the detection of gait events, and for the purposes of this report, a summary and brief description of some of the commonly used methods will be given in this section.

At this stage, however, it might be useful to provide a definition for the gait events conventionally used in the literature. A clear definition of each of the four events is critical in avoiding any ambiguity when discussing these events. The following definitions are taken from a report prepared for the Gait and Clinical Movement Analysis Society (Ounpuu 1994).

Heel contact (HC): When initial contact (see below) is made with the heel. It is also referred to as heel strike.

Initial contact (IC): The point in the gait cycle when the foot initially makes contact with the ground; this represents the beginning of the stance phase. It is suggested that heel strike not be a term used in clinical gait analysis as in many circumstances initial contact is not made with the heel.

Toe-off (TO): When terminal contact (see below) is made with the toe.

Terminal contact: The point in the gait cycle when the foot leaves the ground: this represents the end of the stance phase or beginning of the swing phase. Also referred to as foot off. Toe-off should not be used in situations where the toe is not the last part of the foot to leave the ground.

Note: For those cases of pathology where the foot never leaves the ground (foot drag), the termination of stance and the onset of swing may be somewhat arbitrary. The termination of stance and onset of swing is defined as the point when all portions of the foot have achieved motion relative to the floor. Likewise, the termination of swing and the onset of stance may be defined as the point when the foot ends motion relative to the floor. This choice can be justified, as the function of the foot during swing is not support but forward progression.

Foot flat (FF): The point in time in the stance phase when the foot is plantar grade.

Heel off (HO): The point in the stance phase when the heel leaves the ground.

Although toe contact (TC) is not included as one of the terms in the report by Ounpuu, it can be thought of as the time when foot flat occurs. A proposed description for TC is as follows: the point in time when the forefoot initially makes contact with the ground. The reported descriptions of these events by Whittle (1996) agree with the above, with the exception of heel off, also called heel rise, which is more specifically defined as “the time at which the heel begins to lift from the walking surface”. It is clear from the above definitions that some confusion might still arise in certain cases, in particular with pathological gait. The confusion can be yet greater with events of a relatively prolonged nature such as heel off. Nevertheless, the above definitions are important for later

discussions. The next section will describe some of the available methods for detecting the timing of gait events, also referred to as the temporal parameters of gait.

4.2.1 Introduction to gait event detection methods

There are several methods that can measure the timing of gait events alone or in addition to other spatial parameters of gait. The following is a list of these techniques:

- Electrically conducting walkways
- Electrical switches placed under or in the shoe
- Pressure sensitive switches placed under the foot
- Pressure sensitive walkways
- Instrumented shoe insoles
- Force platform data
- Marker or video data (used in an automated way or through visual inspection by a rater)

In addition to the above-mentioned methods, temporal parameters are sometimes inferred from the analysis of motion signals recorded by a single or combination of transducers. Accelerometers, gyroscopes, tilt sensors are a few examples of such sensors, and are used as was discussed in the previous chapter (section 3.3). With respect to such approaches, however, there is no standard method for using any of these sensors for gait event detection, and hence their use as a standard gait event detection method was not considered appropriate. This decision was further emphasized by the fact that the standard detection method is to be used for the evaluation of our Gyro sensor system – one example of those sensors.

4.2.2 Overview of gait event detection methods

A variety of approaches can be used to extract temporal parameters of gait by making the subject walk over instrumented surfaces or walkways. Signals from conducting wires or metal strips embedded into a walkway or placed under the foot or shoe can be recorded by a data collection system. Varying the design of the walkway or the placement and number of conductors at the foot will alter how much information one can obtain. Other options that have been explored are instrumented walkways that have embedded pressure-sensing elements. In addition to the temporal information, most of these walkways provide some

information on the magnitude of forces and pressures applied by the foot. Some of these walkways are available commercially such as the MatScan[®] system from Tekscan.

A more common approach is the use of pressure or force sensors or electrical switches placed under the foot or embedded in a shoe insole. The “closing” or “opening” of such switches can be used to infer foot or shoe contact with the floor. Increasing the number of sensors under the foot will improve the resolution of the system in determining the foot contact pattern. Calibrating these sensors (*e.g.*, force sensitive resistors) can provide some measure of the force or pressure values under the foot. There are commercially available insole systems used in foot pressure measurement that accommodate several hundred individual sensing elements per foot with reasonable sampling rates. Some examples of these are F-Scan[®] from Tekscan, Footscan[®] insole from RSScan, and Pedar[®] system from Novel.

Force plate systems can be used to extract initial and terminal foot floor contact by looking at the ground reaction force values. These are often used for this purpose within the conventional gait analysis set-up. Time resolution and accuracy are normally high and as a result these are often considered the gold standard in determining IC and TC. One major limitation is the need for more than one plate in order to obtain timings for multiple successive events for more than one stride, taking into account the cost of these systems. In addition, the data cannot be used to detect heel off or toe contact in conventional “normal” gait.

An alternative approach to all the techniques mentioned so far is the use of a foot imaging system where the motion of the foot can be utilised to infer the temporal parameters. Using video image and a reasonably trained rater, is one approach that has been used in order to detect the timings of the different gait events. Time resolution is often an issue with this technique, not to mention the time consumption when large data sets are to be analysed. An alternative to this is the use of captured 3D data of markers placed on the foot in order to derive the temporal parameters. This approach is discussed in further detail in the following section.

4.3 Kinematic-based techniques

Following on from the above overview, special focus will be made on techniques that are based on kinematic data and used for gait event detection. The reasons behind this choice are given below. The approach used in this set of methods utilises kinematic data only as opposed to some techniques that use a combination of kinematic data and other data, for example ground reaction forces (Hansen *et al.* 2002). The need for additional measurement systems such as force plates for gait event detection is seen as an additional requirement on the patient which may alter their gait. This is in addition to the limitations that were discussed earlier, and are encountered when using such measurement systems for gait event detection.

4.3.1 Reasons for this choice

There were several reasons behind the decision to choose a kinematic-based technique for gait event detection. These can be summarised in the following:

- Resolution and accuracy: Marker detection systems tend to have a high sampling rate and accuracy. The systems available for use in the University of Surrey and in Queen Mary's Hospital sample at frequencies up to 240 Hz and 60 Hz respectively. (Qualisys ProReflex and MacReflex marker detection systems – Qualisys Medical AB, Gothenburg, Sweden). These sampling frequencies will provide a resolution of 4.2ms and 16.7 ms respectively.
- The encumbrance to the patient is minimal as the only addition to the patient is a set of markers, both lightweight and small (a sphere of mass approximately 1 gram and 15 mm radius) attached to the skin using double-sided adhesive tape.
- Marker data is a fairly representative description of what is happening at the foot during walking, and theoretically can be used to infer the gait event timings. This is conditional on the use of appropriate marker locations and a sufficient number of markers to closely represent the body segment and its joints.
- Gait events from more than one stride can be obtained as the subject walks through the measurement volume. Measurement volumes can have a length of a few metres.

- Encouraging results from literature: searching the literature revealed a set of papers that showed encouraging results when using kinematic data for gait event detection. These papers are reviewed in the following section. The data are readily available for use, as these systems are used in the assessment of patients' gait and are normally part of a gait lab set-up. Hence, there will be no additional sensors or costs for collection. This was certainly the case within our research centre, and purchasing a different system for gait event detection (such as a foot pressure measurement system) would not have been an economically viable decision.

4.3.2 Literature

The literature was reviewed for existing methods in order to explore the possibility of using a readily available method for the purposes of this study. This and the following section are a review and discussion of six key papers that describe and validate methods, utilising kinematic data for the purpose of detecting the timings of gait events or phases.

Stanhope *et al.* published a paper entitled “Kinematic-based technique for event time determination during gait” in 1990. The method is based on a subject-defined kinematic model. The determination of a gait event time is dependent on the identification of relative kinematic patterns similar in shape to the kinematic-model for a previous occurrence of the same event. The first occurrence is determined by a different sensing device, in this case a force platform. The positions of two retroreflective markers placed bilaterally at the lateral malleolus were sampled at 50 Hz in the lateral (X), progression (Y), and vertical (Z) direction. 2 subjects (1 healthy and 1 pathological walker) performed 3 trials each for which the detected times of initial foot contact (IFC) and terminal foot contact (TFC) were determined. A set of predictors was used to evaluate the model detection capability which included XYZ, YZ, X, Y, and Z. The model order (K) was also varied between 1 and 9 taking each of these values 1,3,5,7, and 9. The detected times were compared against those given by the force plates by calculating the difference between the two. None of the differences were above 20 ms when using the XYZ predictor with any value of K. This was also the case when using the YZ (sagittal) predictor except for one event when K was set to 1.

Wall *et al.*, 1996 reported on the “accuracy and reliability of temporal gait measurement” when determined using a field counting technique (visual inspection) of video recordings (50 Hz) of the foot in the sagittal plane. The times of make and break of foot to floor contact were determined by multiple raters (4 in this case) and compared to times determined using foot switches attached to the heel and big toe, and force plates mounted centrally along a 7m walkway. 5 subjects performed 3 trials for each of the 3 conditions, barefoot, wearing training shoes, and outdoor shoes. From the contact times, left total support, right total support and double support phase times were calculated and compared across the three methods. 95% of the calculated times from the observations made by the raters were within 60 ms of actual values determined by the force plates. This difference was 80 ms in some of the cases, in particular the double support phase time when wearing shoes. Intraclass correlation analysis was used to investigate the inter-rater reliability. These values showed high correlation for the calculated durations, except for some inconsistencies between raters in determining the double support times.

Speed distribution analysis was used in a study by Peham *et al.*, 1999 in order to determine stance phase durations. Kinematic data from one marker placed at the distal limb (captured at 240 Hz) were used to plot a histogram of the horizontal speed over 1 motion cycle. The most frequent speed in the histogram was used as the threshold to determine the start and end of the stance phase. The resulting durations were compared to those measured by a force plate, and the mean difference was 10.8 ms. Although this technique was designed for application in equine studies and evaluated using 7 horses, it was believed that the same approach would be feasible in the case of human gait.

In a study by Mickelborough *et al.*, 2000 eleven multiple raters were given a set of rules to determine the following four gait events: swing heel off (heel off from a gait initiation step), swing toe-off (toe off from a gait initiation step), swing heel contact (heel contact from a step during gait), and stance toe off (toe off from a step during gait). The raters used vertical displacement and velocity plots of toe and heel markers (captured at 50 Hz) in order to discern the gait events from specific features of the curves. 12 subjects performed a series of 10 trials for each one of three different starting set-ups. Each set-up had a different foot and plate relative position so that heel off could be detected from ground reaction force measurements. The resultant times were compared against those obtained from simultaneously collected ground reaction force data. For all four events,

between 78 and 95% of all differences were within 20 ms and the intraclass correlation coefficients for inter-rater agreement produced high coefficients (0.993 to 0.999), which is the result of the precision of the definitions used by the raters to determine the events.

Hreljac *et al.*, 2000 presented the results from a study that used algorithms to determine heel strike and toe off times from kinematic data. 2 healthy subjects performed a set of 6 trials at a variety of walking speeds when the motion of two markers (placed at the heel and 5th metatarsal) was captured at 60 Hz with simultaneous ground reaction force data. The algorithm determined the two events using local maxima in the heel vertical acceleration and toe horizontal acceleration. Linear interpolation was used to estimate the actual time (inter-sample time) when the maxima occurred using the zero crossing of jerk (derivative of acceleration). No significant differences were found between the algorithm and force plate timings. The average of absolute differences was 4.7 ms and 5.6 ms for heel strike and toe off respectively.

In a more recent study by Hansen *et al.*, 2002 another kinematic-based technique is described and assessed for the detection of heel contact and toe off. This approach, however, also depended on the availability of data on the centre of pressure simultaneously with ankle marker data. Multiple force plates were used to detect the position of the centre of pressure. For this reason, this method will not be described with any further details, as it is not strictly kinematic-based.

4.3.3 Limitations

This section presents some criticism of the above reported techniques, and includes a summary of limitations and constraints with the methods used, as follows:

- Lack of automation, and hence time consuming in particular when analysing large data sets.
- Subjectivity as a result of dependence on individual or multiple raters.
- The need for additional instrumentation for example ground reaction force data from force platforms.

- Increased encumbrance to the patient and interference with normal walking patterns due to controlling walking speed or step length.

In the case of the first study by Stanhope *et al.*, there is a need to determine the occurrence of the event once using force plate data. This is possible for initial and terminal contact but not without difficulty or interference with the subjects' gait when foot flat or heel rise are considered. In theory, another method can be used to determine the occurrence of the event in order to set the kinematic model. For example, visual inspection can be used which will eliminate the need for force plate data; however, this will increase the subjectivity and dependence on individual raters. In addition, this method can be also prone to errors resulting from the inability of the subject to perform cyclical movement.

The approach used by Peham *et al.* was evaluated in detecting the stance phase of horses. The approach can be expected to be feasible in the case of human gait, but needs some testing in order to prove this feasibility. When applying this technique some issues remain to be clarified that are mainly related to the choice of the width of the histogram classes which affects the sensitivity of the method. The noise in the signal is stated as a factor in the choice of the class width but not explicitly related to that choice. Another and perhaps less important issue is the exact value of the threshold used for the detection of the events. The choice of the upper or lower or median of the most frequent histogram class will have a minor, but nevertheless some effect on the detected times.

The approaches taken in the studies by Wall *et al.* and Mickelborough *et al.* both suffer from the main constraints of being tedious, slow, and time consuming. In addition, Mickelborough's study only considered the heel off event during gait initiation and not continuous gait. Further investigations are needed to assess the approach taken for the detection of heel off during continuous gait. In addition, the detection of toe contact was not assessed in the latter study.

The method adopted by Hreljac *et al.* appears to be accurate in estimating the times of heel contact and toe off in the evaluation carried out. This however was done with only 2 healthy subjects and might need further evaluation by a larger group and a mixture of both normal and pathological gait patterns. Differentiation (velocity), double differentiation (acceleration), and triple differentiation (jerk) of kinematic data are a common issue when

dealing with human movement data collected from marker detection systems. Filtering of data prior to multiple differentiations is essential in order to minimise the effects of noise. The detection algorithms in this study, by using acceleration local maxima and jerk zero crossing times, depended on smoothing the data prior to analysis which might have masked some of the features in the signal and hence affected the estimation of the event times. Moreover, the above approach was limited to the detection of heel contact and toe off, and did not address the detection of heel off and toe contact.

As all these methods lacked one or more of the requirements set out in the specification, so a new method was then proposed for the detection of the four gait events.

4.4 Proposed method

Following the literature review above, an additional set of requirements becomes apparent:

- The method should not depend on individual or multiple raters.
- The method should be automated.
- The subject encumbrance should be minimal or none, i.e. should not affect his/her gait.
- Restrictions must be also minimised, that is no control on the walking speed or step length.
- Utilises the 3D co-ordinates of foot markers only, as opposed to a combination of force and kinematic data.

4.4.1 From Visual Inspection to Automation

The available 3D co-ordinate data of foot markers, in particular heel and toe markers, has been shown to be useful for the detection of gait events such as heel contact and rise and foot flat and toe off. One possible way of achieving this is by visually inspecting the movement of these markers using a suitable software package to display the data and run through it frame by frame. A trained observer (or multiple observers) can then estimate the timings of the gait events. This technique is similar to that adopted by Wall *et al.* and was also used in earlier work at Surrey (Ghoussayni 2000). The two main issues with such an approach are time consumption and dependence on the judgements made by an individual or multiple raters. This dependence can be minimised firstly by having a clear

definition of these events. This is a pre-requisite for any observer to consistently estimate the gait event timings. The mind of the observer is after all applying some algorithms in order to judge the occurrence of these events. Secondly, in situations where a significant volume of data is to be analysed, the time consumption factor can be minimised by automation. Thus, an automated method that can consistently reproduce the criteria used by individuals in estimating the event times is a reasonable and elegant approach worth exploring.

4.4.2 Criteria selection

After defining the 4 gait events (heel contact, toe contact, heel off or heel rise, and toe off), the next step was to develop a set of criteria to be used for detecting each one of these events. Some of the studies reported earlier used one or more features of the measured or calculated motion signals in order to detect each event. A rater performing visual inspection (eyeballing) is also effectively applying a set of criteria to do the detection. Formulating the right set of criteria for each event becomes critical for the correct detection. One way of selecting each event's criteria is by using ground reaction force data for example. By looking at simultaneously collected data from a comparative method and kinematic data, it is possible to look for features in measured or calculated motion signals that correlate directly to the occurrence of the event as determined by the comparative method. These features can then be used in order to detect the event. Force plate data, foot switch recordings, and foot pressure measurements can be used as comparative methods. Another possibility for finding the criteria is by writing down the selection parameters used by a rater eyeballing the events. By doing this, intrinsic errors to the comparative detection method can be avoided.

During the period of foot floor contact the movement of a foot surface marker is expected to be minimal and only the result of minor skin or tissue movements (or shoes if shod) relative to the bones, or due to noise and errors by the measurement system. The start of movement of a marker indicates that the foot segment concerned is in the process of breaking foot to floor contact. The main aim hence becomes differentiating true movement from artefacts and noise. If faced by a situation like this, the rater eyeballing the marker motion can inspect the motion over a few frames in order to reach a decision. A continuous motion in the direction of progression or vertical direction after a particular frame means that the movement seen at that frame is not an artefact. On the other hand, if

a marker stops moving in the forward or upward direction after that frame, then it is likely that the observed movement is due to noise or minor foot movement and not the start of breaking a foot to floor contact.

The choice of the location of the foot markers obviously had to reflect the movement of the heel and the toe (Figure 4-1). The markers were placed on the posterior end of the lateral border of the calcaneus, and the fifth metatarsal head of the right foot.



Figure 4-1: Figure showing the marker placement used in this study

The choice of position had to minimise occlusion of the marker by other body parts, which will prevent it from being seen by the cameras. The metatarsal head, instead of the toe, was chosen because the detection of toe-off from the kinematic method was to be used to compare the Gyro sensor system to the foot switches. Usually the toe foot switch used for FES triggering is placed under the head of the first metatarsal head. Thus the event detected can be thought of as the start of the toe-off phase, when force transmission to the ground, through the metatarsal heads diminishes. An alternative name to toe-off for this event could be “start of forefoot progression”.

The above predictions about foot marker motion were used to set the criteria for the detection of each event. Heel and toe contact times are defined as the times when the respective marker “stops” moving in the vertical and progression directions. The initiation of the rise phases was defined as the first frame around the estimated event time after which the marker has a continuous motion in the vertical and progression directions.

In order to implement these statements as part of an automated algorithm, the following assumption was made. During the period when the heel (or toe) is in contact with the

ground, any observed marker movement is the result of minor skin or tissue movements or noise. The heel is considered stationary and thus its velocity should be zero. The result of measurement noise and minor movement artefacts at the foot create a baseline value for the velocity even when the foot part with the marker on is stationary. This measured marker velocity at zero foot movement, if known, can be used in conjunction with the marker instantaneous velocity to decide whether the foot part is in contact with the floor or not during cyclic walking movements.

4.4.3 Practical issues with implementation

The implementation of the visual inspection approach into an automated algorithm requires addressing some of the issues that became clear from the previous section. Firstly, there exists the issue of differentiating between noise and artefacts on one hand and real foot movement on the other. The change of position or movement is reflected in velocity values, which can be obtained by differentiating the position data. Differentiation of noisy signals is known to degrade the signal to noise ratio. This issue will be discussed in detail in the course of the coming chapter. The main frequency components of gait kinematic signals are band limited and of relatively low frequency, and hence low-pass filtering of data is one way to minimise the effect of wide band noise differentiation. The second issue was the feasibility of using the same criteria for multiple subjects, walking at different speeds, both shod and barefoot.

4.4.4 Development of method

The details of the filtering approach are dealt with in the next chapter. After low-pass filtering the co-ordinate data, derivatives were calculated using finite difference equations.

Equation 4-1

$$V_{x_i} = \frac{X_{i+1} - X_{i-1}}{\Delta t}$$

where

V_{x_i} = Velocity at i^{th} sample

X_{i+1} = Magnitude of signal X at (i+1) sample

X_{i-1} = Magnitude of signal X at (i-1) sample

Δt = Sampling time duration

As walking motion signals mainly take place in two directions, it was decided to use the co-ordinates in the progression and vertical directions only, *i.e.* the sagittal plane. The velocities in the progression and vertical directions were added (vector addition) to obtain the magnitude of the sagittal velocity. The second step was to obtain information on the amount of movement that takes place during the foot to floor contact period. After visually inspecting the data and deciding on the times of the make and break of contact of each foot part, the velocity of these markers during the contact period was calculated and averaged in both directions separately and combined.

Figure 4-2 shows the velocity of the heel marker calculated from both raw and filtered co-ordinates (4th-order, zero lag Butterworth filter with a 10 Hz cut-off frequency). The data is from a representative trial of a healthy subject walking shod at a self-selected normal speed. The figure shows the time period during which the foot starts descending and decelerating towards the floor. By visually inspecting the combined movement on the screen, the heel contact time was given at 2.23 s. The main observations from this plot are the following:

- The presence of sudden changes in the values of velocities calculated from raw position data.
- The effect of filtering the velocity data, in particular the effect seen in the calculated sagittal velocity of the marker (FVelHXZ).
- The presence of a residual amount of movement after contact with the ground. This is not very surprising as it can be interpreted as a result of noise differentiation, and skin/tissue and shoe movement relative to the floor and foot bones.

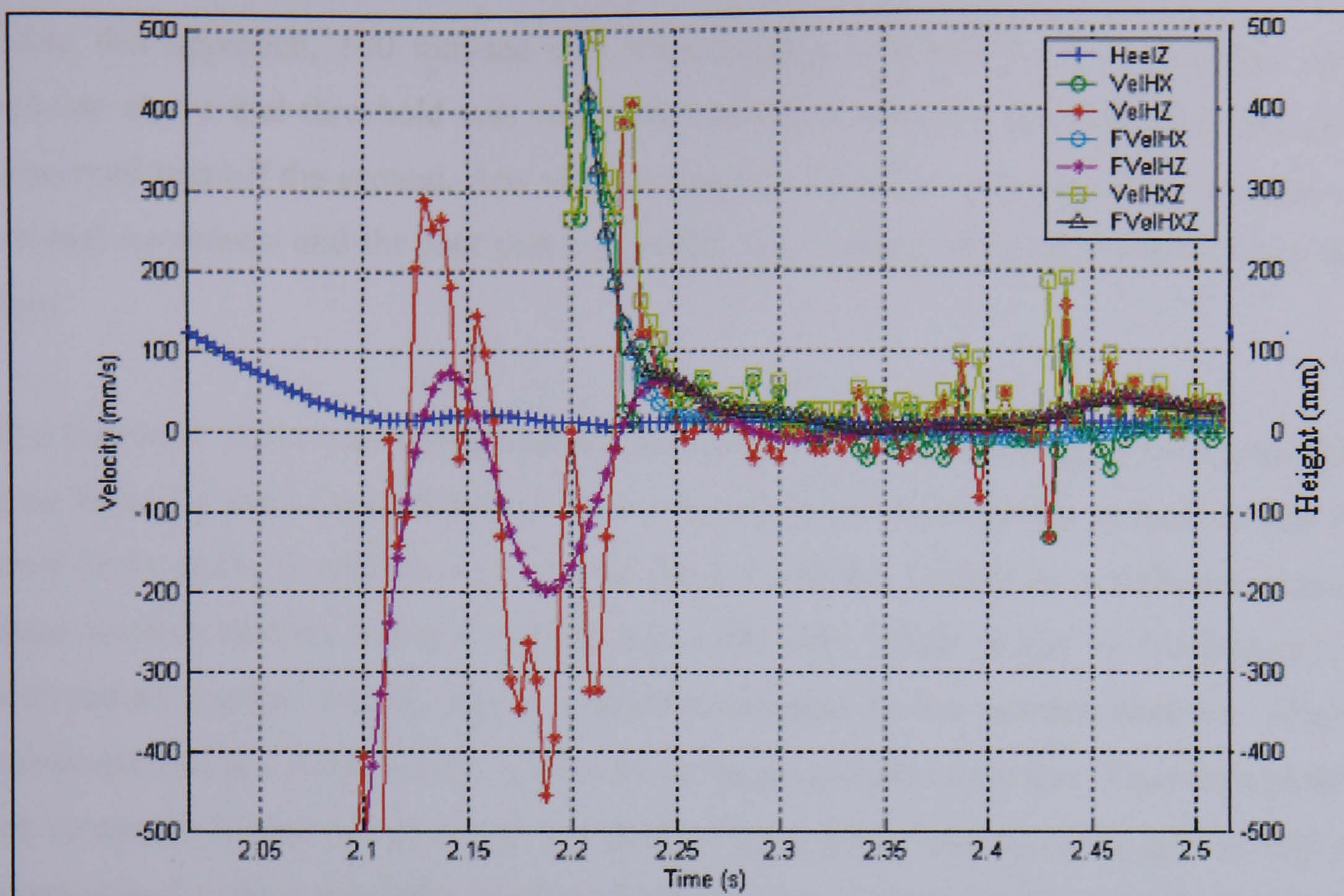


Figure 4-2: A plot of the heel marker velocities in both progression and vertical directions versus time. X =progression direction; Z=vertical direction; Vel=velocity; H=heel; F=filtered (Sampling rate 240 Hz)

The assumption that the heel (or toe) becomes stationary during floor contact, means that the velocity in the x (progression) and z (vertical) direction for that marker should be zero or minimal. The combination of these two velocities, the sagittal velocity should also be zero. Allowing for noise and minor movement, one can define the event by using an appropriately set threshold on the sagittal velocity. In order to calculate the value of these thresholds, the following method was used. Visually inspect data from a total of 4 trials, from 2 subjects (2 each), and determine the times of heel and toe contact and break of contact. Look at the averaged values of sagittal velocities for each marker during the foot part contact period and then choose a threshold value to exclude 95% of the observed values during that period (Upper limit of the 95% confidence interval).

Equation 4-2

$$\text{Threshold} = \text{Average} + 2 \times \delta$$

where δ = standard deviation

Using this approach, 100 mm/sec was selected as a threshold for both markers. Any velocity above that threshold was considered as real movement and hence the foot part concerned was off the ground. Any value below that threshold was considered as noise or residual movement and the foot part concerned was considered to be in contact with the floor.

This threshold value was appropriate for the detection of the four events. One issue that arose from the use of this threshold value was related to the detection of heel contact in some of the trials of subjects with a particular gait pattern. During the weight acceptance phase between heel contact and foot flat, also called the “initial rocker” or “heel pivot”, a heel surface marker usually shows a slight movement in the upward direction. Slight movement, but to a lesser extent, also exists in the progression direction. The result of this can be seen in Figure 4-3 in the second peak of the sagittal velocity of the heel at 6.88 s. Average heel marker velocities in the sagittal plane at and immediately after heel contact were in the range of 100 to 250 mm/s for representative walking trials. Oscillations in the marker are also seen in some other cases directly after heel contact. Assume the marker detection system identifies a 1 mm change in the position of the centroid of the marker in any of the 3 directions after 1 frame of data acquired at 100 Hz. This is equivalent to a velocity of 100 mm/s in each direction. On these grounds, the threshold for heel contact was adjusted to a value of 300 mm/s. (Tranberg evaluated the relative movement of skin-mounted markers on the foot using roentgen photogrammetry and found that markers mounted on the foot moved between 1.8 and 4.3 mm corresponding to the underlying bones (Tranberg *et al.* 1998). Thus the thresholds used to discern between noise or skin movement and real movement are not exaggerated).

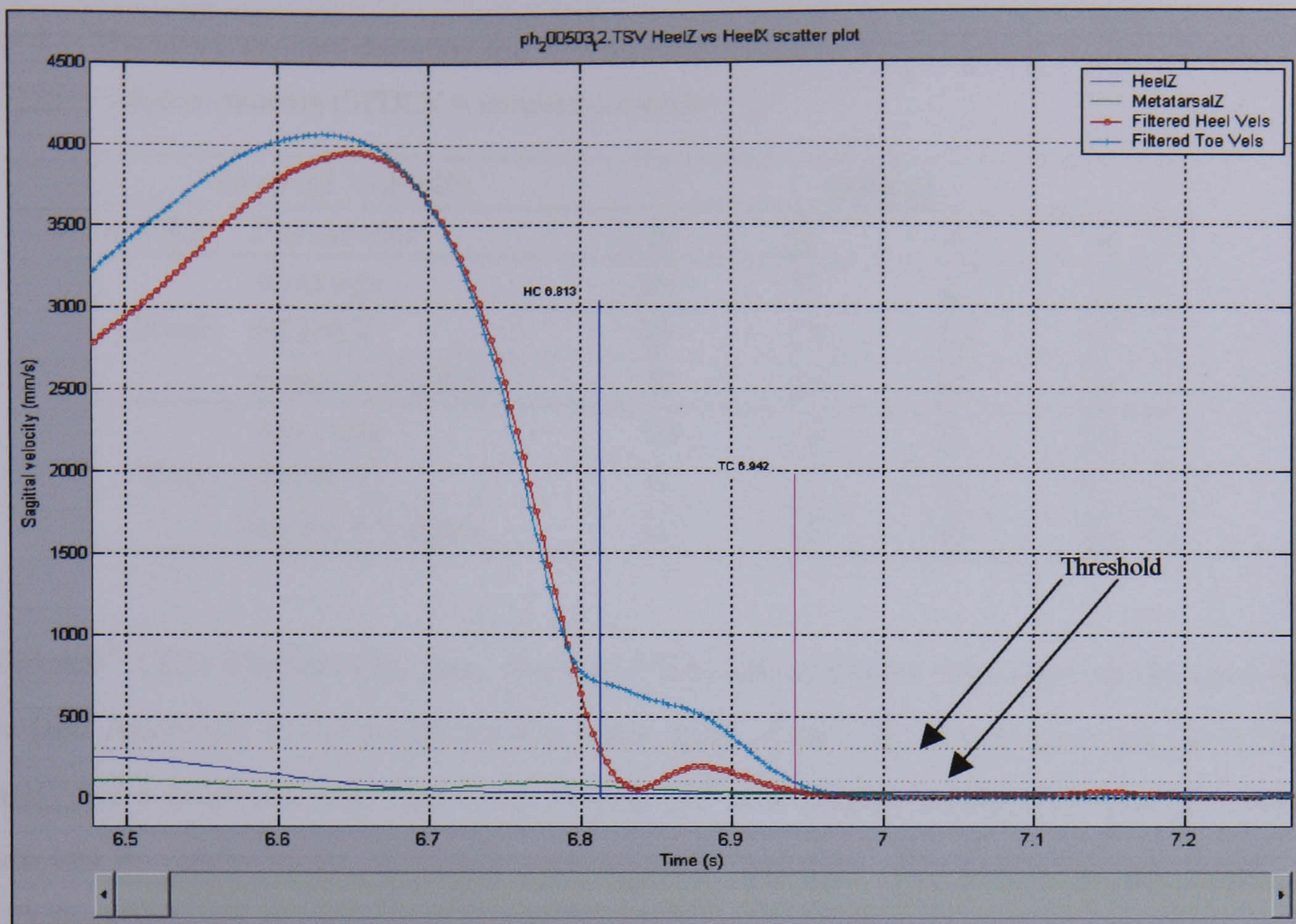


Figure 4-3: A plot of the heel and toe sagittal velocities during swing to stance period. Z = vertical coordinate; Vels = velocity; HC = heel contact, TC = toe contact. (healthy subject, self-selected normal walking speed)

One more issue that needed consideration at this stage was the effect of different factors on the choice of thresholds. The importance of this issue lies in its effect on deciding whether it is feasible to use the same thresholds for different subjects or different trials. Factors that are expected to affect the amount of residual movement during contact periods include type of footwear if any, walking speed, noise from the measurement system, marker positions, amount of skin and tissue movement. In order to assess this, position data was gathered from 4 subjects while standing. This was expected to enable us to predict sagittal velocity values of heel and toe markers when the foot is in contact with the floor. The results from this can be seen in Table 4-1. This allowed two assumptions to be made. First, the threshold values can be used for multiple subjects. This can be justified as the sum of the mean and 2 standard deviations values were within the threshold limit and comparable between subjects. Second, the threshold values selected are suitable for discerning between real movement and the lack of it.

Table 4-1: The mean, standard deviation and 95% confidence interval limit of marker sagittal velocities (in mm/s) for 4 subjects standing (STDEV = standard deviation)

Sagittal Velocity		subject			
marker	Parameter	1	2	3	4
Heel	Average	29	32	23	18
	STDEV	25	18	14	10
	mean + 2 stdev	79	68	52	39
Toe	Average	19	16	20	20
	STDEV	11	9	15	12
	mean + 2 stdev	42	35	49	44

MATLAB[®] (The Mathworks, Inc., Natick, USA) environment was used to develop the code (see Appendix A for code) for the processing of the 3D co-ordinate data (TSV file format) and a graphical user interface. MATLAB[®] was chosen mainly because of its ease of use and its powerful set of inbuilt mathematical functions. The graphical user interface (GUI) development environment in MATLAB[®] facilitates the creation and programming of user interfaces and setting their layout. The processing of the 3D marker data, acquired from the marker detection system in a TSV file format, takes place in a few stages and is controlled by user input through a series of push buttons and menu items:

- Stage 1 Data input: This is done by displaying a dialogue box that is used to retrieve the data file. The co-ordinate data is read together with the other information in the file, including the sampling frequency and marker names. The software looks for heel or toe marker names in the file and if found, they are displayed as the markers to be used for gait event detection. User input is requested if either heel or toe marker names are not found. The user can select different markers than the ones found if needed.
- Stage 2 Gait cycle choice: This is achieved by searching for the maxima in the heel z-co-ordinate (vertical). The heel z values are plotted together with the detected times of the peaks. A gait cycle is defined as the time between consecutive peaks. The start of the cycle is the time at which the first peak occurs, and the end is the frame before the next peak occurs. The user can select which cycle is to be analysed for gait event detection. The user can also ignore any of the peaks as false starts or ends of cycles. Foot contact is asserted when the sagittal velocity of the marker on that part of the foot

goes below the threshold for the first time. Break of contact is asserted the last time the velocity crosses the threshold during the cycle.

- Stage 3 Gait event detection: during this stage the code filters the data from each cycle and calculates the sagittal velocities for both the heel and toe markers. The thresholds are applied in order to detect the occurrence of each of the four gait events. Heel contact is assigned to the first frame when the heel sagittal velocity falls below the threshold. The same applies to toe contact. Heel rise is defined as the first frame when the velocity of the heel sagittal velocity goes above the threshold. The same applies for toe off. If multiple crossings of the threshold occur, the first crossing of the threshold is used for heel and toe contact detection. The last crossing is used for the detection of heel rise and toe off. The results are then displayed together with the sagittal velocity plots (Figure 4-4).

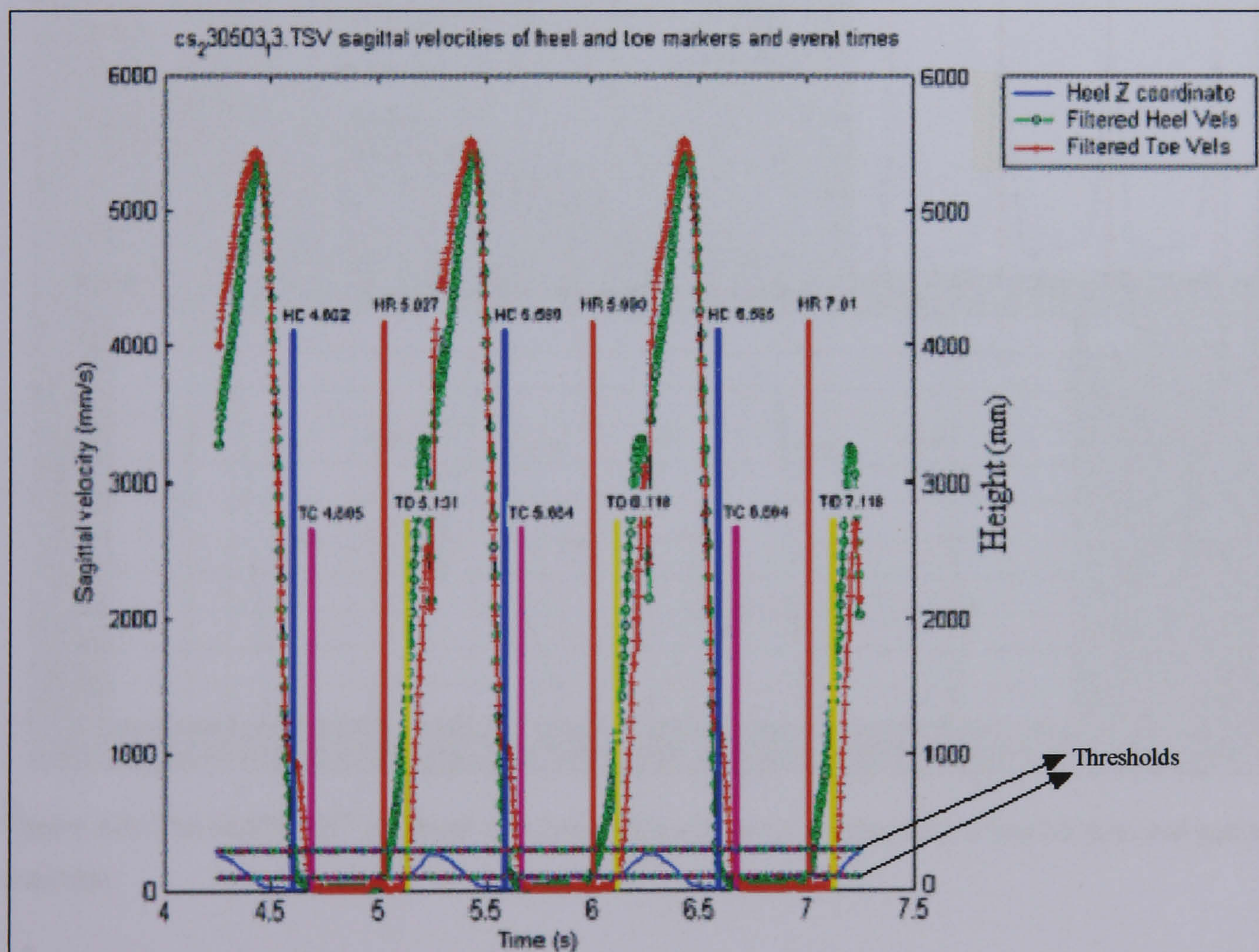


Figure 4-4: Plot of the sagittal velocities of the heel and toe markers and the times of detected events shown. HC=Heel contact; TC=Toe contact; HR=Heel rise; TO=Toe-off.

Additional functions are available and these include:

- Synchronisation option: if the data needs to be synchronised to a time scale used by another system used for simultaneous collection of data during that trial.
- Save data: the timing of the gait events, the walking speed (calculated from the speed of a sacral marker), the start and end times of each cycle (useful for normalisation) can be exported into a text file.
- Zoom option: this allows the user to look with greater detail on the data displayed using a separate figure and plot.

The graphical user interface developed in MATLAB[®] can be seen in Figure 4-5.

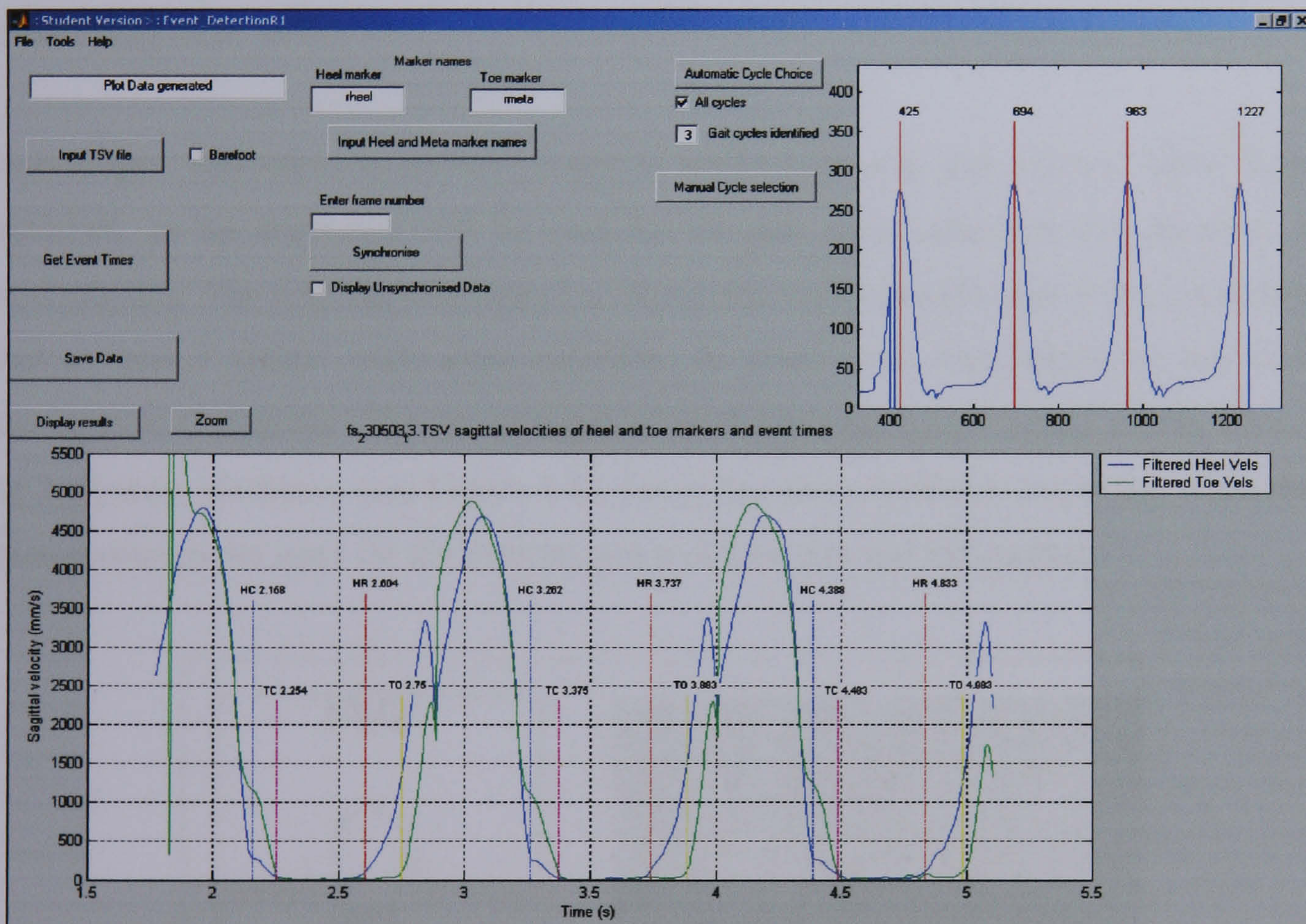


Figure 4-5: The MATLAB[®] graphical user interface used for processing the 3D marker data and gait event detection.

4.4.5 Pilot study

A pilot study was carried out in order to assess the performance of the proposed method in the detection of gait events (Ghoussayni *et al.* 2002). Ground reaction force data were

simultaneously collected from force plates, and used to assess the performance of the algorithms. The marker data were also visually inspected to determine the timings of the events. Five subjects (3 males and 2 female, ages 11, 12, 14, 23, and 58 years), without discernable gait abnormalities, performed a total of 30 steps (same number of steps per subject) across two adjacent force platforms (Figure 4-6). Each wore two retroreflective markers (radius 15 mm); one on the posterior end of the lateral border of the calcaneus and the other on the fifth metatarsal head. The purpose of the study was explained to each subject before they were asked to give their consent to take part in this study. The start point of their walk was marked and the subject was asked to start from the same point for each trial. This starting point was selected to be at least 3 strides away from the measurement volume to ensure the subjects acquired their target speed. This choice of 3 strides was chosen according to clinical experience and confirmed in results presented by (Yuancheng *et al.* 1993)

Each subject was asked to perform 2 sets of walks both with and without shoes. This is important, as the algorithm will be used for the gait event detection with barefoot and shod subjects. The subjects were asked to repeat the walks in each one of the 2 conditions until at least 3 'clean' trials were recorded. A 'clean' trial was judged by one of the investigators (using the video recordings) when the subject's foot landed evenly between the 2 adjacent platforms (see Figure 4-6). Satisfying this criterion is important when the 2 force platforms are used for the determination of heel rise and toe contact.

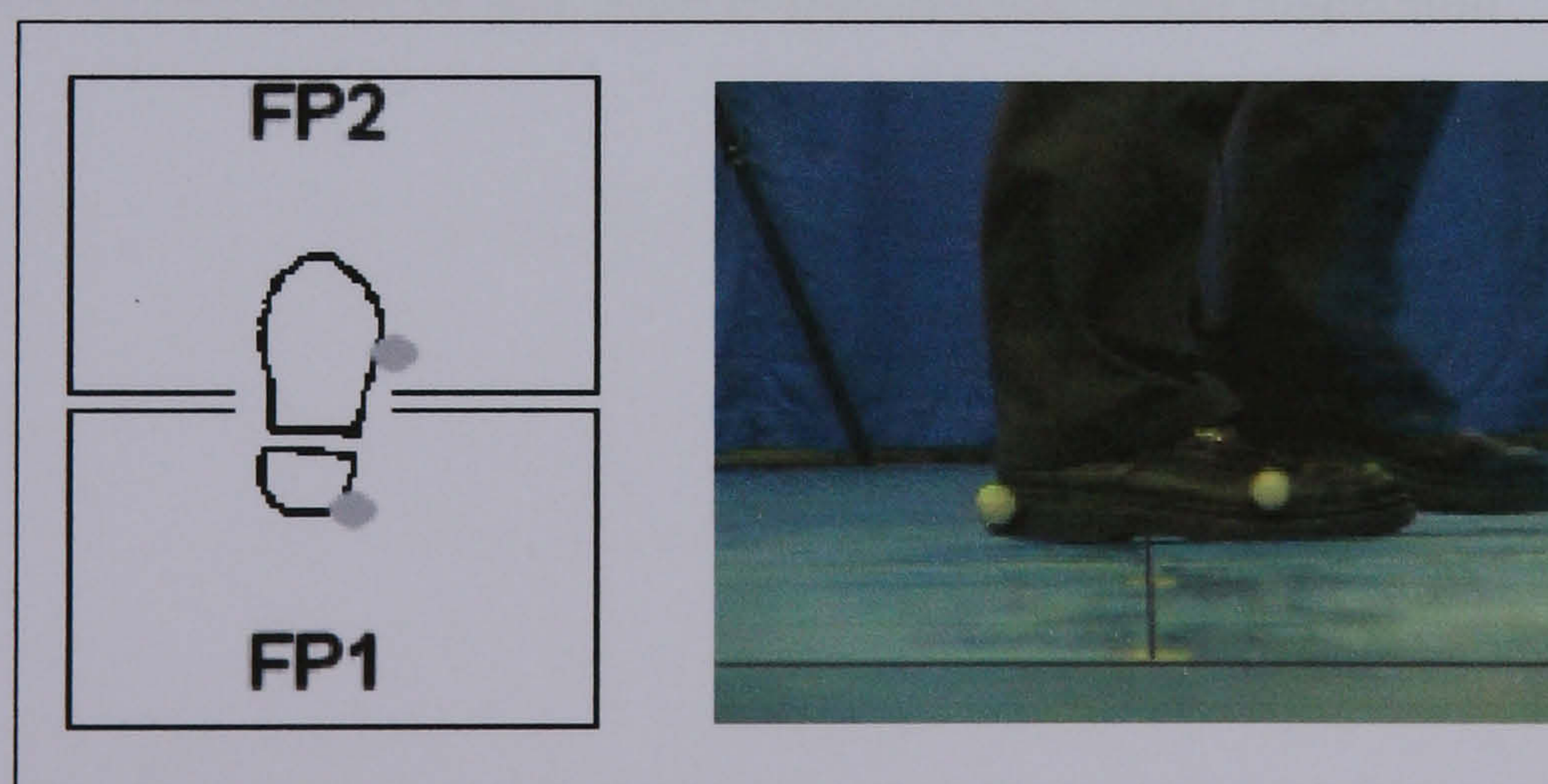


Figure 4-6: Foot placement across the two force platforms (FP) in a clean trial and an image capture of the video recordings.

Ground reaction forces (GRF) were measured using two force platforms (Hynd *et al.* 2000) sampled at 2000Hz, re-sampled down to 60Hz and synchronised with the marker system. The 3D coordinates of the markers were detected using a six camera 60 Hz MacReflex motion detection system (Qualisys Medical AB, Partille, Sweden). A lateral view of the foot motion was recorded on video and used to check foot position on the force platforms.

For GRF data, heel contact and the termination of the heel rise phase were estimated using a 10N threshold from the vertical component, measured by the first platform. Initial toe contact and end of toe contact times were determined in the same way using data from the second platform.

MacReflex 3.42f2 PPC software was used to track the motion data. For visual inspection, the two markers 3D motion trajectories were displayed using Q Trac View version 2.74p (Qualisys Medical AB) (Figure 4-7). The timings of heel and toe contact, and the initiation of the heel- and toe-rise phases, were estimated by a trained observer using the rules set in section 4.4.2. This process is very time consuming and tedious. In order to avoid any bias in the determination of the timings, an additional observer to the author of this work volunteered to perform the inspection. There was no bias and the occasional differences between the two observers were no more than 1 frame using the same set of rules to determine the gait events. Hence, for the subsequent formal assessment (described later in this chapter), the author of this work performed the visual inspection.

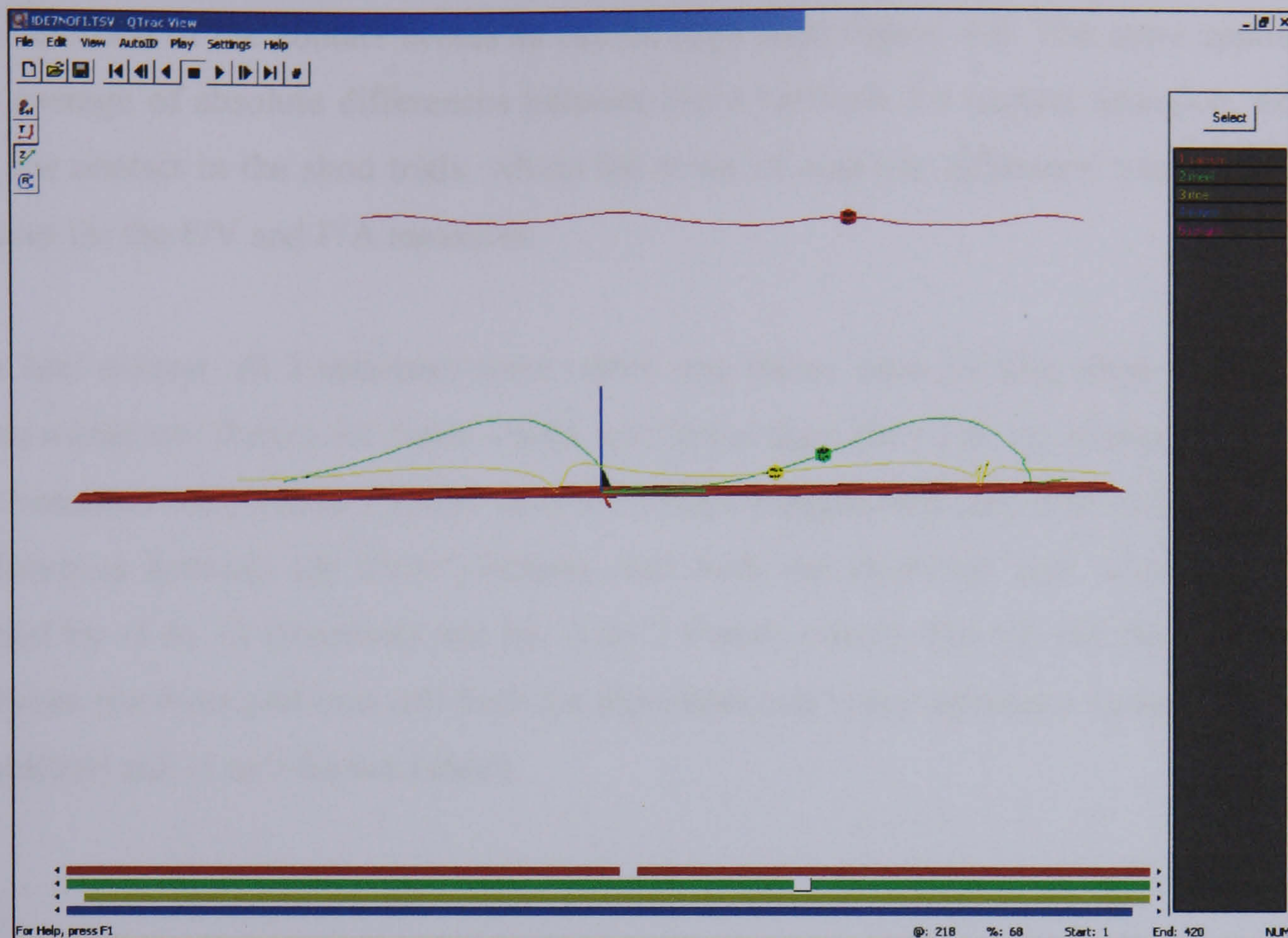


Figure 4-7: Screenshot of Q Trac View used for display of marker trajectories and visual inspection (Trajectories of sacral, heel, and toe markers in red, green, and yellow respectively).

The different timings given by the three methods were then compared for three trials from each subject in each of the two conditions, giving a total of 30 steps. The differences between the three methods were averaged and analysed using descriptive statistics at first. The absolute differences were also calculated and averaged in order to avoid any misleading conclusions from only averaging the differences.

The differences between the three methods in determining the time of each gait event were calculated as follows:

$$F/V = \text{Force platform} - \text{visual inspection estimated time}$$

$$V/A = \text{Visual inspection} - \text{algorithm estimated time}$$

$$F/A = \text{Force platform} - \text{algorithm estimated time}$$

A negative difference means that the first method estimated the event to have occurred earlier than the second method.

Figure 4-8 shows the mean differences between the 3 methods, while Figure 4-9 shows the mean of absolute differences. All three methods agreed to within 1 frame (16.7 ms) in

the detection of the contact events as can be seen from Figure 4-8. The same applied to the average of absolute differences between the 3 methods for contact detection, except for toe contact in the shod trials, where the mean of absolute difference was less than 2 frames for the F/V and F/A measures.

For heel contact, all 3 measures were within one frame, save for four shod trials, which were within two frames for force/ visual, and force/ algorithm. For toe contact, the f/v and f/a measures were within 1 frame save for 6 trials (ranged between -4 to 6). For heel off, differences between the force platform, and both the algorithm and visual estimates, varied by -1 to 13 (barefoot) and by -3 to 7 frames (shod). For toe off, the differences between the force platform and both the algorithm and visual estimates varied by 0 to 10 (barefoot) and -1 to 9 frames (shod).

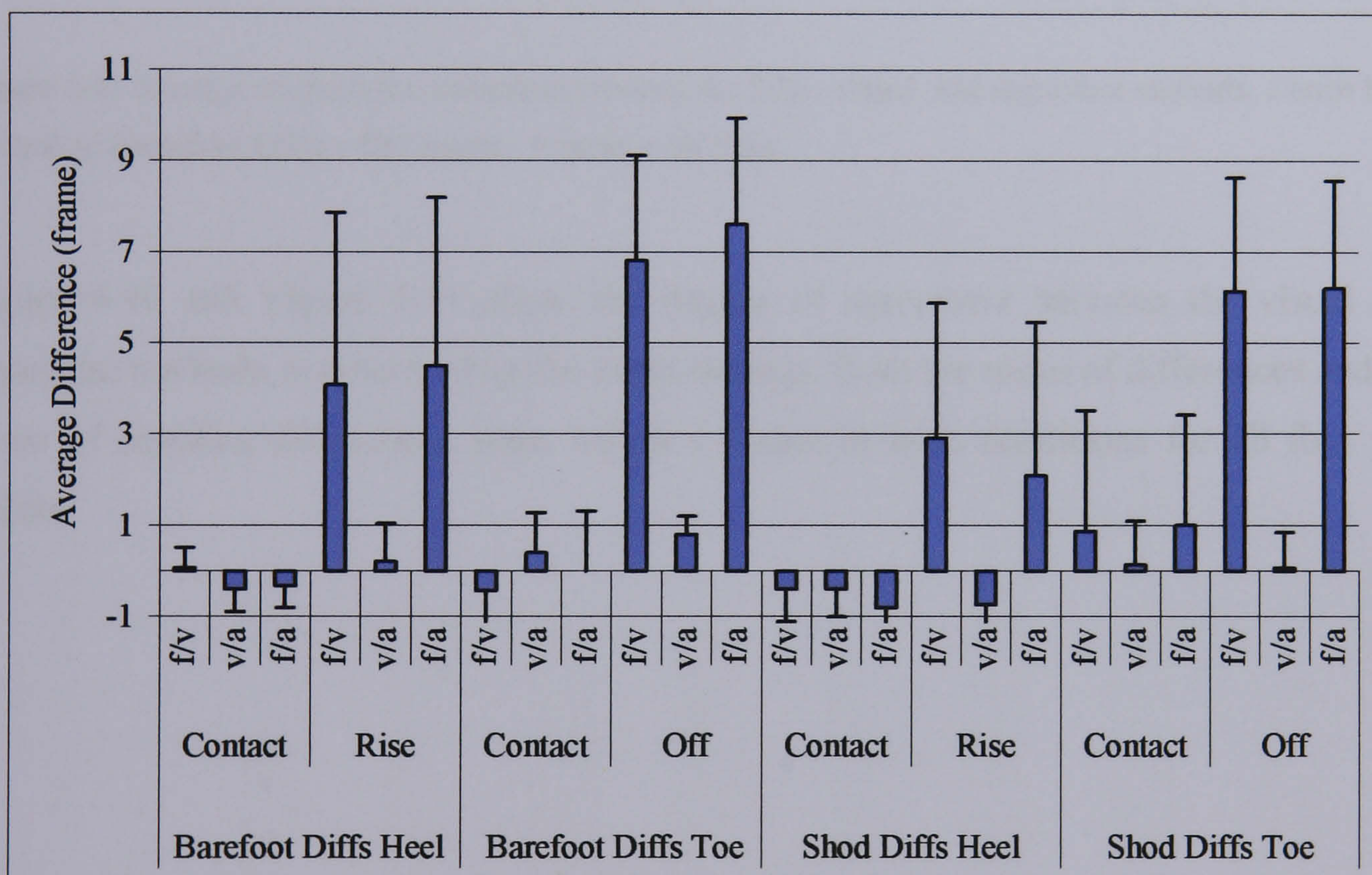


Figure 4-8: Average of differences between the force, visual, and algorithm methods. 1 error bar = 1 standard deviation; Diffs = Difference; 1 frame = 16.7 ms.

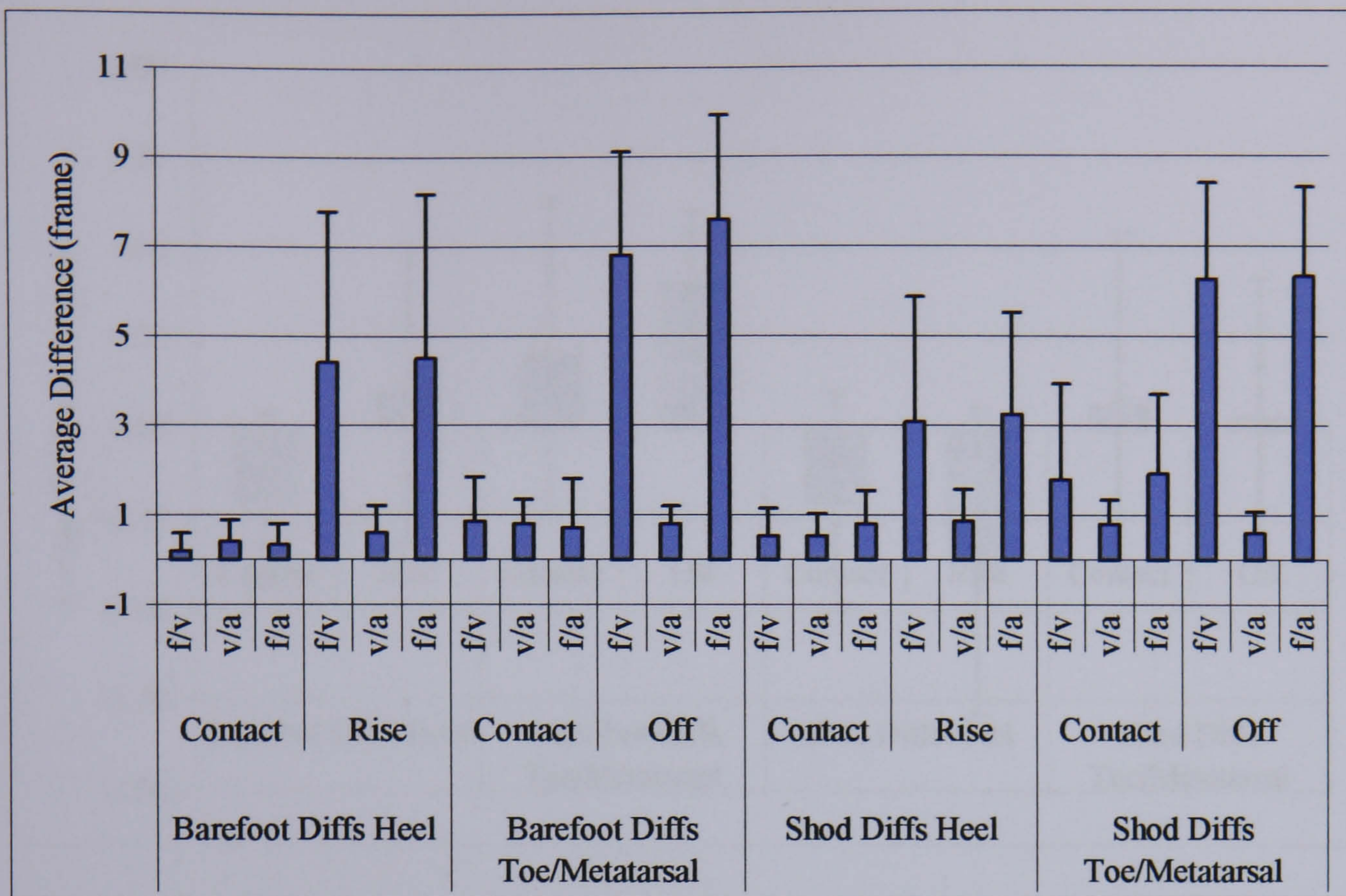


Figure 4-9: Average of absolute differences between the force, visual, and algorithm methods. 1 error bar = 1 standard deviation; Diffs = Difference; 1 frame = 16.7 ms.

Figure 4-10 and Figure 4-11 show the degree of agreement between the visual and algorithm methods in determining the event timings. Both the mean of differences and the mean of absolute differences were within 1 frame in both conditions for all four gait events.

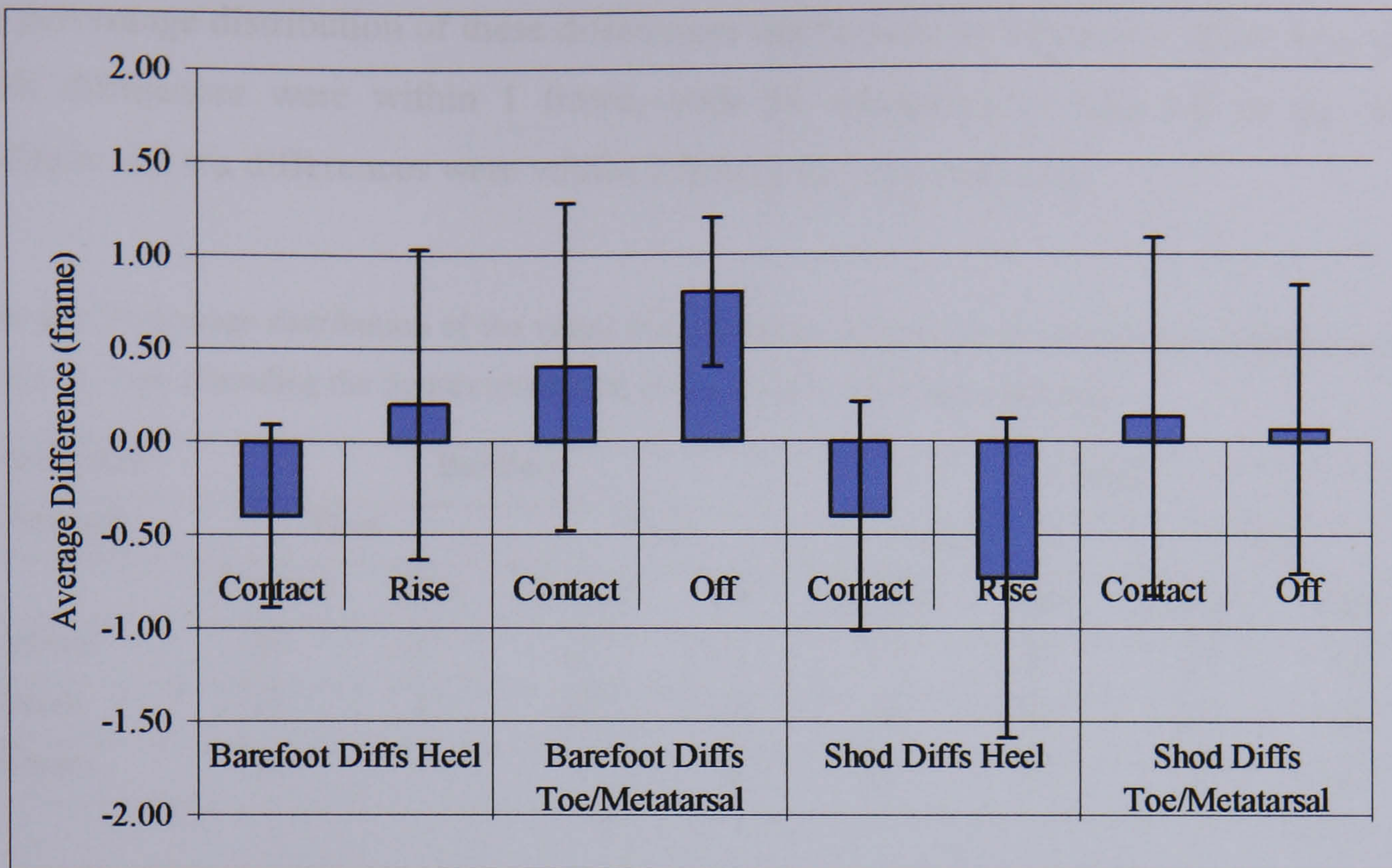


Figure 4-10: Average of differences between the visual and algorithm methods. 1 error bar = 1 standard deviation; Diffs = Difference; 1 frame = 16.7 ms.

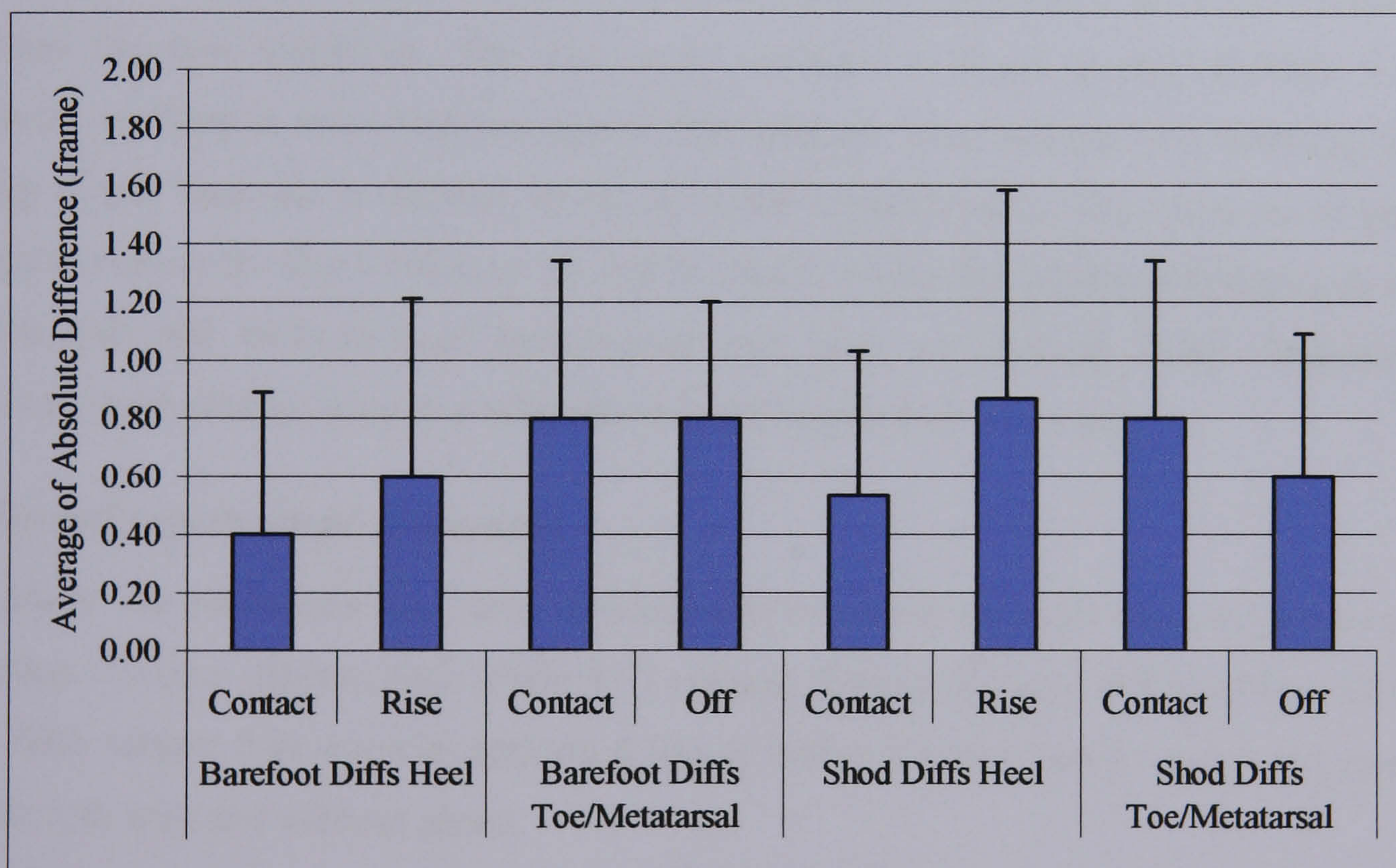


Figure 4-11: Average of absolute differences between the force, visual, and algorithm methods. 1 error bar = 1 standard deviation; Diffs = Difference; 1 frame = 16.7 ms.

The percentage distribution of these differences can be seen in Table 4-2. More than 90% of all differences were within 1 frame, with the exception of heel off in the shod condition. All v/a differences were within 2 frames for all conditions.

Table 4-2: Percentage distribution of the visual and algorithm differences (% occurrence of difference). 1 frame = 16.7 ms. (rounding the figures resulted in a total of 101 in 3 of the columns)

Trial/Event:	Barefoot				Shod			
	Heel		Toe		Heel		Toe	
	Contact	Rise	Contact	Off	Contact	Rise	Contact	Off
0 frames	60	47	27	20	47	33	27	40
1 frame	40	47	67	80	53	47	67	60
2 frames	0	7	7	0	0	20	7	0

The main conclusion to note from the above results is the close agreement between the visual and algorithm methods in detecting all gait events. The disparities between the force and visual or algorithm methods seen in the f/v and f/a differences will be discussed towards the end of this chapter. A more extensive study was undertaken in order to further evaluate the new technique. The new study included a larger normal database (12 subjects), walking at more than one speed. The methods were assessed in evaluating the timing of gait intervals in addition to the detection of gait events. The durations of gait intervals, such as the Heel-Toe interval, can be used to assess the degree of deviation from normal gait and evaluation of pathological gait such as Cerebral Palsy. Statistical measures were used in order to statistically test the results from the study.

4.5 Formal experimental assessment

This study was performed as a more thorough assessment of the algorithms in gait event detection. Twelve subjects (see Table 4-3) without discernable gait abnormalities, took part. Each subject was asked to perform 4 sets of walks at self-selected normal and slow speeds both with and without shoes.

Table 4-3: Table showing subject data details with average and standard deviation.

Subject	Age (years)	Sex (M/F)	Height (m)	Weight (kg)
Average:	34.3	-	1.74	71.9
Standard Deviation	10.7	-	0.13	10.3
1	25	M	1.79	99.6
2	31	F	1.68	66.5
3	27	F	1.58	55.8
4	45	F	1.60	57.4
5	23	M	1.86	67.4
6	59	M	1.80	78.8
7	23	F	1.57	57.6
8	45	M	1.87	82.3
9	39	M	1.78	77.4
10	25	M	1.91	80.7
11	36	M	1.83	80.5
12	33	M	1.59	58.1

The reason for performing the trials at both speeds was to cover a range of walking speeds, which would be the case in a real life situation, where the algorithm will be used in pathological gait. Both speeds were self-selected and not controlled to minimise the effect of the experimental protocol on the subjects' gait and to simulate best the range of walking speeds in both the able-bodied and pathological populations. A third retroreflective marker was placed on the sacrum. Data from the sacral marker was used to calculate the walking speed, as the mean of the magnitude of the sacral marker velocity vector in the progression and medial-lateral plane.

The different timings given by the three methods were then compared for three representative trials from each subject in each of the four conditions, giving a total of 144 steps. Each set of three readings from one subject was used to produce a single mean, reducing the data points into twelve points for each condition. The differences between the three methods were averaged and analysed using descriptive statistics at first. The absolute differences were also calculated and averaged. The differences in the event timings were normalised as a percentage of the gait cycle duration (% of gait cycle) for each trial and the resulting percentages were analysed. In addition to the above

comparisons, the 3 methods were compared in the determination of 3 intervals in the gait cycle: HC-TC [Heel contact to Toe contact], TC-HR [Toe contact to Heel rise], and HR-TO [Heel rise to Toe off].

The degree of agreement between the methods was assessed using Passing and Bablock regression and identity line plots for method comparison and agreement (Passing *et al.* 1983) and Bland and Altman plots (Bland *et al.* 1986). Nonparametric Repeated Measures ANOVA (Friedman test - Dunn's post test) was used to judge the statistical significance of differences between the three methods in the determination of both the timings of the four gait events and the duration of the three gait phases.

4.5.1 Results and discussion

Table 4-4 shows the average values of both walking speed and gait cycle duration times for all 12 subjects under the four conditions: barefoot-normal speed (b/f-n), barefoot-slow (b/f-s), shod-normal (shod-n), shod-slow (shod-s).

Table 4-4: Descriptive statistics of the walking speed and gait cycle duration of the 12 subjects. b/f: barefoot, -n: normal, -s: slow, STDEV: standard deviation

Parameter		Test Condition			
		b/f-n	shod-n	b/f-s	shod-s
Walking speed (m/s)	Average	1.39	1.48	1.05	1.11
	STDEV	0.12	0.12	0.17	0.16
Cycle duration (frames)	Average	64	65	75	76
	STDEV	5	5	11	9

The differences between the 3 methods in determining the gait event timings were initially computed for each speed and footwear separately. The differences however showed no significant variation between the two different walking speed trial sets. As a result of this each figure will present both slow and normal walking speed results together. The average difference between estimates for both normal and slow speed walking are shown in Figure 4-12. These show the differences f/v, v/a and f/a for all four

events when walking shod and barefoot. One error bar on the graph is equivalent to one standard deviation. The absolute average differences are plotted in Figure 4-13.

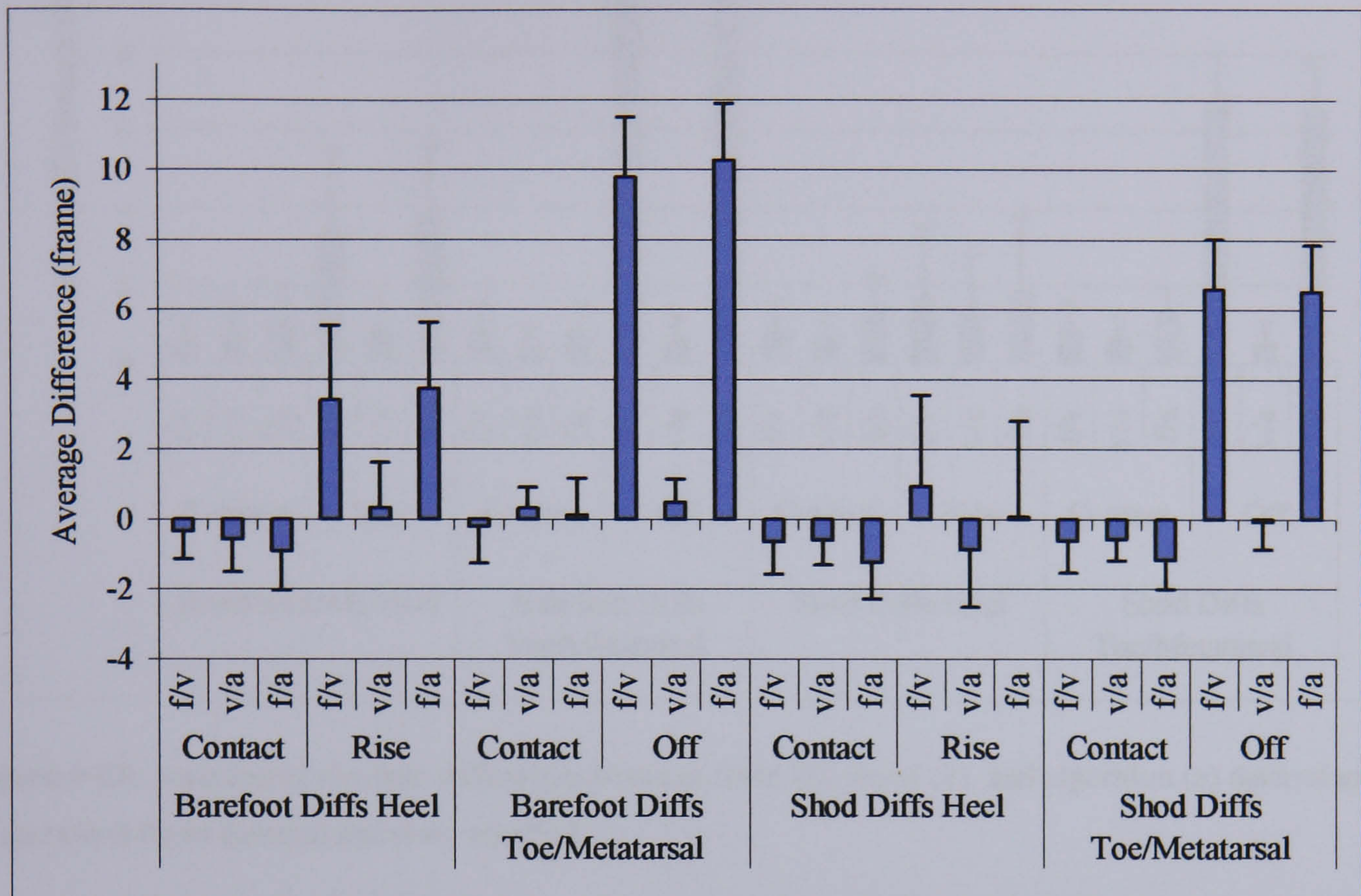


Figure 4-12: Average of differences between force (f), visual (v), and algorithm (a) determination of gait event times (normal and slow velocity).

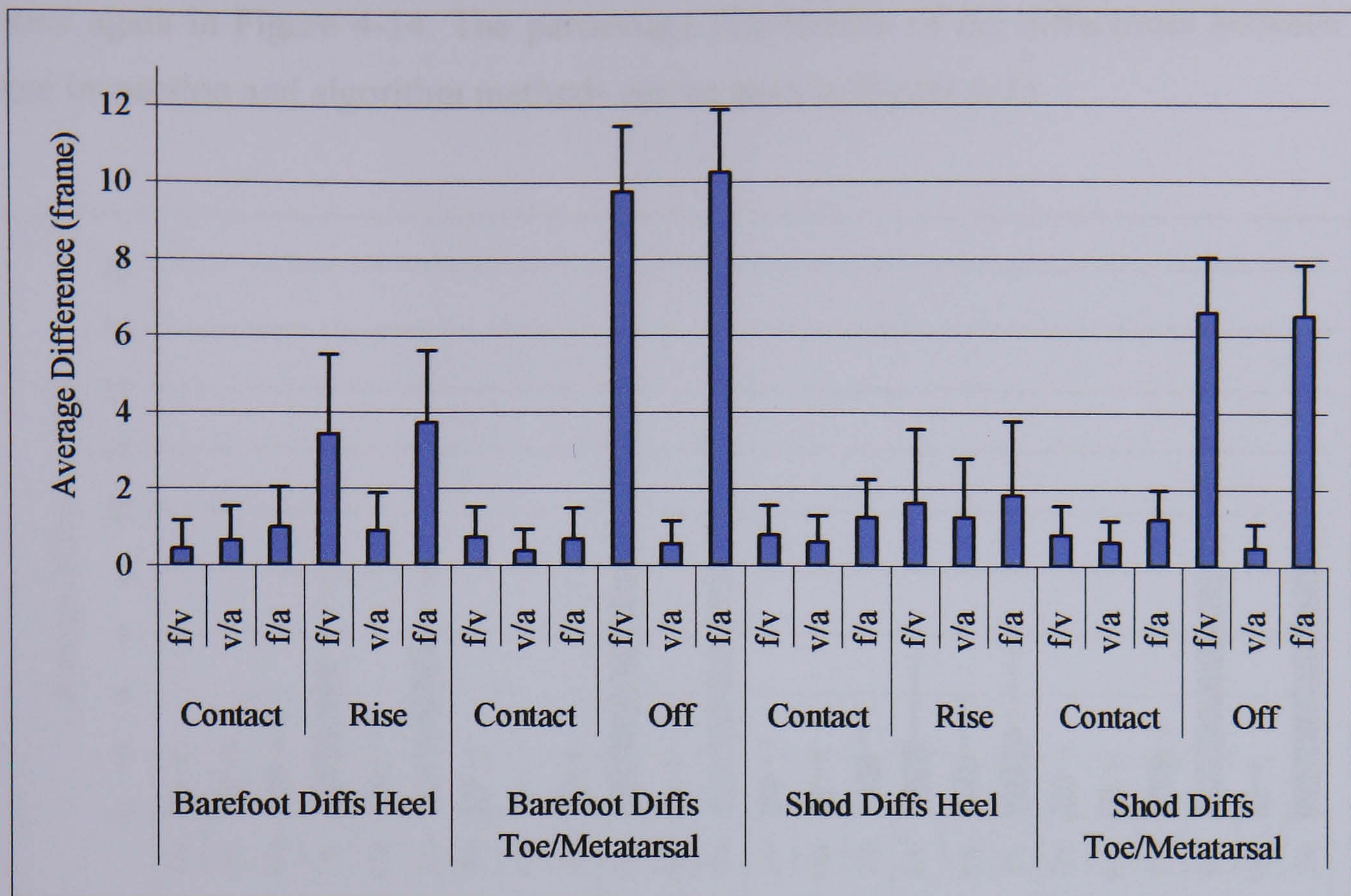


Figure 4-13: Average of absolute differences between force (f), visual (v), and algorithm (a) determination of gait event times (normal and slow velocity).

For both heel contact and toe contact, the average differences and the average of absolute differences between the 3 methods were within 1.5 frames, equivalent to 2.3% of the average gait cycle time. The v/a average of absolute differences was less than 1 frame for all four conditions.

For heel rise, the average differences between the force platform, and both the algorithm and visual estimates (f/v and f/a), were mainly positive (varied between 0 and 4 frames). The average of absolute differences f/v and f/a were very similar in each condition, but slightly higher in the barefoot trials (3-4 frames) than the shod trials (1-2 frames).

For toe off, the average of differences and absolute differences between the force platform and both the algorithm and visual estimates (f/v and f/a), were between 6 and 7 frames for shod and 9 to 10 frames in the barefoot trials.

After normalising the differences as percentages of one gait cycle time (T is equal to one gait cycle time for this figure and all others in this thesis), the absolute differences are

plotted again in Figure 4-14. The percentage distribution of the differences between the visual inspection and algorithm methods can be seen in Figure 4-15.

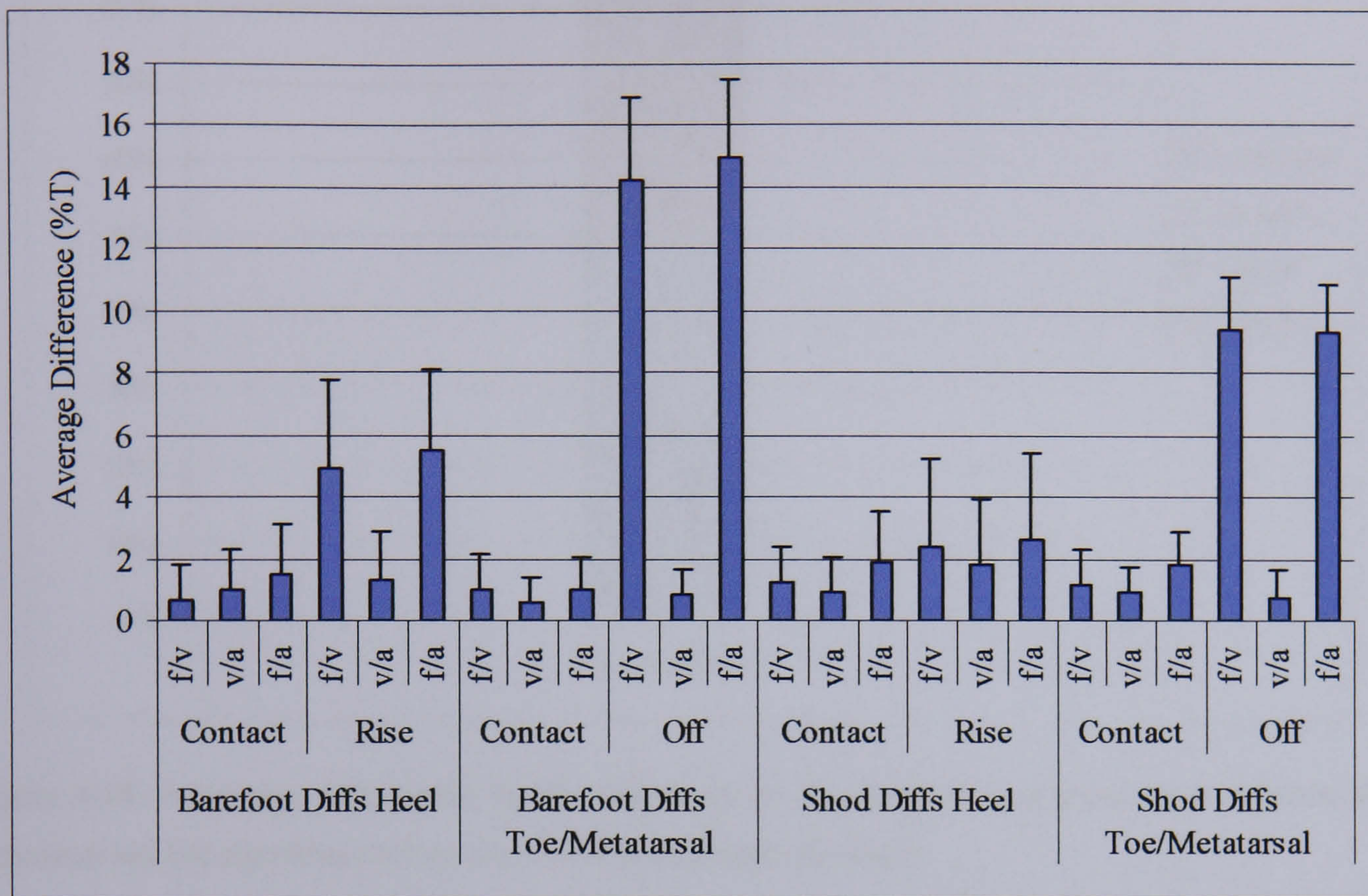


Figure 4-14: Normalised average of absolute differences between force (f), visual (v), and algorithm (a) determination of gait event times (normal and slow velocity).



Figure 4-15: Percentage distribution for the differences in the estimated gait event times between visual inspection and the algorithm (All events, both footwear and velocities).

For all four events visual inspection and algorithm timings agreed to within 1 frame in 90% of the cases and to within 2 frames in 96% of the cases. Also, the v/a difference was within 2% of the average gait cycle time in 90% of the cases.

Figure 4-16 and Figure 4-17 show the averages of the normalised durations of the 3 intervals considered as given by the 3 methods for normal and slow walking speed respectively. The f/v and f/a differences seen in the determination of HR and TO resulted in the Visual and Algorithm giving shorter estimates of the TC-HR and HR-TO intervals (Figure 4-16 and Figure 4-17). All 3 methods estimates of the HC-TC interval were very close, with the exception of the Algorithm estimate being 1% shorter in the barefoot trials. The difference between the visual and algorithm estimates of all 3 intervals was within 1% of the average gait cycle time.

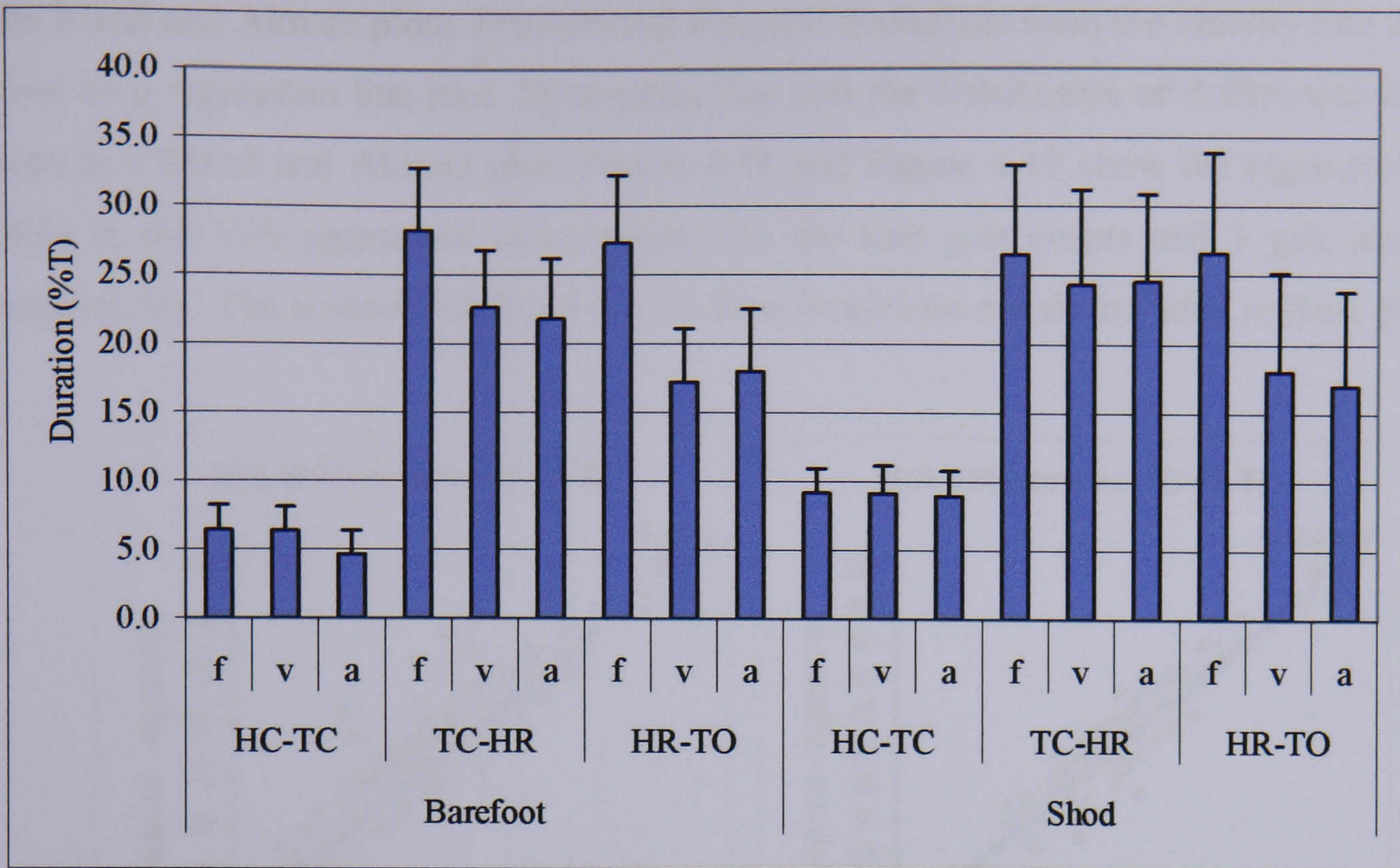


Figure 4-16: Normalised average interval durations as determined by the 3 methods for the normal speed trials (HC-TC: Heel contact to toe contact, TC-HR: Toe contact to heel rise, HR-TO: Heel rise to toe off).

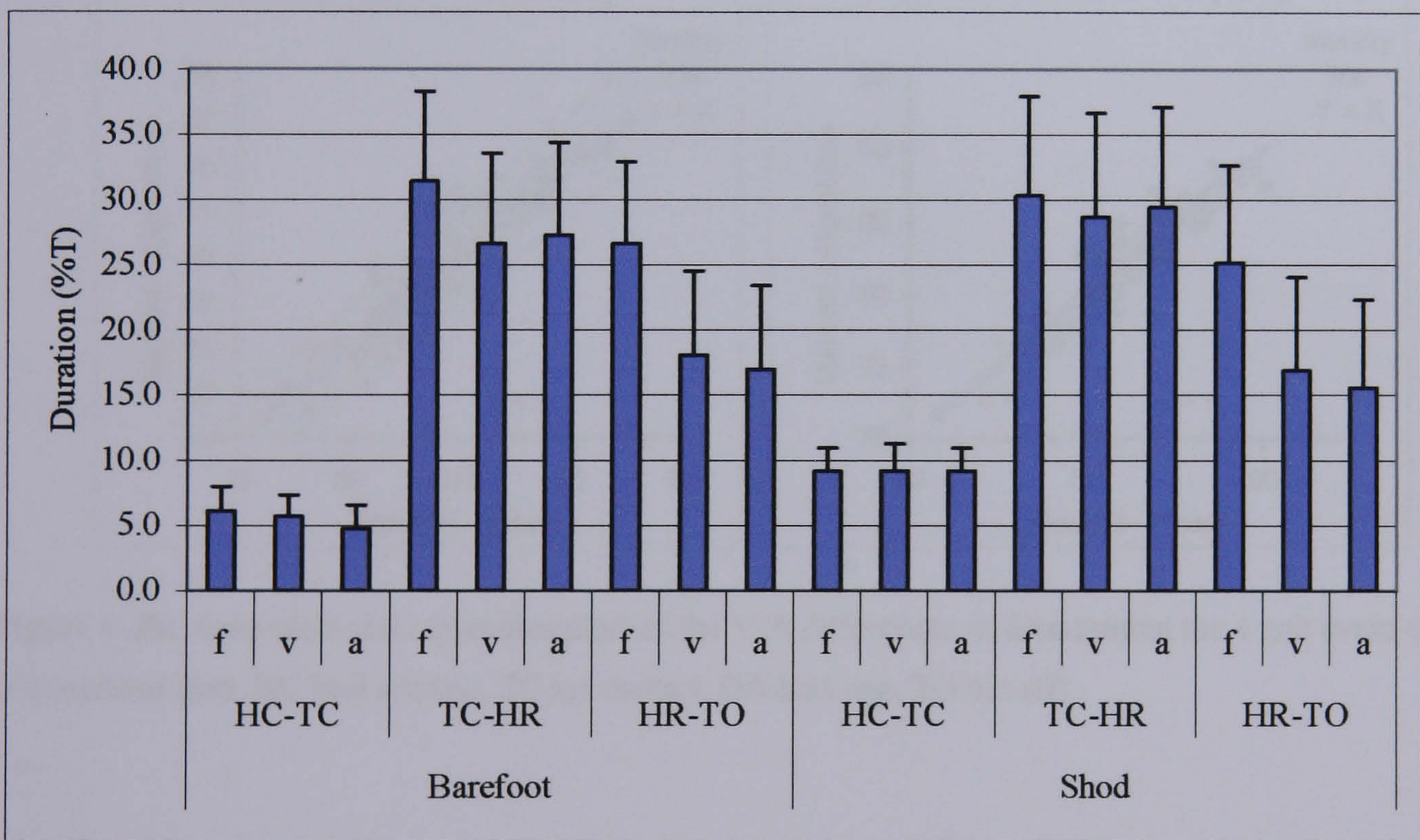


Figure 4-17: Normalised average interval durations as determined by the 3 methods for the slow speed trials (HC-TC: Heel contact to toe contact, TC-HR: Toe contact to heel rise, HR-TO: Heel rise to toe off).

The agreement between the visual and algorithm estimates in determining the four gait events and intervals was assessed using the Passing and Bablock regression method and

the Bland and Altman plots. Proportional bias and deviations from the identity line can be seen on a regression line plot. Systematic bias and the distribution of differences can be seen in a Bland and Altman plot. Figure 4-18 and Figure 4-19 show the regression line plots in the V/A agreement comparisons for the four gait events and 3 gait intervals respectively. The normalised data from the four conditions are all included in these plots.

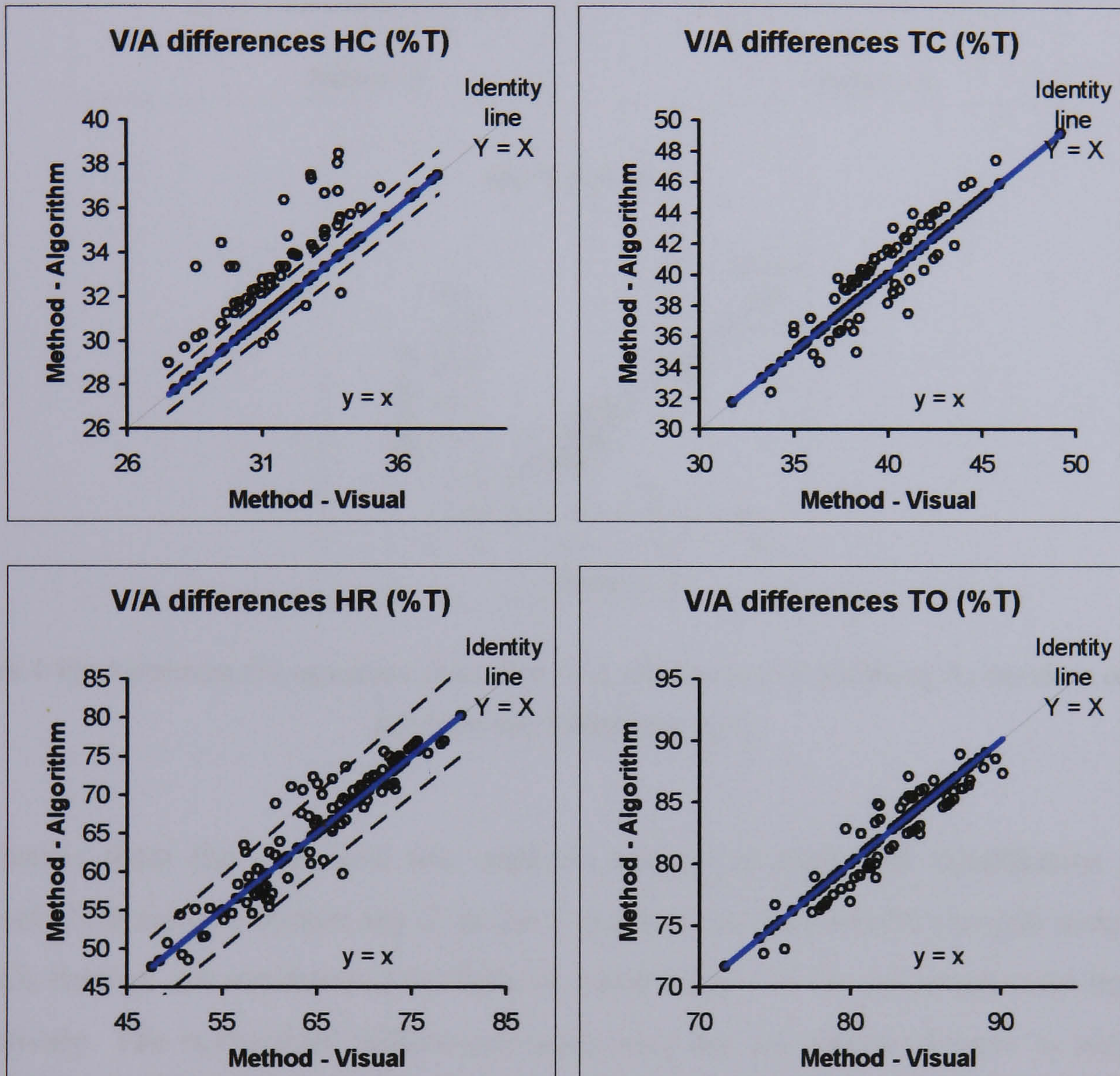


Figure 4-18: Agreement test regression plots of the V/A differences in determining the 4 gait event timings (Normalised data; HC heel contact, TC toe contact, HR heel rise, TO toe off).

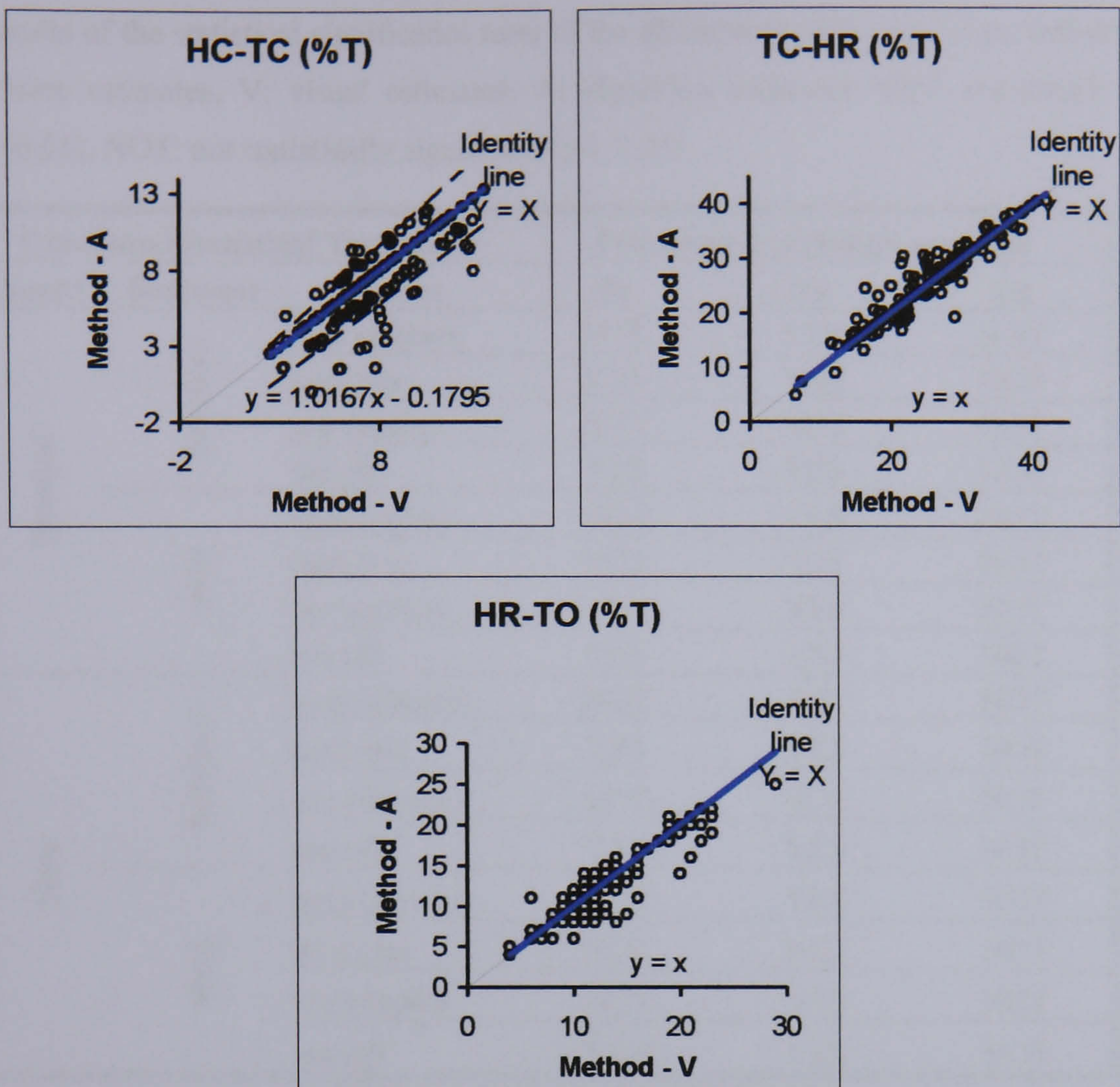


Figure 4-19: Agreement test regression plots of the V/A differences in determining the durations of the 3 gait intervals (Normalised data).

The results from the statistical test used to assess the statistical significance in the observed differences between any 2 of the 3 methods in determining the gait events and intervals timings are summarised in Table 4-5 and Table 4-6 for gait events and intervals respectively. The normalised differences were used for the statistical tests to judge the differences in light of their real life significance in gait analysis.

Table 4-5: Results of the statistical significance tests of the differences in the gait event detection by the 3 methods. F: force estimates, V: visual estimates, A: algorithm estimates YES: statistically significant difference ($p < 0.05$), NOT: not statistically significant ($p > 0.05$).

Condition\Statistical Test-result			Friedman test/Dunn's post test		
Speed	Footwear	Event	f/v	f/a	v/a
Normal	barefoot	heel contact	NOT	YES	NOT
		heel rise	YES	YES	NOT
		toe contact	NOT	NOT	NOT
		toe off	YES	YES	NOT
	shod	heel contact	NOT	YES	NOT
		heel rise	NOT	NOT	NOT
		toe contact	NOT	YES	NOT
		toe off	YES	YES	NOT
Slow	barefoot	heel contact	NOT	YES	NOT
		heel rise	YES	YES	NOT
		toe contact	NOT	NOT	NOT
		toe off	YES	YES	NOT
	shod	heel contact	NOT	YES	NOT
		heel rise	NOT	NOT	NOT
		toe contact	NOT	YES	NOT
		toe off	YES	YES	NOT

Table 4-6: Results of the statistical significance tests of the differences in the gait interval estimation by the 3 methods.

Condition\Statistical Test-result			Friedman test/Dunn's post test		
Speed	Footwear	Interval	f-v	f-a	v-a
Normal	barefoot	HC-TC	NOT	YES	YES
		TC-HR	YES	YES	NOT
		HR-TO	YES	YES	NOT
	shod	HC-TC	NOT	NOT	NOT
		TC-HR	NOT	YES	NOT
		HR-TO	YES	YES	NOT
Slow	barefoot	HC-TC	NOT	YES	NOT
		TC-HR	YES	YES	NOT
		HR-TO	YES	YES	NOT
	shod	HC-TC	NOT	NOT	NOT
		TC-HR	NOT	NOT	NOT
		HR-TO	YES	YES	NOT

There were no statistically significant ($p > 0.05$) differences between the visual and algorithm methods in determining the timing of 4 gait events in any of the conditions. The only statistically significant difference seen between the visual and algorithm estimates of the 3 gait intervals was in the HC-TC estimate in the b/f-n trials. This is mainly due to a relative bias of about 1.5 % (1 frame) earlier estimate of HC by the visual method as can be seen on the Bland and Altman plot (Figure 4-20).

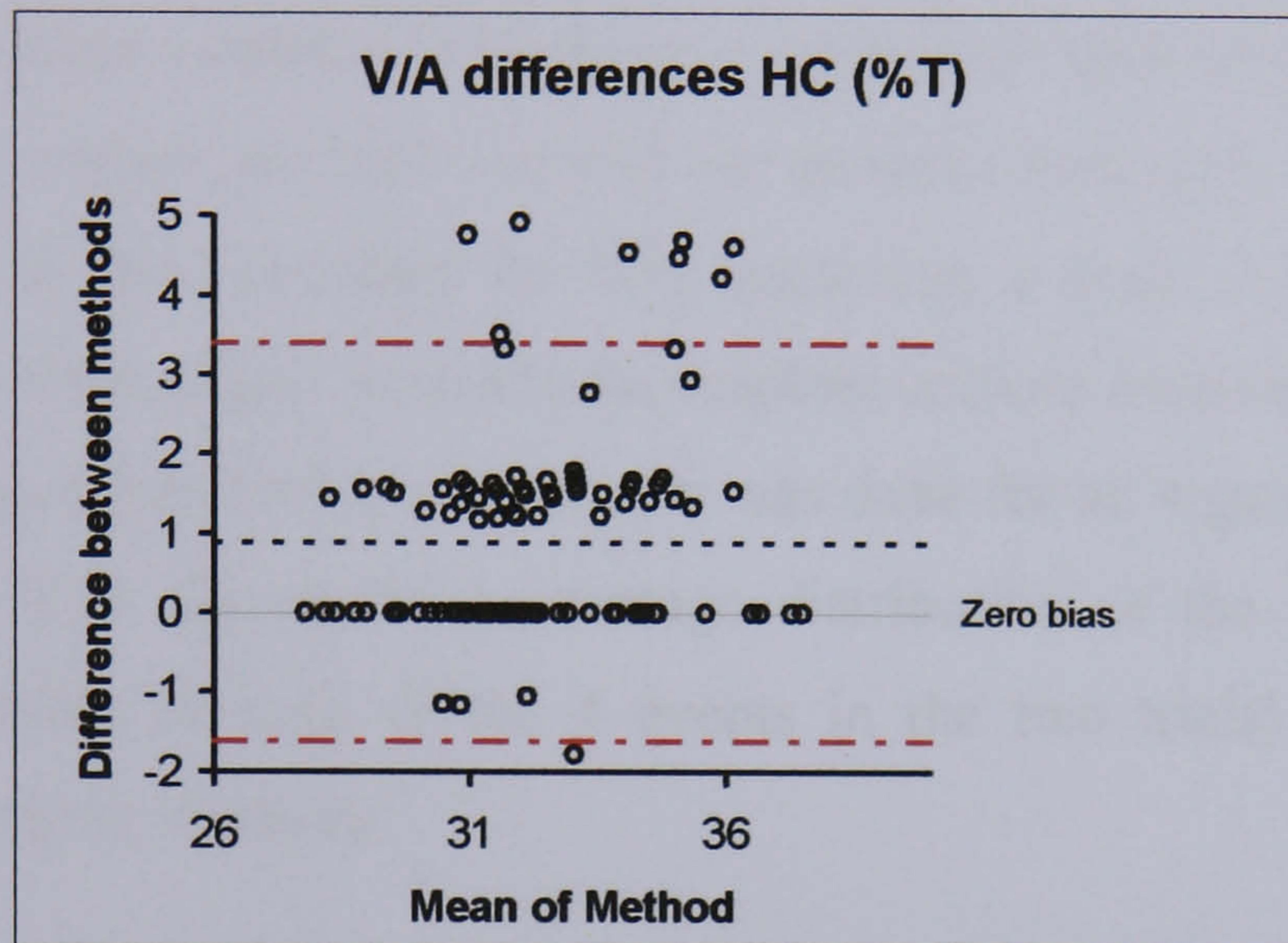


Figure 4-20: Bland and Altman plot for the V/A differences in determining HC in the b/f-n condition (Normalised data to gait cycle time T).

- shows the 95% limit of agreement
- bias of Algorithm method compared with visual inspection method

The statistically significant differences occurring in F/V and F/A comparisons for both HR and TO (except for HR in shod conditions) are expected due to the nature of the events and the experimental set-up. In the cases of HC and TC, however, the F/A and F/V differences were relatively small and expected to be statistically insignificant. The statistical test results agreed with the expectation except for the F/A differences in HC in all 4 conditions and TC in the shod condition (Table 4-5). These statistically significant F/A differences for HC and TC are believed to be the result of a bias between the 2 methods. However, the average of the absolute F/A differences for HC and TC are within 2.5 % of gait cycle time (1.5 frames).

4.6 Pathological gait case study

In order to test whether the approach used is applicable in the case of pathological gait, one subject with hemiplegic gait performed two walking trials. The subject had a foot drop condition and performed 2 walks through the measurement volume, one with the aid of a foot drop stimulator and one without, providing data from 3 consecutive gait cycles per walk. The protocol set for the earlier data collection, in particular foot placement across the force platforms, meant that it was not suitable for patient testing. Conventional force platform data were available from the case study and could only be used to compare initial and terminal contact, but heel rise and toe contact times were not available. As the timing of heel rise is very important for FES triggering, a study to assess the kinematic algorithms for pathological gait would be incomplete without assessing the timing of heel rise. A visual vs. algorithm timing comparison was done for all 4 gait events as described previously. Figure 4-21 shows the percentage distribution of the absolute differences (total of 8 occurrences of each of the 4 events in the two trials) between the visual inspection and algorithm methods.

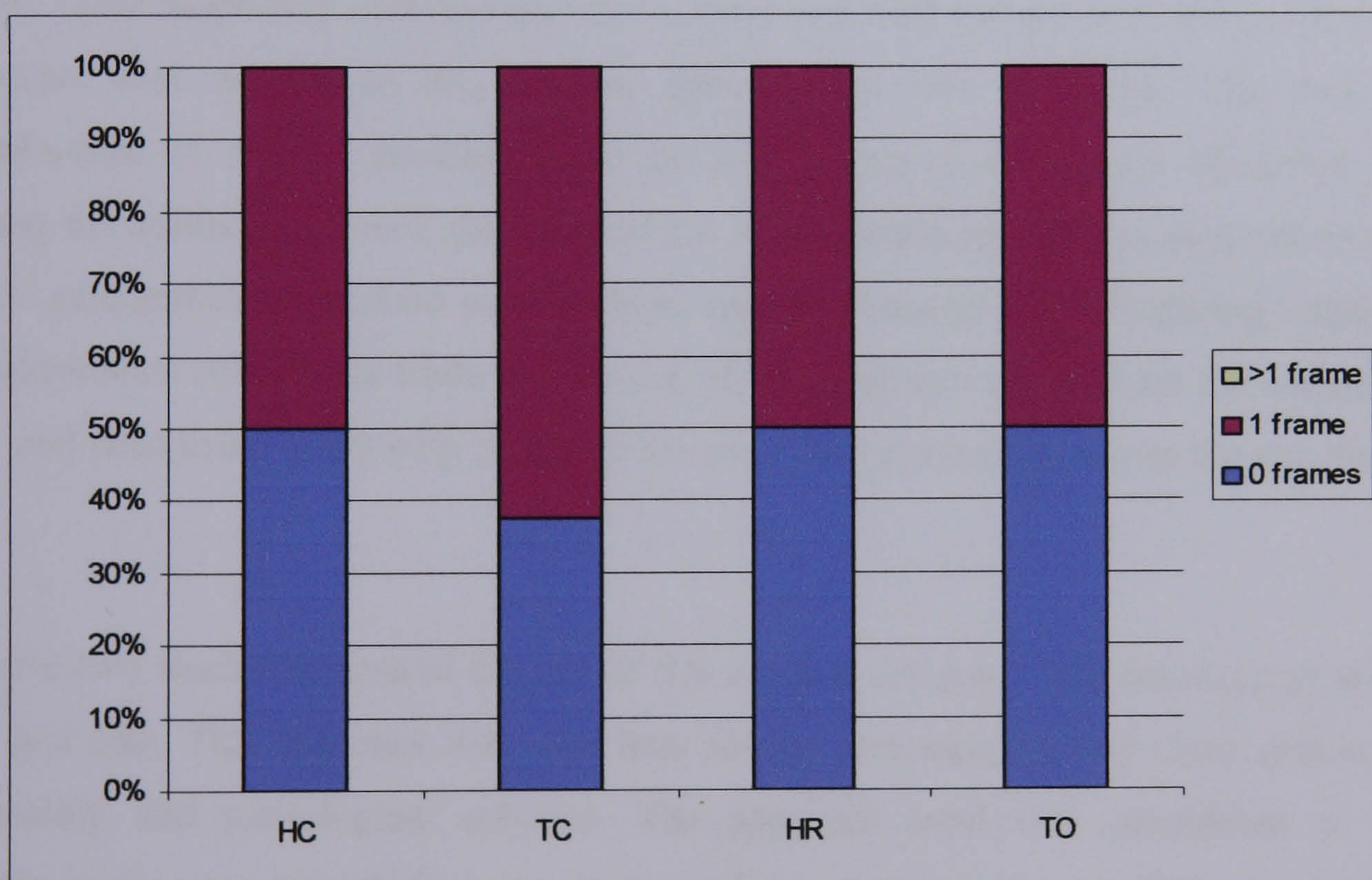


Figure 4-21: Percentage frequency distribution for the V/A absolute differences in estimating the gait events.

None of the V/A differences were above 1 frame difference (Sampling frequency = 60 Hz). These results are comparable to those seen in the able-bodied trial, and would suggest a similar performance by the algorithm method in the case of pathological gait.

4.7 Conclusions

Due to the experimental set-up and nature of recorded data, the 3 methods have differences, mainly F/V and F/A, for some of the events and intervals. The force platform data are measures of the start of contact events and end of the take-off phases, whereas the visual and algorithm methods (based on marker data) measure the end of the same contact events and the start of take-off phases. Thus, the discrepancies between the marker and force detection times for heel rise and toe off are acceptable as these are in reality phases and not single events in time. One suggestion worth considering is redefining or renaming these events to reflect whether the event considered is the start or end of each of these phases. Heel contact is a rapid event and so the different measures can be expected to be in agreement. This is also true of toe contact, although with more variation. For heel rise and toe off the differences are marked, with a greater variation, both within and between subjects. Video inspection showed that this is correlated with variations in the position of the contact foot relative to the junction between the two platforms. The lack of standardisation of contact position could be a criticism of this study. However, by following the outlined protocol, the effect of the experimental set-up was minimal on the subjects' gait, and eliminated the need to target specific areas on the plate during walking. The performance of multiple trials and the use of video images allowed for the choice of 'clean' and acceptable trials with regard to the even foot placement across the two force plates.

The above two studies evaluated the use of this method for gait event detection in able-bodied gait data. This approach was used later for the assessment of the Gyro system in both healthy and pathological subjects. The approach used was considered to be applicable in the case of pathological gait, in particular hemiplegic gait. This assumption was tested with data collected in a case study. Criteria used by the algorithm, such as threshold values, are believed to be sufficient for a similar performance in the case of pathological gait. Data from the case study reflected similar differences between the visual and algorithm timings to those seen in able-bodied gait, and suggested that the new method is a feasible approach for the detection of gait events in pathological gait

Another potential application for the technique is the determination of gait interval durations. One example for this application is the use of these durations as an outcome measure in the assessment of interventions such as FES in correcting gait deviations in cerebral palsy “toe gait” (Stevens *et al.* 2001).

In conclusion, the algorithm appears to be a reliable measure in comparison to the visual inspection method. The study suggests that the automated algorithm is both timesaving and as accurate in detecting gait events as visual inspection. It is useful in automatically detecting the events for several strides within the measurement volume and could be used in the assessment of the Gyro sensor system and its comparison to the foot switches.

The issue highlighted in section 4.4.3 related to the use of filtering to smooth kinematic data prior to processing will be the subject of discussion in the next chapter.

Chapter 5: Choice of cut-off frequency for the filtering of gait kinematic data

This Chapter describes the techniques that were used in the treatment of the 3D coordinate data prior to using them for gait event detection. The discussion is made with particular reference to the choice of cut-off frequency for low-pass filtering the data before differentiation. Noise magnification as a result of differentiating data is a well-known issue. This issue has been a major area of research and debate, and hence a review of some of the commonly used techniques and methods is presented. The review highlighted the importance of the frequency characterisation of kinematic signals and enabled a better understanding of their frequency content. An experimental study was carried out in order to look at the frequency domain characteristics of the gait signals in 10 subjects who performed a total of 180 trials at different walking speeds both shod and barefoot. The results from this study, presented in this chapter, were used to guide towards a more informed choice of cut-off frequency.

5.1 Choice of cut-off frequency

Both the applications and measurement methods of human locomotion have changed with time. There are a number of approaches for the measurement of kinematic variables during walking. These include the use of strobe light and reflective strips, electrogoniometry, video/cine film, and active/passive automated marker detection systems. Cost, validity, efficiency, and encumbrance to the subject being measured are some of the considerations when the choice of measuring system is made.

Video/marker detection systems have gained widespread use within movement analysis systems for the purposes of kinematic data collection. Often the captured movement of a set of markers attached to the skin is used to infer the skeletal movement. The system captures marker position data within an absolute reference set of co-ordinates. In such systems, one can derive higher order kinematic variables by differentiating the position data. This process, however, selectively magnifies high frequency components of the position signal. One way of reducing the effect of differentiation on the signal to noise ratio (SNR) is by low pass filtering the position data to eliminate the mainly noise part of

the spectrum and preserve the mainly signal part. This is based on the fact that the signal is band-limited and lies within a low frequency range. The choice of cut-off frequency is often a compromise between minimising the signal distortion and the degree of noise reduction. This choice is usually made with some consideration of the intended application of the data. Hence, it is commonly emphasized that the choice of cut-off frequency should be optimised for the particular application.

5.2 Differentiation magnifies noise

For this work, the first and higher derivatives of gait kinematic signals are required but cannot be directly measured to a satisfactory level with available equipment. The computation of these derivatives using noise contaminated signals deteriorates the signal to noise ratio. This can be shown in the following example. If we accept that a periodic signal $X(t)$ (time changing parameter of gait such as the global position of a body segment as a function of time) is composed of a series of sinusoidal waves (Fourier series), then we can write:

Equation 5-1

$$x(t) = a_1 \sin(\omega t + \theta_1) + a_2 (\sin 2\omega t + \theta_2) + \dots a_n \sin(n\omega t + \theta_n)$$

The amplitudes of each of the sinusoidal harmonics of frequencies ω , 2ω , $n\omega$ are a_1 , a_2 , and a_n (θ is the phase angle for each component). The amplitudes of the same harmonics are however ωa_1 , $2\omega a_2$, and $n\omega a_n$ for the first time derivative of X and $\omega^2 a_1$, $2\omega^2 a_2$, and $n\omega^2 a_n$ for the second time derivative. Hence, any higher frequency components in the position signal will have a relatively higher contribution to the signal power in the first and second derivatives than in the original position signal.

Normal gait kinematic signals are generally believed to have relatively low frequency content and limited bandwidth. The main components of the gait signals are believed to be within 10 Hz (Winter *et al.* 1974; Winter 1990; Angeloni *et al.* 1994). The noise seen in the recorded signals, however, has a wide frequency band and extends beyond the gait signal limits. This makes the application of low-pass filtering a useful approach to reduce the effect of noise and to improve the SNR of the gait kinematic signal.

5.3 Reported techniques for the filtering of kinematic signals

The presence of noise superimposed from various sources of error in kinematic analysis has led many researchers to investigate ways of reducing its effect on the quality of computed derivatives and parameters of gait. A literature survey of proposed techniques to deal with this problem revealed several studies which include Jackson 1979; Hatze 1981; Woltring 1986; Winter 1990; D'Amico *et al.* 1990; Challis 1999; and Giakas *et al.* 2000. Essentially, these techniques apply some numerical method in order to solve the problem of noise and are successful to varying degrees when the control variables are set appropriately.

In the paper by Jackson in 1979, a set of biomechanical data was fitted with a Fourier series. The data used were the angular flexion recordings of the elbow during normal walking. The residual or average error between the data and the derived data from the series was calculated as a function of series order. The higher the order of the series used, the closer the fit, and hence, the smaller the error. Above a certain level of series order, the increase in order produces no significant decrease in the average error. The second derivative of the average error with respect to the changing series order was calculated and plotted. The cut-off frequency/order of polynomial is chosen at the point where the absolute value of second derivative of residual falls below a "prescribed level" for 3 consecutive order values. First and second derivatives of the motion signals can then be calculated from the mathematical function resulting in effective filtering of the data.

In 1981, Hatze proposed a method that is based on optimally regularised Fourier series (ORFS) for the estimation of higher-order derivatives of noisy data. The data from the study by Pezzack *et al.* in 1977 were used to assess the effectiveness of the above approach. The statistical properties of the signal are used in order to find the optimum filter function. This is done by minimising a certain logarithmic function of the signal which contains the Fourier coefficients. The regularisation of the Fourier series determines an optimal low-pass filter window and hence an optimal cut-off frequency for smoothing the signal and obtaining its derivatives.

The study by Woltring in 1986 uses generalised cross-validatory spline (GCVS) smoothing and differentiation of the data. Both GCVS and ORFS are based around the same minimisation technique. The extent of smoothing in GCVS is controlled by the statistical characteristics of the data and the choice of the smoothing parameters is automated.

D'Amico *et al.*, 1990 reported yet another technique, which is called linear-phase autoregressive model-based derivative assessment algorithm (LAMBDA). The cut-off frequency is automatically chosen based on the desired SNR. The SNR value used was 50 dB after examining many biomechanical data recordings. An autoregressive model is fitted to the data and used in order to estimate the power spectrum density.

The residual analysis method used by Winter is based on calculating the residual between the signal and filtered output using a Butterworth filter with varying cut-off frequency. The choice of cut-off frequency is made to equalise the amount of signal distortion and allowed noise. This is considered a good compromise, however it is a subjective and arbitrary one. This method has also proved to be prone to other considerations that will become clear later in this chapter (Winter 1990).

Challis 1999 described another procedure for the automatic determination of filter cut-off frequency. The cut-off frequency is chosen so that the difference between the filtered and unfiltered data is the best approximation to white noise, *i.e.* a residual with a minimum auto-correlation coefficient. The noise is assumed to be white, *i.e.* stationary, uncorrelated and with a mean value of zero.

Giakas *et al.*, 2000 used the Wigner function to represent the signal in the time-frequency domain. Filtering in this domain is achieved by considering only those components within a “suitable” region of the time-frequency plane. This requires some knowledge about the characteristics of the signal in terms of its time-frequency distribution. Also, the “suitable” region for filtering is to be based on well-educated subjective choice. In a more recent paper, Georgakis *et al.*, 2002 described some developments and improvements on

the time frequency filtering technique presented in the earlier paper. The controlling parameters for the filter were optimised and chosen automatically without user intervention or knowledge of the reference acceleration. The technique was shown to be superior to other conventional methods in the filtering of kinematic signals with high impacts. This performance however was not maintained when low frequency content signals were used for its assessment. A different issue with this approach is related to the effects of the uncertainty principle on time-frequency analysis. Detailed consideration of this issue is not relevant to the current work, however, briefly the principle entails that accurate representation in one domain compromises the accuracy in the other.

Some important observations can be made in relation to the methods discussed above, and are summarised in the following points:

- Most of these methods assume that the sampling rate of data is relatively high in order to provide a high number of data points for each signal. This is important in order to avoid the aliasing effects. The Nyquist criterion that states that the sampling frequency should be at least twice the highest signal frequency component is often met and higher sampling frequencies are almost always used. This minimises the amount of white noise that will be mapped into the signal region.
- The assumption that the noise and signal frequency spectra do not significantly overlap. This is a result of the signal main components being of relatively low frequency, while that of noise extending over the whole spectrum.
- Systematic errors due to noise or other sources that have frequency content within the signal region, such as movement in skin markers, tissue (loose connective, or muscular) movement, cannot be removed by filtering generally. Some techniques might be available to remove these artefacts by estimating the amount of movement and removing it.

- Most of these methods assume that the noise is white or uncorrelated. In other words, the noise is stationary, additive, and has a mean value of zero, with its autocorrelation function set at zero.
- If the signal is to be filtered in either the time or frequency domain, it can be argued that the signal statistical properties do not change with time and that the filter is applied for the whole period of the signal. This might not be the case for some signals where there are times of impact or high frequency content events, and a dramatic change in the frequency content. In such cases the filtering might need to be adjusted to retain the high frequency components during the impact, but remove them during the rest of the signal.

More recently, wavelet-based techniques have been employed for filtering noisy data including kinematic data (Ismail *et al.* 1999; Wachowiak *et al.* 2000). Wavelets are known to be relatively powerful in analysing signals with time-varying frequency content, which can be argued to be the case for some of the gait kinematic signals. A good example is the change in frequency content due to sharp changes and impacts such as heel strike. Both studies reported a good performance when compared to other conventional methods. The data used was that of Pezzack encompassing simultaneous camera and accelerometer recordings of an aluminium “arm” moving with displacements within the range of many human motor tasks. The second paper used accelerometer signals from a subject’s hand hammering a table. The displacement data was obtained by direct numerical integration and noise (zero-mean and white) was added to the displacement data to test the effectiveness of the technique. These techniques are yet to gain widespread use in kinematic data smoothing and filtering. This might be due to the fact that conventional methods produce satisfactory results for most applications. Some comparative studies utilising real kinematic gait data are needed to better evaluate the performance advantage of these novel approaches.

The above survey shows that the area of smoothing and differentiation of noisy kinematic data has been well investigated. One conclusion from this survey is that each one of the above methods makes certain assumptions about the data or the noise inherent in the signal

or both. Thus the issue becomes one of knowing what the assumptions are and whether they are applicable for that particular application, rather than finding the best method. It is made obvious in some of the studies that assess these techniques that some methods have certain advantages over others but no method is declared as the universal or most suitable technique for all applications (Giakas *et al.* 1997). A better understanding of the motion signal, including its frequency content, and the noise added, including its sources and characteristics, becomes a prerequisite for selecting the suitable approach for smoothing and differentiating the data in each particular application.

The survey also showed that a “well-educated”, “arbitrary”, or “subjective” choice of a “suitable”, “prescribed”, “good”, or similar nature has to be made in the process of deciding on a cut-off frequency. This choice can be viewed as application dependent and one way of optimising this choice is by finding an objective way of representing the signal. As the subject of this work is the study of the band-limited kinematic signals from gait, with relatively no high impact events, it was reasonable to use the approach of low-pass filtering for data smoothing and noise suppression. It was therefore decided to analyse the frequency content of the raw position data signal, before deciding on a choice of cut-off frequency for low-pass filtering of the data.

5.4 More on the residual analysis method

Before proceeding to describe the experimental work done for frequency content analysis, it is worth discussing in some more detail the very common residual analysis method of Winter for the filtering of gait kinematic data (Angeloni *et al.* 1994; Hreljac *et al.* 2000).

This technique is based on calculating the residual differences between filtered and unfiltered signals for a different range of cut-off frequencies. The signal is filtered using a 2nd order Butterworth low-pass and zero-phase-shift filter (data filtered twice: once in each direction). The residuals are calculated as the root mean square differences between the filtered and raw data. The residuals are then graphed against the filter cut-off frequency. At high frequencies, where the signal is mainly composed of noise, the residuals are expected to be small and reflect the noise content of the signal. As the cut-off frequency is decreased, the signal content of the data increases and hence the residuals increase. Hence, the lower the cut-off frequency, the more signal attenuation and the

higher the signal distortion is. The higher the cut-off, the lower the signal distortion, but the more noise is allowed through the filter. Winter selects the optimal cut-off frequency as the one that equates the amount of signal distortion to allowed noise through the filter.

Winter also suggests doing a power or harmonic analysis of the data, and selecting a cut-off frequency based on how much power (99% for example) is to be accepted or rejected (Winter *et al.* 1974); and (Winter 1990). He criticises this approach, however, on the basis that the filtering on that basis assumes that the filter response is ideal and has an infinitely sharp cut-off. The above residual analysis method is proposed as a better alternative.

The main objective of the study described below was to assess the frequency content of lower limb kinematic signals. The residuals were also calculated as described by Winter and a comparison between the two approaches was drawn.

5.5 Study plan and methods

10 subjects with no observable gait abnormalities took part in the study (see Table 5-1).

Table 5-1: Detailed data of subjects who took part in this study.

Subject	Age (years)	Sex (M/F)	Height (m)	Weight (kg)
Average:	32.4	-	1.73	78.2
Standard Deviation	10.8	-	0.07	19.5
1	25	M	1.86	125
2	57	M	1.75	75
3	23	M	1.80	90
4	29	F	1.67	67
5	46	M	1.68	68
6	27	F	1.76	83
7	27	F	1.60	53
8	27	F	1.73	65
9	28	M	1.70	80
10	35	M	1.72	76

A Qualisys ProReflex motion capture system was used to capture the position of 7 retroreflective markers. These were placed lateral to the centre of the thigh, anterior to the shank (2 markers 15 cm apart the higher marker approximately 5 cm below the knee), on

the lateral malleolus, on the posterior end of the lateral border of the calcaneus, on the fifth metatarsal head, and dorsal to the first metatarsal head. Two of the foot marker positions are the same as those previously used for the kinematic gait event detection, while the other two are commonly used positions for gait analysis. The shank markers positions were chosen so to allow the calculation of the shank angular velocity relevant to the Gyro sensor work. The frequency content of the thigh marker was expected to be lower than that of more distal markers, and thus the location of the thigh marker was used to confirm this expectation. The Qualisys QTrac Capture 2.74p was used to track the motion data.

Each subject performed a total of 18 trials. The subjects were barefoot and performed three trials at each one of three self-selected speeds (normal, fast, and slow). This was repeated with the subjects walking shod. The data was sampled at 240 Hz, tracked and then 1 cycle was extracted from each traverse. Any marker with one or more missing frames in any of the three co-ordinates resulted in ignoring the data for that marker in that particular traverse.

5.5.1 Data analysis

Two consecutive maxima in the heel Z co-ordinate were used to decide on 1 cycle time. The mean of each of the co-ordinate data was removed and the resulting zero-mean X, Y and Z (X anterior-posterior, Y medial-lateral, and Z vertical) co-ordinates were detrended before applying a Fourier Transform. Detrending the data compensated for the non-periodic cyclic nature of the data. The power spectrum of each signal was calculated from the periodogram using the conventional power spectrum estimation Welch method. Selecting a finite time-domain sequence of a signal for power calculation, results in limited frequency resolution and a bias in the power estimate and leads to errors in the spectrum. Longer data recordings reduce the bias and improve on the frequency resolution, but compromise the variance. The Welch method and the application of a time window to the sampled data signal were utilised to achieve a compromise in the estimation of the power spectrum (Welch 1967). A Hanning window was chosen to improve on the frequency resolution and to minimise 'leakage' in the calculated spectrum of the kinematic signals. From the power spectrum of each signal a set of descriptive parameters were calculated. These were:

- FC99 the frequency below which $\geq 99\%$ of the power exists
- FC95 the frequency below which $\geq 95\%$ of the power exists
- FC1 the minimum frequency at which the component power and any higher harmonics falls below 1% of the total power

FC99, FC95, and FC1 from all 10 subjects were averaged for each speed and footwear, and the standard deviations were calculated.

The 3D co-ordinate data from the normal speed and barefoot trials were also filtered in both directions using a second order Butterworth filter with a varying cut-off frequency in steps of 0.25 Hz from 0.25 Hz to 120 Hz (half the sampling frequency).

The averaged residuals (same as the root mean square error (RMSE)) for each co-ordinate of the 7 markers between the filtered and unfiltered data (over 1 cycle) were calculated and plotted as described by Winter:

Equation 5-2

$$RMSE = \sqrt{\frac{1}{N} \sum_{i=1}^N (X_i - \hat{X}_i)^2}$$

Where X_i is the raw value of the signal X at the i^{th} sample

\hat{X}_i is the filtered value of the signal X at the i^{th} sample

N is the number of sample points in time for the signal X

The compromise used by Winter to select the cut-off frequency, as that equating signal distortion to allowed noise through the filter, can be derived graphically from the residual versus filter frequency plot (see Figure 5-1). The linear part of the residual plot represents the best estimate of the noise residual. Any cut-off frequency (above Fc1) will allow a proportion of the noise to go through the filter (line 2). A linear line is then fitted to the noise residual estimate (dashed green line) and the y-intercept (R1) is defined. The sharp increase in the residual value at low filter cut-off reflects the loss of signal data or signal

distortion (line 1). The cut-off frequency, $Fc1$, is then chosen as the frequency where the residual and a horizontal line projected from $R1$ intersect. This represents a compromise where the signal distortion and the amount of noise allowed through are equal.

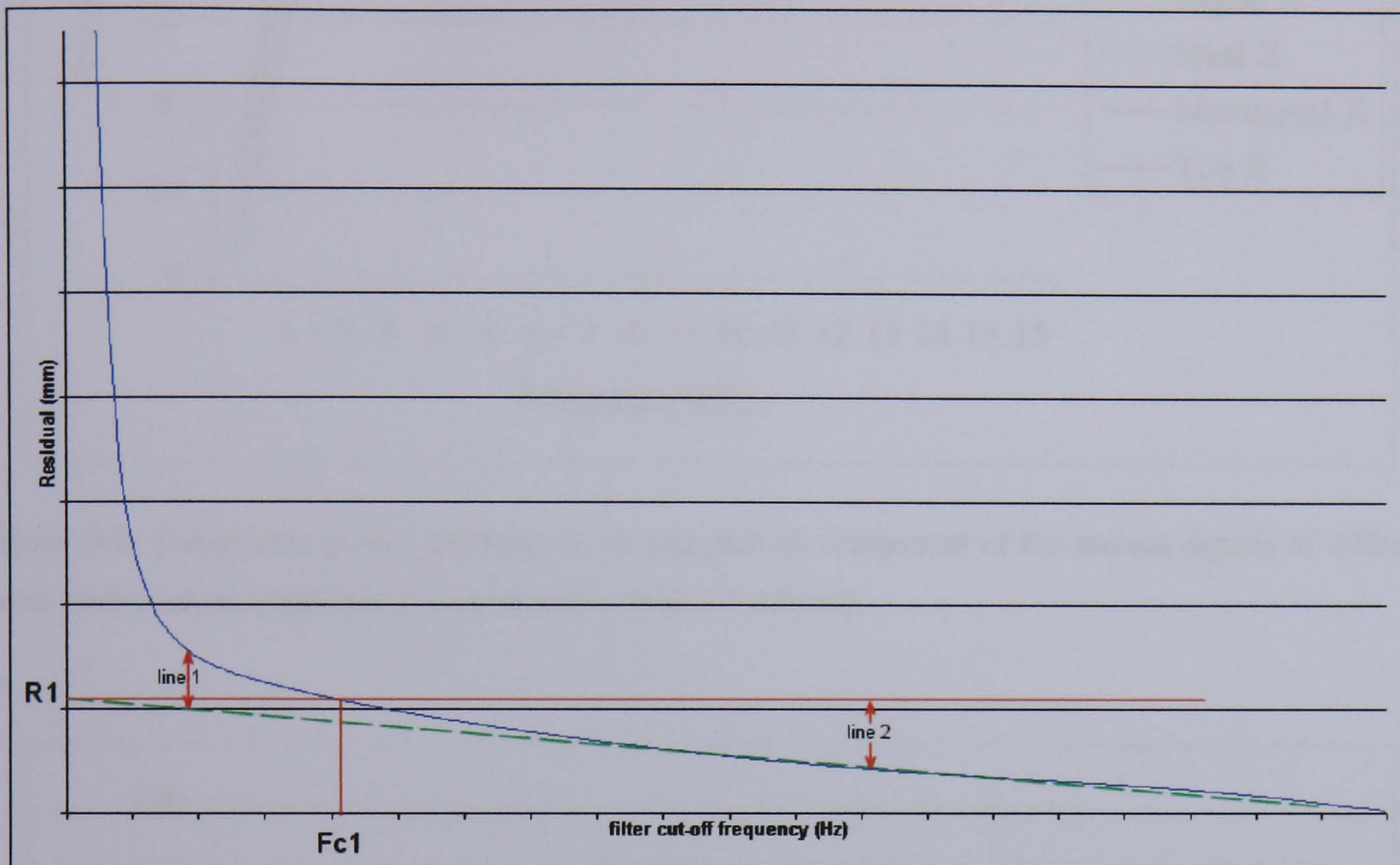


Figure 5-1: A representative plot of residual between filtered and unfiltered data vs. filter cut-off frequency (Winter 1990).

5.5.2 Results

Figure 5-2, Figure 5-3, and Figure 5-4 show the cumulative power spectra for the 3 directions using data from 1 representative trial by one of the subjects walking barefoot at self-selected normal speed. It can be seen from those three Figures that the major part of the signals in all 3 directions is in the low frequency range. The power distribution appears very similar among different markers for the X direction but more varied for the Y and Z directions (X anterior-posterior, Y medial-lateral, and Z vertical).

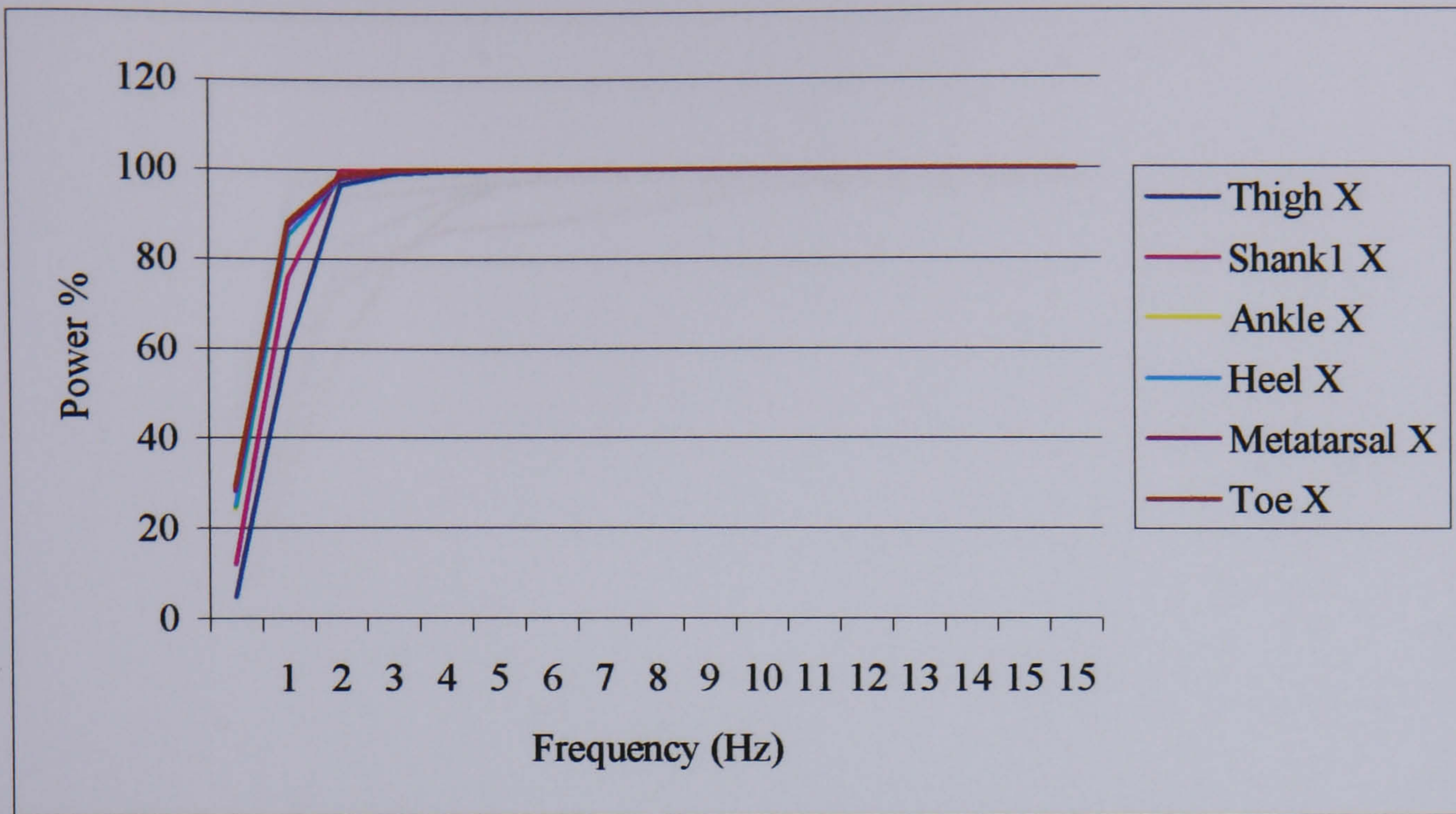


Figure 5-2: Cumulative power spectrum in the progression component of the motion signals of different lower limb markers (data from 1 representative trial of 1 subject).

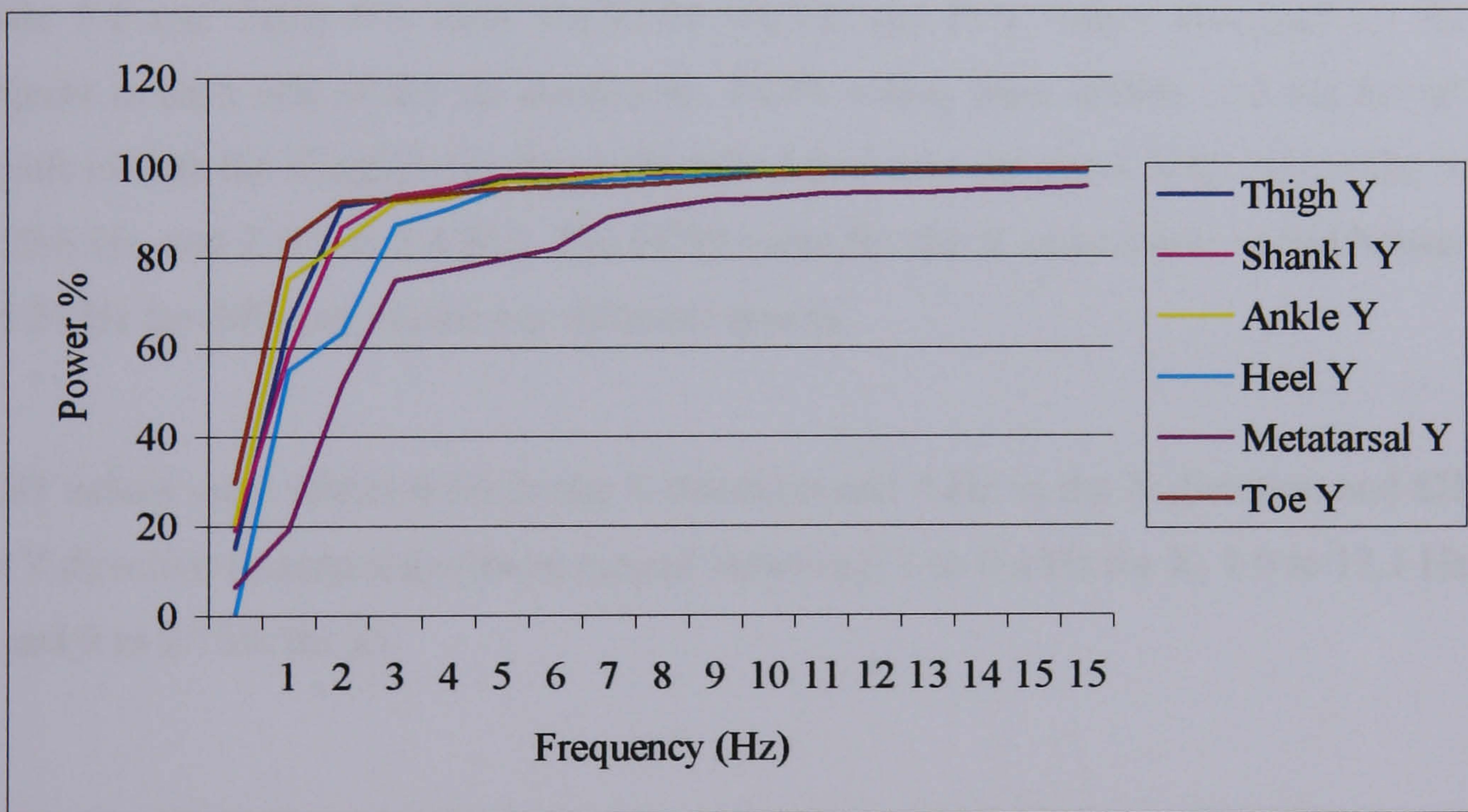


Figure 5-3: Cumulative power spectrum in the medial-lateral component of the motion signals of different lower limb markers (data from 1 representative trial of 1 subject).

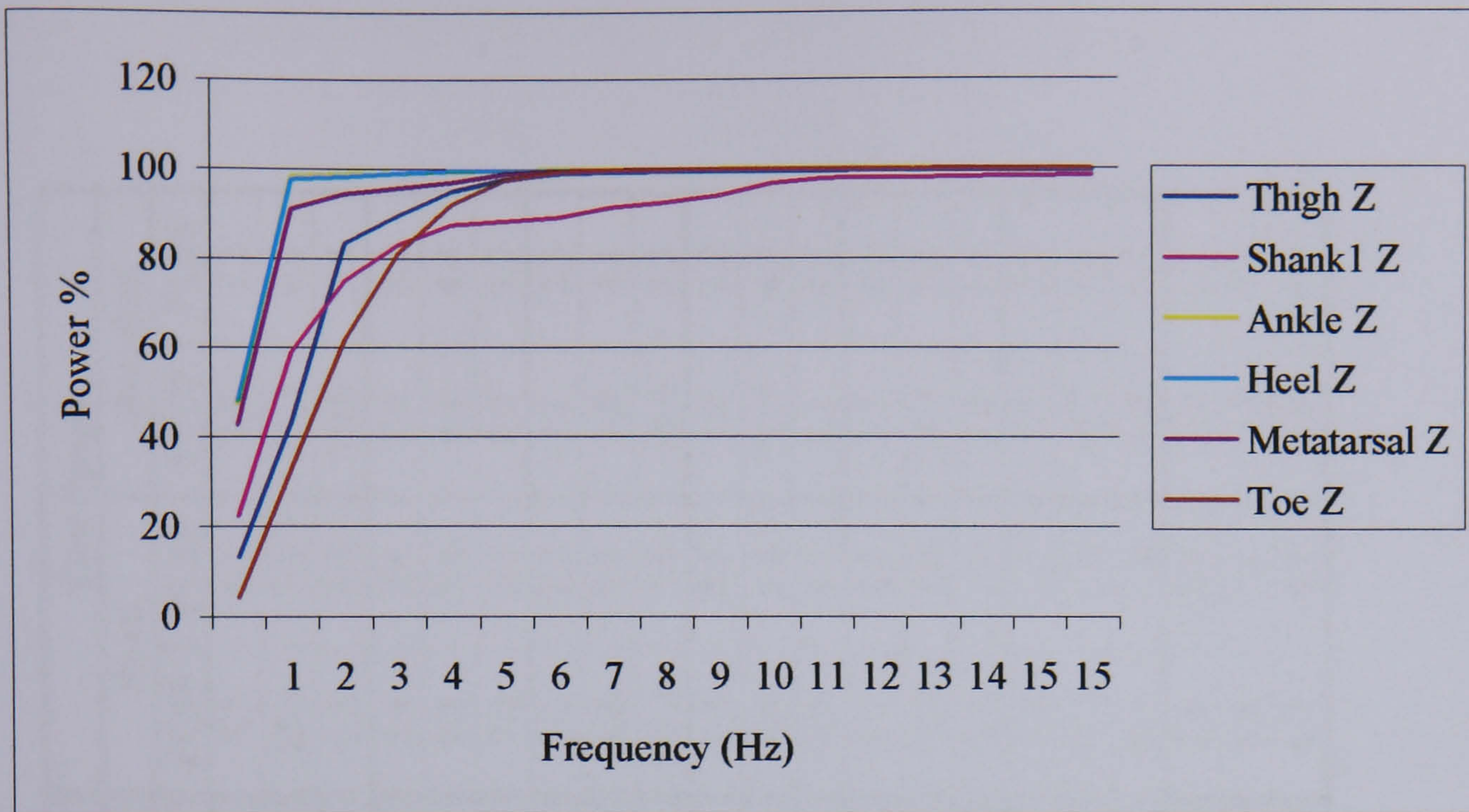


Figure 5-4: Cumulative power spectrum in the vertical component of the motion signals of different lower limb markers (data from 1 representative trial of 1 subject).

Table 5-2 and Table 5-3 show the FC99, FC95, and FC1 values averaged for the 10 subjects in each one of the six conditions. FC99 values were within 10.6 Hz for all the signals in both the X and Z directions (Standard deviation ranges in X 0.1 to 1.5 Hz, Y 2.0 to 29.6 Hz, and Z 0.3 to 5.4 Hz). The FC99 value for the Y co-ordinate varied between 6 and 24 Hz for different markers at different speeds.

FC95 values were within 6 Hz in the Z direction and 4 Hz in the X direction and 8 Hz in the Y direction (standard deviation ranged between 0.1 to 0.4 Hz for X, 1.0 to 12.1 Hz for Y, and 0 to 2.7 Hz for Z).

When FC1 is considered, all values were within 5 Hz for X, 8 Hz for Z and 9 Hz for the Y direction (standard deviation ranges in X 0.1 to 0.7 Hz, Y 1.0 to 3.5 Hz, and Z 0.4 to 3.0 Hz). This indicated that any components above 9 Hz contribute less than 1% of total power.

Table 5-2: The FC99 and FC95 values (in Hz) for the 7 markers for different speeds and footwear.

Speed: Footwear: MARKER	Normal Speed						Slow Speed						Fast Speed					
	Shod			Barefoot			Shod			Barefoot			Shod			Barefoot		
	FC99	FC95	FC99	FC99	FC95	FC95	FC99	FC95	FC99	FC99	FC95	FC95	FC99	FC95	FC99	FC99	FC95	FC95
Thigh X Y Z	3.4	2.0	3.1	3.0	1.9	2.0	3.0	1.9	3.0	1.8	1.8	3.2	2.1	3.3	3.3	2.2	2.2	2.2
	12.5	4.5	8.7	6.2	2.8	4.0	6.5	2.8	6.5	3.0	3.0	15.5	7.0	11.3	11.3	6.1	6.1	6.1
	7.8	4.1	8.1	7.1	3.9	4.4	8.1	3.9	8.1	4.2	4.2	8.5	4.7	10.0	10.0	5.5	5.5	5.5
Shank1X Y Z	2.3	1.9	2.0	2.0	1.7	1.9	2.1	1.7	2.1	1.7	1.7	2.4	2.1	2.6	2.6	2.2	2.2	2.2
	9.5	4.6	7.7	7.0	3.9	3.5	7.6	3.9	7.6	3.3	3.3	9.3	5.4	9.1	9.1	4.4	4.4	4.4
	6.5	3.2	8.2	5.8	2.8	3.4	7.7	2.8	7.7	3.0	3.0	7.0	3.7	8.7	8.7	3.7	3.7	3.7
Shank2 X Y Z	1.9	1.9	1.9	1.7	1.7	1.9	1.7	1.7	1.7	1.7	1.7	2.2	2.2	2.3	2.3	2.3	2.3	2.3
	9.1	5.1	7.6	9.1	4.5	3.4	7.5	4.5	7.5	4.0	4.0	8.8	5.5	8.0	8.0	4.1	4.1	4.1
	8.7	4.4	10.6	8.7	4.5	5.2	8.7	4.5	8.7	4.3	4.3	10.1	5.5	10.6	10.6	5.5	5.5	5.5
Ankle X Y Z	2.7	1.9	2.8	2.5	1.6	1.9	2.6	1.6	2.6	1.7	1.7	2.7	2.1	3.2	3.2	2.2	2.2	2.2
	7.4	3.5	16.9	7.4	3.2	5.4	19.0	3.2	19.0	3.8	3.8	9.4	4.6	12.5	12.5	4.3	4.3	4.3
	2.8	0.9	3.1	2.2	0.8	1.0	2.5	0.8	2.5	0.9	0.9	4.0	1.1	4.1	4.1	1.1	1.1	1.1
Heel X Y Z	2.8	1.9	2.9	2.5	1.7	1.9	2.6	1.7	2.6	1.7	1.7	3.2	2.1	3.3	3.3	2.2	2.2	2.2
	15.2	6.7	23.3	18.2	6.1	7.1	14.3	6.1	14.3	4.1	4.1	16.0	5.8	14.1	14.1	5.2	5.2	5.2
	2.7	0.9	2.8	2.0	0.8	1.0	2.5	0.8	2.5	0.9	0.9	3.3	1.1	3.2	3.2	1.1	1.1	1.1
Metatarsal X Y Z	2.8	1.9	4.3	2.5	1.7	1.9	2.6	1.7	2.6	1.7	1.7	3.2	2.1	3.3	3.3	2.2	2.2	2.2
	21.3	6.1	22.4	16.5	4.4	8.2	22.7	4.4	22.7	6.3	6.3	17.3	5.5	19.7	19.7	7.1	7.1	7.1
	5.5	4.0	5.9	5.0	3.4	3.5	5.1	3.4	5.1	3.0	3.0	6.1	4.8	6.5	6.5	4.3	4.3	4.3
Toe X Y Z	2.6	1.9	2.9	2.4	1.7	1.9	2.6	1.7	2.6	1.7	1.7	2.5	2.1	3.3	3.3	2.2	2.2	2.2
	8.5	4.4	8.1	8.5	4.0	3.8	9.1	4.0	9.1	4.1	4.1	8.9	5.1	11.9	11.9	4.2	4.2	4.2
	5.6	4.3	6.0	5.3	4.1	4.7	5.6	4.1	5.6	4.3	4.3	6.2	4.7	6.9	6.9	5.4	5.4	5.4

Table 5-3: The FC1 values (in Hz) for the 7 markers for different speeds and footwear.

Speed:	Normal Speed		Slow Speed		Fast Speed	
Footwear:	Shod	Barefoot	Shod	Barefoot	Shod	Barefoot
MARKER	FC1	FC1	FC1	FC1	FC1	FC1
Thigh X	3.8	4.0	3.7	3.6	4.1	4.3
Y	6.1	6.1	4.3	4.5	8.9	8.6
Z	5.7	6.2	5.4	5.9	6.4	7.2
Shank1 X	2.8	2.9	2.6	2.6	3.3	3.4
Y	6.8	5.6	5.7	4.9	7.8	6.2
Z	5.4	5.4	4.7	4.7	6.1	6.8
Shank2 X	2.8	2.9	2.5	2.6	3.2	3.4
Y	6.7	5.5	6.1	5.7	8.1	7.0
Z	6.7	7.1	6.4	6.1	7.9	7.9
Ankle X	3.4	3.8	3.0	3.4	3.5	4.1
Y	5.4	6.4	4.9	5.1	6.8	6.4
Z	2.6	2.5	2.2	2.0	3.2	3.3
Heel X	3.7	3.8	3.3	3.5	4.3	4.4
Y	6.2	7.3	5.7	5.6	7.5	6.8
Z	2.0	2.2	1.8	1.8	2.6	2.8
Metatarsal X	3.7	3.9	3.3	3.5	4.3	4.5
Y	6.1	6.6	5.4	6.0	7.1	8.1
Z	6.0	6.0	5.5	5.3	6.7	7.0
Toe X	3.4	3.8	3.0	3.4	3.4	4.2
Y	6.3	5.8	5.4	5.4	7.4	6.1
Z	6.2	6.6	5.8	6.1	6.9	7.7

Figure 5-5, Figure 5-6, and Figure 5-7 show the residual plots for the 3D co-ordinates of the 7 markers in the barefoot and normal speed walking trials. The scale on the vertical axis was chosen in a way to show the low residual values, however the residual values were much higher than 10 mm at the lower end of the frequency range. For example, the residual value for a number of marker co-ordinates was around 500 mm when the filter cut-off frequency was set to 0.25 Hz.

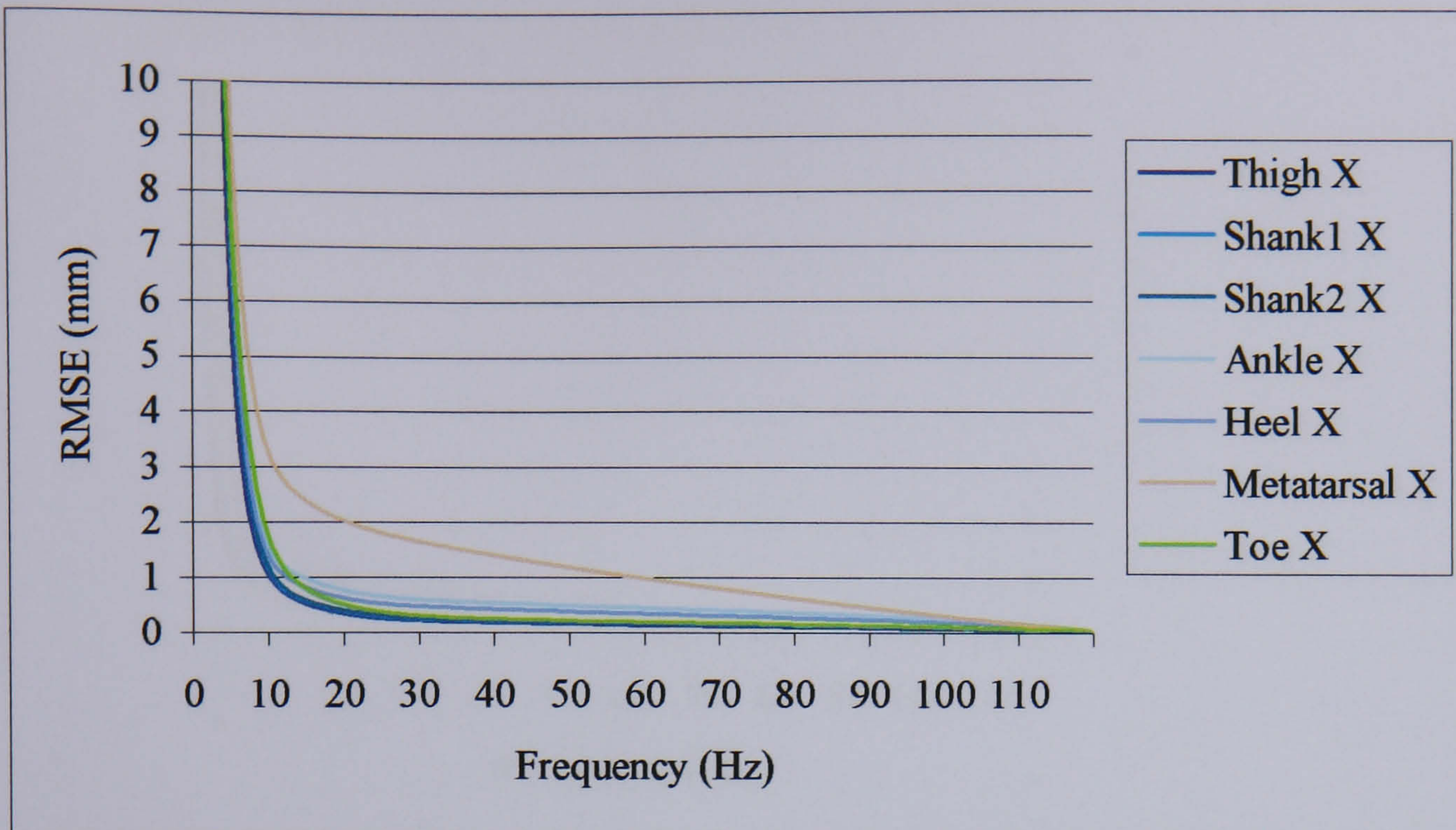


Figure 5-5: The residuals in the X components of the 7 markers. Data averaged from the 30 barefoot normal speed walking trials.

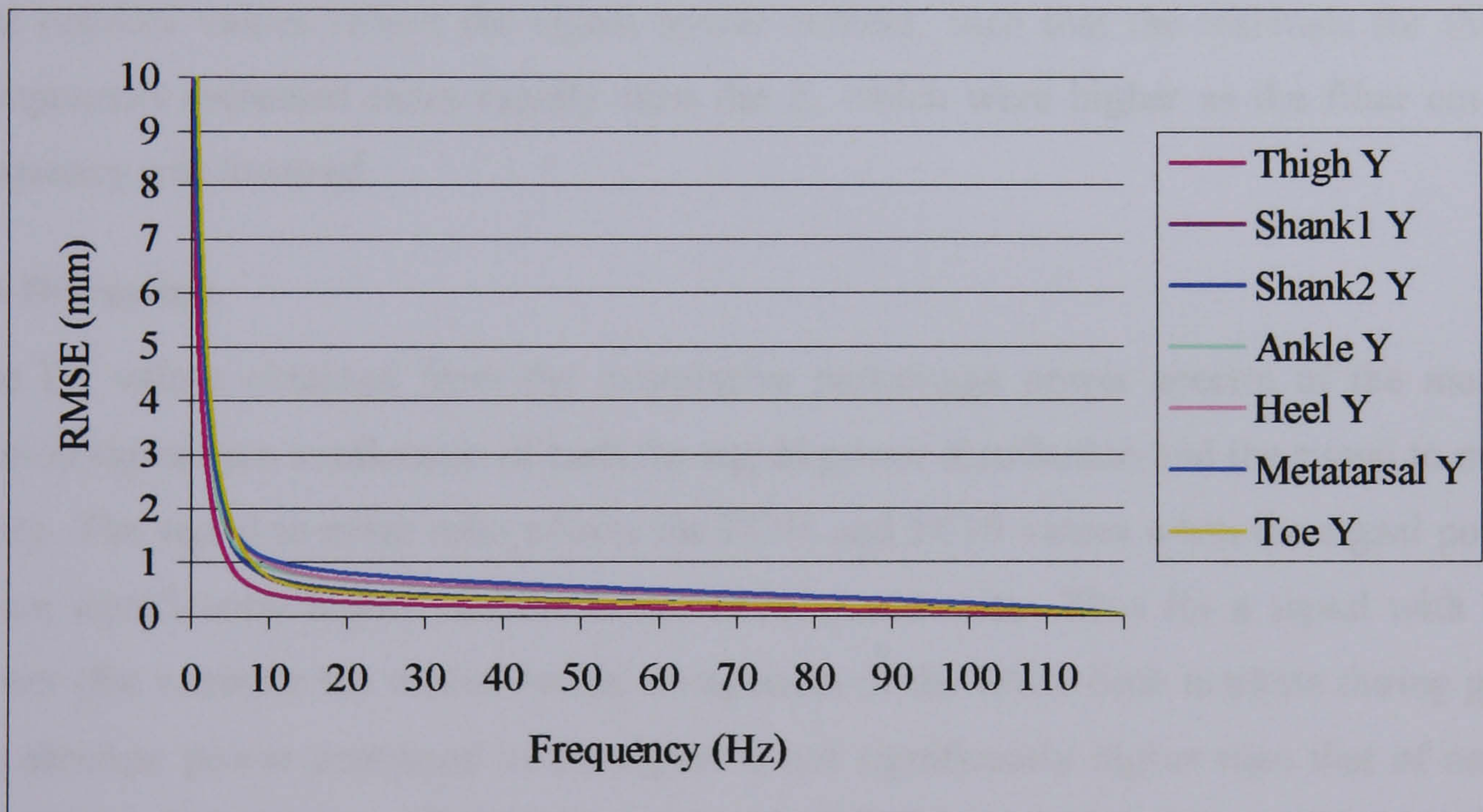


Figure 5-6: The residuals in the Y components of the 7 markers. Data averaged from the 30 barefoot normal speed walking trials.

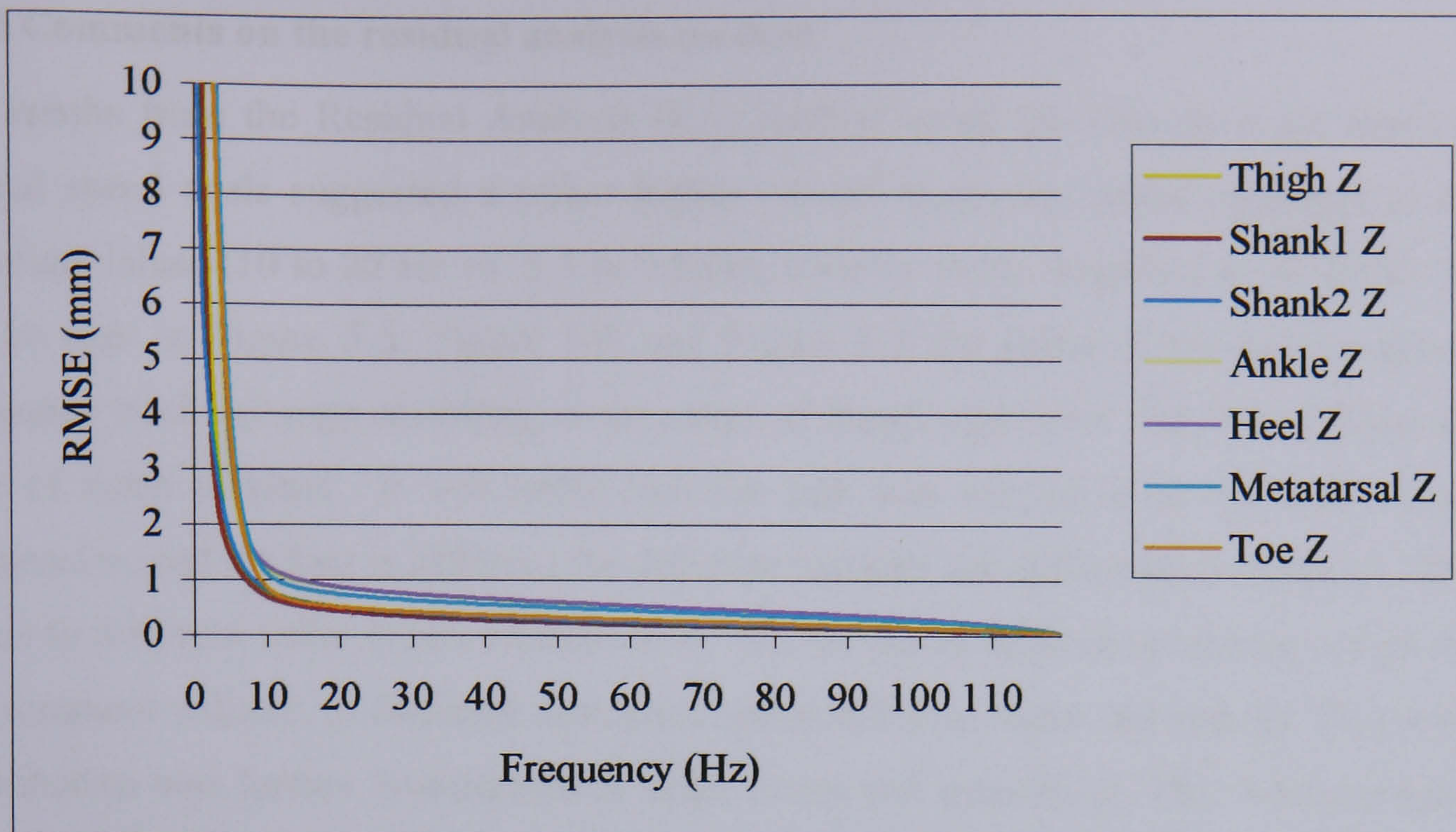


Figure 5-7: The residuals in the Z components of the 7 markers. Data averaged from the 30 barefoot normal speed walking trials.

The residual values reflect the signal power content, such that the residuals for the X components increased more rapidly than the Z, which were higher as the filter cut-off frequency was lowered.

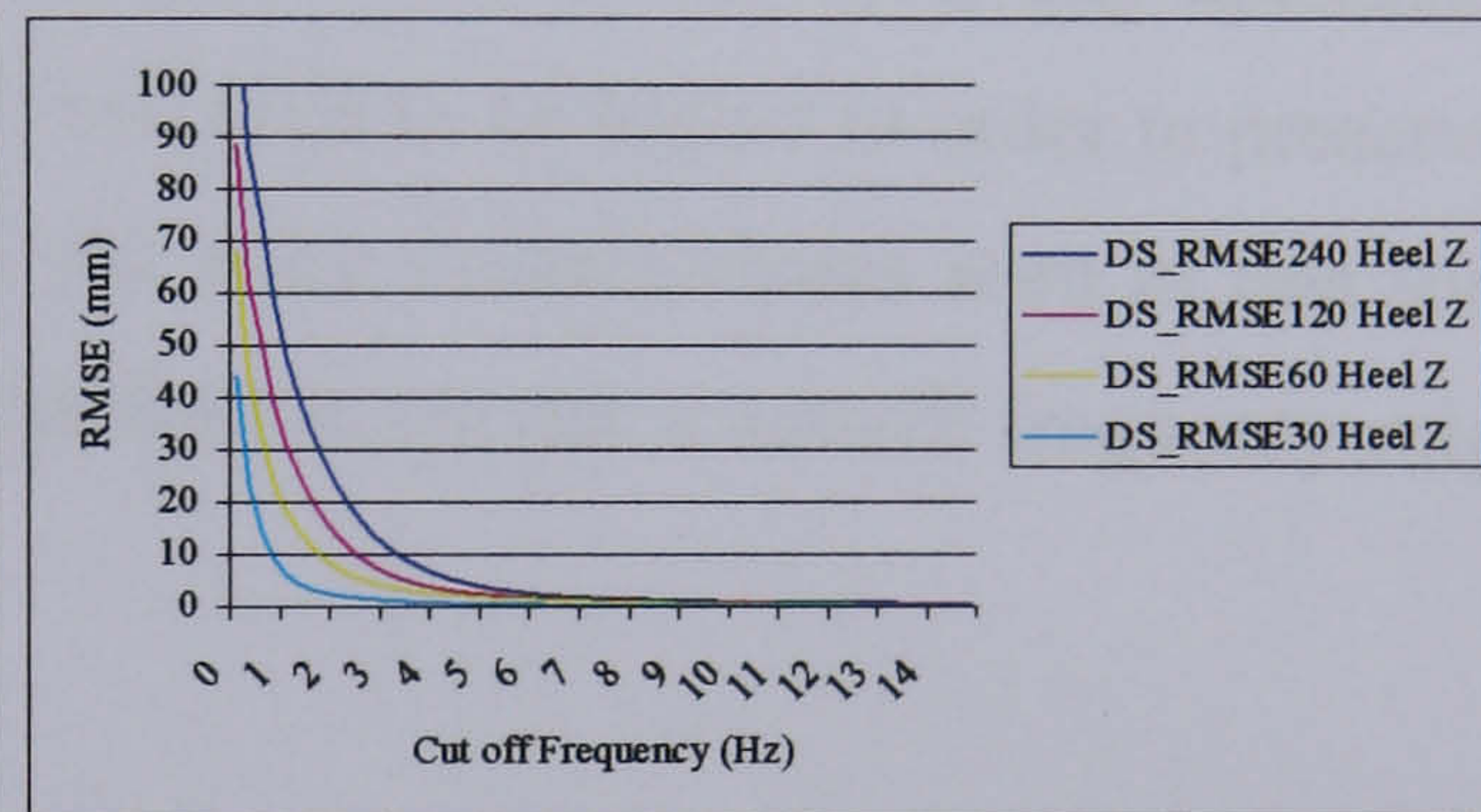
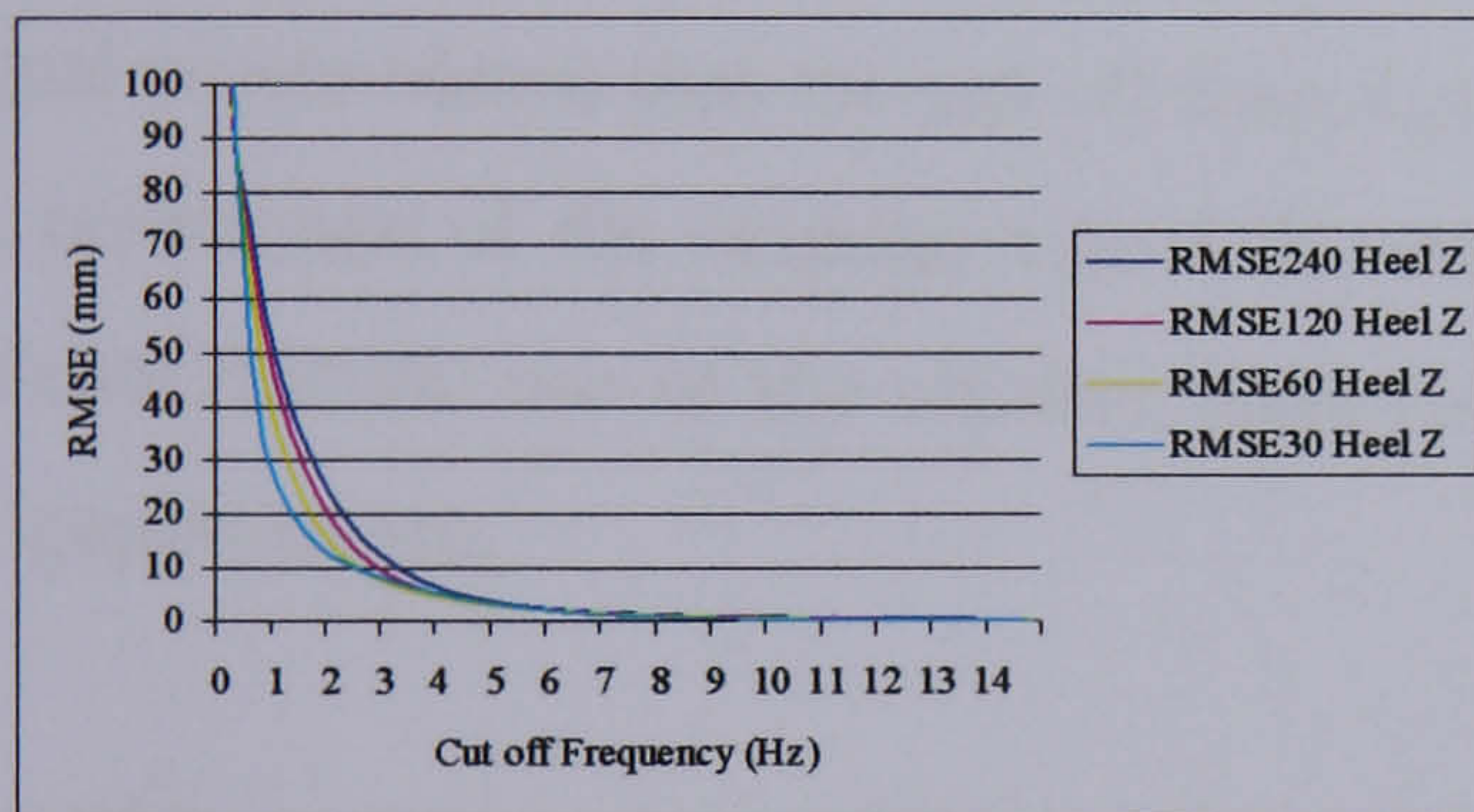
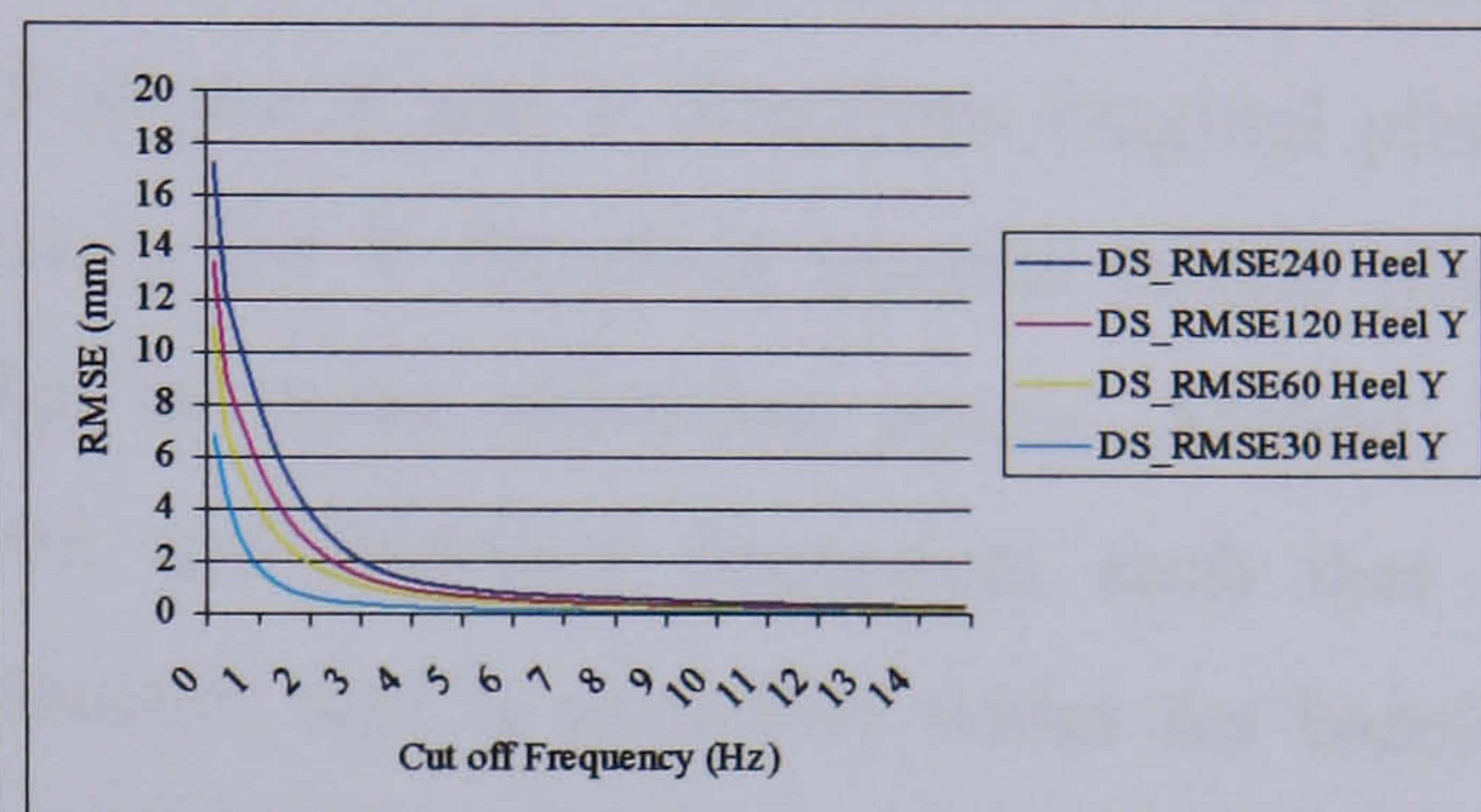
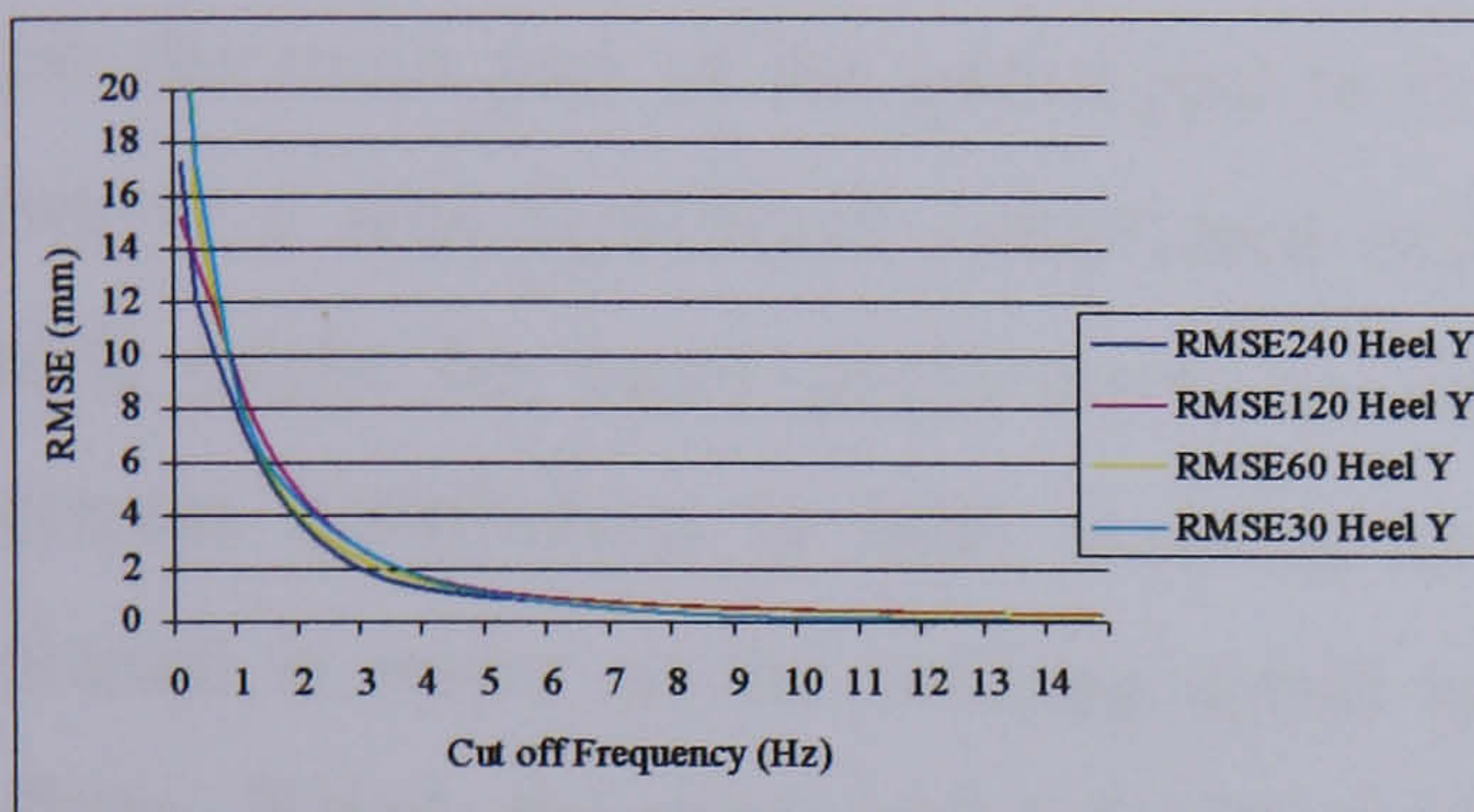
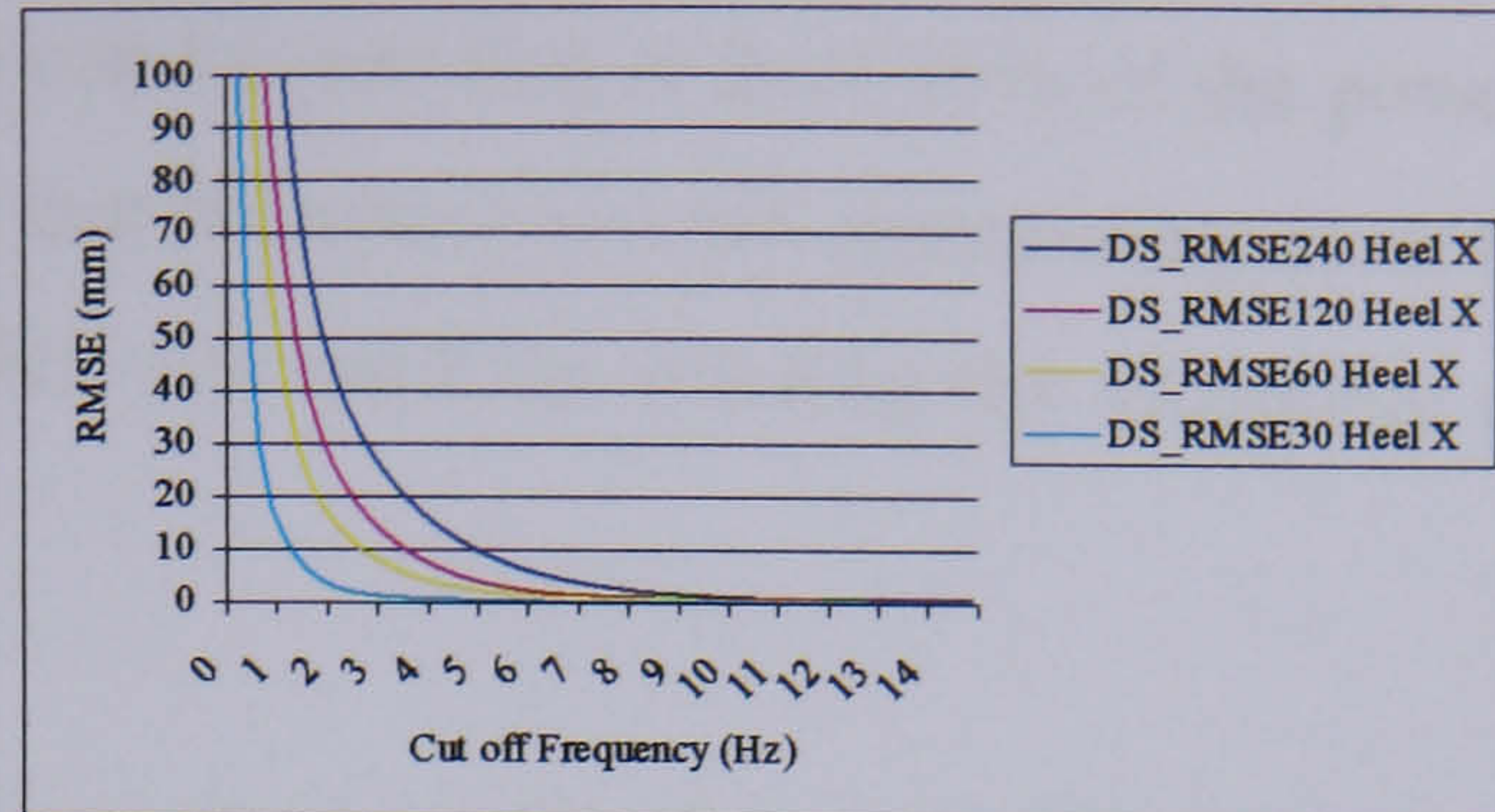
5.6 Discussion

The FC values obtained from the cumulative percentage power spectra of the marker motion signals are a reflection of both the signal power distribution and the signal to noise ratios. The signal to noise ratio affects the FC95 and FC99 values when the signal power is not significantly higher relative to the wide spread noise. Thus for a signal with low power (for example the medial-lateral component of the lower limb markers during gait) the absolute power contained in the signal is not significantly higher than that of noise, and hence the FC95 and FC99 values end up being high (around 20 Hz in some of the cases). This observation limits to a certain extent the usefulness of this approach. However, in these cases the FC1 value becomes a very significant adjunct in determining whether the FC95 and FC99 high value is a result of high frequency signal components or a result of the low signal to noise ratio. Any significant high frequency signal components will be reflected in a high value of FC1, and hence a low value of FC1 combined with high values of FC95 and FC99 are an indication of a very low signal to noise ratio.

5.6.1 Comments on the residual analysis method

The results from the Residual Analysis (RA) method using the data from the barefoot normal speed trials suggested a rather higher cut-off frequency when compared to the literature values (10 to 20 Hz vs. 5.5 to 9.8 Hz) (Winter 1990; Angeloni *et al.* 1994). As can be seen in Figure 5-5, Figure 5-6, and Figure 5-7 the value of the chosen cut-off frequency would change according to the range of frequencies over which we project the 'line of noise residual'. It was noted that the line was not linear at the high cut-off frequencies, and the line is different for different markers and different co-ordinates. This is due to different noise levels introduced by the system at different positions within the measurement volume, in different directions and at different times and speeds. This noise contribution was further investigated in order to try and quantify it. This was attempted using recordings of both static and moving markers with some known relationship between their co-ordinates; however this proved to be a virtually impossible task. This is because the noise in the resulting 3D co-ordinates depends on a variety of parameters that cannot be standardised as such. One could, in theory, compensate for variable noise levels depending on the position within the measurement volume. However noise levels depended on other factors such as orientation relative to the cameras, obstruction, and speed.

The noise level also varied with the sampling frequency. For example, the total power in a signal from a static marker was similar for different sampling frequencies, and hence at the lower end of the spectrum the component power was higher for lower sampling frequencies, with the exception of the Y direction data. This meant the residual between the filtered and unfiltered data was lower for the lower sampling frequencies with a higher slope at very low cut-off frequencies. When the same data was down sampled to 120, 60 and 30 Hz (Figures 5-11, 12 & 13), the RA method suggested a cut-off frequency within previously reported ranges (5 to 10 Hz). This was also the case when the sampling rate was decreased to 120, 60 and 30 Hz (Figures 5-8, 9 & 10). This added another parameter on which the choice of cut-off frequency depended if we were to use the RA method outlined by Winter.



Figures 5-8, 5-9, and 5-8: Plot of the residuals for the 3 co-ordinates of the heel marker. Data sampled at four different frequencies (240, 120, 60, and 30) for 1 shod and normal speed trial.

Figures 5-11, 5-12, and 5-13: Plot of the residuals for the same heel marker data sampled at 240 Hz and down sampled to 3 different frequencies (120, 60, and 30).

5.7 Conclusions

The use of gait kinematic data for gait event detection, as described in Chapter 4, required the differentiation of noise contaminated raw position data. Differentiation of noisy signals is known to degrade the signal to noise ratio. The main frequency components of gait kinematic signals are band limited and of relatively low frequency, and hence low-pass filtering of data is one way to minimise the effect of wide band noise differentiation. The study described in this chapter was utilised for a more informed choice of cut-off

frequency. As can be seen from the results, selecting 10 Hz as a cut-off frequency for the low-pass filtering of the above data set, one can be sure that at least 95% of the power is maintained, and also any components above that frequency are not contributing more than 1 % of the total power. This value of 10 Hz was used for filtering the kinematic data before its use in gait event detection.

The results from the power-frequency analysis done on the data set collected confirm previously reported characteristics of kinematic gait data and highlight a few new points. First, the main part of the gait signal is in both the X and Z directions (sagittal plane), however a less significant component exists in the Y direction (medial lateral plane) which might be more problematic in terms of noise reduction issues. Second, the spectrum distribution is both walking speed and footwear dependent such that the spectrum is wider as the walking speed increases, and is generally wider for barefoot walking. Third, the total power in the marker signals increases as the marker is moved from a proximal to a more distal position on the lower limb. However any decrease in signal power means that the cut-off frequency will need to be higher in order to preserve a set percentage of the original signal. Fourth, the noise characteristics seen in this study indicate that the use of the residual analysis method to choose a cut-off frequency might be inappropriate.

In a wider context, the problem of kinematic data smoothing and differentiation remains an issue worth investigating and a challenge for anyone in the field. The considerable development to existing methods and innovative techniques to deal with it has resulted in many acceptable methods. The improvement in measurement systems, digitisation techniques, and computing technologies help reduce the errors and noise in recordings. Systematic errors, such as marker shifting, movement or erroneous positioning, can hopefully be minimised by standardisation and good practice. It is believed, however, that further improvements can be achieved by a better understanding of the kinematic data statistical properties and frequency domain characteristics.

This chapter in combination with chapter 4 described the development of a kinematic based gold standard method for gait event detection. This method is to be used in the evaluation of the new Gyro sensor system for a FES foot drop correction system. The following chapter will describe the methods used to obtain gait temporal data from the

gyroscopic angular rate recordings, and the development of the necessary hardware and software for the Gyro sensor system. The theory, equipment used, experimental protocols, and data analysis procedures will also be considered.

Chapter 6: Theory and methods for the Gyro sensor system

This chapter outlines the methods used in utilising the gyroscope (Gyro) as an artificial sensor for detecting the occurrence of gait events (temporal parameters) and triggering a foot drop FES correction system. The chapter starts by presenting the evidence behind the processing method used in extracting useful information from the angular velocity signals. The experimental protocols, data collection methods and equipment used in the course of this study are then described. At the end, a description of the tools used for analysing the data is given.

6.1 Theory

In the first paper reporting the use of FES to correct for foot drop, Liberson synchronised the application of the electrical current to the peroneal nerve to the swing phase of gait using a heel switch. The main reason behind this choice of synchronisation is the activity pattern of the Tibialis Anterior (TA) muscle during gait. Reported patterns of dorsiflexor activity during gait vary slightly (Figure 6-1), but all state that it initiates in pre-swing, continues throughout the swing phase and terminates briefly after initial contact (loading response), with the peak of activity occurring either slightly before or after initial contact (Winter 1991; Perry 1992; Craik *et al.* 1995; Whittle 1996).

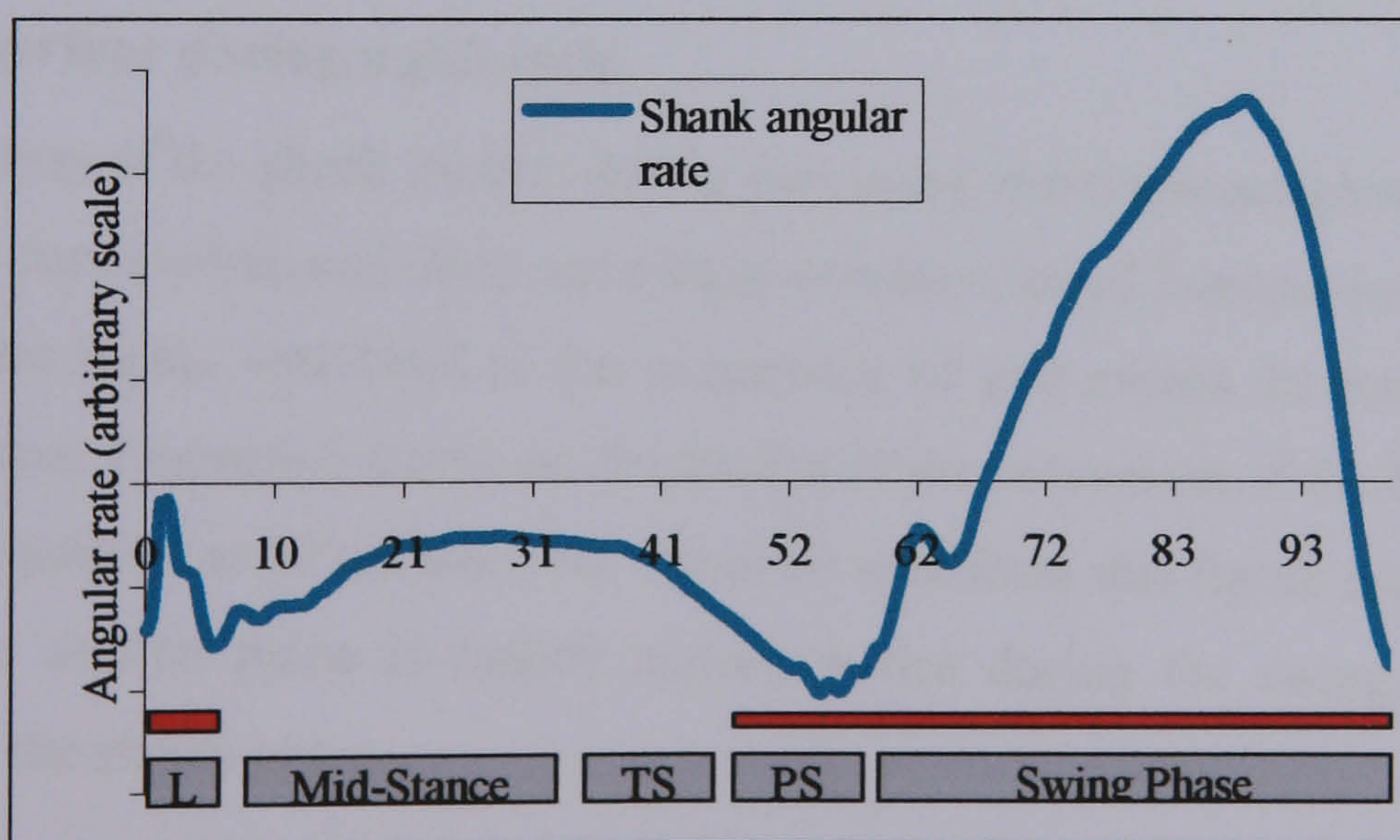


Figure 6-1: The shank angular rate (arbitrary scale) for a representative gait cycle (0 to 100%) with the tibialis anterior active period (in red). (LR = loading response; TS = terminal stance; PS = pre-swing).

In order to stimulate the peroneal nerve at the right time, previous work has suggested that detection of heel rise or terminal stance will be suitable to start the stimulation (with or without a delay /ramp in stimulator output) before the start of pre-swing, and that detection of initial contact will be suitable to terminate (with or without delay/ramp down in stimulator output) stimulation (Figure 6-2). Thus for most applications, effective stimulation requires, at the very minimum, a binary input reflecting the heel state: "Heel On" and "Heel Off".

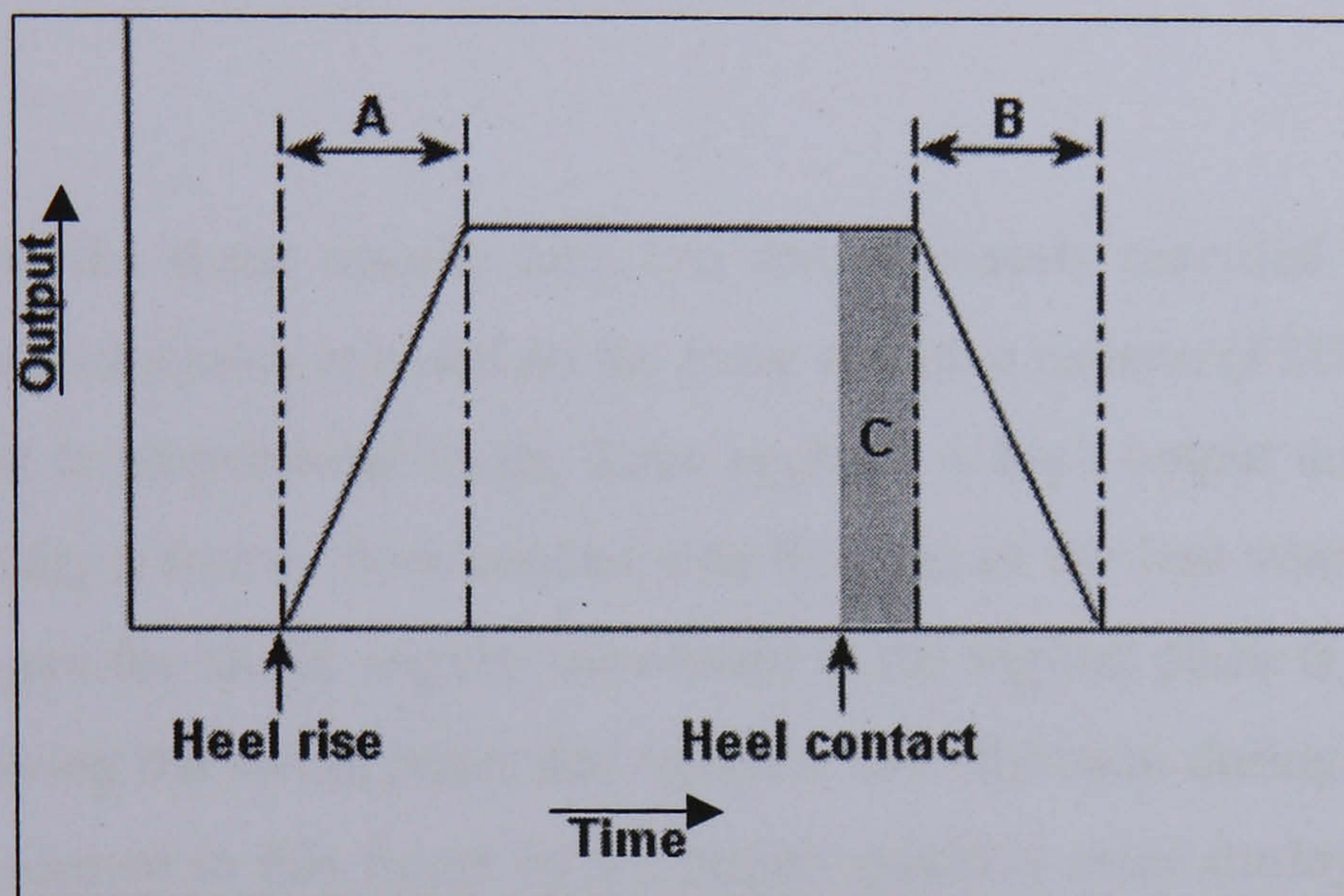


Figure 6-2: Typical stimulator output envelope. Stimulation is started after heel rise with a rising edge ramp (A) and stopped after heel contact with a falling edge ramp (B). An extension to the stimulation time (C) can be applied after heel contact for a better control of plantarflexion.

6.1.1 Shank behaviour during a gait cycle

Careful examination of the shank motion during gait using simultaneous ground reaction force, kinematic, foot switch, and Gyro recordings reveals a set of features in the angular rate signal that are highly correlated to the occurrence of gait events, in particular heel contact and heel rise. Figure 6-3 shows an illustration of the movement of the leg during a single gait cycle sampled at 40 ms intervals. It can be seen from this figure that the shank movement in the sagittal plane is mainly anti-clockwise during the swing phase and clockwise during the stance phase.

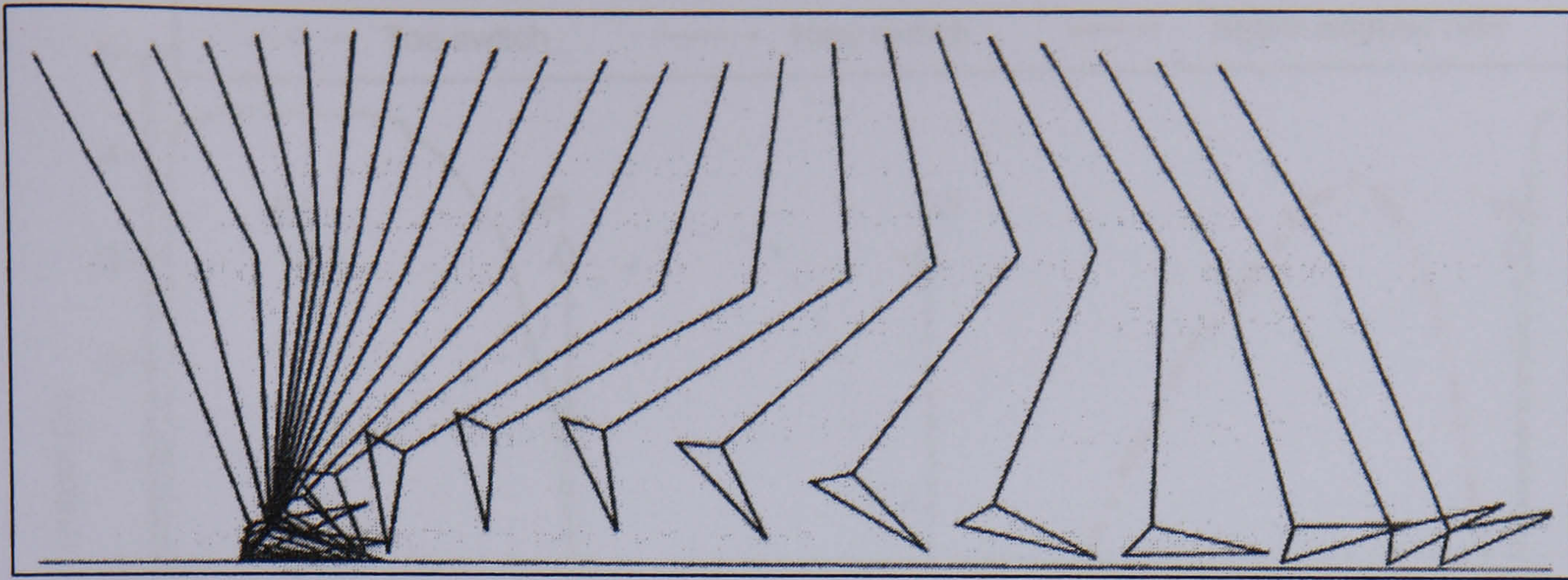


Figure 6-3: An illustration of a single gait cycle showing the position of the right leg at 40 ms intervals. (Whittle 1996).

Figure 6-4 shows the shank angular rate, and simultaneously recorded heel and toe foot switch data. The foot switch is based on the force sensitive resistor (FSR) technology, and hence the output is proportional to the force applied. A high output implies force being applied and usually a foot to floor contact over the area of the foot where the switch was placed. During gait the shank angular movement in the sagittal plane is predominantly in one direction during the swing phase and opposite that direction during the stance phase. This can be confirmed in this figure by the largely positive value during the swing phase and negative value during the stance phase. The occurrence of the heel contact and toe off events can be correlated to two negative peaks in the shank angular rate at the start and end of the stance phase. Between HC and foot flat, the magnitude of the shank angular rate tends to decrease (less negative) and reaches a plateau. As the heel starts to rise off the ground, the shank angular rate starts to increase (more negative) again. The detection of the decreasing slope in the angular rate can be correlated to the occurrence of heel rise. These distinctive features were exploited for the detection of the gait phases and events using a purpose written rule-based algorithm. Although the magnitude and duration of these peaks in the angular rate vary slightly, depending on the particular gait pattern exhibited by the subject, they can always be detected provided we allow for these variations (Ghoussayni 2000).

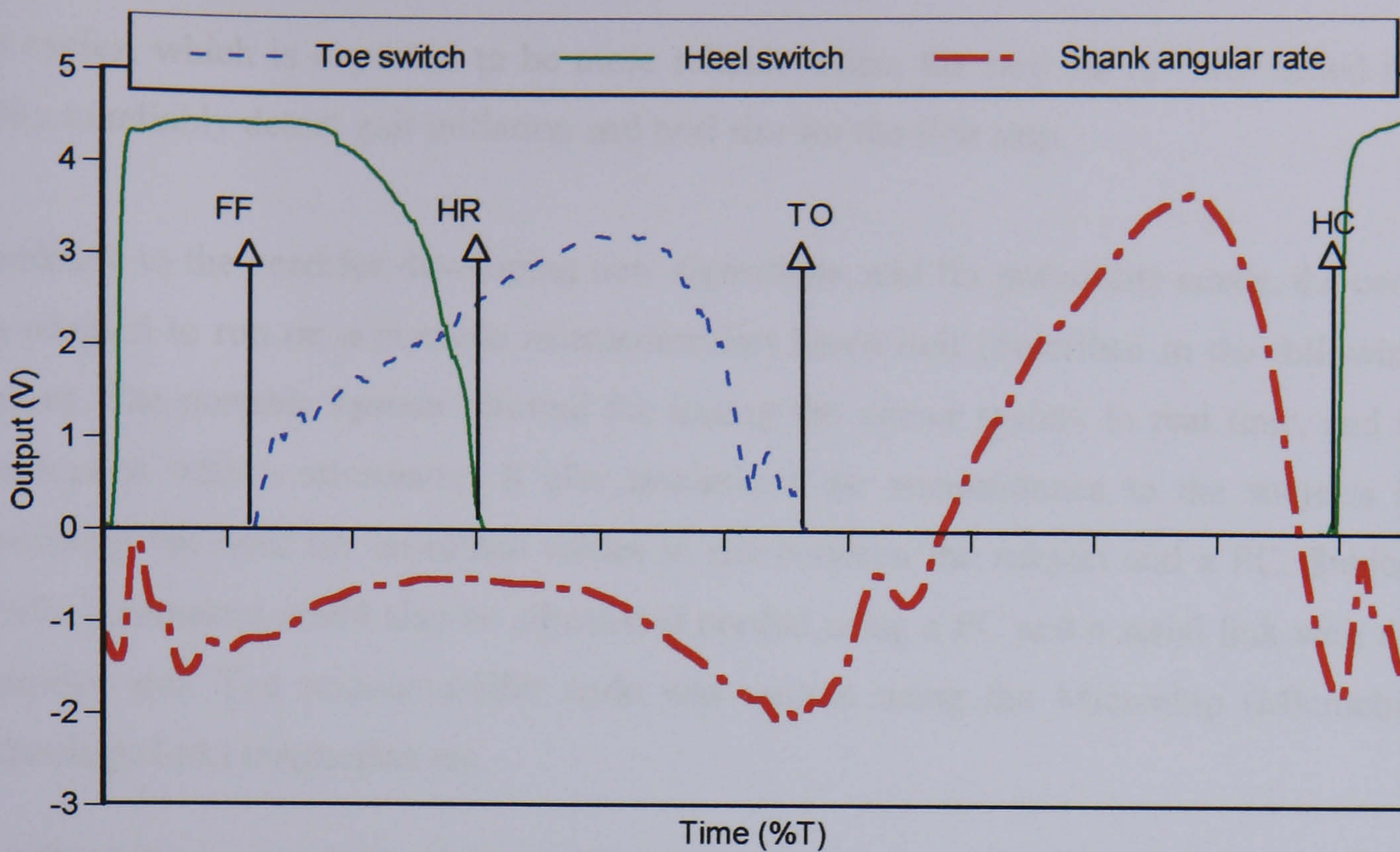


Figure 6-4: A typical gait cycle shank angular rate and foot switch (force sensitive resistor based) recording (HC heel contact, FF foot flat, HR heel rise, TO toe off).

6.1.2 Development of detection algorithms

The above criteria were used in a rule-based algorithm in order to detect heel contact and heel rise. Previous work carried out by the author of this work as part of a MSc highlighted areas of difficulty and challenge for the detection algorithms. The results of the previous work helped guiding the new developments (Ghoussayni 2000). In the previous work, the original code was implemented on a desktop PC, with LabVIEW (National Instruments Corporation) used for data collection and display, interfaced through a code interface node with a detection algorithm written in C code. Pilot tests were performed in order to assess and make necessary adjustments to the system prior to any formal evaluation. The sensor system was tested by 2 able-bodied subjects walking at different walking speeds both shod and barefoot. The sensor detection times of heel contact and rise compared were similar to the foot switch timings. The system was also tested by one subject suffering from foot drop. These tests highlighted areas for further development. The features used for the detection of heel contact and the swing phase in the previous work were used in the new set of rules. However, the new algorithms (described in detail in section 6.1.3.3) were more detailed in breaking the gait cycle to sequential states, and resulted in a different way of identifying heel rise during repetitive

gait cycles, which is expected to be more reliable. Also, the new set of rules added the ability to reliably detect gait initiation and heel rise for the first step.

In addition to the need for developing new algorithms, and for portability needs, the code was adapted to run on a portable microcontroller based unit (described in the following section). The portable system allowed for testing the sensor system in real time, and in combination with a stimulator. It also minimised the encumbrance to the subjects in eliminating the need for umbilical cables to run between the subject and a PC. Subject specific parameters could also be adjusted if needed using a PC and a serial link with the controller unit. The microcontroller code was written using the Microchip (Microchip Technology Ltd.) instruction set.

6.1.3 Experimental approach: hardware and software description

The timing of the gait cycle phases can be obtained from force platform data, foot switch data, shoe insole pressure measurement systems or other techniques. Simultaneous recording of the shank angular rate will be one way of correlating the occurrence of gait events and subsequently the timings of gait phases to the angular rate. The gyroscope sensor output is continuously proportional to the shank angular rate, which was utilised by a controller unit running a rule-based algorithm for the detection of the gait events in real-time. The output of the controller unit can then be used to control the timing of the stimulation to the peroneal nerve. In our work, the commonly used ODFS was used for stimulation. Figure 6-5 shows a block diagram of the experimental set-up.

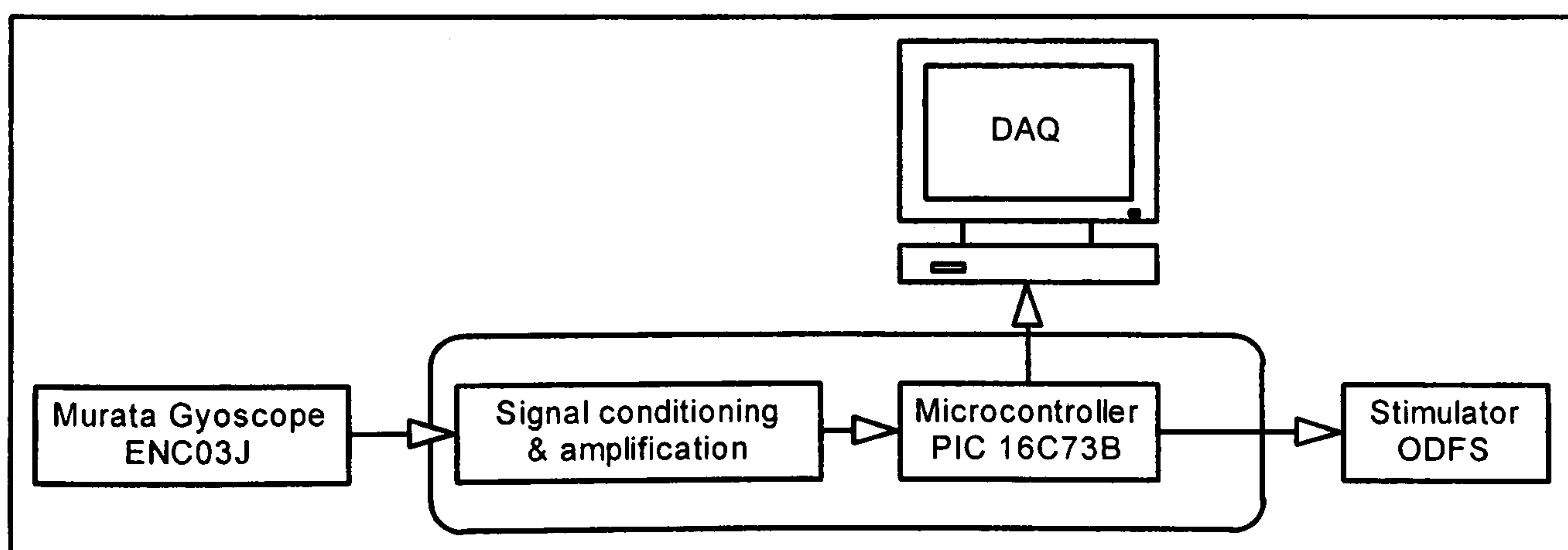


Figure 6-5: A block diagram describing the main components in the experimental set-up used.

6.1.3.1 The sensor

The gyroscope chosen for use in this study is the ENC-03J from the ENC series of Gyrostar® by Murata (Murata Manufacturing Company Ltd, Japan). This choice was made on the following basis:

- The measurement range (quoted value of ± 300 degrees/s). This range proved satisfactory for the measurement of lower limb segment angular velocity measurement (Ghoussayni 2000) and (Henty 2004).
- Sensor performance as tested and shown in (Henty 2004) and (Ghoussayni 2000), using comparisons with an optical sensor and a 3D marker detection system.
- Availability and cost on the market. Cost is an important aspect in developing medical devices for clinical use. The cost of this sensor is approximately £18 and may be reduced for bulk orders. This is in comparison to approximately £33.60 for one foot switch and its lead and £272.25 for the ODFS stimulator (prices according to the Salisbury Newsletter April 2004 – from the Salisbury group web site www.salisburyfes.com).

The combination of range, sensitivity, size, weight, and cost made the Murata ENC-03J sensor a more favourable choice among other sensors that were available on the market. Table 6-1 shows a list and details of those sensors and others that were made available recently. Refer to Appendix D for manufacturers' addresses.

Table 6-1: Details of other gyroscope sensors available on the market.

Part number or name	Manufacturer	Mass (g)	Dimensions (mm)	Range (deg/s)	Scale factor (mV/deg/s) unless otherwise stated	Comments
ENV-05G	<i>Murata Manufacturing</i>	5	12x8x18	± 70	25	Released 2003-2004
ENC-03M		0.4	13x7x2.8	± 300	0.67	Released 2002
VSG-LTD-C1x5	<i>Watson Industries</i>	250max	108x64x57	± 500 max	6 to 100 deg/sec/V	

Single axis VSG-E		130	75x43x40	±200 max	10 to 40 deg/s/V	
ADXRS150	<i>Analog</i>	0.5max	7x7x3	±150	12.5	
ADXRS300	<i>Devices</i>	0.5max	7x7x3	±300	5	
IS-300	<i>Intersense</i>	59	27x34x30	±1200	-	
MicroRing Gyro™	<i>Microsensors</i>	-	-	±60	25	Under development
CRS02	<i>Silicon</i>	25	59x26x25	±150	12.75	
CRS03	<i>Sensing</i>	25	29x29x18	±100	20	
CRS04	<i>Systems</i>	12	30x30x8	±150	12.75	
SiRRS01	<i>BAE Systems</i>	35max	32x32x17	±110	18.2	
VSG series	<i>BAE Systems</i>	135	76x43x41	±50 to 1000	50	
KX210-xxx series	<i>Kionix</i>	-	16x7x2	±75 to 300	6.7 to 26.7	Under development
CG-L43	<i>Token</i>	-	8x16x5	±90	0.66	
QRS11- 0xxxx-10x series	<i>BEI Technologies Inc</i>	60max	∅ 38max	± 50 to 1000	-	
QRS14- 0xxxx-10x series		50max	69x26x26	± 50 to 1000	-	
AQRS- 0075-11x		125max	80x45x45	±75	-	
HZ1-xxx- 100		60max	58x25x25	±90	-	
EWTS53	<i>Panasonic</i>	65	84x35x30	±90	20	
EWTS62		-	20x13x11	±300	6	
EWTS82		-		<±100	25	
-	<i>ETB</i>	-	∅ 15 max	10- 2000	-	Under development

The Murata ENC-03J miniature (15.5 x 8 x 4.3 mm and 1.0 gram max) piezoelectric vibrating gyroscope (Murata Manufacturing Company Ltd., see Appendix C for data sheet) was used to capture the shank instantaneous angular rate. The gyroscope (Gyro) scale factor as quoted by the manufacturer is 0.67 mv/deg/s. The Gyro was housed within an enclosure of dimensions (27 x 17 x 4.5 mm). Velcro attached to this rectangular box was used to mount the sensor package on the subject's shank with a Velcro strap. The Gyro senses the angular rate in a single plane, which was aligned parallel to the sagittal plane. The angular rate measured by the gyro placed on the anterior aspect of the shank is the component of the shank rate located in the sensing plane of the gyro, which is close to the sagittal plane, but does vary with the tibia's internal and external rotation during the gait cycle. The power consumption of the Gyro is low (5 mA max) and hence it is suitable to be battery powered. A 1m flexible cable was used to transmit the signal from the Gyro to the micro-controller based unit located at the subject's waist (total weight of Gyro module and cable is 20 g).

The gyroscopic sensor used in this study is based on the Coriolis force principle to measure the angular rate input (Figure 6-6). The Coriolis force (F) is an apparent force that results when rotation is applied to a moving body (mass m , velocity v) in a rotating reference frame, and is proportional to the angular rate of rotation (w).

Equation 6-1

$$\vec{F} = 2m(\vec{v} \times \vec{w})$$

An elinvar (elastic invariable metal) equilateral prism is excited in one direction and the generated Coriolis force is sensed in the orthogonal direction. Three ceramic piezoelectric elements are attached to the three faces of the prism. Two of the elements are used to drive the prism into oscillation. The third element is used to control the oscillation in a feedback loop configuration. The two elements used for driving the prism are also used for detection. When there is no rotation, all 3 signals from the three elements are the same. When the prism is rotated, the signals on the detection elements become different and the differences is electronically processed to provide an output proportional to the angular velocity of rotation.

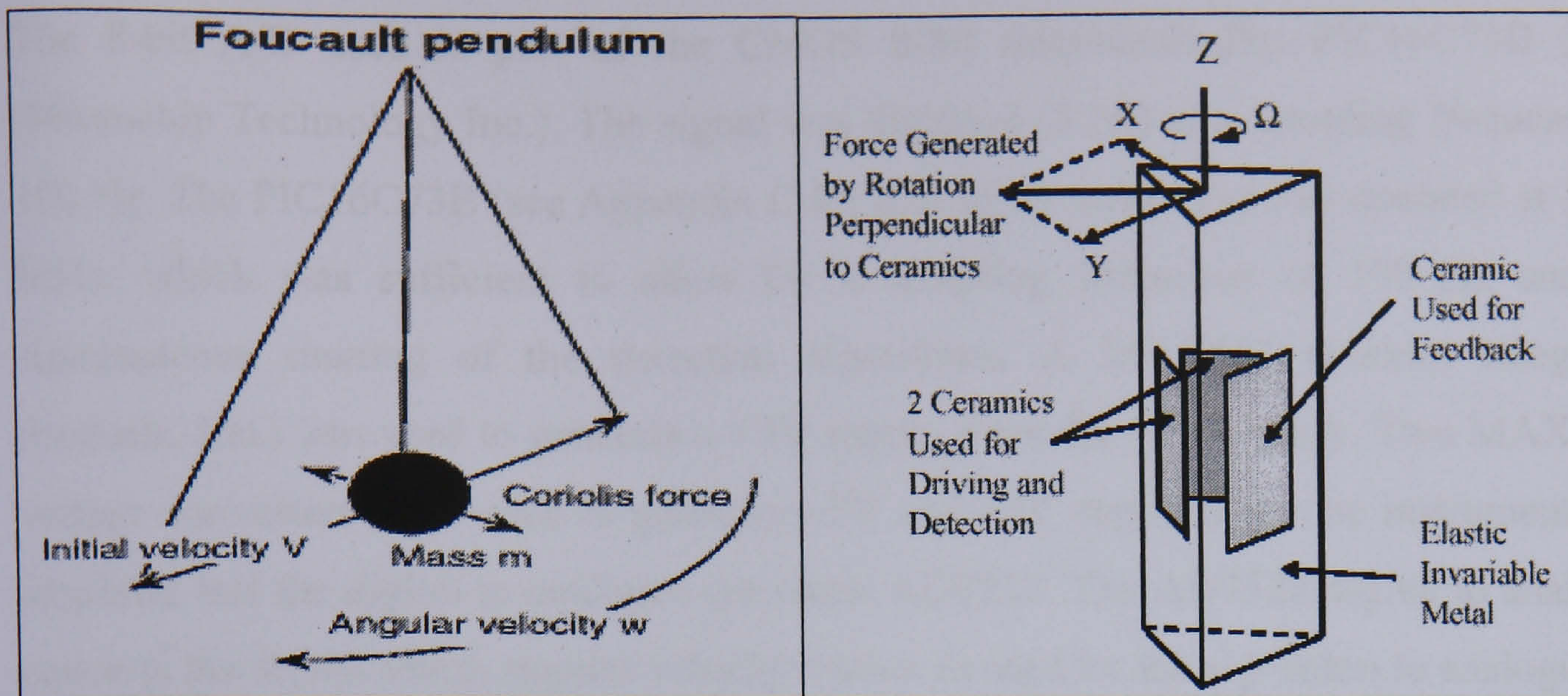


Figure 6-6: The principle of the Coriolis force (left), and the metallic triangular prism vibrator used in the GYROSTAR[®] from Murata (right). (Murata).

In June 2002, Murata introduced a new GYROSTAR[®] model ENC-03M, a compact and surface-mount gyroscope. The new sensor measures 12.2 x 7.0 x 2.6 mm and weighs 0.4 g making it 60% smaller than the ENC-03J, and therefore a more compact and potential alternative to the sensor used in this study. This work however has started when this sensor was introduced, and hence, the ENC-03J version was used for the purposes of this study.

6.1.3.2 Microcontroller Unit

The circuitry of the microcontroller unit (Figure 6-7) is housed within a battery-powered (single 9V PP3 battery) unit (weight approx. 200 gram with battery) enclosed in a box of dimensions (108 x 79 x 35 mm). This choice was made with consideration to both size and weight of the unit for practical use. The output from the Gyro was amplified using an instrumentation amplifier (INA 101HP Burr-Brown Corporation) with a gain of 5 giving a scale factor of 3.35 mV/deg/s. The output from the instrumentation amplifier was then biased using a micropower quad operational amplifier in a summer configuration (LP324 National Semiconductor Corporation). The other input to the summer comes from a three terminal fixed positive voltage regulator (ZMR250 Zetex). The output from the adder is set at 2V5 for no movement. This output at zero movement is essential as a result of the 0 to +5 V input limits for the analogue-to-digital converter (A/D).

The 8-bit A/D used is part of the CMOS 8-bit microcontroller PIC16C73B (PIC) (Microchip Technology Inc.). The signal was digitised (8 bit) at a sampling frequency of 100 Hz. The PIC16C73B (see Appendix C for data sheet summary) was operated at 3.579 MHz, which was sufficient to allow for a sampling frequency of 100 Hz and the simultaneous running of the detection algorithms. A MAX667 (Maxim Integrated Products, Inc.) was used to generate a +5V supply from the +9V battery. Two MAX7660 voltage converters were used to generate -5V and -9V supplies for the instrumentation amplifier and the digital to analogue converter AD7528. The AD7528 digital to analogue converts the digital shank angular velocity values as used by the algorithm to analogue for data acquisition and debugging purposes.

A 5-pin connector was used to connect between the unit and the Gyro sensor box. A 2.5 mm standard audio socket was used to connect the microcontroller unit to the stimulator transmitting the heel state signal (0 to +5V digital signal). Another 5-pin connector was used for transmitting the data from the unit to an external recording device for data acquisition purposes. A red low-power LED was used as an indicator of the heel state as determined by the algorithm.

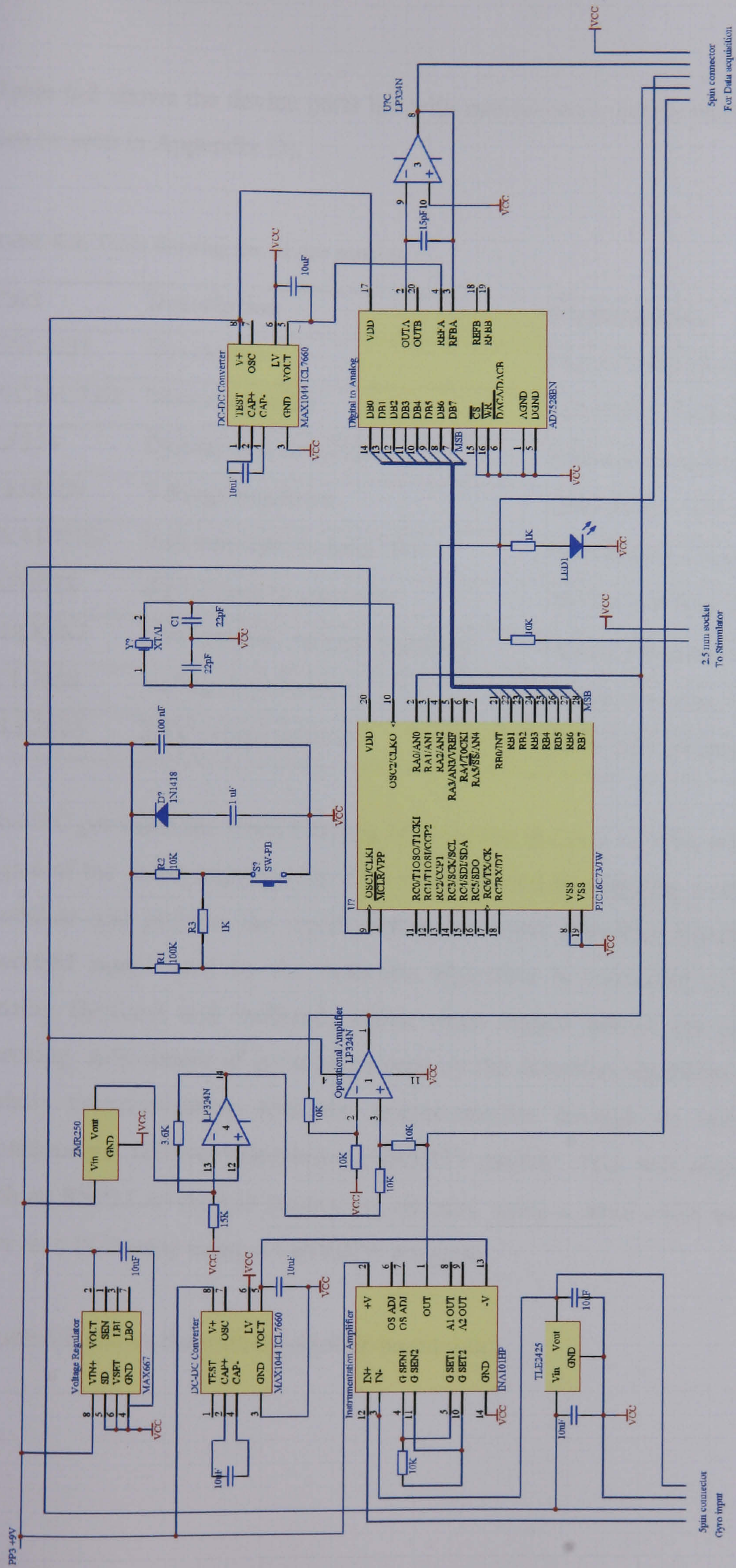


Figure 6-7: Schematic circuit diagram of the microcontroller unit.

Table 6-2 shows the device parts list with manufacturer details (full manufacturer details can be seen in Appendix D).

Table 6-2: Table showing the device parts list

Part	Description	Manufacturer
ENC-03J	Gyroscope	Murata Manufacturing Company
PIC16C73B	Microcontroller	Microchip Technology Inc
LP324	Operational Amplifier	National Semiconductor Corporation
ZMR250	Voltage regulator	Zetex Semiconductors
INA101HP	Instrumentation Amplifier	Burr-Brown Corporation
AD7528	digital/analog converter	Analog Devices Inc
MAX667	Low-dropout voltage regulator	Maxim Integrated Products
ICL7660	Voltage Converters	Maxim Integrated Products
TLE2425	2.5V virtual ground	Texas Instruments

The PIC performs the main function of detecting the heel state by analysing the digitised signal of the shank angular rate. This was achieved by applying a set of subroutines that modulate and prepare the signal before the main detection algorithm. The software-modified signal used by the detection algorithm is converted to analogue (AD7528 Analog Devices) and buffered, which when logged allows for code debugging and checking. Adjustment of parameters used by the detection algorithm can be achieved by serially communicating with the microcontroller through its universal synchronous asynchronous receiver transmitter (USART) module. This was connected to a module with an RS232 driver and supporting circuitry using a serial cable and controlled by the user on a PC/laptop using a LabVIEW program.

Figure 6-8 shows the microcontroller-based unit.



Figure 6-8: The microcontroller-based unit with labelled buttons and connectors (dimensions are 108, 79, 35 mm).

- “A” is used to connect to a serial communication module that in turn can be connected to a serial port on a PC (not seen in figure; symmetrical to “F”).
- “B” is a 5-pin connector used to connect to the Gyro sensor box.
- “C” is a 2.5 mm standard audio socket that can be used to connect the microcontroller unit to the stimulator transmitting the heel state signal (0 to +5V digital signal)
- “D” is a red low-power LED that reflects the heel state as determined by the algorithm
- “E” is a 5-pin connector allows for transmitting data through a cable to a desktop PC for data logging. These include the heel state, the shank angular rate input to the PIC, the output from the digital-to-analogue converter, and the stimulator on/off timing.
- “F” is the input of the stimulator On/Off timing. This gave the option of monitoring the stimulator on/off times by connecting this to data logging equipment through connector E.
- “G” is a reset button.
- “H” is the unit power switch.
- “I” is the 9V PP3 battery compartment.

6.1.3.3 Software

What follows is a description of the main subroutines and their function and flowchart diagrams for the PIC code (see Appendix B for code) written using Microchip instruction set:

- Initialise (see Figure 6-9): Initialises the PIC input and output ports, interrupts, A/D, special function and general-purpose registers, and timer modules.

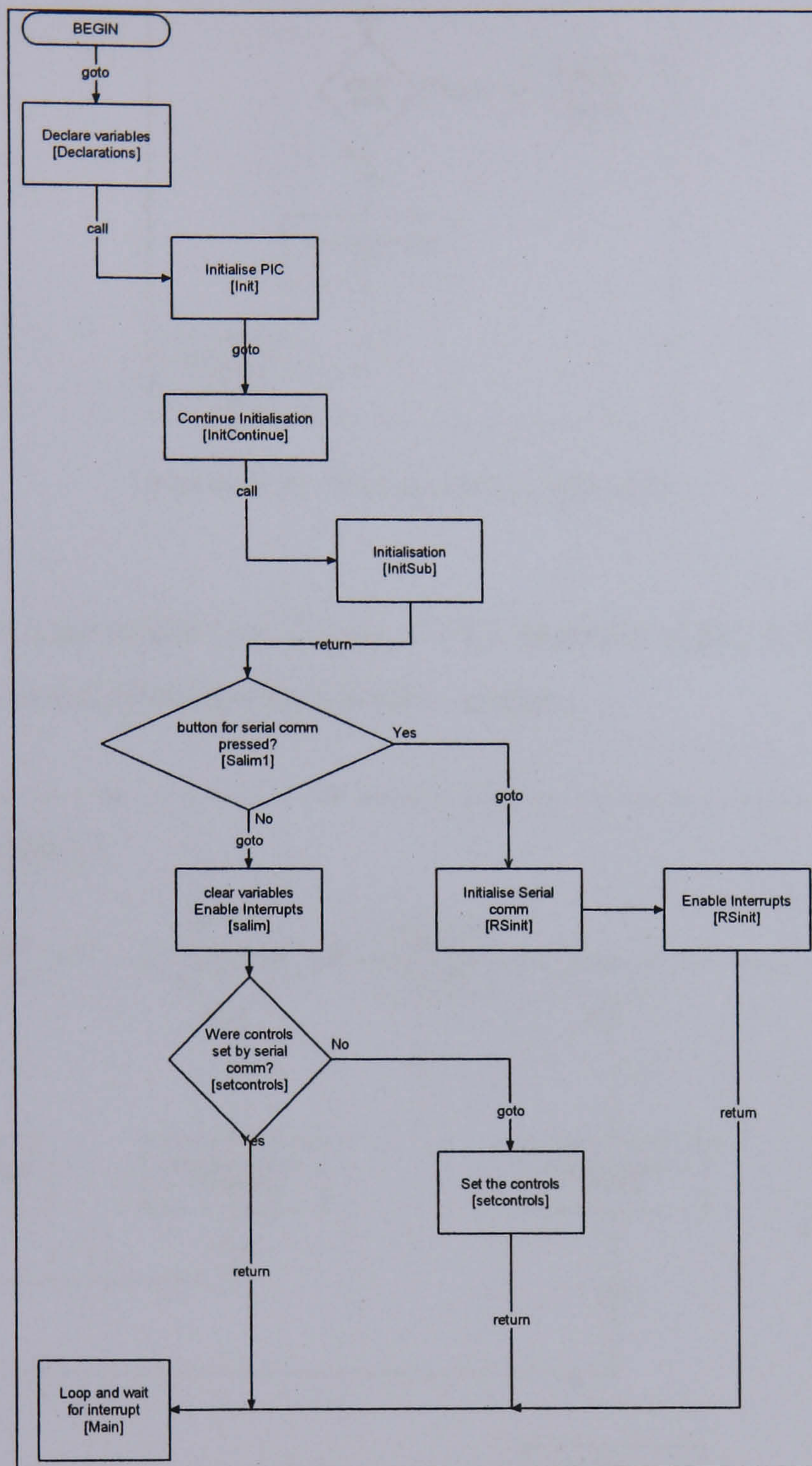


Figure 6-9: Initialisation subroutine.

- Interrupt service routines (see Figure 6-10): on timer interrupt (set at 100 Hz) sends the PIC into either analysis mode or serial communication mode.

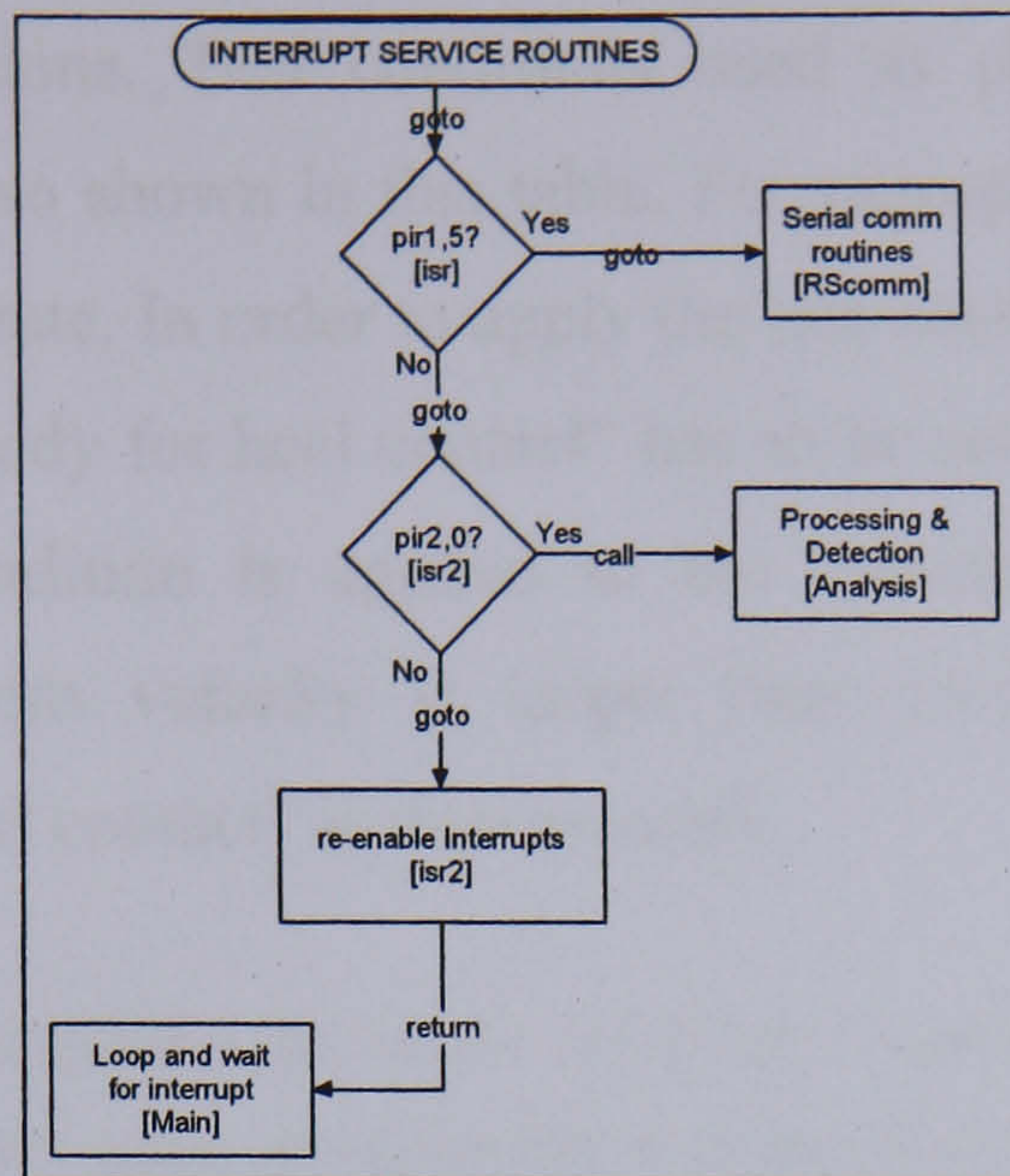


Figure 6-10: Interrupt service subroutine

- Communication subroutine (see Figure 6-11): receives eight, 8 bit numbers at high speed, asynchronously through the USART module.

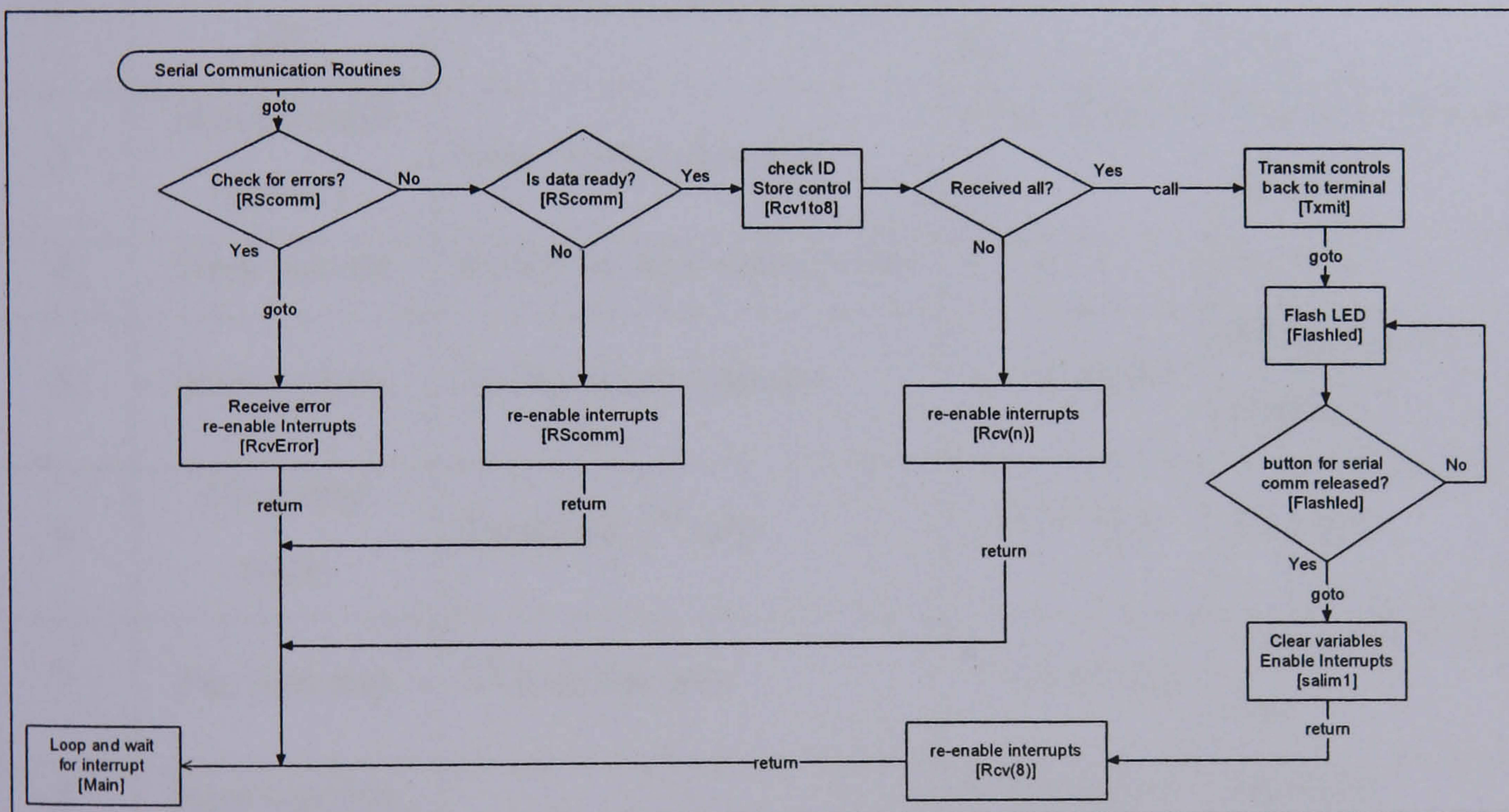


Figure 6-11: Serial communication subroutine

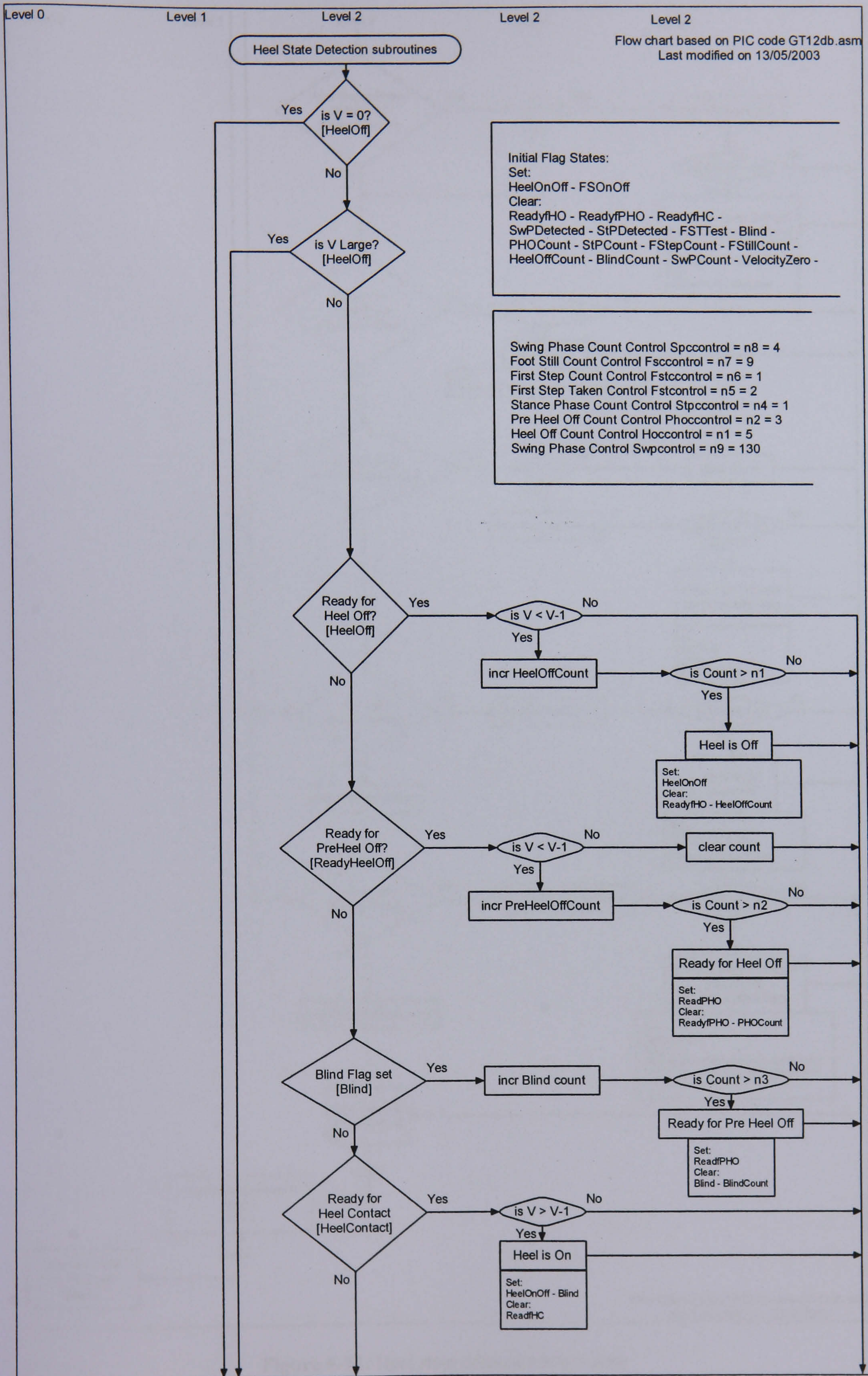
- The heel state detection subroutine encodes the cycle into 9 sequential phases, based on the temporal knowledge of the 'normal' gait cycle. A set of rules is applied to the shank angular rate in order to effect any of the transitions. The heel state (on or off) is changed in accordance to specific conditions applied to the angular rate within each phase. Table 6-3 summarises the 9 phases and

their pre-conditions. Test conditions used as part of each phase and the outcomes are also shown in this table. For example, consider phase 4 and the “heel contact” state. In order to apply the test condition for this phase, the pre-condition of “ready for heel contact” has to be set true. If this pre-condition is true, a test condition is applied to the measured shank rate. If this test condition (current velocity is larger than previous velocity) is met, the outcome of “heel contact” is then asserted.

Table 6-3: Heel state detection algorithm description. (n1 to n8 = algorithm parameters – \underline{n} = consecutive count condition – V and V^{-1} are the values of angular rate in current frame and previous frames)

Phase	State name	Pre-condition	Test condition	Outcome
1	Heel off	V not 0 & not > 0 & Ready for HO true	$V < V^{-1}$ for n1	<i>Heel off</i>
2	Ready for heel off	Ready for pre-heel off true	$V < V^{-1}$ for <u>n2</u>	Ready for heel off true
3	Blind (initial stance)	Heel contact detected	After time $>$ n3	Ready for pre-heel off true
4	Heel contact	Ready for heel contact true	$V > V^{-1}$	<i>Heel on</i>
5	Stance phase	Swing phase detected	$V < 0$ for n4	Ready for heel contact
6	First step taken	Ready for 1 st step	$V > V^{-1} + n5$	<i>Heel off</i>
7	Pre first step	1 st step flag true	$V < 0$ for <u>n6</u>	Ready for 1 st step true
8	Foot inactive	-	$V = 0$ for <u>n7</u>	<i>Heel on</i>
9	Swing phase	-	$V > n9$ for <u>n8</u>	<i>Heel off</i>

The detailed stages of the analysis subroutine for heel state detection can be seen in the flowchart in Figure 6-12 on the following 2 pages.



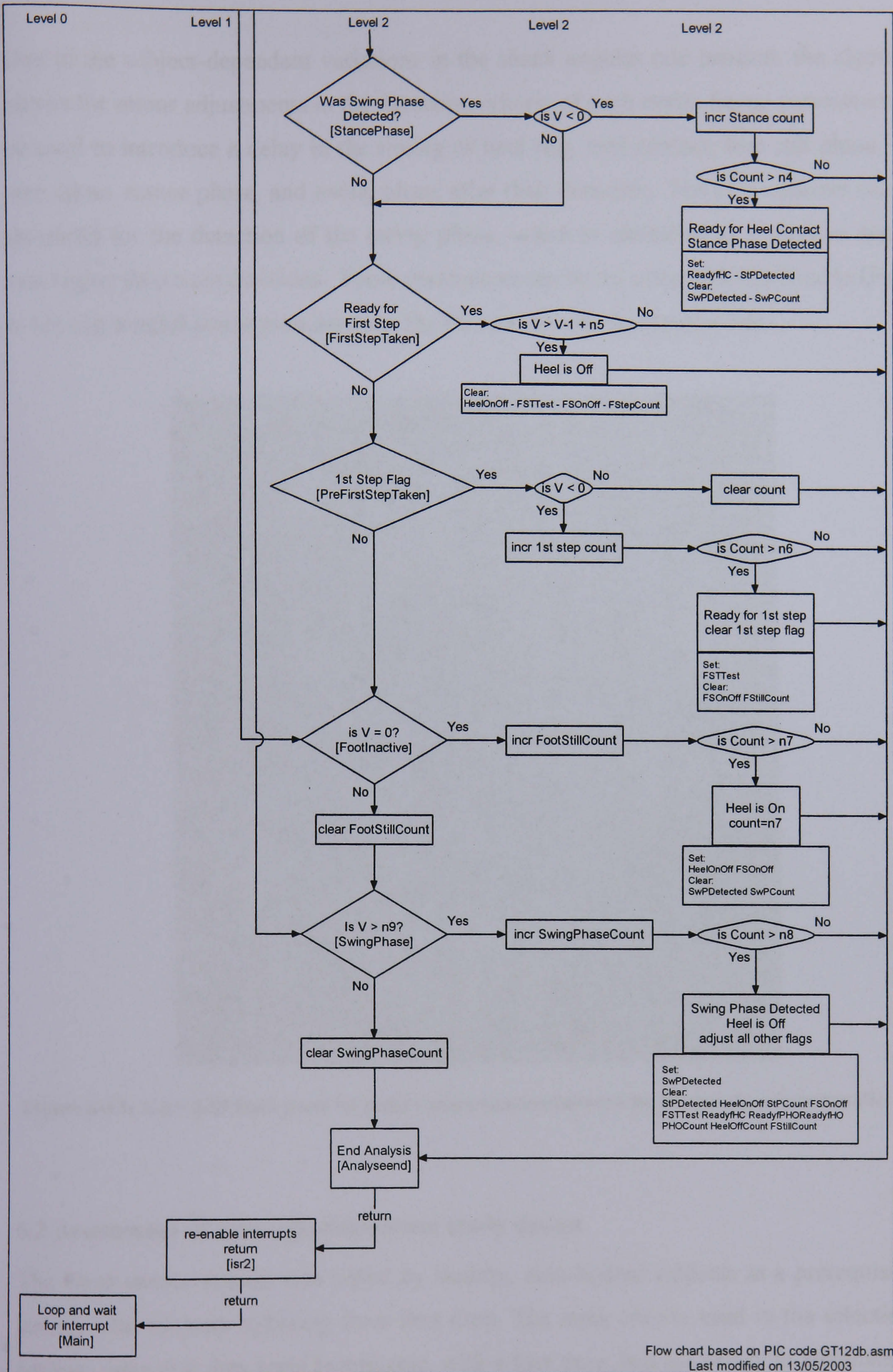


Figure 6-12: Heel state detection subroutine

Due to the subject-dependent variations in the shank angular rate patterns, the algorithm allows for minor adjustments in the detection criteria of each event. Seven parameters can be used to introduce a delay in the timing of heel rise, heel contact, foot still phase, first step taken, stance phase, and swing phase after their detection. The 8th parameter sets the threshold for the detection of the swing phase, which is identified as a positive angular rate higher than a set threshold. These parameters can be set using LabVIEW code (Figure 6-13) and a serial connection between the PC and the microcontroller unit.

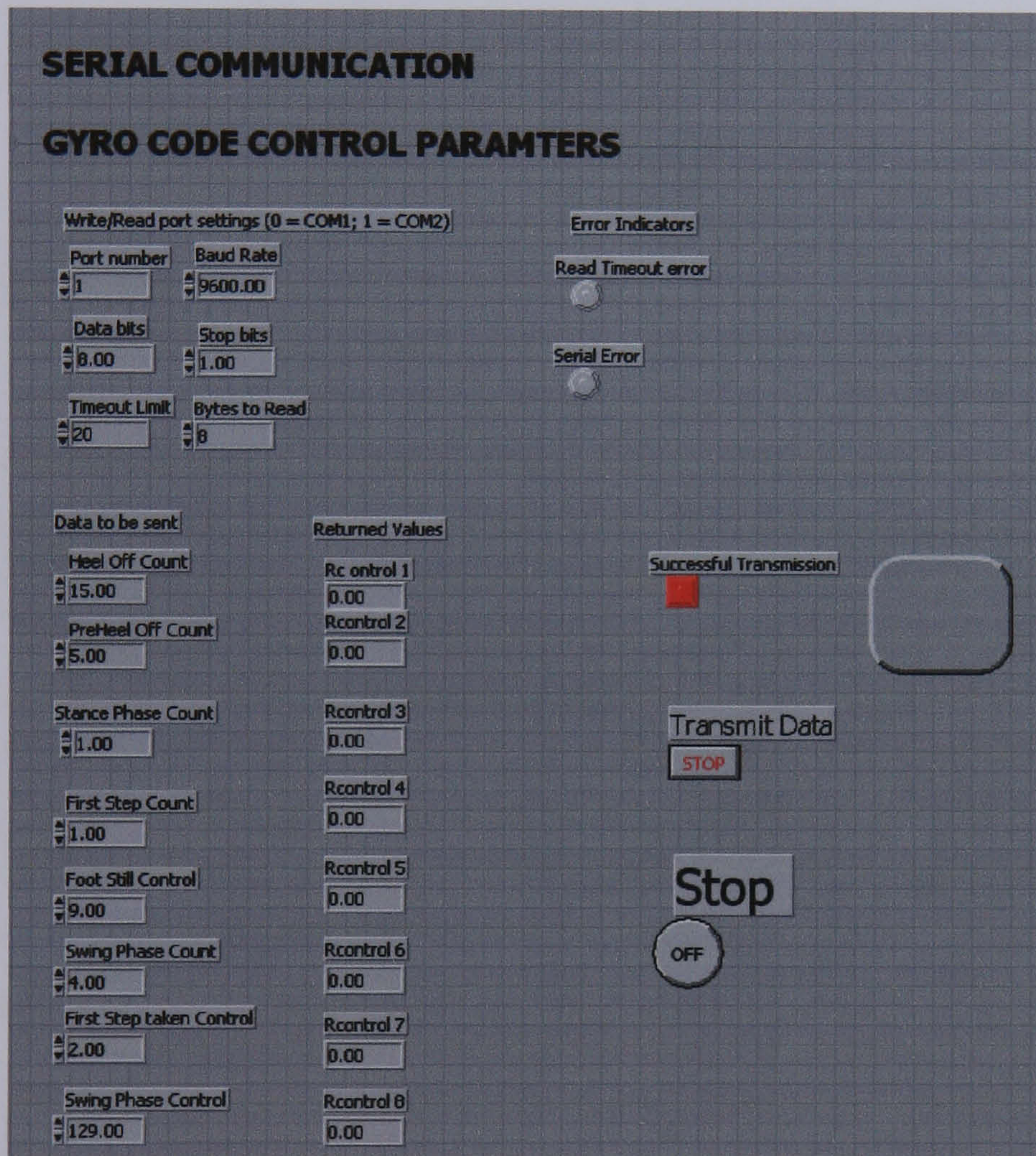


Figure 6-13: LabVIEW front panel for serial communication between the PC and the microcontroller unit.

6.2 Assessment of sensor performance: study design

The Gyro sensor system was tested by healthy, able-bodied subjects as a prerequisite to testing with subjects suffering from foot drop. The main criteria used in the selection of patients were that they were hemiplegic, with a foot drop, had the ability to ambulate, had no contractures, and had been using a foot drop FES correction system.

6.2.1 Equipment and data collection

Simultaneous recordings from a 3D motion capture system (MCS), foot switches, Gyro, and video were made. 3D foot marker data were used to determine reference times for gait events as described in Chapter 4. Force platform data were also available for the trials performed in the second part of the study. Figure 6-14 shows the experimental set-up used throughout the data collection trials.

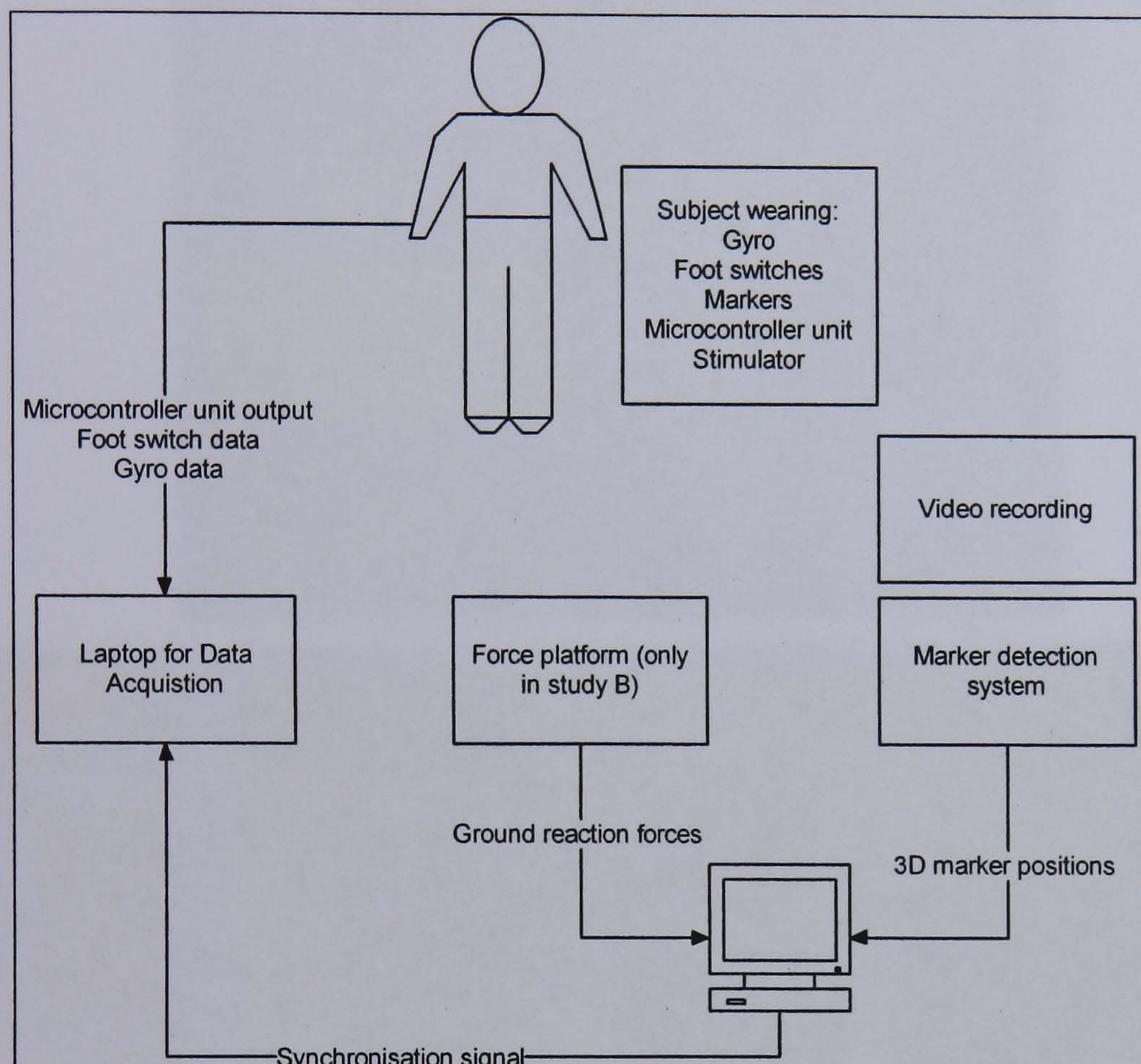


Figure 6-14: Diagram showing the different components of the experimental set-up.

The 3D co-ordinates were recorded using Qualisys systems (Qualisys Medical AB, Partille, Sweden). In the first part of the study, a seven-camera 240 Hz ProReflex motion detection system (Qualisys Medical AB, Partille, Sweden) was used to capture the motion data. QTrac Capture 2.74p was used to track the data. For the second part of the study, a six-camera 60 Hz MacReflex motion detection system was used. MacReflex 3.42f2 PPC software was used for tracking the data. The reason behind using two different systems is the fact that the two parts of the study took place in two different laboratories: Centre for Biomedical Engineering at the University of Surrey, and the Clinical Biomedical Engineering Centre at Queen Mary's Hospital. A National Instruments data acquisition card (DAQCardTM-700) was used to acquire the analogue signals from the microcontroller

unit and the foot switches. LabVIEW code was written for data logging and display Figure 6-15. The acquisition was done on a laptop (electric safety considerations). The trigger signal to the MCS was also recorded by the DAQCard and used for synchronisation between the MCS and the acquired microcontroller and foot switch outputs.

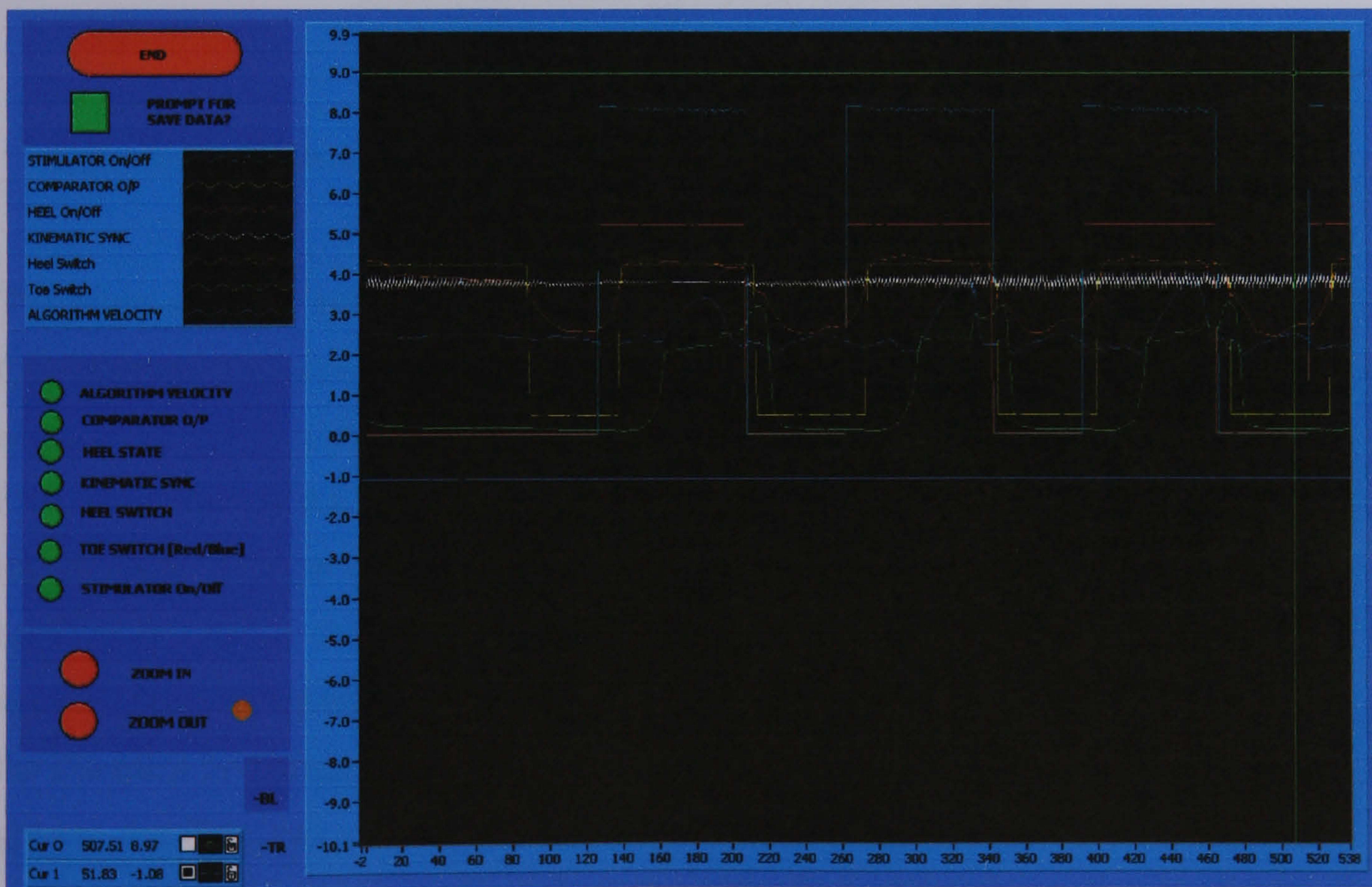
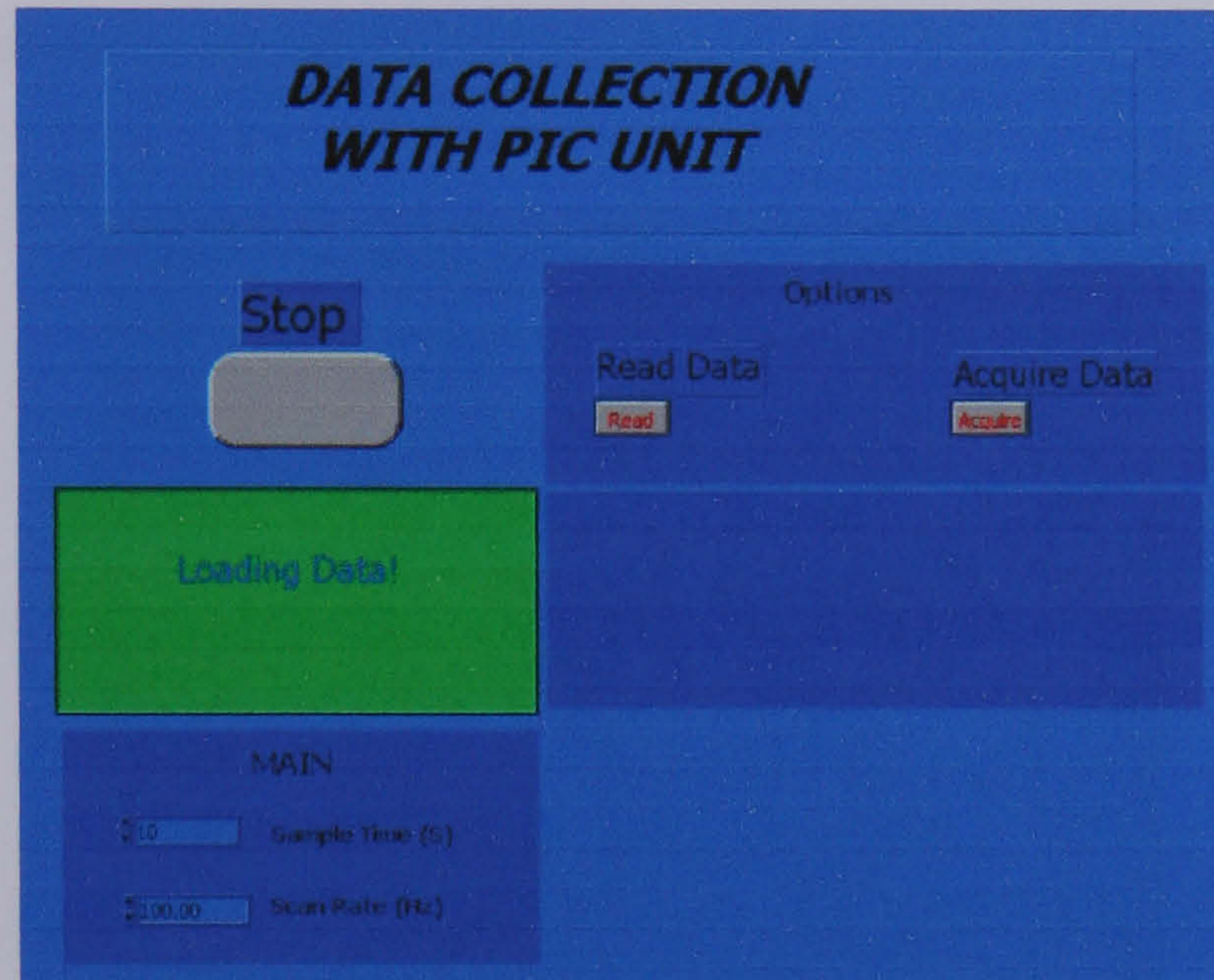


Figure 6-15: Front panel and user interface (top) and data display (bottom) of the LabVIEW code used for data collection.

The two Qualisys motion capture systems used consist of a set of cameras that flash infrared light which is reflected from the retroreflective markers and used to provide a 2D image. The images from 2 or more cameras are used to calculate the 3D position of the marker in a global laboratory reference system (Figure 6-16). The system is usually calibrated for a measurement volume (typically in the order of 2 to 3 metres in each direction). A set of retroreflective markers placed on the subject is used to determine the kinematic data of the body segments and joints.

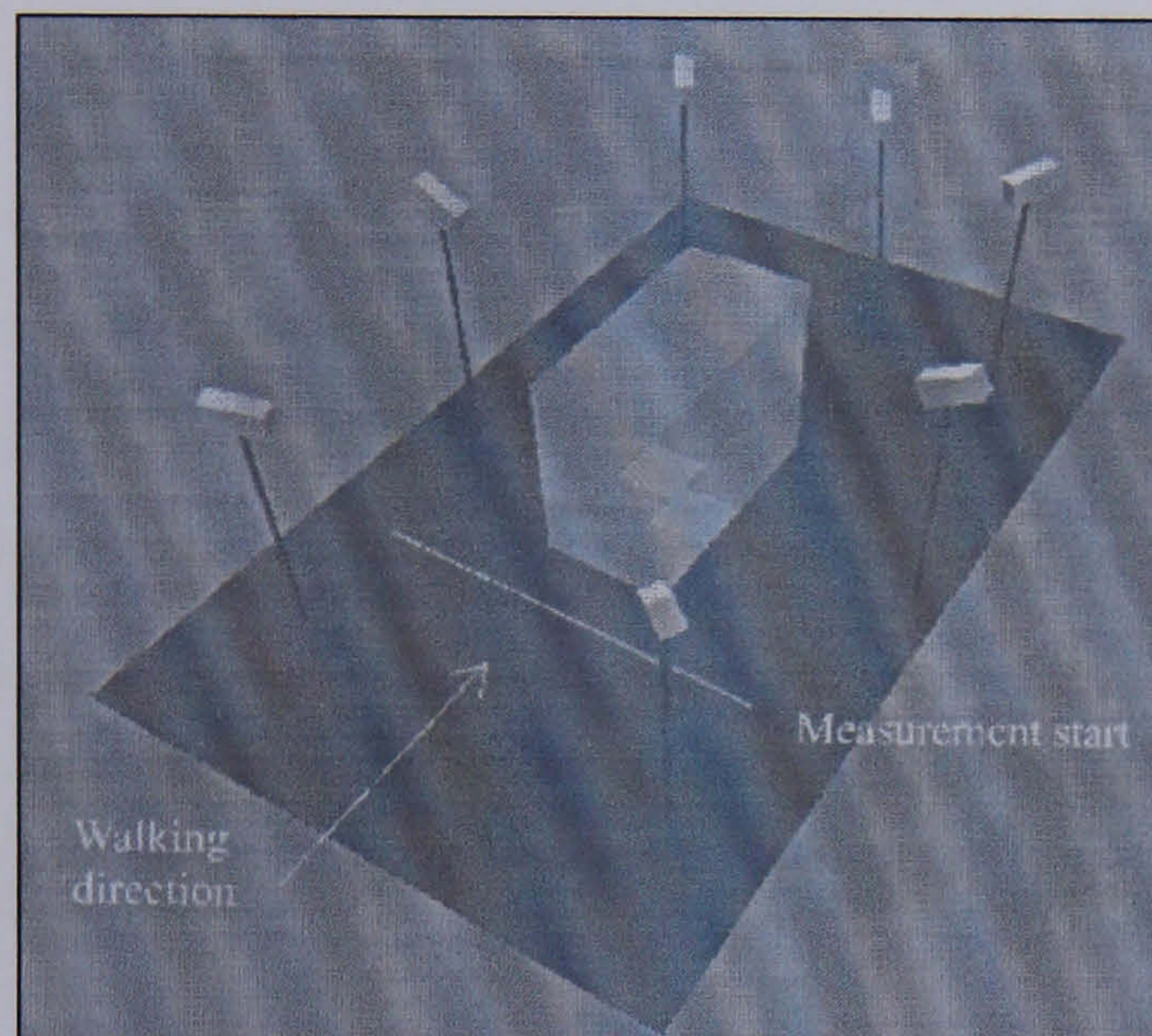


Figure 6-16: A schematic of the motion capture system with the cameras and measurement volume

The force sensitive resistor-based foot switches (Interlink Electronics) used throughout this study are the same as the foot switches used for triggering the stimulator. The force-sensing resistor is a polymer thick film device, which decreases its resistance when a force is applied to the active surface (Figure 6-17). The sensor consists of 2 conducting interdigitated patterns deposited on a thermoplastic polyetherimide film. A spacer placed between the plastic sheets permits electrical contact between the 2 sheets when force is applied. The contact area between the 2 layers is increased with the applied force and thus the electrical resistance decreases. A typical FSR will exhibit a change in resistance from greater than 1 M Ω to a few k Ω upon the application of force. The output of a comparator was used to derive the timings of the gait events from the FSR-based foot switch. This circuit replicates that in the stimulator and therefore generates the same event times as the stimulator used in this study.

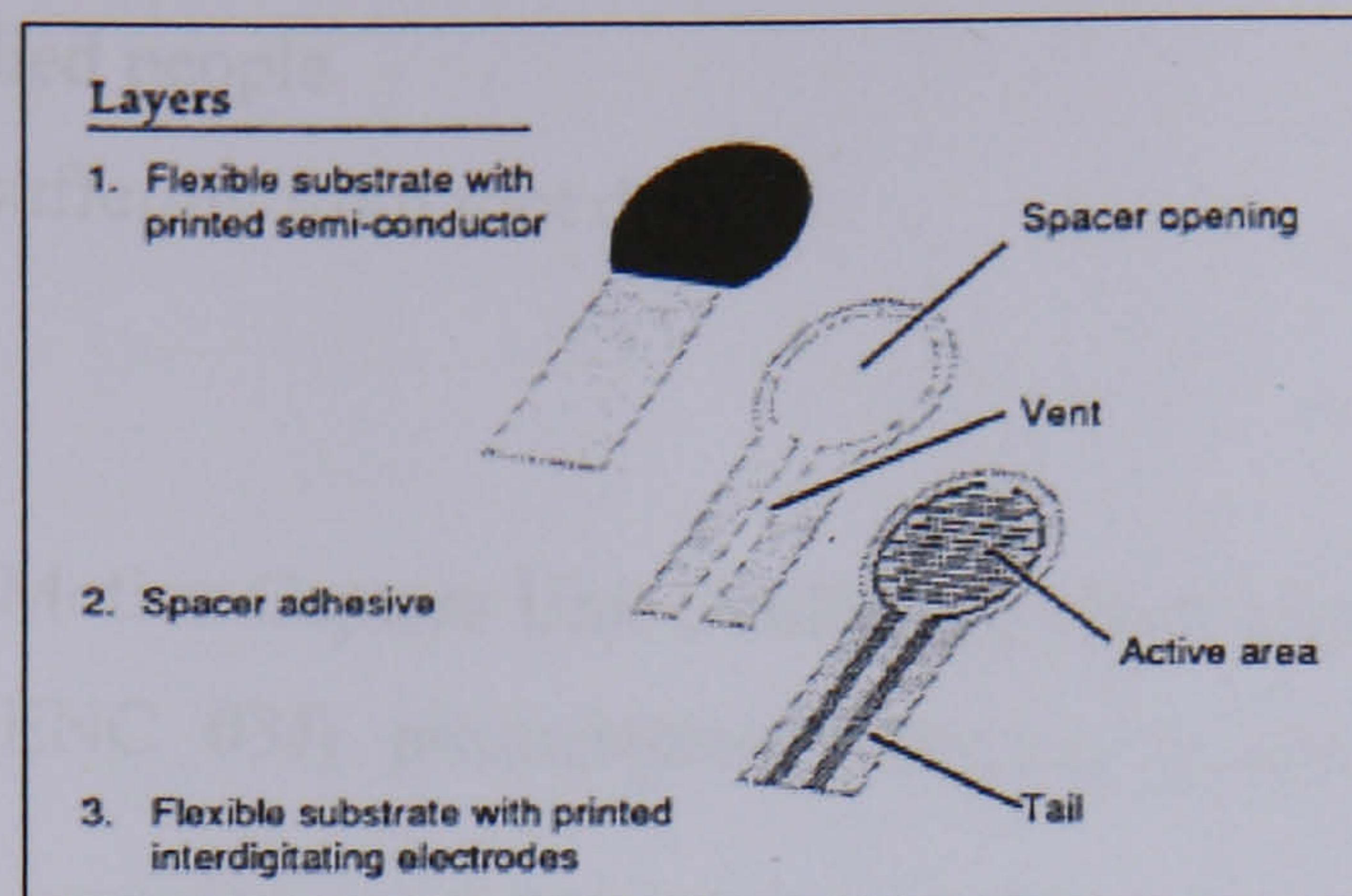


Figure 6-17: Force sensitive resistor technology (Interlink Electronics).

The stimulator used in this study is the Odstock Dropped Foot Stimulator (ODFS) (Figure 6-18). It is a single channel stimulator (dimensions 95 x 60 x 25 mm) used for the correction of foot drop. The stimulation is triggered by a foot switch, and consists of 40 Hz voltage driven current symmetrical or asymmetrical pulses. A front panel control adjusts the stimulation level by varying the stimulation pulse width from 3 to 350 μ s. Internal controls allow the adjustment of the output current amplitude, waveform, falling edge ramps, rising edge ramps, extension time, and time duration for fixed time stimulation.



Figure 6-18: ODFS single channel foot drop stimulator (Salisbury District Hospital, UK)

6.2.2 Protocols

This section describes the protocols used for the data collection in the two assessment studies.

Purpose: Evaluate the gyroscope as a sensor for gait event detection by

- A- Able-bodied people
- B- Patients suffering from foot drop

Equipment:

- Qualysis Motion Capture Unit (ProReflex/MacReflex)
- Murata (ENC 03J) piezoelectric vibrating gyroscope, plus supporting circuitry
- 2 Foot switches (Interlink Electronics)
- Data acquisition card (DAQCardTM-700)
- Micro-controller based unit for gait event detection
- Video image recording (sagittal view)
- (Force plate data)

Software:

- Motion capture and tracking software from Qualisys. (QTrac v 2.74 provided by Qualisys or Qualisys Track Manager)
- LabVIEW program for collecting and displaying data
- (Force platform software)

Markers/Sensors Placement:

- 5 retroreflective markers: placed on the posterior end of the lateral border of the calcaneous, the fifth metatarsal head of the right foot and the third on the sacrum. 2 markers placed on the frontal aspect of the shank (see Figure 6-19)
- Gyro placed on anterior aspect of the shank using a Velcro strap
- 2 Footswitches placed under the heel and the first metatarsal head

Number of subjects:

- A. 5 able-bodied with no observable gait deviations
- B. 3 patients suffering from unilateral foot-drop who were using a foot-drop stimulator for functional purposes; preferably with no contralateral complications

Trial conditions:

- A. Level floor walking at self-selected normal and slow speed, and a simulated pathological gait pattern (foot drag or circumduction)
- B. Walking at their self-selected comfortable speed
 - § Stimulator Off (No Stim)
 - § Stimulator On triggered by foot switch (FSR Stim)
 - § Stimulator On triggered by gyroscope (Gyro Stim)

Number of traverses/condition:

- A. 5 traverses of the calibration volume (self-selected normal 2, slow 2, and simulated pathological-1). Each traverse would ideally allow for the comparison of events over 3 strides.
- B. 6 traverses:
 - i. 2x Stimulator Off
 - ii. 2x Stimulator On triggered by foot switch
 - iii. 2x Stimulator On triggered by gyroscope

Process:

1. Explain to subject what we are trying to do
2. Place the footswitches inside their shoe
3. Place the Gyro on the shank
4. Place the 5 markers
5. Do a practice walk to make them familiar with the lab and attached wires and sensors
6. Collect data
7. A: normal → slow → simulated pathological
8. B: Stimulator off → Stimulator on (FSR trigger) → Stimulator on (Gyro trigger)
9. Collect feedback from subjects

Figure 6-19 shows both a frontal and side view of two subjects who took part in the part B of the study. A typical set-up of the sensors and markers can be seen prior to start of assessment.



Figure 6-19: Two of the subjects who took part in the study (surface electrodes, Gyro, markers and connecting wires in these frontal and side views).

Subject Data: The average age of the able-bodied subjects was 34.8 years (ranged between 24 and 60 years), average weight 75.3 kg, and average height 1.8 m (see Table 6-4).

Table 6-4: Subject data for study A participants

Subject	Age (years)	Weight (kg)	Height (m)
1	28	56	1.58
2	25	103	1.93
3	37	71	1.83
4	24	68	1.78
5	60	79	1.80

Subject data on the 3 patients with foot drop who took part in this study are shown in Table 6-5. The 3 subjects were regular users of FES for foot drop correction. All 3 subjects had their right side affected.

Table 6-5: Subject data for the 3 patients who took part in Study B.

Subject	Condition	Age (years)	Weight (kg)	Time since Diagnosis (years)
1	MS	54	89	5
2	MS	42	73	9
3	MS	67	75	11

6.3 Data analysis and presentation

Each subject performed 5 trials in study A and 6 trials in study B. Each trial data was processed in order to determine the timings of heel contact and rise according to the three systems: kinematic reference (Ref) using method described in chapter 4, foot switches (FSR) and Gyro. Due to the limited size of the calibrated measurement volume of the MCS, a limited number of strides could be analysed from each trial. This number varied between 2 and 5 and depended on the subject's stride length. The timings of the FSR and Gyro were compared against the Ref times for each of the 3 conditions. For part "A" these were: self-selected normal walking speed, slow speed, and simulated pathological. For part "B" of the study, the 3 conditions were: no stimulation (No Stim), stimulation on and triggered by the FSR (FSR Stim), and stimulation on and triggered by the Gyro (Gyro Stim). The differences (diff) in timing were calculated arithmetically as follows:

Equation 6-2

$$Gyro\ diff = Gyro\ time - ref\ time$$

Equation 6-3

$$FSR\ diff = FSR\ time - ref\ time$$

Hence a negative difference indicates an earlier detection of the event, while a positive difference indicates a delayed detection. Average and standard deviations (STDEV) were calculated for each condition and event.

Averaging positive and negative differences can result in misleading outcomes, and hence the absolute values of the individual differences were calculated and used to calculate the average and standard deviations. The timings of the 2 events were also normalised to the gait cycle duration. Gait cycle duration was calculated as the time span between 2 occurrences of the same gait feature. The feature used was the peak of heel vertical

elevation. Thus, the start of the gait cycle was defined as the frame when the heel starts descending towards the floor and the end is the frame just before the heel has reached its peak elevation after toe off. The peak times were determined using the kinematic data recorded. Normalised differences allow for the differences among subjects in gait cycle times.

Percentage accuracy was used to assess the overall performance of both sensor systems. This was calculated (using Equation 6-4) as the percentage of data points where the sensor system and reference system detection outputs agreed. The output of the system can be in one of two states (Heel on the ground or heel off the ground). If 1 stride with a stride time of 1s and data sampled at 100 Hz is considered, an error of 2 samples in the detection of each event will result in an accuracy of 96%.

Equation 6-4

$$Accuracy (\%) = \frac{\text{number of correct samples}}{\text{total number of samples}} \times 100$$

6.3.1 Power analysis

In order to estimate the number of subjects that need to be recruited in order to detect a significant improvement in performance, power calculations were made. If 100 ms is considered to be a significant difference, and 1 s as an average gait cycle time, 99 % power will be present in an observed difference of 9 % (or 90 ms) for a sample size of 5. The power calculation is done assuming a 3 % standard deviation in the timing of each gait event.

In order to detect statistical significance in the comparison between the Gyro and foot switch for smaller observed differences, significantly larger sample sizes would be necessary. However, it is believed that a comparable or improved performance, even without statistical significance, would still justify the use of the alternative sensor when the additional advantages are considered.

This chapter has described the methods and theory behind the use of the Gyro sensor system. The experimental approach and study design were also discussed. The following

chapter presents and examines the results obtained from the Gyro sensor assessment studies by both able-bodied subjects and patients with foot drop.

Chapter 7: Evaluation of the Gyro sensor system: results and discussions

This chapter presents the results of the comparison of event detection by the Gyro and foot switch as compared against the kinematic-based reference method. As noted in chapter 6, the two parts of the assessment study have been referred to as Study A and Study B. “A” refers to the results from the testing performed with the able-bodied subjects, while “B” refers to those from patients suffering from foot drop. The second part of the chapter discusses the results of this assessment with respect to the accuracy and reliability of detection of both systems.

7.1 Results of the evaluation

The correlation between the feature used for the detection of heel rise and the occurrence of heel rise was in part subject dependent. This subject dependency was accounted for in the detection algorithms by allowing the user to set a heel rise detection parameter. This parameter effectively introduces a delay to the detection of heel rise. This parameter was kept constant during the testing procedures for all subjects; however, the offline processing of data showed the need to modify this control for different subjects in order to improve the accuracy of heel rise detection. For this reason, the heel rise detection times as given by the Gyro were transformed to reflect this need for adjusting the delay. The correct delay was calculated by considering the shank angular rate and event times given by the reference system. The results presented here are those obtained after this transformation. The need for setting this parameter affects the practical use of the sensor system. However, this can be achieved as part of the clinical session during which the patient is set up with the stimulator. One suggested means for doing this is to data log the shank angular rate signal from the Gyro and the heel rise detection times as the patient performs a test walk with the stimulation. In a similar way to setting up the appropriate delays when using the foot switch, the data can be used to adjust the heel rise detection parameter, based on clinical judgement of the patient’s gait. The availability of reference times (e.g. from a kinematic system) of the occurrence of the gait events, particularly heel rise, would be an advantage.

7.1.1 Study A

7.1.1.1 Performance accuracy for both Gyro and FSR sensors

Figure 7-1 presents the mean timing of both heel contact and heel rise as determined by the three systems. The means of the normalised timings (%T = % of gait cycle duration) are presented for each of the 3 conditions for both events, where “N” refers to walking at a normal self-selected speed, “S” refers to slow walking, and “SP” refers to the simulated pathological gait patterns. 1 error bar reflects 1 standard deviation for all the graphs in this chapter.

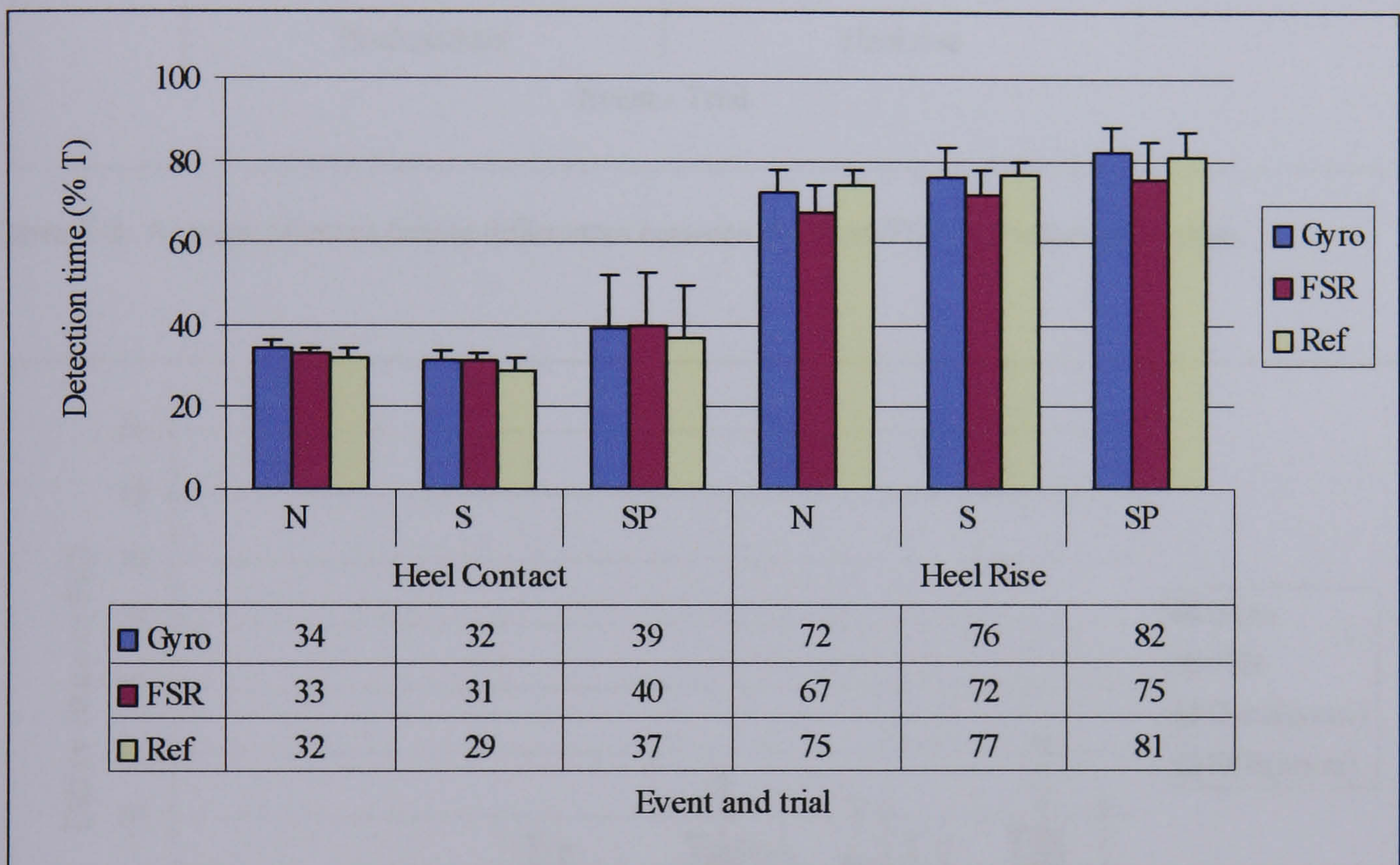


Figure 7-1: Normalised detection times of heel contact and rise as given by the Gyro, FSR, and reference system. (number of observations are 33, 34, and 19 for N, S, and SP trials respectively)

Figure 7-2 and Figure 7-3 show the average of event timing differences using the arithmetic and absolute differences respectively. “Diff” refers to the difference between timings and is presented in frames (multiples of 10 ms) for the raw timings and as a percentage of the gait cycle duration (%T) for the normalised (“norm”) time differences.

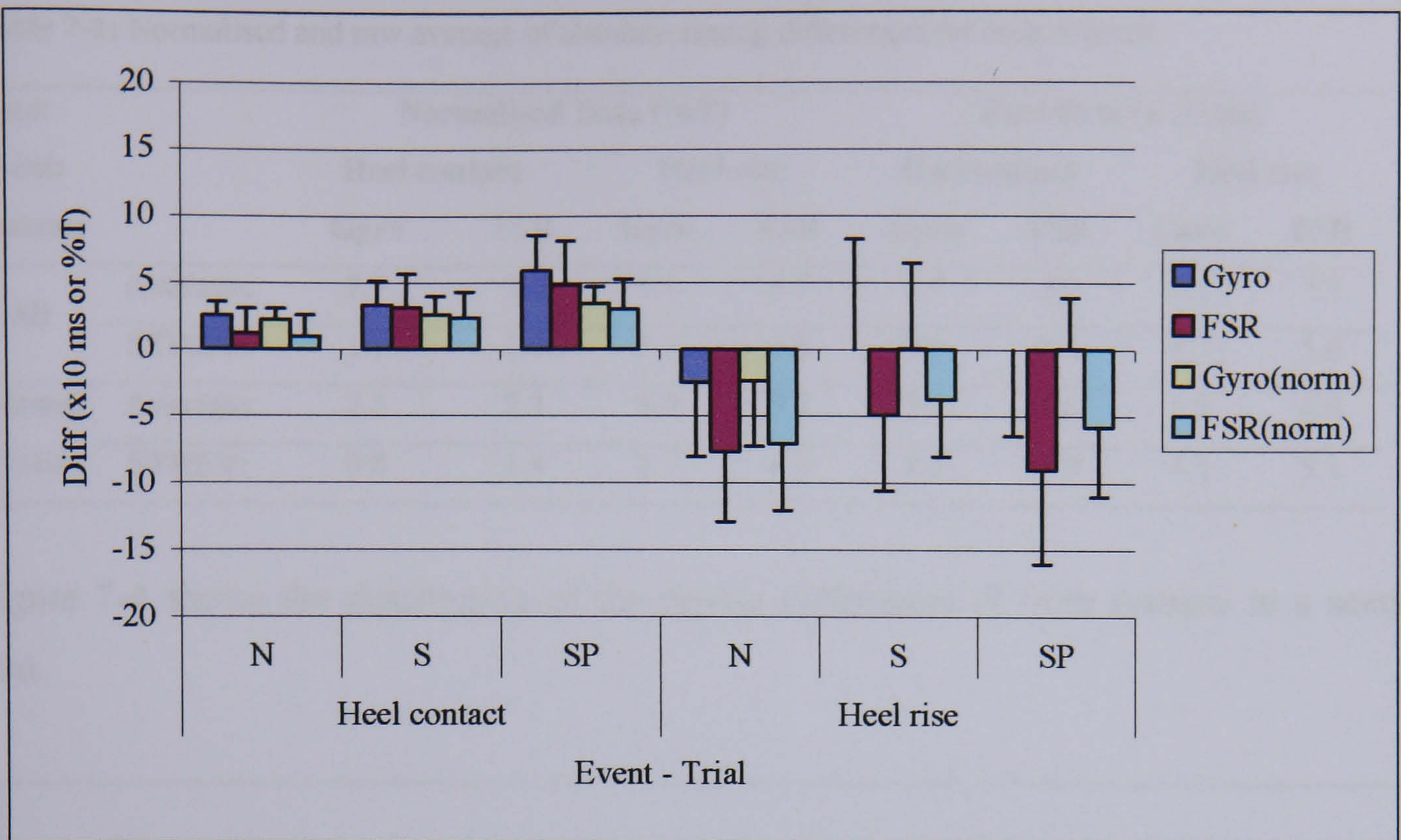


Figure 7-2: Average of event timing differences between the Gyro/FSR and reference system.

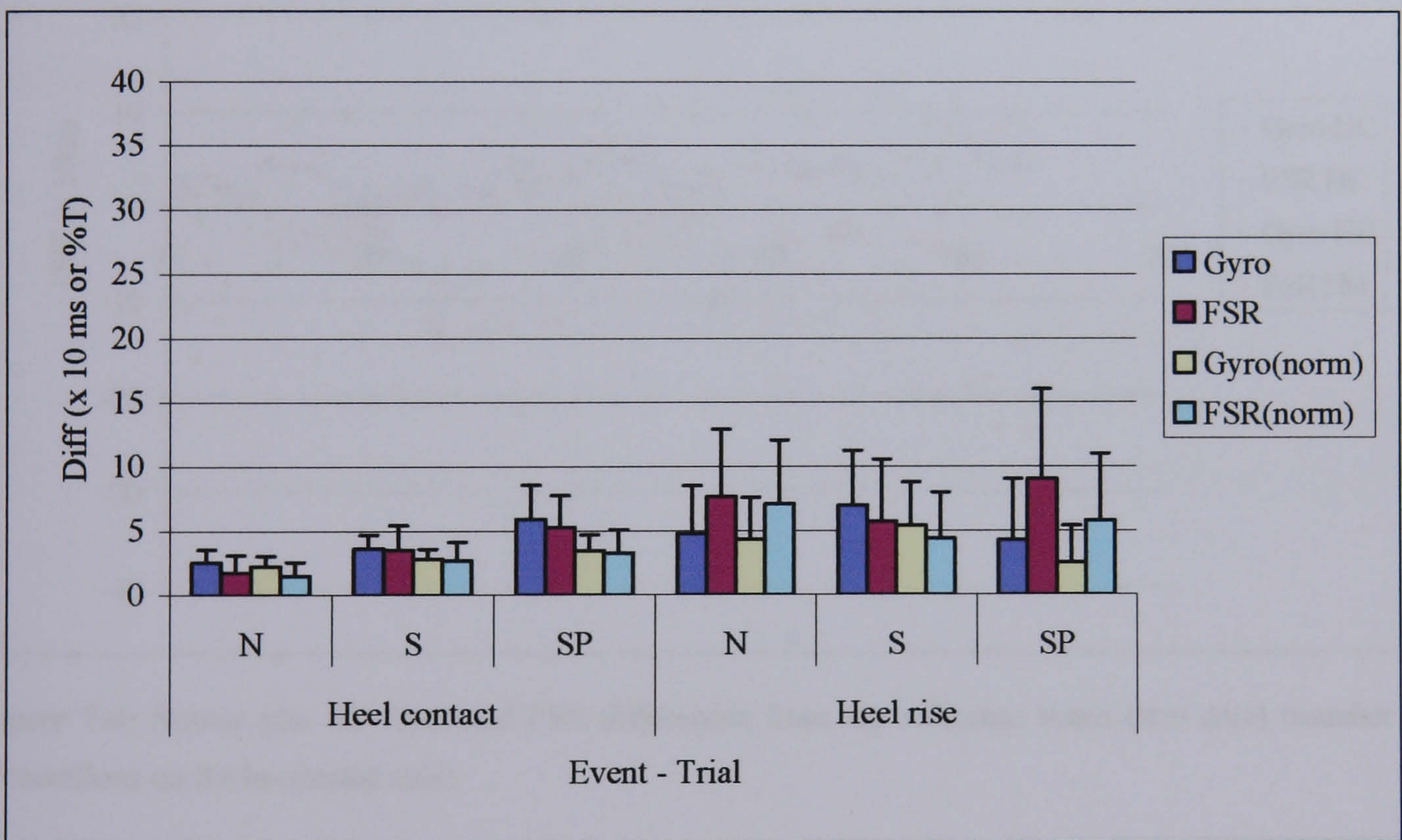


Figure 7-3: Average of absolute event timing differences between the Gyro/FSR and reference system.

Table 7-1 presents the timing accuracies for the Gyro and FSR for the detection of both events. The means for both normalised and raw absolute timing differences are presented for a combination of the differences in all 3 conditions and for the combined normal and slow trials.

Table 7-1: Normalised and raw average of absolute timing differences for both systems

Data:		Normalised Data (%T)				Raw Data (x 10 ms)			
Event:		Heel contact		Heel rise		Heel contact		Heel rise	
System:		Gyro	FSR	Gyro	FSR	Gyro	FSR	Gyro	FSR
All	Average:	2.7	2.4	4.4	5.7	3.7	3.2	5.5	7.2
	STDEV:	1.0	1.6	3.4	4.6	2.0	2.3	4.3	5.6
Normal & Slow	Average:	2.5	2.1	4.9	5.7	3.1	2.6	5.9	6.6
	STDEV:	0.8	1.4	3.3	4.5	1.2	1.9	4.1	5.1

Figure 7-4 shows the distribution of the timing differences of both systems in a scatter plot.

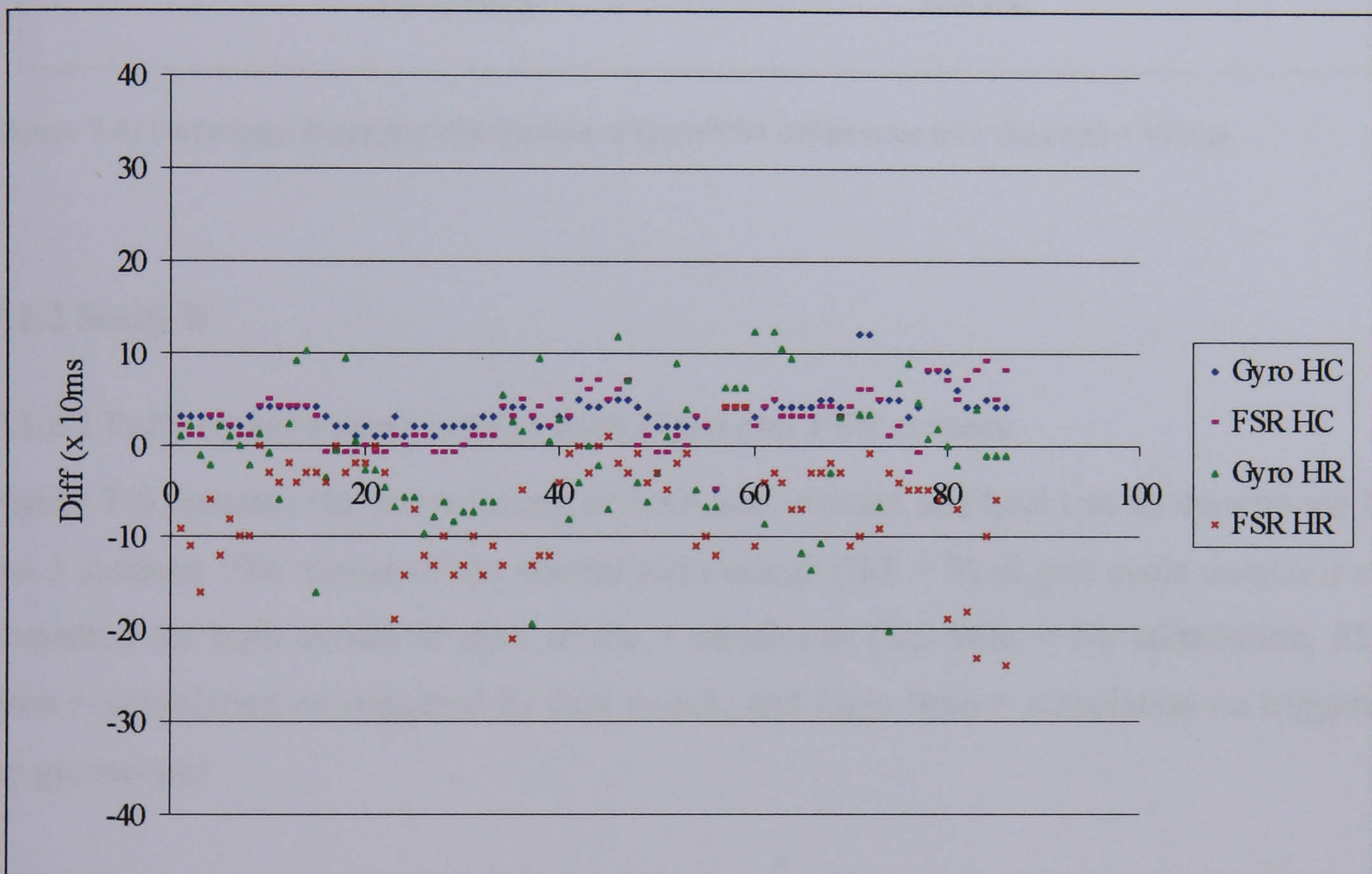


Figure 7-4: Scatter plot for Gyro and FSR differences from the reference times (raw data) (number of observations on the horizontal axis).

7.1.1.2 Frequency distribution of timing differences

Figure 7-5 presents the percentage frequency distribution of the absolute timing differences for both systems in all 3 conditions for heel contact and rise.

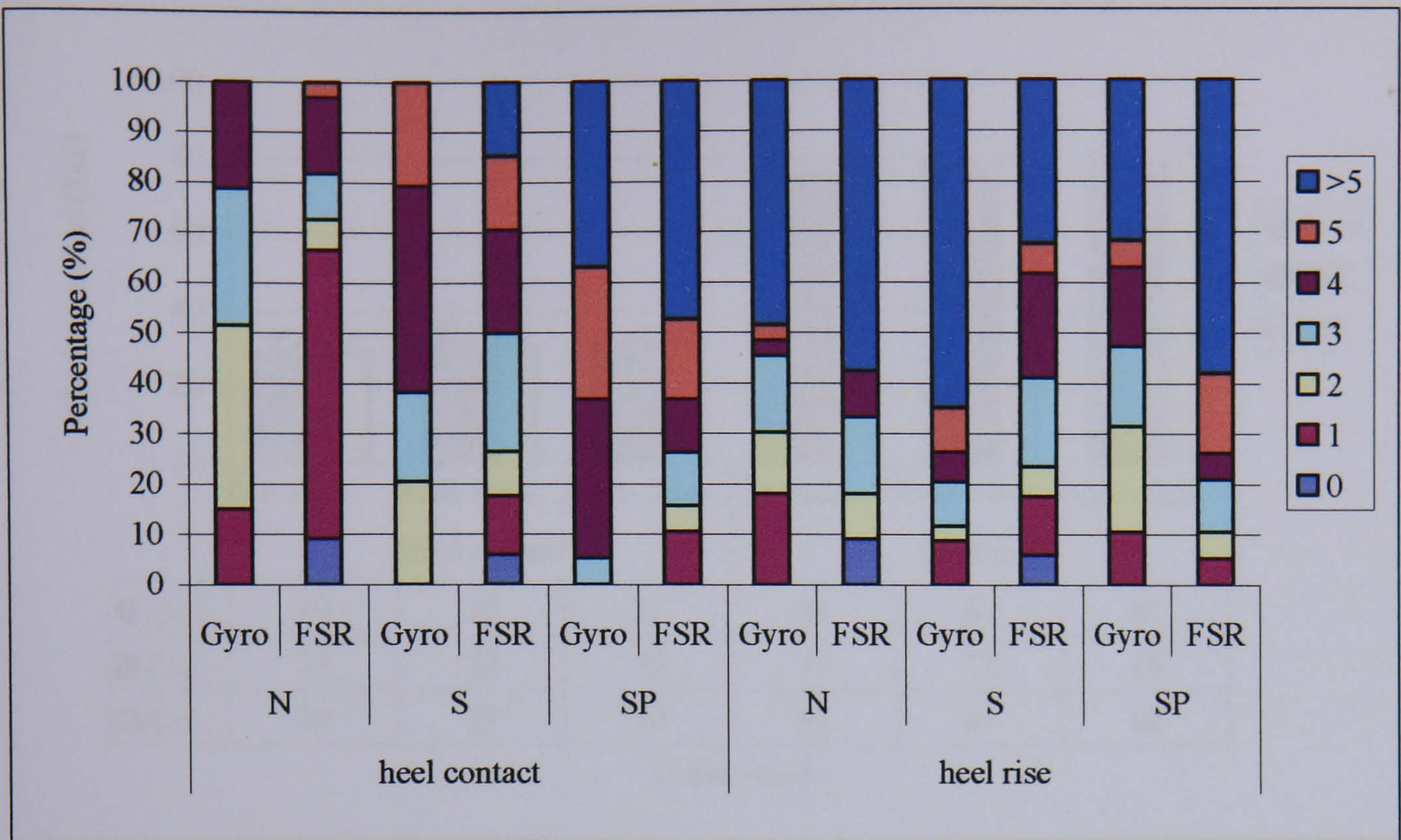


Figure 7-5: Percentage frequency distribution of Gyro/FSR differences (raw data and x 10 ms)

7.1.2 Study B

7.1.2.1 Performance accuracy for both Gyro and FSR sensors

Figure 7-6 presents the mean timing of both heel contact and heel rise as determined by the 3 systems. The means of the normalised timings (%T = % of gait cycle duration) are presented for both events in each of the 3 conditions (No Stim = No stimulation, FSR Stim = stimulation on triggered by foot switch, and Gyro Stim = stimulation on triggered by gyroscope).

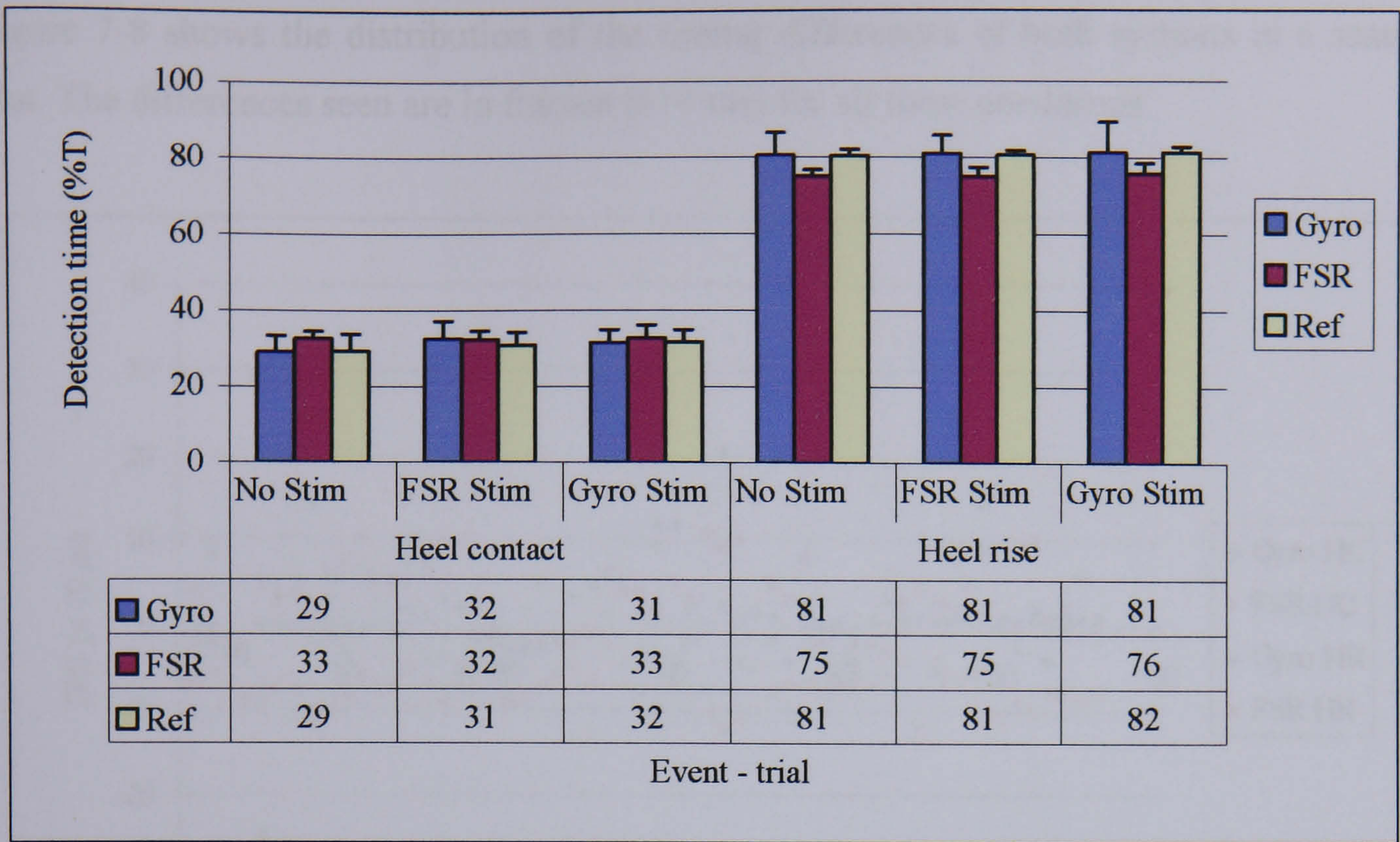


Figure 7-6: Normalised detection times of heel contact and rise as given by the Gyro, FSR, and Reference system

Figure 7-7 shows the average of absolute event timing differences for both systems (data in frames and normalised to gait cycle duration).

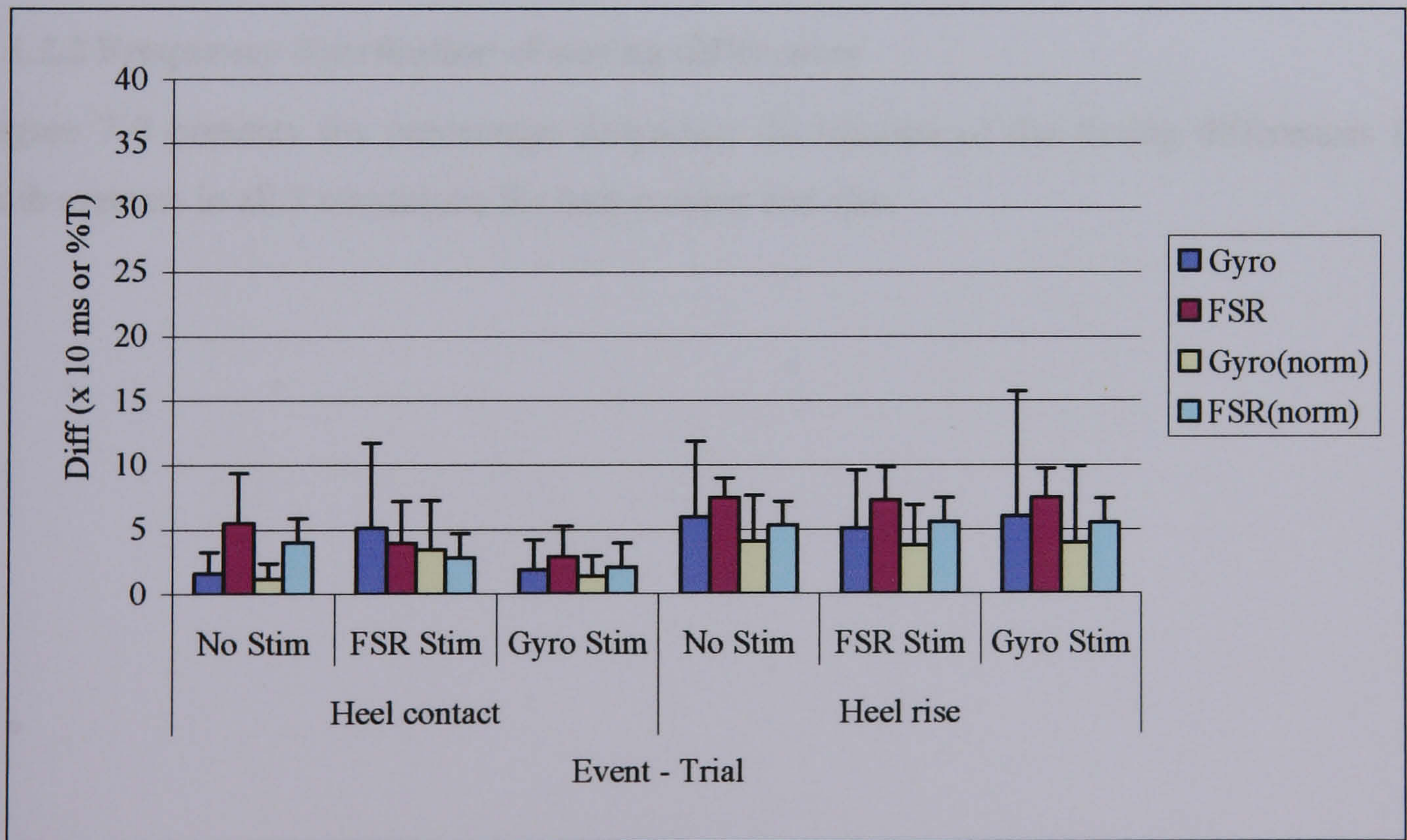


Figure 7-7: Average of absolute event timing differences between the Gyro/FSR and reference system.

Figure 7-8 shows the distribution of the timing differences of both systems in a scatter plot. The differences seen are in frames ($\times 10$ ms) for all three conditions.

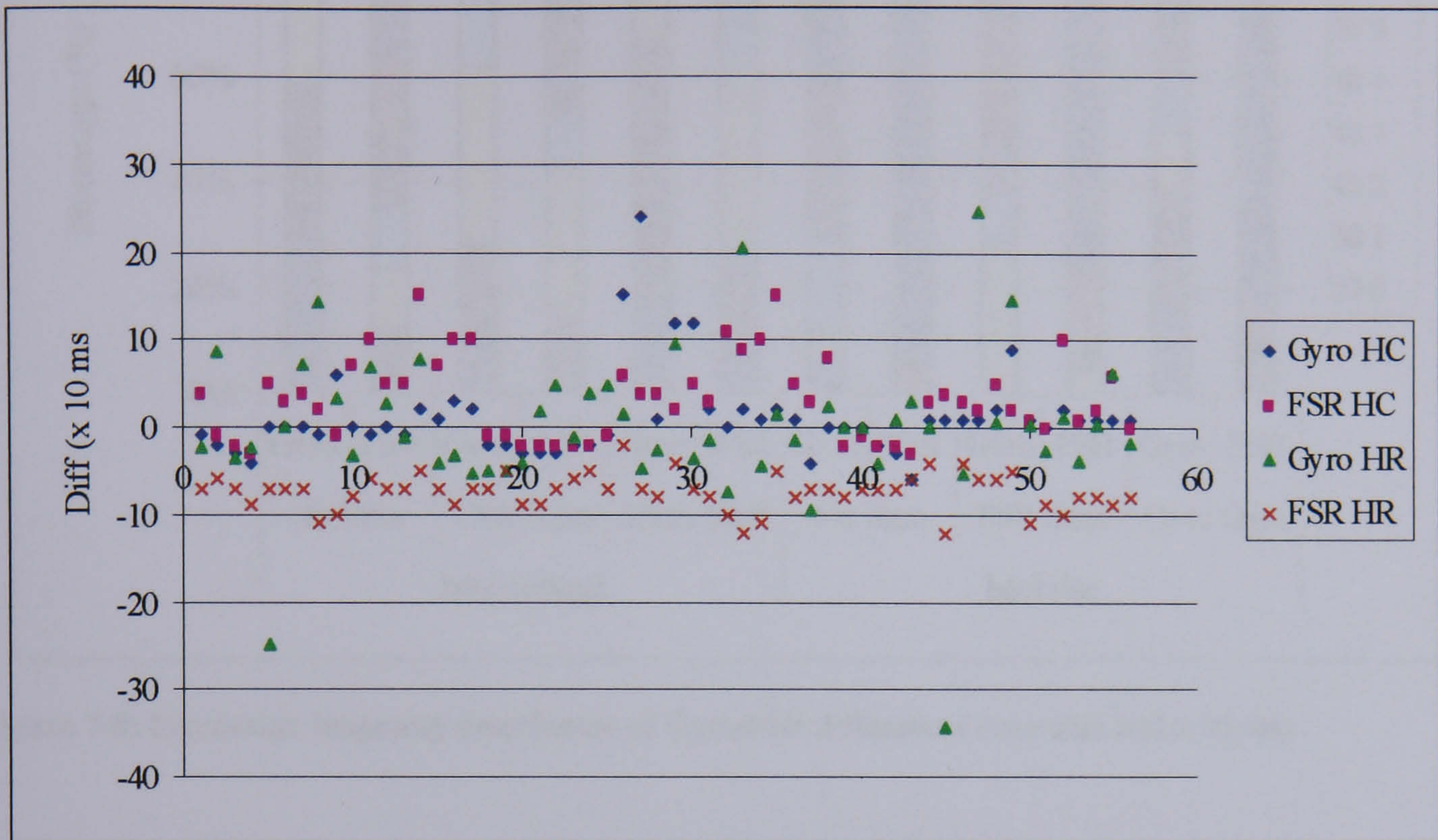


Figure 7-8: Scatter plot for Gyro and FSR differences from reference times (raw data-all conditions) (number of observations on the horizontal axis).

7.1.2.2 Frequency distribution of timing differences

Figure 7-9 presents the percentage frequency distribution of the timing differences for both systems in all 3 conditions for heel contact and rise.

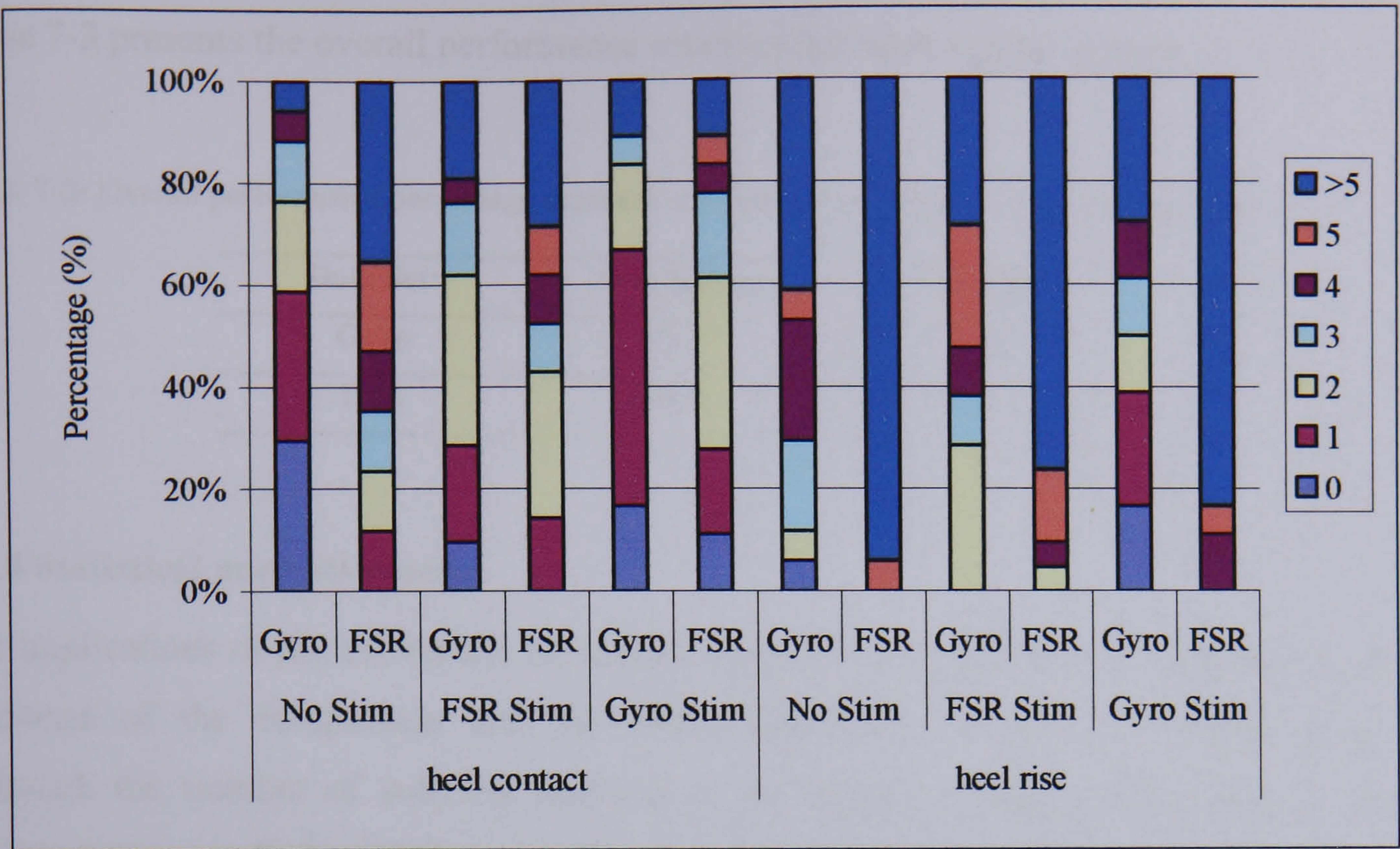


Figure 7-9: Percentage frequency distribution of Gyro/FSR differences (raw data and x 10 ms)

7.1.3 Detection accuracy

Table 7-2 shows the detection accuracy of both systems in each of the 3 conditions per subject group. The accuracy is measured as described in section 6.3.

Table 7-2: Performance percentage accuracy of both sensor systems for all three conditions in both data sets.

Tests:	Able-bodied			Patients		
	N	S	SP	No Stim	FSR Stim	Gyro Stim
Gyro	96.6	96.4	94.4	94.7	93.1	93.8
FSR	95.8	96.2	91.6	90.9	91.2	91.6

Table 7-3 presents the overall performance accuracy for both subject groups.

Table 7-3: Overall performance percentage accuracy for both sensor systems in the two data sets.

Data Set:	Able-bodied	Patients
Gyro	95.9	93.8
FSR	94.8	91.2

7.1.4 Statistical analysis results

The implications of the results can be judged in light of the statistical significance in the outcomes of the comparison and the representation of the selected patient group. Although the number of subjects involved in the study is limited, the results of the statistical tests applied are believed to be useful in highlighting the differences between the three systems.

For the statistical analysis of the results, the normalised differences were used. Differences were averaged and reduced to one data point for each subject in each condition. Making no assumption about the distribution of the data and taking into account that the data are matched, the nonparametric Friedman test (two-way analysis on ranks) was used to test and compare the 3 groups and Dunn’s post test to test and compare each one of the 3 pairs of systems (Dunn 1964).

Table 7-4 shows the results of the statistical significance test applied to the results from Study A. statistical significance was tested between all 3 possible pairs of systems. This was repeated for data from both N and S trials separately, combined, and all 3 conditions.

Table 7-4: Statistical analysis results, with * indicating statistical significance at the $p < 0.05$ level.

	Normal speed			Slow speed			Normal and slow			All conditions		
	Gyro	Gyro	FSR	Gyro	Gyro	FSR	Gyro	Gyro	FSR	Gyro	Gyro	FSR
	FSR	Ref	Ref	FSR	Ref	Ref	FSR	Ref	Ref	FSR	Ref	Ref
HC	Not	*	Not	Not	Not	Not	Not	*	Not	Not	*	*
HR	Not	Not	*	*	Not	Not	*	Not	*	*	Not	*

Table 7-5 shows the results of the statistical significance test applied to the results from Study B.

Table 7-5: Statistical analysis results, with * indicating statistical significance at the $p < 0.05$ level.

	FSR Stim			Gyro Stim			With Stim			All conditions		
	Gyro FSR	Gyro Ref	FSR Ref	Gyro FSR	Gyro Ref	FSR Ref	Gyro FSR	Gyro Ref	FSR Ref	Gyro FSR	Gyro Ref	FSR Ref
HC	Not	Not	Not	Not	Not	Not	Not	Not	Not	Not	Not	Not
HR	Not	Not	Not	Not	Not	Not	*	Not	*	*	Not	*

7.1.5 Reliability of the system

Three types of detection errors are identified:

- False positive (F+ve): the sensor system detects an event that is not real as determined by the reference system.
- False negative (F-ve): the sensor system misses the detection of an event that the reference system identified.
- Significant difference (SD): the sensor system detected the event but either significantly early or late. Any difference greater than 150 ms was described as being significant. This decision is mainly the result of the commonly used stimulation frequency of 40 Hz. Although no experimental investigations have been made into the effect of delaying (or starting the stimulation earlier), a 150 ms difference or six stimulation pulses is expected to be a significant difference. This is equivalent to approximately 12 % of an average gait cycle, 20% of stance phase duration, and 100% of double support phase duration.

The errors from both parts of the assessment study are presented in Table 7-6 and Table 7-7 respectively.

Table 7-6: Description of detection errors by both systems in study A

		Normal speed			Slow speed			Simulated Path.		
		F+ve	F-ve	SD	F+ve	F-ve	SD	F+ve	F-ve	SD
HC	Gyro	-	-	-	-	-	-	2	-	-
	FSR	-	-	-	-	-	-	2	-	-
HR	Gyro	-	-	1	-	-	1	-	-	2
	FSR	-	-	1	-	-	1	-	-	4

Table 7-7: Description of detection errors by both systems in Study B

		No Stim			FSR Stim			Gyro Stim		
		F+ve	F-ve	SD	F+ve	F-ve	SD	F+ve	F-ve	SD
HC	Gyro	1	-	1	-	-	-	-	-	-
	FSR	-	-	-	-	-	-	-	-	-
HR	Gyro	2	-	-	1	-	-	-	-	5
	FSR	1	-	-	1	-	-	-	-	-

7.2 Discussion

7.2.1 Detection accuracy in able-bodied subjects

The means of the normalised timings of heel contact and rise as given by the 3 systems varied between 29 and 40 % for HC and 67 to 82 % for HR. In the case of HR, the Gyro was closer to the Ref estimates in all 3 conditions, and in the SP trials for the HC detection. The 3 systems agreed to within 3% for each condition in the HC case, while an 8 % difference was seen between the FSR and Ref means of HR timing in the N trials. The FSR mean timings of HR were consistently earlier than both the Gyro and Ref.

The timings of heel contact and rise as shown in Figure 7-1 reflect two main findings. A relatively higher standard variation, and hence variability, can be seen in the event detection by both the Gyro and FSR systems in the SP trials. In addition a higher standard

deviation in the detection of heel rise compared to heel contact in both the N and S trials. The higher variation in the SP trials can be the result of a relatively poorer performance of the detection system, but more likely a result of the inter-subject variability in gait due to the requirement to walk with a simulated pathological gait. This is supported by the higher standard deviation in the detection timings of the reference system.

Comparing the differences for either system as shown by Figure 7-2 and Figure 7-3 highlights the importance of averaging the absolute differences to avoid any misleading calculations. This is particularly the case for the Gyro system heel rise detection. A similar pattern is seen to the previous figure with higher standard deviations for heel rise and for the SP trials. For all 3 conditions, the Gyro and FSR performed very similarly in the detection of HC (37 and 32 ms respectively), and HR (55 and 72 ms). The Gyro performance was slightly better for HR while in the case of HC, the FSR performed slightly better (Table 7-1).

The scatter plot in Figure 7-4 emphasizes the wider distribution of differences for both systems in the detection of HR compared to HC. It can be seen from this figure that the majority of FSR HR detections (90%) were earlier than the Ref timings. This is also the case for the Gyro system but to a lesser degree (55%). As to the detection of HC, both the Gyro and FSR were delayed in a majority of cases (99% and 84% respectively).

The percentage frequency distribution (see Figure 7-5) of these differences reveals a systematic difference in the HC detection by the Gyro system (more than 80% of differences between 20 and 40 ms). A similar distribution can be noted for the FSR system but with a wider range (85% between 10 and 50 ms). For HR detection both systems had about 50% of differences within 50 ms, with a slightly better performance by the Gyro in the N and SP trials (52 & 68% compared to 42 and 42% respectively within 50 ms) and a better performance by the FSR-base system in the S trials (35% compared to 68% within 50 ms). The detection of HC for both systems is more accurate than that of HR. This can be seen if the frequency distribution of the differences is calculated for all 3 conditions. In the case of HC 92% of the Gyro differences and 84% of the FSR differences were within 50 ms, while for HR 49% and 52% were within 50 ms respectively.

7.2.2 Detection accuracy in patients

Figure 7-6 shows the timings of both events as given by the 3 systems, with three findings worth noting. First the Gyro timing was closer to the Ref system in the detection of HR. The same applies to HC with the exception of the FSR Stim trials, where the Gyro and FSR detection of HC were on average the same. Second, the standard deviation for HR detection was relatively higher in the case of the Gyro system (5 to 8 %) compared to both the FSR and Ref systems.

The timings of HC and HR for foot drop patients were similar to those for the able-bodied population (Compare Figure 7-1 to Figure 7-6). The timing of HC for both populations varied between 29 and 32%, with the exception of the SP trials (37%). The average HR timing for the 3 conditions in Study B was 81% compared to 75 - 77% in the S and N trials and 82% in the SP trials for able-bodied subjects. Walking with a simulated pathological gait seems to have caused a delayed occurrence of both HC and HR. It is suggested that this could be the result of an extended swing phase for that particular limb. As the timing of events was calculated using its relative position to the point in time when the heel elevation is maximal, an extended swing phase could be the cause for the observed timings.

Considering the mean of absolute timing differences for both systems (Figure 7-7), it can be seen that the Gyro outperformed the FSR in both HC and HR detection, with the exception of HC in the FSR Stim trials. The standard deviations in the HR timing differences of the Gyro system were consistently higher than those of the FSR system (3 to 6 % compared to 1 to 2 %). HR detection by the FSR shows a systematic difference where the FSR detected HR earlier than the Ref system (see Figure 7-8). This error (mean -80 ms) could be partly explained by the two different principles used by each system to detect heel rise. It is suggested that there is a delay between the time the patient off-loads the heel and the start of movement of the heel.

The distribution of the timing differences for both systems can be seen in Figure 7-9. Combining the FSR and Gyro Stim trials, 85 % and 72 % of the Gyro timing differences were within 50 ms for HC and HR respectively, compared to 79 % and 21 % in the case of the FSR timings.

7.2.3 Detection accuracy and reliability

The calculated accuracies of both systems' performance in the detection of the correct phase (Table 7-2 and Table 7-3) reflect a similar performance by the Gyro sensor system compared to the FSR system. This is true for all 6 conditions in both data sets. The overall accuracy (Table 7-3) of the Gyro was 96 % in the able-bodied sample and 94 % in the patient sample. The FSR accuracy was similar but slightly lower (95 % and 91 %). Both systems had a higher accuracy in the able-bodied tests than the patient tests. The SP trials also highlighted a slightly lower accuracy by both systems when compared to the results from the S and N trials in the able-bodied tests. This decrease in accuracy is believed to be the result of the higher inter-subject variability in pathological or simulated pathological gait when compared to normal gait. The effect of this on the performance when used by patients is expected to be minimised by setting subject specific parameters in the detection algorithms of the Gyro sensor system, in particular for heel rise detection. Currently used foot switch and simulator systems, such as the ODFS, are usually set by the scientist/physiotherapist to suit each patient's gait by adjusting delays and extension times and ramps in stimulator output.

The number of available data points that were used for statistical tests of the results was limited; Nevertheless, the statistical analysis results are believed to be useful in highlighting any significance in the differences between the 3 systems. For the combined data of able-bodied tests, the Gyro differences from the reference system were statistically significant in the case of HC detection, while the FSR differences were statistically significant in both HC and HR detection. The timing differences between the Gyro and FSR were statistically significant in the case of HR detection only.

For the data from patient tests, there was no statistical significance in the timing differences between any of the 3 systems in the detection of HC. In the case of HR, statistical significance was detected between the FSR and reference system both when data was combined from all 3 conditions, and for the FSR Stim and Gyro Stim trials. There was no statistical significance between any of the 3 systems when considering data from either the FSR Stim or Gyro Stim trials separately. This is expected due to the limited power of the statistical test with a small sample (3 data points per condition).

The three patients were asked for feedback on the Gyro Stim trials.

- Subject 1: Stimulation not coming in so sharply; feels less intense; not working as well
- Subject 2: Stimulation felt ok
- Subject 3: Stimulation felt ok

7.2.4 Agreement between methods

Figure 7-10 and Figure 7-11 show the Bland and Altman plots where the difference between the two methods is plotted against the mean timing as given by both methods. Bias plots are useful in the visual assessment of the differences between two methods. The difference plot shows the difference between the methods (on the Y axis), plotted against the estimation of the true value (the X axis). These plots can highlight any changes in the variance that are dependent on the timing of the event. The normalised timings from all subject trials in both studies were used for these plots. The grey line shows the zero bias line while the dotted line shows the bias of each method compared with the reference method. The red dash-dot line shows the 95% limits of agreement. If the differences are normally distributed, 95% of the differences will likely lie within the range. Larger limits of agreement indicate larger variation of differences, and therefore a lower degree of agreement.

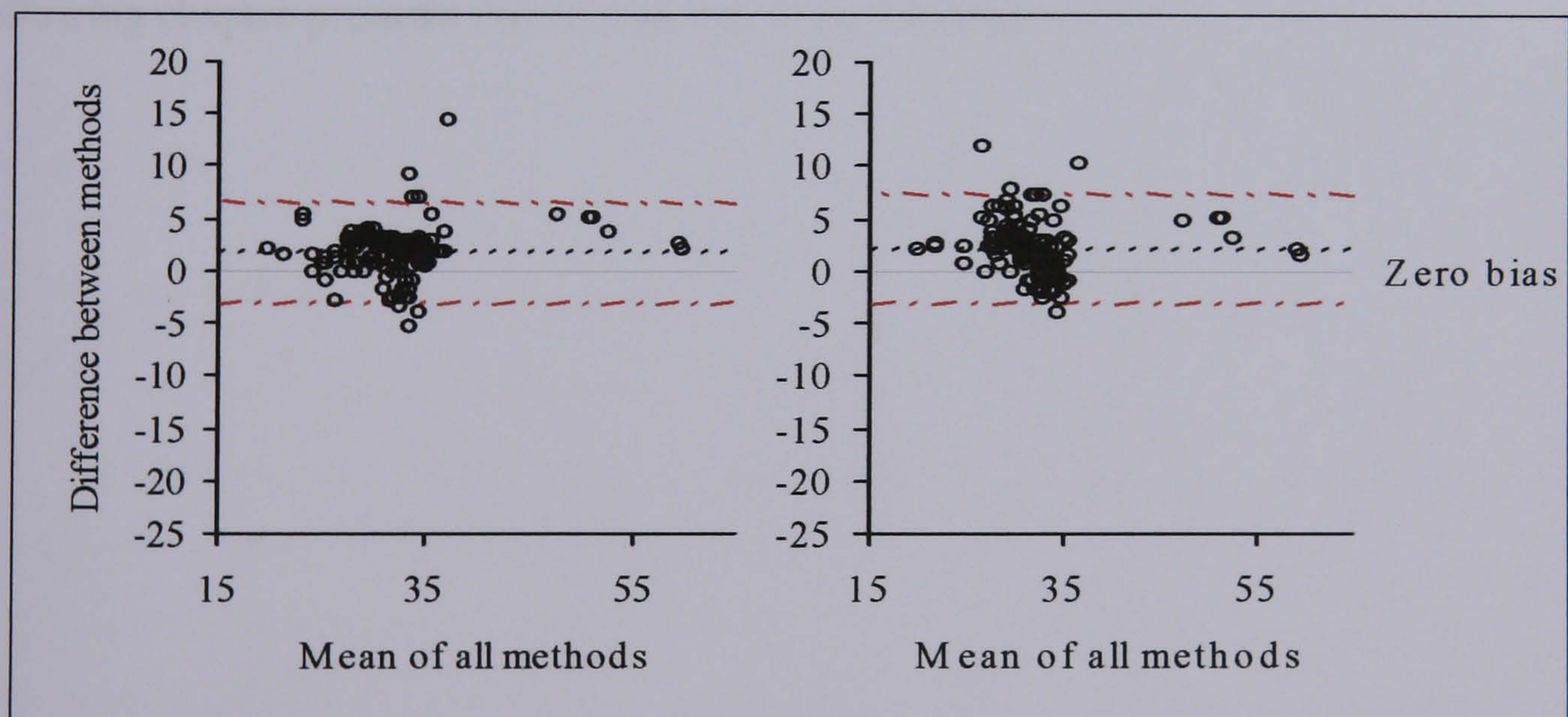


Figure 7-10: Bias plot for HC detection comparison between the Gyro vs Ref (left) and FSR vs Ref (right) (normalised timings as % of gait cycle).

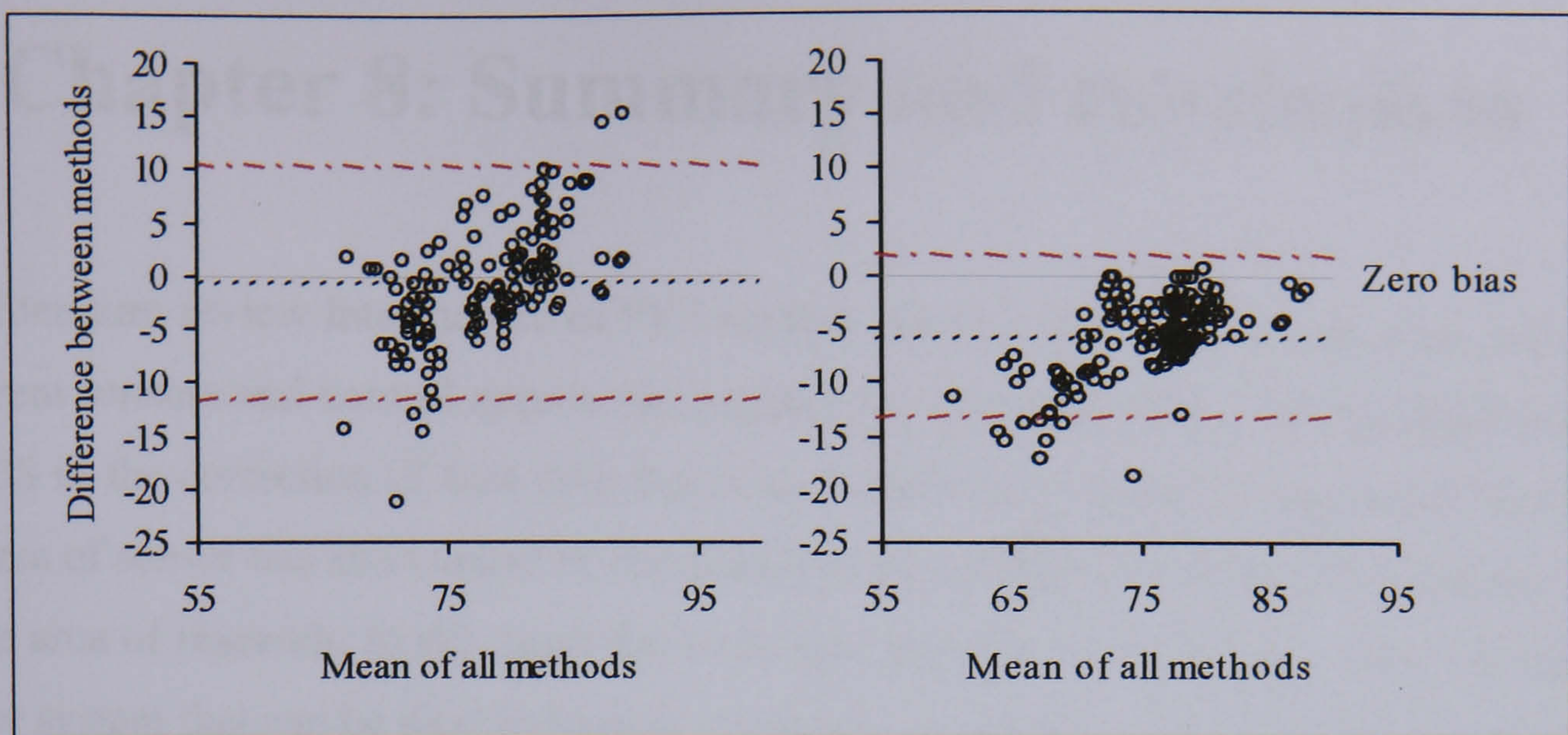


Figure 7-11: Bias plot for HR detection comparison between the Gyro vs Ref (left) and FSR vs Ref (right) (normalised timings as % of gait cycle).

In the case of heel contact detection, Figure 7-10 shows a bias of 2 % for the Gyro and 2 % for the FSR. The lower and upper limits of agreement are -3 and 7 % for the Gyro and -3 and 8 % for the FSR. For heel rise detection the bias for the Gyro timings is -1 % and in the case of the FSR timings -6 % (Figure 7-11). The lower and upper limits of agreement are -12 to 10 % and -13 to 2 % for the Gyro and FSR respectively.

After this discussion of the results seen in the evaluation of the new sensor system, the following chapter presents the conclusions from this work.

Chapter 8: Summary and conclusions

The literature review into the use of FES systems for the correction of foot drop and the different sensors and control approaches highlighted two main facts. First the application of FES in the correction of foot drop has been a useful and beneficial approach. Second, the area of sensor use and control of stimulation has been well investigated but remains an active area of research. In this study the main aim has been to design, test, and validate a sensor system that can be used to trigger stimulation in a FES foot drop correction system. Such a sensor should make it feasible to work towards a totally self-contained device with the surface stimulator, sensor, and electrodes part of one unit to be worn on the shank. A novel approach of using a single gyroscope placed on the shank of the affected side to obtain feedback for the triggering of the stimulation was taken.

The evaluation of such a sensor required the availability of a reference method for gait event detection. This was achieved using a kinematic-based approach and an algorithm for the automated detection of gait events from three dimensional co-ordinate data of foot markers. An investigation was carried out into the processing of three dimensional gait data for the purposes of noise reduction in differentiation. A summary and the main conclusions drawn from the work undertaken in each one of the three areas are presented in the following sections. The last section highlights some of the constraints and limitations of this study.

8.1 Kinematic-based gait event detection

A review of available methods for gait event detection was completed and a decision was made to develop a new method utilising kinematic data. The 3D co-ordinates of two retroreflective markers, placed on the heel and toe, were acquired using a marker detection system and utilised in the detection of the timings of heel contact, heel rise, toe contact, and toe-off. MATLAB routines were written to process the data and to apply a set of rules for the detection of each one of the four gait events. The new method was validated using gait event timings obtained from force platform data and visual inspection of marker data by trained observers. 12 able-bodied subjects took part in the main validation study. The subjects performed a total of 144 steps walking barefoot and shod and at different walking speeds. The timings of the 4 gait events as given by the 3

methods were then evaluated. The new method was also assessed in determining the durations of 3 intervals in the gait cycle: HC-TC [Heel contact to Toe contact], TC-HR [Toe contact to Heel rise], and HR-TO [Heel rise to Toe off]. For all four gait events the visual and algorithm method agreed to within 17 ms in 90% of the cases, and to within 33 ms in 96% of the cases. The results from this study showed that the new method is both reliable and time saving for the detection of gait events and interval durations. The study also allowed for a better understanding of the relatively slower events of break of contact such as heel rise and toe-off. The results suggest that the use of phases to describe such events would be more appropriate. Force data recorded using foot switches, instrumented shoe insoles, or plantar pressure measurement systems from the area under the heel and toe do indeed reflect a gradual off loading. The time from the start of the break of contact to the point in time where the force value is zero is sufficiently significant to consider an alternative to the commonly used event definition for heel rise and toe-off.

8.2 The choice of cut-off frequency for kinematic data analysis

The adopted approach for kinematic-based gait event detection involved processing of the 3D co-ordinate data with a differentiation step. The problem of differentiating biomechanical data contaminated with noise made it necessary to apply some means of noise reduction for an improved estimation of first or second derivatives. As this has been a well-investigated issue, a review into the literature was carried out for an understanding of existing and commonly used techniques and their operation. The importance of the frequency characterisation of kinematic signals became evident from this review. 10 able-bodied subjects were recruited and participated in an experimental study that was carried out in order to look at the frequency domain characteristics of lower limb segments gait signals. In retrospect, the conventional set of marker positions (e.g. Helen Hayes marker set) should have been used, which would have allowed for expanding the conclusions reached from this analysis to other applications. However, it is the author's belief that the frequency content will not change significantly so as to affect the conclusions reached from this study.

The results from this study suggest that 95 % of the signal power is within 10 Hz. The study also showed that any components above 10 Hz contribute less than 1 % of the overall signal power. 10 Hz was hence chosen as the cut-off frequency for low pass filtering of 3D co-ordinate data prior to differentiation. Previously reported characteristics

of kinematic gait data were confirmed by the results from this study. The study also highlighted the need for extra care when applying the commonly used residual analysis method, in particular when deciding on a choice of cut-off frequency for low-pass filtering of gait kinematic data. .

8.3 Development of the Gyro sensor system for use in FES foot drop correction

A gyroscope-based sensor system was further developed, and aimed to control the timing of stimulation applied to the peroneal nerve in foot drop patients. The sensor system relies on a feedback signal from a Murata (ENC 03J) piezoelectric gyroscope that senses the shank angular rate in the sagittal plane. The feedback signal is utilised by a purpose written algorithm running on the PIC 16C73B microcontroller to detect the timings of heel contact and heel rise. The supporting electronics and microcontroller are housed within a portable unit (dimensions 108 x 79 x 35 mm) that was carried by the subject. The gyroscope sensor and its supporting components were housed within a sensor package (dimensions 27 x 17 x 4.5 mm) and attached to the shank of the subject using a Velcro strap. The sensor connected by a wire to the controller unit (placed at the waist), provides a control signal that was used to trigger the foot drop stimulator.

One group of able-bodied subjects (Study A) and a group of 3 patients suffering from foot drop (Study B) used and evaluated the sensor system. The system's ability to correctly identify and detect two gait events was assessed and compared to that of the commonly used foot switches. For this purpose, simultaneous recordings from a 3D motion capture system, foot switches, Gyro, and video were made. Each subject performed multiple trials at different walking speeds and conditions in study A, and with different stimulation conditions in study B. Each trial data was processed in order to determine the timings of heel contact and rise according to the gyro sensor system and foot switches, and compared against the reference times determined from the reference kinematic system.

The overall accuracy of the Gyro was 96 % in the able-bodied trials and 94 % in the patient trials. The FSR accuracy was similar but slightly lower (95 % and 91 %). The performance of the Gyro sensor system would suggest that it is sufficient for its use in a FES foot drop correction system under the conditions tested. In addition to its similar performance to the foot switch, the new sensor system is believed to offer a number of advantages due to its nature and the way it has been used. The commonly used foot switch

is subjected to significant loading cycles leading to a relatively short lifetime, while the new sensor is expected to have a much longer lifetime. In addition, weight shifting or foot sliding which is reported to cause erroneous triggering of stimulation when the foot switch is used does not affect the new sensor system. Walking barefoot while using the stimulator with foot switches is another limitation that is overcome by the use of the new sensor system. In addition, the single gyroscope based sensor system allows for the potential detection of additional gait events (such as toe off and foot flat), which are often required for dual channel stimulation used in gait assist.

8.4 Other conclusions drawn from this work

The second half of this dissertation described the work undertaken for the development of the Gyro sensor system and its evaluation in gait event detection. The literature review carried out into the application of FES for foot drop correction and the sensor technology used in such systems emphasized the following points:

- Growing evidence is available to support the beneficial use of FES in foot drop correction.
- The area of sensor technology and feedback control of FES foot drop systems is a very active area of research. A variety of both artificial and natural sensors and control approaches have been used or tested. These approaches, however, are yet to result in a system that is both reliable and sufficiently easy to use in the clinical setting and the everyday life of the patient.
- Recently a substantial amount of research has been focused on the development of more (desirable) implantable and cosmetically acceptable systems. This is in combination with the use of natural sensors and bio-signals such as the ENG.
- There is a very limited use of FES foot drop systems particularly when we consider the incidence and prevalence rates of the conditions leading to foot drop.
- The majority of the currently used systems in clinical settings, particularly in the UK, are single-channel surface stimulators and very similar to the original system designed and described by Liberson and his group in 1961. These systems are still

dependent on the use of foot switches and have the potential for both cosmetic and functional improvement. The reliability and use of such systems are partly constrained by the use of foot switches.

It is the author's belief that future developments to FES foot drop correction systems should focus on the needs of two types of users. One of these is the patient who would benefit from the system, but will not opt to use the device permanently or long term. The benefits of FES to this group of patients stop due to either sufficient natural or otherwise recovery, or due to a deterioration in their condition where ambulation becomes dependent on other means. A reversible means of correcting the foot drop in this group would benefit from a reliable and an easy to use external system that requires minimal or no surgical intervention. On the other hand, the patient who could benefit from FES long term use should be considered for a fully implantable system (seen in Figure 8-1 – D). Patients who are not suitable for surface stimulation (for example due to a skin condition) could also benefit from such a system. The sensor approach used in this project or alternative approaches using bio-signals for controlling the stimulator could be appropriate.

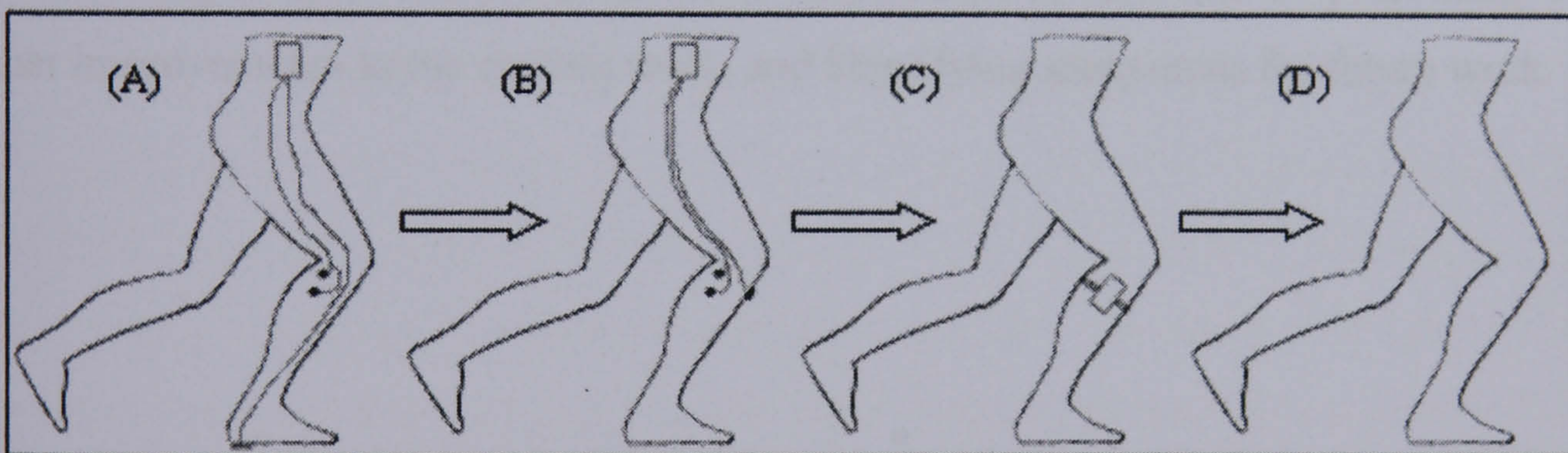


Figure 8-1: Schematic showing the evolution in the design of FES foot drop correction systems.

The main aim behind developing the Gyro sensor system was to improve the currently used surface system and to overcome a number of limitations with the use of the foot switch. The new sensor system further improves the cosmetic appearance by reducing the number of wires and sites of attachment. With this new approach no wires will run lower than the proximal part of the shank and no sensors are to be attached to the foot. This fact also reduces the hindrance to the patient and should make it easier to don and doff the system. This transition from the traditional set-up (seen in Figure 8-1 – A) to the

arrangement seen in (seen in Figure 8-1 – B) also makes it feasible to develop a totally self-contained device with an integrated stimulator, sensor, control, and electrodes compact package (seen in Figure 8-1 – C). A strap holding the system in place could incorporate the electrodes and some easy means of adjusting the position of electrodes for both the clinician and patient. Electrode positioning is a common problem and challenge to both the patient and therapist as evident from the literature review. One suggested solution to this issue would be the use of steerable electrodes. A strap will incorporate multiple electrodes so that different combinations of these electrodes can be connected to form virtual electrodes, and produce a more optimal response to stimulation.

8.5 Limitations of the study

The work presented does suffer from a number of limitations. Of particular note are:

- The limited number of patients used for testing the Gyro sensor system.
- All testing of the Gyro sensor system was carried out in the laboratory.
- The kinematic reference method for gait event detection was not validated in an experimental study using pathological gait data.

The following chapter will address these limitations, in addition to presenting some further improvements to the current work, and identifying main areas for future work.

Chapter 9: Future work

This chapter identifies areas of the work undertaken in this project that could be the subject of future investigations. The results of this work in conjunction with the literature review will also be used to highlight some areas where further work is necessary.

9.1 Gyro sensor system and FES for foot drop

Further work in this area can be separated into software and hardware areas and can be summarised in the following points:

- ❖ Further testing of the new sensor system is needed to establish its reliability when walking outside the laboratory, walking over ramps, and stair climbing. Some testing is also needed for sit to stand and stand to sit transfers. Additional testing by a patient group with a larger size and a wider set of pathological causes for foot drop would be necessary prior to clinical use of a system based on the Gyro sensor. Although the results are not expected to be different, the additional data would reinforce the conclusions drawn from this study.
- ❖ Design of a totally self-contained device: this will be a natural step after the above. Miniaturisation can be achieved by the re-design of the sensor system circuitry and control box and its integration with the stimulator module. The availability of new gyroscopes on the market (such as ENC-03M, a SMD type sensor from the Gyrostar[®] series by Murata) and the use of surface mount technology would be two useful assets. The availability of a prototype of such a device would allow for some clinical trials and for the patient to use such a device more freely and provide additional feedback.
- ❖ Modify the detection algorithm to include the ability to detect additional gait events. The same data collected could be used to evaluate the detection of two other events – foot flat and toe-off. Toe-off, for example, is evidently derivable from the occurrence of a negative peak after heel rise. The timings of these two events will allow increased flexibility to the clinician in setting up the stimulator. One example where these timings would be useful is in triggering the stimulation for different muscle groups at different times during the gait cycle.

- ❖ Technology has made it possible to design injectable microstimulators (Arcos *et al.* 2002) and implantable artificial sensors (Johnson *et al.* 1999). Such technology can be used in combination with external units for power and control and allow for the development of systems that are more acceptable to the patient, in particular the long-term user.
- ❖ Adaptive algorithms: by undertaking further processing on temporal parameters of past gait cycles some predictions can be made in order to adapt the timing and intensity of stimulation. The detection of slowing down or speeding up, for example, could be achieved by using some form of extrapolation computation based on previous stride times, length or velocities. This is particularly useful for FES use by children with CP. Published work has shown the possibility of extracting such temporal and spatial parameters from lower limb segment angular velocity recordings (Aminian *et al.* 2002).
- ❖ Closed loop control of FES in foot drop correction is believed to significantly improve the functionality of current systems. Few attempts have been made at designing systems for foot drop correction with closed-loop control. The practicality of such systems remains an issue with the current sensors available for such applications. The availability of either natural or implantable artificial sensors suitable for closed-loop control will further advance these applications and make them useful for patients in their daily activities and environment. For example, in the case of a foot drop stimulator, one could account for fatigue and a changing muscle response to stimulation by monitoring the gyroscope output and derived spatio-temporal parameters. The stimulation parameters and stimulation envelope can be accordingly modified in real-time. A literature search and an experimental investigation into such relationships will be pre-requisites for this work. One possibility will be to consider the duration and maximal positive angular rate during swing (its integration) and their relationship to the muscle response and gait quality. Normative measures of angular velocities and temporal parameters could be also used to adapt the stimulation in order to approximate such measures in the patient's gait.

9.2 Gait event detection and kinematic algorithms

Further work into the area of kinematic-based gait event detection should focus on the testing of the kinematic algorithms for gait event detection by using pathological gait data. A similar experimental protocol to that used in this project could be used to test the performance in pathological gait. The use of an insole pressure measurement system is believed to be useful for such a study. It is also believed to be useful to test the kinematic algorithms for gait event detection using conventional gait analysis marker locations on the heel and toe. This will avoid the need for additional markers and would allow for the use of this algorithm in detecting gait events timing during routine gait analysis.

With hindsight, the study that was performed into the frequency content of gait kinematic data should have used conventional landmarks for the positioning of surface markers. It is however believed that this will not have any significant effects on the conclusions drawn from the described study.

Two additional modifications are suggested to the algorithm. Firstly, it will be useful to adapt this program for bilateral detection of both right and left gait events. Secondly, to add a set of rules to the algorithm in order to improve the accuracy of detection. This can be done by creating a matrix that describes each data frame in relation to the heel and toe markers. The matrix will be a set of indexes given to describe different parameters of the marker position, velocity, and acceleration. If the marker parameters at contact and break of contact are defined or approximated, then the set of parameters and matrix that best describes the event can be also defined. Finding the identical or most similar frame matrix in the data to each events matrix will further improve the accuracy in detecting these events. Using such a method the detection of the events will be based on a combination of marker parameters such as velocities, position, and accelerations, and it is believed that this will improve the robustness and accuracy of the algorithm.

The availability of an automated reference method for gait event detection will be of use in achieving issues not directly related to the objectives of this work. Some future work could focus on developing a database of gait event timings. This will be useful in gait evaluation and assessment of pathological gait and response to interventions. The method can also be used to shed more light on gait intervals durations and their dependence on

other variables or pathologies. One such example is the heel-toe interval, sometimes used as an outcome measure, and its dependence on variables like walking speed.

References

- Aminian, K., B. Najafi, C. Bula, P. F. Leyvraz and P. Robert (2002). "Spatio-temporal parameters of gait measured by an ambulatory system using miniature gyroscopes." Journal of Biomechanics **35**: 689-699.
- Aminian, K., K. Rezakhanlou, E. De Andres, C. Fritsch, P. F. Leyvraz and P. Robert (1999). "Temporal feature estimation during walking using miniature accelerometers: An analysis of gait improvement after hip arthroplasty." Medical & Biological Engineering & Computing **37**(6): 686-691.
- Ando, S., Y. Shimada, K. Sato, G. Obinata, Y. Abe, T. Matsunaga, Y. Tsutsumi, A. Misawa, T. Minato, M. Sato, S. Chida and K. Hatakeyama (2000). Application of the acceleration sensor in functional electrical stimulation for the restoration of gait in stroke patients. 5th Annual Conference of the International Functional Electrical Stimulation Society, Aalborg, Denmark.
- Angeloni, C., P. O. Riley and D. E. Krebs (1994). "Frequency content of whole body gait kinematic data." IEEE Transactions on Rehabilitation Engineering **2**(1): 40-46.
- Arcos, I., R. Davis, K. Fey, D. Mishler, D. Sanderson, C. Tanacs, M. J. Vogel, R. Wolf, Y. Zilberman and J. Schulman (2002). "Second-generation microstimulator." Artificial Organs **26**(3): 228-231.
- Bajd, T., A. Kralj, M. Stefancic and N. Lavrac (1999). "Use of functional electrical stimulation in the lower extremities of incomplete spinal cord injured patients." Artificial Organs **23**(5): 403-409.
- Baker, L. L., D. R. McNeal, B. L.A., B. B.R. and R. L. Waters (1993). Neuromuscular electrical stimulation - a practical guide, Rehabilitation Engineering Program, Los Amigos Research & Education Institute, Rancho Los Amigos Medical Center.
- Baysefer, A., E. Erdogan, A. Sali, S. Sirin and N. Seber (1998). "Foot drop following brain tumors: Case reports." Minim Invasive Neurosurg **41**(2): 97-98.
- Bland, J. M. and D. G. Altman (1986). "Statistical methods for assessing agreement between two methods of clinical measurement." The Lancet: 307-310.
- Bogataj, U., M. Kijajic, N. Gros, R. Acimovic and M. Malezic (1993). The rehabilitation of gait in stroke patients: A comparison between conventional therapy and multichannel neuromuscular electrical stimulation therapy. The Ljubljana FES Conference.
- Bogataj, U., M. Kljajic, U. Stanic, R. Acimovic and N. Gros (1984). Gait pattern behavior of hemiplegic patients under the influence of a six-channel microprocessor stimulator in a real environment. Proc 2nd Int Conf Rehab Eng.
- Bowker, P. and G. H. Heath (1995). Control of peroneal functional electrical stimulation using a magneto transducer to monitor the angular velocity of the knee. Proc World Cong Int Soc Prosthet Orthot, Melbourne.

- Bowman, B. R. and L. L. Baker (1985). "Effects of waveform parameters on comfort during transcutaneous neuromuscular electrical stimulation." Annals of Biomedical Engineering **13**(1): 59-74.
- Burridge, J., P. Taylor, S. Hagan and I. Swain (1997). "Experience of clinical use of the odstock dropped foot stimulator." Artificial Organs **21**(3): 254-260.
- Burridge, J. H. (2001). "Does the drop-foot stimulator improve walking in hemiplegia?" Neuromodulation **4**(2): 77-83.
- Burridge, J. H., P. N. Taylor, S. A. Hagan, D. E. Wood and I. D. Swain (1997). "The effect of common peroneal nerve stimulation on the effort and speed of walking. A randomised controlled trial with chronic hemiplegic patients." Clinical Rehabilitation **11**: 201-210.
- Challis, J. H. (1999). "A procedure for the automatic determination of filter cutoff frequency for the processing of biomechanical data." Journal Of Applied Biomechanics **15**: 303-317.
- Craik, R. L. and C. A. Oatis (1995). Gait analysis: Theory and application, Mosby. Pages 310-315, 413.
- Dai, R., R. B. Stein and B. Andrews (1996). "Application of tilt sensors in functional electrical stimulation." IEEE Transactions on Rehabilitation Engineering **4**(2): 63-71.
- D'Amico, M. and G. Ferrigno (1990). "Technique for the evaluation of derivatives from noisy biomechanical displacement data using a model-based bandwidth selection procedure." Medical & Biological Engineering & Computing **28**: 407-415.
- Dunn, O. J. (1964). "Multiple comparisons using rank sums." Technometrics **6**: 241-252.
- Edwards, S. (1996). Neurological physiotherapy : A problem-solving approach. New York ; Edinburgh, Churchill Livingstone.
- Frigo, C., M. Ferrarin, W. Frasson, E. Pavan and R. Thorsen (2000). "Emg signals detection and processing for on-line control of functional electrical stimulation." Journal of Electromyography and Kinesiology **10**(5): 351-360.
- Georgakis, A., L. K. Stergioulas and G. Giakas (2002). "Automatic algorithm for filtering kinematic signals with impacts in the wigner representation." Medical & Biological Engineering & Computing **40**(6): 625-633.
- Ghoussayni, S. (2000). Use of the angular rate gyroscope as a sensor for fes foot drop correction. MSc Thesis. School of Mechanical and Materials Engineering. Guildford, University of Surrey.
- Ghoussayni, S., C. Stevens, S. Durham and D. Ewins (2002). Gait event detection: A comparison of force platform, visual inspection, and kinematic algorithm based methods. Gait and Clinical Movement Analysis Society Seventh Annual Meeting, Chattanooga, Tennessee.

- Giakas, G. and V. Baltzopoulos (1997). "A comparison of automatic filtering techniques applied to biomechanical walking data." Journal of Biomechanics **30**(8): 847-850.
- Giakas, G., L. K. Stergioulas and A. Vourdas (2000). "Time-frequency analysis and filtering of kinematic signals with impacts using the wigner function: Accurate estimation of the second derivative." Journal of Biomechanics **33**(5): 567-574.
- Graham, J. (2000). What is ms? London, Multiple Sclerosis Society.
- Granat, M. H., D. J. Maxwell, A. C. B. Ferguson, K. R. Lees and J. C. Barbenel (1996). "Peroneal stimulator: Evaluation of the correction of spastic foot drop in hemiplegia." Archives of Physical Medicine and Rehabilitation **77**: 19-24.
- Graupe, D. K.H. Kohn, A. Kralj, S. Basseas.(1983). Patient controlled electrical stimulation via EMG signature discrimination for providing certain paraplegics with primitive walking functions. Journal of Biomedical Engineering **5**(3): 220-226.
- Hambrecht, F. T. (1992). A brief history of neural prostheses for motor control of paralyzed extremities. Neural prostheses replacing motor function after disease or disability. R. B. Stein, P. Hunter Peckham and D. B. Popovic. New York, Oxford University Press.
- Hambrecht, F. T. and J. B. Resnik (1977). Functional electrical stimulation : Applications in neural prostheses. New York, M. Dekker.
- Hansen, A. H., D. S. Childress and M. R. Meier (2002). "A simple method for the determination of gait events." Journal of Biomechanics **35**(1): 135-138.
- Hansen, M., M. Haugland, T. Sinkjaer and N. Donaldson (2002). "Real time foot drop correction using machine learning and natural sensors." Neuromodulation **5**(1): 41-53.
- Hansen, M., M. K. Haugland, A. Kostov and T. Sinkjaer (2000). Machine learning for real time control of foot-drop correction using natural sensors. Proceedings of the 5th Annual Conference of the International Functional Electrical Stimulation Society, Aalborg, Denmark.
- Hansen, M., M. K. Haugland and F. Sepulveda (2003). "Feasibility of using peroneal nerve recordings for deriving stimulation timing in foot drop correction systems." Neuromodulation **6**(1): 68-77.
- Hatze, H. (1981). "The use of optimally regularized fourier series for estimating higher-order derivatives of noisy biomechanical data." Journal of Biomechanics **14**: 13-18.
- Haugland, M., C. Childs, M. Ladouceur, J. Haase and T. Suinkjaer (2000). An implantable foot drop stimulator. Proceedings of the 5th Annual Conference of the International Functional Electrical Stimulation Society, Aalborg, Denmark.
- Haugland, M. K. and T. Sinkjaer (1995). "Cutaneous whole nerve recordings used for correction of footdrop in hemiplegic man." IEEE Transactions on Rehabilitation Engineering **3**(4): 307-317.

- Henty, J. (2004). Detection of gait events using a gyroscope sensor in fes drop-foot correction. PhD Thesis. School of Engineering. Guildford, University of Surrey.
- Henty, J. R. and D. Ewins (1998). Applications of gyroscopic angular velocity sensors in fes systems. 6th Viennal International Workshop on Functional Electrical Stimulation, Vienna.
- Henty, J. R., D. E. Wood and D. Ewins (1999). Detection of gait events using a vibratory gyroscope. Proceedings of the 4th Annual conference of the IFESS, Japan.
- Holsheimer, J., G. Bultstra, A. J. Verloop, H. E. Aa van der and H. J. Hermens (2000). Implantable dual channel peroneal nerve stimulator. Proceedings of the Ljubljana FES conference.
- Holsheimer, J., G. Bultstra, A. J. Verloop, H. E. van der Aa and H. J. Hermens (1993). Implantable dual channel peroneal nerve stimulator. The Ljubljana FES Conference, Ljubljana, Slovenia.
- Hreljac, A. and R. N. Marshall (2000). "Algorithms to determine event timing during normal walking using kinematic data." Journal of Biomechanics **33**(6): 783-786.
- Hynd, D., S. C. Hughes and D. Ewins (2000). "The development of a long, dual-platform triaxial walkway for the measurement of forces and temporal-spatial data in the clinical assessment of gait." Journal of Engineering in Medicine **214**: H193-201.
- Ilic, M., D. Vasiljevic and D. B. Popovic (1994). "A programmable electronic stimulator for fes systems." IEEE Transactions on Rehabilitation Engineering **2**(4): 234-239.
- Ismail, A. R. and S. S. Asfour (1999). "Discrete wavelet transform: A tool in smoothing kinematic data." Journal of Biomechanics **32**: 317-321.
- Jackson, K. M. (1979). "Fitting of mathematical functions to biomechanical data." IEEE Transactions on Biomedical Engineering **26**(2): 122-124.
- Jeglic, A., E. Vanken and M. Benedik (1970). Implantable muscle/nerve stimulator as part of an electronic brace. Proc. 3rd Int. Symp. External Control of Human Extremities.
- Johnson, M. W., P. H. Peckham, N. Bhadra, K. L. Kilgore, M. M. Gazdik, M. W. Keith and P. Strojnik (1999). "Implantable transducer for two-degree of freedom joint angle sensing." IEEE Transactions on Rehabilitation Engineering **7**(3): 349-359.
- Jones, R. and T. White (2002). Upstairs, downstairs - emg triggering for fes applied to foot-drop. Poceedings of the 1st annual conference of FESnet, University of Strathclyde, Glasgow.
- Junqueira, R. C. and A. P. C. Fonseca (1998). The utilisation of the functional electrical orthosis - km 25 in rehabilitation of hemiparetic patients. 6th Viennal International Workshop on Functional Electrical Stimulation, Vienna.
- Juul, P. R., M. Ladouceur and K. D. Nielsen (2000). Coding of lower limb muscle force generation in associated eeg movement related potentials: Preliminary studies toward a

fee-forward control of fes-assisted walking. Proceedings of the 5th International Functional Electrical Stimulation Society Meeting, Aalborg, Denmark.

Kelih, B., J. Rozman, U. Stanic and M. Kljajic (1988). "Dual channel implantable stimulator." Electrophysiological Kinesiology: 127-130.

Kenny, L., G. Bultstra, R. Buschman, P. Taylor, G. E. Mann, H. Hermens, J. Holsheimer, A. Nene, T. Martin, A. Hans and J. Hobby (2002). "An implantable two channel stimulator: Initial clinical results." Artificial Organs 26(3): 267-270.

Kershaw, R. A., R. Jones and A. Bateman (1993). The use of emg for real time closed loop control of functional electrical muscle stimulation. The Ljubljana FES Conference, Ljubljana.

Kershenbaum, A., T. Jaffa, A. Zeman and S. Boniface (1997). "Bilateral foot-drop in a patient with anorexia nervosa." International Journal of Eating Disorders 22(3): 335-337.

Kirkwood, C. A., B. J. Andrews and P. Mowforth (1989). "Automatic detection of gait events: A case study using inductive learning techniques." Journal of Biomedical Engineering 11: 511-516.

Kljajic, M., R. Acimovic and M. Malezic (1993). Long term follow up of gait hemiparetic patients using subcutaneous peroneal electrical stimulation. Ljubljana FES Conference, Ljubljana.

Kostov, A., B. J. Andrews, D. B. Popovic, R. B. Stein and W. W. Armstrong (1995). "Machine learning in control of functional electrical stimulation systems for locomotion." IEEE Transactions on Biomedical Engineering 42(6): 541-551.

Kostov, A., M. Hansen, M. Haugland and T. Sinkjaer (1999). "Adaptive restrictive rules provide functional and safe stimulation pattern for foot drop correction." Artificial Organs 23(5): 443-446.

Kottink, A. I. R., L. J. M. Oostendorp, J. H. Buurke, A. V. Nene, H. J. Hermens and M. J. IJzerman (2004). "The orthotic effect of functional electrical stimulation on the improvement of walking in stroke patients with a dropped foot: A systematic review." Artificial Organs 28(6): 577-586.

Kralj, A., T. Bajd and L. Vodovnik (1995). Fes for mobility: The lesson learned in 30 years. Proceedings of the 5th Vienna International Workshop on Functional Electrical Stimulation, Vienna (Austria).

Kralj A, B. T. (1989). Functional electrical stimulation: Standing and walking after spinal cord injury, CRC Press.

Kralj, A., A. Trnkoczy and R. Acimovic (1971). Improvement in locomotion in hemiplegic patients with multichannel electrical stimulation. Human locomotor engineering - a review of developments in the field including advances in prosthetics and the design of aids and controls. London, Inst Mech Eng: 45-50.

Lauer, R. T., P. H. Peckham and K. L. Kilgore (1999). "Eeg-based control of a hand grasp neuroprosthesis." Neuroreport 10(8): 1767-1771.

- Lauer, R. T., P. H. Peckham, K. L. Kilgore and W. J. Heetderks (2000). "Application of cortical signals to neuroprosthetic control: A critical review." IEEE Transactions on Rehabilitation Engineering **8**(2): 205-208.
- Liberson, W. T., H. J. Holmquest, D. Scot and D. Margot (1961). "Functional electrotherapy: Stimulation of the peroneal nerve synchronised with the swing phase of the gait of hemiplegic patients." Archives of Physical Medicine and Rehabilitation **42**: 101-105.
- Lyons, G. M., T. Sinkjaer, J. H. Burridge and D. J. Wilcox (2002). "A review of portable fes-based neural orthoses for the correction of drop foot." IEEE Transactions on Neural Systems and Rehabilitation Engineering **10**(4): 260-279.
- Lyons, G. M., P. C. Sweeney, M. E. Bradley, T. F. Hourigan and D. T. O'Keeffe (1997). The university of limerick drop foot stimulator. Proceedings of the 5th IPEM Clinical FES meeting.
- Malezic, M., U. Bogataj, N. Gros, I. Decman, P. Vrtacnik, M. Kljajic and R. Acimovic-Janezic (1992). "Application of a programmable dual-channel adaptive electrical stimulation system for the control and analysis of gait." Journal of Rehabilitation Research & Development. **29**(4): 41-53.
- Mann, G. E., J. H. Burridge, D. Ewins, D. L. McLellan, I. D. Swain, P. N. Taylor, D. E. Wood and P. A. Wright (2000). Optimising two channel stimulation to improve walking following stroke. 5th Annual Meeting of the International Functional Electrical Stimulation Society, Aalborg, Denmark.
- Mansfield, A. and G. M. Lyons (2003). "The use of accelerometry to detect heel contact events for use as a sensor in fes assisted walking." Medical Engineering & Physics **25**(10): 879-885.
- Matsunaga, T., Y. Shimada, M. Sato, K. Hatakeyama, S. Chida, K. Sato, S. Ando, T. Minato, N. Konishi and K. Iizuka (2000). The akita heel sensor system (ahss) for the correction of dropped foot gait in hemiplegic patients. 5th Annual Conference of the International Functional Electrical Stimulation Society, Aalborg, Denmark.
- McNeal, D. R. (1977). 2000 years of electrical stimulation. Functional electrical stimulation. Applications in neural prostheses. J. B. R. F. Terry Hambrecht. New York.
- Merletti, R., A. Andina, M. Galante and I. Furlan (1979). "Clinical experience of electronic peroneal stimulators in 50 hemiparetic patients." Scandinavian Journal of Rehabilitation Medicine. **11**(3): 111-21.
- Michael, P. (1996). Developments in surface electrical orthoses for the re-education of hemiplegic gait. PhD Thesis. Biomedical Engineering Group. Guildford, University of Surrey.
- Mickelborough, J., M. L. v. d. Linden, J. Richards and A. R. Ennos (2000). "Validity and reliability of a kinematic protocol for determining foot contact events." Gait and Posture **11**(1): 32-37.

- Moe, J. H. and H. W. Post (1962). "Functional electrical stimulation for ambulation in hemiplegia." The Lancet **82**: 285-288.
- Mourselas, N. and M. H. Granat (2000). Correction of foot drop using a fuzzy logic controlled miniature stimulator. 5th Annual Conference of the International Functional Electrical Stimulation Society, Aalborg, Denmark.
- Ng, S. K. and H. J. Chizeck (1997). "Fuzzy model identification for classification of gait events in paraplegics." IEEE Transactions on Fuzzy Systems **5**(4): 536-544.
- O'Keeffe, D. T. and G. M. Lyons (2002). "A versatile drop foot stimulator for research applications." Medical Engineering & Physics. **24**(3): 237-42.
- Ounpuu, S. (1994). Terminology for clinical gait analysis (draft #2), Clinical Gait and Movement Analysis Society: 1-19.
- Pappas, I. P. I., M. R. Popovic, T. Keller, V. Dietz and M. Morari (2001). "A reliable gait phase detection system." IEEE Transactions on Neural Systems and Rehabilitation Engineering **9**(2): 113-125.
- Passing, H. and W. Bablock (1983). "A new biometrical procedure for testing the equality of measurements from two different analytical methods." Journal of Clinical Chemistry and Clinical Biochemistry **21**: 709-720.
- Pedersen, E., T. Petersen, C. Hansen and B. Klemar (1986). "Videnskab og praksis - original meddelelse - kilisk erfaring med en ny drop fodstimulator - clinical experience with new peroneal stimulator." Ugeskrift for Laeger **148**(21): 1272-1275.
- Peham, C., M. Scheidl and T. Licka (1999). "Limb locomotion - speed distribution analysis as a new method for stance phase detection." Journal of Biomechanics **32**(10): 1119-1124.
- Perry, J. (1992). Gait analysis normal and pathological function. New York, McGraw-Hill, Inc. Pages 52-57.
- Pezzack, J. C., R. W. Norman and D. A. Winter (1977). "An assessment of derivative determining techniques used for motion analysis." Journal of Biomechanics **10**: 377-382.
- Pinzur, M. S., L. P. Dimonte, J. Trimble, K. Haag and R. Sherman (1984). "Qualitative and quantitative gait phase analysis by continuous monitoring of inter-ankle distance." Rehabilitation Research and Development **21**(2): 50-53.
- Popovic, D. B., R. B. Stein, K. L. Jovanovic, R. Dai, A. Kostov and W. W. Armstrong (1993). "Sensory nerve recording for closed-loop control to restore motor functions." IEEE Transactions on Biomedical Engineering **40**(10): 1024-1031.
- Popovic, M. R., T. Keller, M. Morari and V. Dietz (1998). "Neural prostheses for spinal cord injured subjects." Journal BioWorld **1**: 6-9.
- Popovic, M. R., T. Keller, I. P. I. Pappas, V. Dietz and M. Monari (2001). "Surface-stimulation technology for grasping and walking neuroprostheses." IEEE Engineering in Medicine and Biology Magazine **20**(1): 82-93.

Popovic, M. R., T. K. Keller, I. P. I. Pappas and P. Y. Muller (2001). Programmable and portable electrical stimulation for transcutaneous fes applications - complex motion. Proceedings of the 6th Annual Conference of the International Functional Electrical Stimulation Society.

Saxena, S., S. Nikolic and D. B. Popovic (1995). "An emg controlled fes system for grasping in tetraplegics." Journal of Rehabilitation Research & Development. **32**(1): 17-23.

Skelly, M. M. and H. J. Chizeck (2001). "Real time gait event detection during fes paraplegic walking." IEEE Transactions on Neural Systems and Rehabilitation Engineering **9**(1): 59-68.

Stanhope, S. J., T. M. Kepple, D. A. McGuire and N. L. Roman (1990). "Kinematic-based technique for event time determination during gait." Medical & Biological Engineering & Computing **28**: 355-360.

Stanic, U., R. Acimovic-Janezic, N. Gros, A. Tmkoczy, T. Bajd and M. Kljajic (1978). "Multichannel electrical stimulation for correction of hemiplegic gait." Scandinavian Journal of Rehabilitation Medicine **10**: 75-92.

Stein, R. B. (1998). Assembly for functional electrical stimulation during movement. Canada, Neuromotion, Inc. U.S. Patent number 5,814,093.

Stein, R. B., M. Belanger, G. Wheeler, M. Wieler, D. B. Popovic, A. Prochazka and L. A. Davis (1993). "Electrical systems for improving locomotion after incomplete spinal cord injury: An assessment." Archives of Physical Medicine and Rehabilitation **74**(9): 954-959.

Stevens, C., S. Durham, L. Eve and D. Ewins (2001). Preliminary findings of a study on the effect of functional electrical stimulation on the gait of children with cerebral palsy. Proceedings of the 6th Annual conference of the International Functional Electrical Stimulation Society, Cleveland, USA.

Strojnik, P., R. Acimovic, E. Vavken, V. Simic and U. Stanic (1987). "Treatment of drop foot using an implantable peroneal underknee stimulator." Scandinavian Journal of Rehabilitation Medicine **19**: 37-43.

Strojnik, P., A. Kralj and I. Ursic (1979). "Programmed six-channel electrical stimulator for complex stimulation of leg muscles during walking." IEEE Transactions on Biomedical Engineering **26**(2): 112-116.

Swain, I. D., J. H. Burridge, S. E. Crook, S. M. Finn, C. A. Johnson, G. E. Mann, P. N. Taylor and P. A. Wright (2001). From circuit design to service delivery - establishing a clinical fes service. Proceedings of the 6th Annual conference of the International Functional Electrical Stimulation Society, Cleveland, USA.

Swain, I. D., J. H. Burridge, C. A. Johnson, G. E. Mann, P. N. Taylor and P. A. Wright (2000). The efficacy of functional electrical stimulation in improving walking ability for people with multiple sclerosis. Proceedings of the 5th Annual conference of the International Functional Electrical Stimulation Society, Aalborg, Denmark.

- Swain, I. D., P. N. Taylor, J. H. Burrige, S. A. Hagan and D. E. Wood (1996). Report to the development evaluation committee common peroneal stimulation for the correction of drop-foot. Salisbury, Medical Physics and Biomedical Engineering, Salisbury District Hospital.
- Sweeney, P. C. and G. M. Lyons (1999). "Fuzzy gait event detection in a finite state controlled fes foot drop correction system." Journal of Bone and Joint Surgery **81-B**(51): 93.
- Takebe, K., C. Kukulka, M. G. Narayan, M. Milner and J. V. Basmajian (1975). "Peroneal nerve stimulator in rehabilitation of hemiplegic patients." Archives of Physical Medicine & Rehabilitation. **56**(June): 237-240.
- Taylor, P. N., J. H. Burrige, D. E. Wood, J. Norton, A. Dunkerly, C. Singleton and I. D. Swain (1999). "Patient perceptions of the odstock drop foot stimulator." Clinical Rehabilitation **13**(5): 439-446.
- Taylor, P. N., P. A. Wright, J. H. Burrige, G. E. Mann and I. D. Swain (1999). Correction of bi-lateral dropped foot using the odstock 2 channel stimulator (o2chs). 4th Annual Conference of the International Functional Electrical Stimulation Society, Japan.
- Teasell, R. W., S. K. Bhogal, N. C. Foley and M. R. Speechley (2003). "Gait retraining post stroke." Top Stroke Rehabil **10**(2): 34-65.
- Teasell, R. W. and L. Kalra (2004). "What's new in stroke rehabilitation." Stroke **35**(2): 383-5.
- Tong, K. Y. and M. H. Granat (1999). "Reliability of neural-network functional electrical stimulation gait-control system." Medical & Biological Engineering & Computing. **37**(5): 633-8.
- Tranberg, R. and D. Karlsson (1998). "The relative skin movement of the foot: A 2-d roentgen photogrammetry study." Clinical Biomechanics **13**(1): 71-76.
- Veltink, P. H., P. Slycke, J. Hemmsem, R. Buschman, G. Bultstra and H. Hermens (2003). "Three dimensional inertial sensing of foot movements for automatic tuning of a two-channel implantable drop-foot stimulator." Medical & Biological Engineering & Computing **25**(1): 21-28.
- Vinci, P. (2003). "Gait rehabilitation in a patient affected with charcot-marie-tooth disease associated with pyramidal and cerebellar features and blindness1." Archives of Physical Medicine and Rehabilitation **84**(5): 762-765.
- Vodovnik, L., C. Long, J. B. Reswick, A. Lippay and D. Starbuck (1965). "Myo-electric control of paralyzed muscles." IEEE Transactions on Biomedical Engineering **12**(3): 169-178.
- Wachowiak, M. P., G. S. Rash, P. M. Quesada and A. H. Desoky (2000). "Wavelet-based noise removal for biomechanical signals: A comparative study." IEEE Transactions on Biomedical Engineering **47**(3): 360-368.

- Wall, J. C. and J. Crosbie (1996). "Accuracy and reliability of temporal gait measurement." Gait and Posture 4(4): 293-296.
- Waters, R. L., D. McNeal and J. Perry (1975). "Experimental correction of footdrop by electrical stimulation of the peroneal nerve." The Journal of bone and joint surgery 57-A(8): 1047-1054.
- Waters, R. L., D. R. McNeal, W. Faloon and B. Clifford (1985). "Functional electrical stimulation of the peroneal nerve for hemiplegia. Long-term clinical follow-up." Journal of Bone and Joint Surgery 67-A: 792-793.
- Welch, P., The use of fast Fourier transform for the estimation of power spectra: A method based on time averaging over short, modified periodograms. Audio and Electroacoustics, IEEE Transactions on. 15(2): p. 70-3, 1967.
- Westcott, P. (2000). Stroke: Questions and answers. London, The Stroke Association.
- Whittle, M. W. (1996). Gait analysis, an introduction, Butterworth-Heinemann.
- Wieler, M., S. Naaman and R. B. Stein (1996). Walkaid: An improved functional electrical stimulator for correcting foot-drop. Proceedings of the 1st IFESS meeting, Cleveland, Ohio.
- Wieler, M., R. B. Stein, M. Ladouceur, M. Whittaker, A. W. Smith, S. Naaman, H. Barbeau, J. Bugaresti and E. Aimone (1999). "Multicenter evaluation of electrical stimulation systems for walking." Archives of Physical Medicine and Rehabilitation 80: 495-500.
- Willemsen, A. T. M., F. Bloemhof and H. R. B. K. Boom (1990). "Automatic stance-swing phase detection from accelerometer data for peroneal nerve stimulation." IEEE Transactions on Biomedical Engineering 37: 1201-1208.
- Williamson, R. and B. J. Andrews (2000). "Gait event detection for fes using accelerometers and supervised machine learning." IEEE Transactions on Rehabilitation Engineering 8(3): 312-319.
- Williamson, R. and B. j. Andrews (2000). "Sensor systems for lower limb functional electrical stimulation (fes) control." Medical Engineering and Physics 22(5): 313-325.
- Winter, D. A. (1990). Biomechanics and motor control of human movement. New York, Wiley.
- Winter, D. A. (1991). The biomechanics and motor control of human gait: Normal, elderly and pathological. Waterloo, Canada, Waterloo Biomechanics.
- Winter, D. A., H. G. Sidewall and D. A. Hobson (1974). "Measurement and reduction of noise in kinematics of locomotion." Journal of Biomechanics 7: 157-159.
- Winters, T. F., J. R. Gage and R. Hicks (1987). "Gait patterns in spastic hemiplegia in children and young adults." Journal of Bone and Joint Surgery 69-A(3): 437-441.

Wolpaw, J. R., N. Birbaumer, W. J. Heetderks, D. J. McFarland, P. H. Peckham, G. Schalk, E. Donchin, L. A. Quatrano, C. J. Robinson and T. M. Vaughan (2000). "Brain-computer interface technology: A review of the first international meeting." IEEE Transactions on Rehabilitation Engineering **8**(2): 164 -173.

Woltring, H. J. (1986). "A fortran package for generalized, cross-validatory spline smoothing and differentiation." Advanced Engineering Software **8**(2): 104-113.

Yuancheng, J., D. A. Winter, M. G. Ishac and L. Gilchrist (1993). "Trajectory of the body cog and cop during initiation and termination of gait." Gait and Posture **1**: 9-22.

Bibliography

- Allard, P. and B. International Society of (1997). Three-dimensional analysis of human locomotion. Chichester, Wiley.
- Baker, L. L., D. R. McNeal, et al. (1993). Neuromuscular electrical stimulation - a practical guide, Rehabilitation Engineering Program, Los Amigos Research & Education Institute, Rancho Los Amigos Medical Center.
- Balmer, L. (1997). Signals and systems an introduction, Prentice Hall.
- Biran, A. and M. Breiner (1995). Matlab for engineers, Addison-Wesley Publishers Ltd.
- Craik, R. L. and C. A. Oatis (1995). Gait analysis: Theory and application, Mosby.
- Gardner, N. (1996). Beginners guide to the microchip pic, Bluebird Electronics.
- Gardner, N. and P. Birnie (1996). Pic cookbook volume 1, Bluebird Electronics.
- Hanselman, D. and B. Littlefield (1998). Mastering matlab 5: A comprehensive tutorial and reference, Prentice-Hall.
- Kralj, A. and T. Bajd (1989). Functional electrical stimulation: Standing and walking after spinal cord injury, CRC Press.
- Perry, J. (1992). Gait analysis normal and pathological function. New York, McGraw-Hill, Inc.
- Porat, B. (1997). A course in digital signal processing, John Wiley and Sons, Inc.
- Tortora, G. J. and S. R. Grabowski (1993). Principles of anatomy and physiology, HarperCollins.
- Wells, L. K. and J. Travus (1997). Labview for everyone: Graphical programming made even easier, Prentice Hall PTR.
- Whittle, M. W. (2003). Gait analysis, an introduction, Butterworth-Heinemann.
- Winter, D. A. (1990). Biomechanics and motor control of human movement. New York, Wiley.
- Winter, D. A. (1991). The biomechanics and motor control of human gait: Normal, elderly and pathological. Waterloo, Canada, Waterloo Biomechanics.

Appendices

Appendix A: MATLAB code used for gait event detection A1-A39

Appendix B: Assembly language code running on the PIC B1-B17

Appendix C: Data sheets C1-C4

Appendix D: Manufacturer details D1-D2

Appendix E: Contents of the compact disc E1-E2

Appendix A

MATLAB code used for gait event detection


```

% KINEMATIC GAIT EVENT DETECTION
% This code encompasses a front panel graphical user interface and the algorithms needed for the
% gait event
% detection using heel and toe marker data
% The program is written for MATLAB environment
% The input to the program is a TSV file that contains the marker data
% Gait event detection results are displayed on the GUI
% Results can be output from the program is in txt format

```

```

function varargout = Event_DetectionR1(varargin)
% EVENT_DETECTIONR1 M-file for Event_DetectionR1.fig
% EVENT_DETECTIONR1, by itself, creates a new EVENT_DETECTIONR1 or raises the
% existing
% singleton*.
%
% H = EVENT_DETECTIONR1 returns the handle to a new EVENT_DETECTIONR1 or the
% handle to
% the existing singleton*.
%
% EVENT_DETECTIONR1('CALLBACK',hObject,eventData,handles,...) calls the local
% function named CALLBACK in EVENT_DETECTIONR1.M with the given input
% arguments.
%
% EVENT_DETECTIONR1('Property','Value',...) creates a new EVENT_DETECTIONR1 or
% raises the
% existing singleton*. Starting from the left, property value pairs are
% applied to the GUI before Event_DetectionR1_OpeningFunction gets called. An
% unrecognized property name or invalid value makes property application
% stop. All inputs are passed to Event_DetectionR1_OpeningFcn via varargin.
%
% *See GUI Options on GUIDE's Tools menu. Choose "GUI allows only one
% instance to run (singleton)".
%
% See also: GUIDE, GUIDATA, GUIHANDLES

```

```

% Edit the above text to modify the response to help Event_DetectionR1

```

```

% Last Modified by GUIDE v2.5 09-Jun-2003 20:16:07

```

```

% Begin initialization code - DO NOT EDIT

```

```

gui_Singleton = 1;
gui_State = struct('gui_Name', mfilename, ...
    'gui_Singleton', gui_Singleton, ...
    'gui_OpeningFcn', @Event_DetectionR1_OpeningFcn, ...
    'gui_OutputFcn', @Event_DetectionR1_OutputFcn, ...
    'gui_LayoutFcn', [], ...
    'gui_Callback', []);
if nargin & isstr(varargin{1})
    gui_State.gui_Callback = str2func(varargin{1});
end

```

```

nargout

```



```

    [varargout{1:nargout}] = gui_mainfcn(gui_State, varargin{:});
else
    gui_mainfcn(gui_State, varargin{:});
end
% End initialization code - DO NOT EDIT

```

```

% --- Executes just before Event_DetectionR1 is made visible.
function Event_DetectionR1_OpeningFcn(hObject, eventdata, handles, varargin)
% This function has no output args, see OutputFcn.
% hObject    handle to figure
% eventdata  reserved - to be defined in a future version of MATLAB
% handles    structure with handles and user data (see GUIDATA)
% varargin   command line arguments to Event_DetectionR1 (see VARARGIN)

```

```

% Choose default command line output for Event_DetectionR1
handles.output = hObject;

```

```

% Update handles structure
guidata(hObject, handles);

```

```

% UIWAIT makes Event_DetectionR1 wait for user response (see UIRESUME)
% uiwait(handles.figure1);

```

```

% --- Outputs from this function are returned to the command line.
function varargout = Event_DetectionR1_OutputFcn(hObject, eventdata, handles)
% varargout  cell array for returning output args (see VARARGOUT);
% hObject    handle to figure
% eventdata  reserved - to be defined in a future version of MATLAB
% handles    structure with handles and user data (see GUIDATA)

```

```

% Get default command line output from handles structure
varargout{1} = handles.output;

```

```

%=====
function Initialise_GUI_Callback(hObject, eventdata, handles)

```

```

axes(handles.axes2);
cla reset
axes(handles.axes3);
cla reset

```

```

set(handles.num_cycles,'String','')
set(handles.edit1,'String','')
set(handles.edit2,'String','')
set(handles.ignored_peaks,'String','')
set(handles.All_cycles,'Value',0)
set(handles.Barefoot,'Value',0)
set(handles.edit3,'String','')
set(handles.Detection_Status,'String','');

```

```

nrcinput=[];

```



```

sync=0;
handles.sync=sync;

w=2; %default to Shod!
handles.w=w;
syncinput = 0;
handles.syncinput=syncinput;

cyclechoice=0;
handles.cyclechoice=cyclechoice;
handles.syncinput=syncinput;
handles.sync=sync;
handles.syncinput=syncinput;
handles.output=hObject;
Guidata(hObject,handles);

set(handles.Detection_Status,'String','Initialisation Complete');
handles.output=hObject;
Guidata(hObject,handles);
%h1 = errordlg('Initialisation complete','Error','modal');
% waitfor(h1)
return

%=====
% --- Executes on button press in Input_TSV.
function Input_TSV_Callback(hObject, eventdata, handles)
% hObject    handle to Input_TSV (see GCBO)
% eventdata  reserved - to be defined in a future version of MATLAB
% handles    structure with handles and user data (see GUIDATA)

% Call the Initialise subroutine
Initialise_GUI_Callback(hObject, eventdata, handles)

message=['Loading TSV file'];
handles.message=message;
handles.output=hObject;
Guidata(hObject,handles);
Detection_Status_Callback(hObject, eventdata, handles)

[fname,pname] = uigetfile('*.TSV','Choose File',200,200);
% function to read a Qualisys TSV file into Matlab
fid=fopen(fname,'rt');
row='first';
num_rows=0;
while ischar(row)
    row=fgetl(fid);
    num_rows=num_rows+1;
    file{num_rows}=row;
end
fclose(fid);

file = textread(fname,'%s','delimiter','\n','whitespace','');
um_frames=str2num(file{1}(14:end));

```



```

num_cameras=str2num(file{2}(15:end));
freq=str2num(file{4}(11:end));
num_analog=str2num(file{5}(14:end));
freq_analog=str2num(file{6}(18:end));
des=file{7}(13:end);
time_stamp=file{8}(11:end);
data_type=file{9}(15:end);

%read the marker names
w=[1:length(file{10})];
tabs=w(double(file{10})==9); %finds the 9 (ASCII tab) in the marker name row
%LHG added a tab in last position:
if(tabs(length(tabs)) < length(file{10})) % if last tab position < length of row
    tabs=[tabs length(file{10})+1] %add tab after last position in row
end
%LHG modified calculation of num_markers
%num_markers=length(tabs)-1;
num_markers=str2num(file{3}(15:end));
for marker=1:num_markers
    marker_names{marker}=file{10}(tabs(marker)+1:tabs(marker+1)-1);
end

%convert the remainder of the file to a matrix
%establish the size of the matrix
scratch=sscanf(file{11},'%f');
[num_data,d2]=size(scratch);

%reserve space
tsv_qq=zeros(num_rows-11,num_data);

for count=11:num_rows-1
    tsv_qq(count-10,:)=sscanf(file{count},'%f');
end

%convert zeros to NaN
%z=find(tsv_qq==0);
%tsv_qq(z)=NaN;

%put into standard form
coord=permute(reshape(tsv_qq',[3,fix(num_data/3),num_frames]),[2,1,3]);

%load the tsv variables into the x structure
x{1}.type='Marker data';
x{1}.data=coord;
x{1}.parameters=[0 freq 1];
%x{1}.notes=notes;
%x{1}.group=group;
%x{1}.subject=subject;
%x{1}.trial=trial;

for mark=1:num_markers
    x{1}.component{mark,1}='X';
    x{1}.component{mark,2}='Y';
end

```



```

x{1}.component{mark,3}='Z';
x{1}.units{mark}='mm';
x{1}.items{mark}=marker_names{mark};
end

%Find the heel and meta marker data
heel_names = {'heel','rheel','sg heel','lheel','Lheel'};
meta_names = {'meta','rmeta','sg meta','lmeta','metatarsal','Lmeta'};
sacrum_names = {'sacral','sacrum','csacral'};
heelname = 0;
metaname = 0;
hname = {'cat'};
mname = {'mouse'};
[m,n] = size(heel_names);
[m2,n2] = size(meta_names);
[m20,n20] = size(sacrum_names);

sacrumname = 0;
sname = {'dog'};

for d = 1:num_markers;
    for d20 = 1:n20;
        C = strcmp(marker_names{d},sacrum_names(d20));
        if C == 1
            i_sacrum = d;
            sname = sacrum_names(d20);
            sacrumname = 1;
            handles.i_sacrum = i_sacrum;
            handles.output=hObject;
            Guidata(hObject,handles);
            break
        end
    end
end

for d = 1:num_markers
    for d2 = 1:n
        C = strcmp(marker_names{d},heel_names(d2));
        if C == 1
            i_heel = d;
            hname = heel_names(d2);
            heelname = 1;
            break
        end
    end
end

for d = 1:num_markers
    for d3 = 1:n2
        C2 = strcmp(marker_names{d},meta_names(d3));
        if C2 == 1
            i_meta = d;

```



```

        mname = meta_names(d3);
        metaname = 1;
        break
        break
    end
end
end

dog = [hname; mname];
if heelname ~= 1 || metaname ~= 1
    h1 = errordlg('Can not find Heel and Metatarsal markers','Error','modal');
    waitfor(h1)
    %request_input_names
else
    set(handles.edit1,'String',hname);
    set(handles.edit2,'String',mname);
    handles.i_heel=i_heel;
    handles.i_meta=i_meta;
    handles.output=hObject;
    Guidata(hObject,handles);
    %S = [dog;{' marker data will be used for gait event detection'}];
    %h = msgbox((S),'Confirm choice of markers','modal');
    %waitfor(h)
    %button = questdlg('Do you want to continue?','Continue Operation','Yes','No','No');
    %if strcmp(button,'Yes')
    %cycle_choice
    %elseif strcmp(button,'No')
    %request_input_names
    %end
end

% Input Data variables to be used by other functions
cyclechoice=0;
handles.cyclechoice=cyclechoice;
syncinput=0;
handles.syncinput=syncinput;
sync=0;
handles.sync=sync;
handles.fname = fname;
handles.coord = coord;
handles.tsv_qq=tsv_qq;
handles.freq=freq;
handles.num_markers= num_markers;
handles.marker_names=marker_names;
handles.i_sacrum = i_sacrum;
handles.output=hObject;
Guidata(hObject,handles);

message=[fname,' data file loaded'];
handles.message=message;
handles.output=hObject;
Guidata(hObject,handles);
Detection_Status_Callback(hObject, eventdata, handles)

```



```

%h1 = errordlg('TSV file loaded','Error','modal');
% waitfor(h1)

%=====
% --- Executes on button press in All_cycles.
function All_cycles_Callback(hObject, eventdata, handles)
% hObject   handle to All_cycles (see GCBO)
% eventdata reserved - to be defined in a future version of MATLAB
% handles   structure with handles and user data (see GUIDATA)

cycleinput=[];
allcycles = get(hObject,'Value'); %returns toggle state of checkbox1

if (get(hObject,'Value') == get(hObject,'Max'))
    cyclechoice = 1;
    handles.cyclechoice=cyclechoice;
end

handles.cyclechoice=cyclechoice;
handles.output=hObject;
Guidata(hObject,handles);

message=['Gait cycles detection in progress'];
handles.message=message;
handles.output=hObject;
Guidata(hObject,handles);
Detection_Status_Callback(hObject, eventdata, handles)

Cycle_choice_Callback(hObject, eventdata, handles)

%=====
% --- Executes on button press in Barefoot.
function Barefoot_Callback(hObject, eventdata, handles)
% hObject   handle to Barefoot (see GCBO)
% eventdata reserved - to be defined in a future version of MATLAB
% handles   structure with handles and user data (see GUIDATA)

% Hint: get(hObject,'Value') returns toggle state of Barefoot

if (get(hObject,'Value') == get(hObject,'Max'))
    w = 1;
else
    w = 2;
end

handles.w = w;
handles.output=hObject;
Guidata(hObject,handles);

%=====
% --- Executes on button press in Manual_Cyclechoice.
function Manual_Cyclechoice_Callback(hObject, eventdata, handles)

```



```

% hObject handle to Manual_Cyclechoice (see GCBO)
% eventdata reserved - to be defined in a future version of MATLAB
% handles structure with handles and user data (see GUIDATA)

set(handles.ignored_peaks,'Visible','on')
set(handles.text7,'Visible','on')
set(handles.peaks_Done,'Visible','on')

tsv_qq=handles.tsv_qq;
i_heel = handles.i_heel;
freq = handles.freq;

cyclechoice=handles.cyclechoice;
HeelZ = tsv_qq(:,i_heel*3);
[f,i] = size(HeelZ);

n = f - i;
% Fs = sampling frequency & R = Resolution and Ts = sampling interval

Ts = 1/freq;
e = f * Ts; %end time
s = i * Ts; %start time

Frame = i:1:(f);
Time = s:Ts:e;
Time = Time';
Frame = Frame';
rpeak=handles.rpeak;

figure;
plot(Frame,HeelZ);
hold on;

lined3 = 1 :(max(HeelZ*1.3)); %vector of data to be used for plotting the events (value goes up to
half of highest velocity)

[m7,n8]=size(rpeak);

xmin = rpeak(1,1) - 100;
xmax = rpeak(1,n8) + 100;
ymax= max(HeelZ)*1.5;

axis([xmin xmax 0 ymax])

for count7=1:n8;
    plot(rpeak(1,count7),lined3,'-r');
    peaktime = num2str(round(rpeak(1,count7)));
    peakstring = [peaktime];
    text(rpeak(1,count7)-0.05,max(lined3),peakstring,'FontSize',8,'BackgroundColor',[1 1 1]);
    hold on
end

prompt = {'Please select the peaks to be ignored:'};

```



```

title = 'False peak deletion';
lines = n8;
def = {};
%answer = inputdlg(prompt,title,lines,def);
%sync = answer{1,1};
%sync = sscanf(sync,'%g',1);

rpeak=handles.rpeak;

[m8,n8]=size(rpeak);
for count=1:n8
    vars(count,1)=num2str(count);
end

set(handles.ignored_peaks,'String',vars);

%=====
% --- Executes on button press in Cycle_choice.
function Cycle_choice_Callback(hObject, eventdata, handles)
% hObject handle to Cycle_choice (see GCBO)
% eventdata reserved - to be defined in a future version of MATLAB
% handles structure with handles and user data (see GUIDATA)

tsv_qq=handles.tsv_qq;
i_heel = handles.i_heel;
freq = handles.freq;
cyclechoice=handles.cyclechoice;
HeelZ = tsv_qq(:,i_heel*3);

suffix = "";

%starting frame = i and final frame = f
% n is the length of the matrix from first Heel Z max to the frame before the next Heel Z max
%footwear = input('Enter 1 for barefoot and 2 for shod trials:');
[f,i] = size(HeelZ);

n = f - i;
% Fs = sampling frequency & R = Resolution and Ts = sampling interval

Ts = 1/freq;
e = f * Ts; %end time

s = i * Ts; %start time

Frame = i:1:(f);
Time = s:Ts:e;
Time = Time';
Frame = Frame';

[b,a] = butter(2,10/(freq/2)); %[b,a] = butterworth filter(filter order, cut-off frequency/half
sampling frequency)

```



```

FHeelZ = filtfilt(b,a,HeelZ); % Each of the signals is filtered twice (2 directions)
FLogHeelZ = [0];
Threshold = max(FHeelZ)/2;
for t = 2:f;
    if FHeelZ(t,:) > Threshold;
        FLogZ = FHeelZ(t,:);
    elseif FHeelZ(t,:) < Threshold;
        FLogZ = 0.00;
    else FLogZ = 0.00;
    end % set any heel z value to zero if it falls below half the maximum of that trial
    FLogHeelZ = [FLogHeelZ;FLogZ];
end

peak = [0];
count = 1;
for t = (1 + peak(count)) : (f - 1);
    A = FLogHeelZ(1:t,1:1);
    B = FLogHeelZ(1:t+1,1:1);
    C = FLogHeelZ(1:t-1,1:1);
    D = max(A);
    E = max(B);
    if E == D;
        if B(t+1,:) < A(t,:);
            if C(t-1,:) < A(t,:);
                peak(count)= Frame(t,:);
                count = count + 1;
            end
        end
    end
end
end
end

% go back to raw data around the estimated peak and look for the real first peak in Z
[m3,n3] = size(peak);
rpeak = [0];
for count2 = 1 : n3;
    HZi = HeelZ(peak(count2)-3:peak(count2)+3);
    for t = 1:7;
        if HZi(t,:) == max(HZi)
            rpeak(count2) = Frame(t - 3 + peak(count2) - 1,:);
            break
        end
    end
end
end

rpeak;
peak;

set(handles.num_cycles,'String',(n3-1));
if cyclechoice ~= 1 ;
    prompt = [num2str(n3 - 1),' gait cycles can be used for gait event detection. Select the cycle
number you want to analyse: or (0) for all cycles'];
    dlg_title = 'Gait Cycle Selection';
    num_lines= 1;

```



```

def = {};
cycle_input = inputdlg(prompt,dlg_title,num_lines,def);
cycle_input = str2num(cycle_input{1});
count4 = cycle_input;
if cycle_input < 1;
    count4 = 0;
    S = ['Gait event times will be determined for all ',num2str(n3 - 1),' available gait cycles'];
    h3 = msgbox(S);
    waitfor (h3)
    set(handles.All_cycles,'Value',1);
else
    if cycle_input == 1
        suffix = 'st';
    elseif cycle_input > 3
        suffix = 'th';
    elseif cycle_input == 3
        suffix = 'rd';
    else
        suffix = 'nd';
    end

    S = ['Gait event times will be determined for ',num2str(cycle_input),suffix,' gait cycle'];
    h3 = msgbox(S);
    waitfor (h3)
end

else
    cyclechoice == 1 ;
    cycle_input = 0;
    count4 = 0;
end

axes(handles.axes2);
plot(Frame,HeelZ);
hold on;

lined3 = 1 :(max(HeelZ*1.3)); %vector of data to be used for plotting the events (value goes up to
half of highest velocity)

axes(handles.axes2);

[m7,n8]=size(rpeak);

xmin = rpeak(1,1) - 100;
xmax = rpeak(1,n8) + 100;
ymax= max(HeelZ)*1.5;

axis([xmin xmax 0 ymax]);

for count7=1:n8;
    axes(handles.axes2);
    plot(rpeak(1,count7),lined3,'-.r');
    peaktime = num2str(round(rpeak(1,count7)));

```



```

    peakstring = [peaktime];
    text(rpeak(1,count7)-0.05,max(lined3),peakstring,'FontSize',8,'BackgroundColor',[1 1 1]);
    hold on
end

```

```

axes(handles.axes2)
hold off

```

```

% Cycle Choice variables to be used by other functions

```

```

handles.suffix=suffix;
handles.cycle_input = cycle_input;
handles.count4=count4;
handles.rpeak=rpeak;
handles.peak=peak;
handles.output=hObject;
Guidata(hObject,handles);

```

```

message=['Cycle Detection Completed'];
handles.message=message;
handles.output=hObject;
Guidata(hObject,handles);
Detection_Status_Callback(hObject, eventdata, handles)

```

```

return

```

```

%=====

```

```

% --- Executes during object creation, after setting all properties.

```

```

function edit3_CreateFcn(hObject, eventdata, handles)

```

```

% hObject handle to edit3 (see GCBO)

```

```

% eventdata reserved - to be defined in a future version of MATLAB

```

```

% handles empty - handles not created until after all CreateFcns called

```

```

% Hint: edit controls usually have a white background on Windows.

```

```

% See ISPC and COMPUTER.

```

```

if ispc

```

```

    set(hObject,'BackgroundColor','white');

```

```

else

```

```

    set(hObject,'BackgroundColor',get(0,'defaultUicontrolBackgroundColor'));

```

```

end

```

```

function edit3_Callback(hObject, eventdata, handles)

```

```

% hObject handle to edit3 (see GCBO)

```

```

% eventdata reserved - to be defined in a future version of MATLAB

```

```

% handles structure with handles and user data (see GUIDATA)

```

```

% Hints: get(hObject,'String') returns contents of edit3 as text

```

```

sync=str2double(get(hObject,'String')); % returns contents of edit3 as a double
syncinput = 1;

```

```

handles.syncinput=syncinput;

```



```
handles.sync=sync;
handles.output=hObject;
Guidata(hObject,handles);
```

Synchronise_Callback(hObject, eventdata, handles)

```
%=====
```

```
% --- Executes on button press in Synchronise.
```

```
function Synchronise_Callback(hObject, eventdata, handles)
```

```
% hObject handle to Synchronise (see GCBO)
```

```
% eventdata reserved - to be defined in a future version of MATLAB
```

```
% handles structure with handles and user data (see GUIDATA)
```

```
syncinput=handles.syncinput;
```

```
sync=handles.sync;
```

```
EventTimes = handles.EventTimes;
```

```
All5 = handles.All5;
```

```
freq = handles.freq;
```

```
rpeak = handles.rpeak;
```

```
cycle_d = handles.cycle_d;
```

```
SpeedS = handles.SpeedS;
```

```
FSpeedS = handles.FSpeedS;
```

```
if syncinput == 1;
```

```
else
```

```
    prompt = {'Please input the synchronisation frame number:'};
```

```
    title = 'Synchronisation with Gyro data';
```

```
    lines = 1;
```

```
    def = {''};
```

```
    answer = inputdlg(prompt,title,lines,def);
```

```
    sync = answer{1,1};
```

```
    sync = sscanf(sync,'%g',1);
```

```
end
```

```
EventTimes2(:,1:4) = (((EventTimes(:,1:4) / freq) * 100) + sync);
```

```
EventTimes2(:,5:8) = EventTimes2(:,1:4) / 100;
```

```
All5(:,2) = ((All5(:,2) * 100) + sync)/100;
```

```
All5(:,1) = (((All5(:,1) / freq) * 100) + sync);
```

```
Startframe = rpeak';
```

```
Startframe = (((Startframe/freq) * 100) + sync);
```

```
[m8,n8] = size(Startframe);
```

```
Startframe = Startframe(1:m8-1,:);
```

```
Starttime = Startframe/100;
```

```
%EventTimes3 = ['a','b','c','d']
```

```
EventTimes2;
```

```
%Synchronise variables to be used by other functions
```

```
handles.Startframe =Startframe;
```

```
handles.Starttime=Starttime;
```

```
handles.All5=All5;
```

```
handles.EventTimes2=EventTimes2;
```

```
handles.output=hObject;
```

```
Guidata(hObject,handles);
```



```

message=['Event times synchronisation completed'];
handles.message=message;
handles.output=hObject;
Guidata(hObject,handles);
Detection_Status_Callback(hObject, eventdata, handles)

set(handles.Unsynchronise,'Value',0);

button = questdlg('Do you want to Update Results Plot?','Continue Operation','Yes','No','No');
if strcmp(button,'Yes')
    message=['Generating Plot Data'];
    set(handles.Detection_Status,'String',message);
    DISPLAY_RESULTS_Callback(hObject, eventdata, handles)
elseif strcmp(button,'No')
end

return

%=====
% --- Executes on button press in DISPLAY_RESULTS.
function DISPLAY_RESULTS_Callback(hObject, eventdata, handles)
% hObject    handle to DISPLAY_RESULTS (see GCBO)
% eventdata  reserved - to be defined in a future version of MATLAB
% handles    structure with handles and user data (see GUIDATA)

message=['Generating Plot Data'];
handles.message=message;
handles.output=hObject;
Guidata(hObject,handles);
Detection_Status_Callback(hObject, eventdata, handles)

axes(handles.axes3);
cla reset

All5 = handles.All5;
fname = handles.fname;
EventTimes2 = handles.EventTimes2;

if get(handles.Barefoot,'Value') == (get(handles.Barefoot,'Max'));
    w=1;
else
    w=2;
end

Time = All5(:,2);
HeelZ = All5(:,5);
FVelHYZ = All5(:,29);
FVelMYZ = All5(:,30);
lined = 1:20:(max(FVelHYZ/(2))); %vector of data to be used for plotting the events (value goes
up to half of highest velocity)
lined2= 1:20:(max(FVelHYZ/1.3));

```



```

% get rid of the zeros on the first and last frame of the cycle in the velocity data
%FVelHYZ(1) = FVelHYZ(2);
%FVelMYZ(1) = FVelMYZ(2);
%[m4,n4] = size(All5);

%FVelHYZ(m4) = FVelHYZ(m4-1);
%FVelMYZ(m4) = FVelMYZ(m4-1);

% get threshold values for velocities
if w < 2; % case = barefoot
    HCThreshold = 300;
    HRThreshold = 100;
    TCThreshold = 100;
    TOThreshold = 100;
elseif w > 1; % case = SHOD
    HCThreshold = 300;
    HRThreshold = 100;
    TCThreshold = 100;
    TOThreshold = 100;
end

xmin = min(Time);
xmin = round(xmin);
if xmin < min(Time)
    xmin = xmin;
else
    xmin = xmin - 0.5;
end

xmax = max(Time);
xmax = round(xmax);
if xmax > max(Time);
    xmax = xmax;
else
    xmax = xmax + 0.5;
end

axes(handles.axes3);
plot(Time,HCThreshold,Time,HRThreshold,Time,TCThreshold,Time,TOThreshold)
plot(Time,FVelHYZ,Time,FVelMYZ)
hold on
axis([xmin xmax 0 5500])
legend('Filtered Heel Vels','Filtered Toe Vels',-1);
xlabel('Time (s)');
ylabel('Sagittal velocity (mm/s)');
titlestring = [fname,' sagittal velocities of heel and toe markers and event times'];
title(titlestring);
grid on;
hold on;

[m6,n6]=size(EventTimes2);
for count6 = 1:m6;
    axes(handles.axes3)

```



```

plot(EventTimes2(count6,5),lined2,'-.b',EventTimes2(count6,7),lined2,'-.r',...
      EventTimes2(count6,6),lined,'-.m',EventTimes2(count6,8),lined,'-.y');
hold on
end

for count6 = 1:m6;
    HCtime = num2str(EventTimes2(count6,5),4);
    HRtime = num2str(EventTimes2(count6,7),4);
    TCtime = num2str(EventTimes2(count6,6),4);
    Totime = num2str(EventTimes2(count6,8),4);
    HCstring = ['HC ',HCtime];
    HRstring = ['HR ',HRtime];
    TCstring = ['TC ',TCtime];
    TOstring = ['TO ',Totime];
    text(EventTimes2(count6,5)-0.05,max(lined2)+50,HCstring,'FontSize',7,'BackgroundColor',[1 1
1]);
    text(EventTimes2(count6,7)-0.05,max(lined2)+125,HRstring,'FontSize',7,'BackgroundColor',[1
1 1]);
    text(EventTimes2(count6,6)-0.05,max(lined)+50,TCstring,'FontSize',7,'BackgroundColor',[1 1
1]);
    text(EventTimes2(count6,8)-0.05,max(lined)+125,TOstring,'FontSize',7,'BackgroundColor',[1 1
1]);
    hold on
end

message=['Plot Data generated'];
handles.message=message;
handles.output=hObject;
Guidata(hObject,handles);
Detection_Status_Callback(hObject, eventdata, handles)

%[newfile,newpath] = uiputfile(fname,'Save file name for the event times');
%output=[Time,FVelHYZ,FVelMYZ] %add speed data to output data to be saved
%dlmwrite(newfile,output,'\t')

return
%legend('HC','HR','TC','TO');
%plot(EventTimes(1,5),lined,EventTimes(2,5),lined,EventTimes(3,5),lined,...
%EventTimes(1,7),lined,EventTimes(2,7),lined,EventTimes(3,7),lined)

%[newfile,newpath] = uiputfile(fname,'Save file name for the event times');
%dlmwrite(newfile,All4,'\t');

%[newfile,newpath] = uiputfile(fname,'Save file name for the data output file');
%dlmwrite(newfile,All,'\t');

%=====
% --- Executes on button press in EXPORT_DATA.
function EXPORT_DATA_Callback(hObject, eventdata, handles)
% hObject handle to EXPORT_DATA (see GCBO)
% eventdata reserved - to be defined in a future version of MATLAB

```



```
% handles    structure with handles and user data (see GUIDATA)
```

```
fname=handles.fname;  
EventTimes2=handles.EventTimes2;  
SpeedS=handles.SpeedS;  
FSpeedS=handles.FSpeedS;  
cycle_d=handles.cycle_d;  
Startframe=handles.Startframe;  
Starttime=handles.Starttime;  
All5=handles.All5;
```

```
[newfile,newpath] = uiputfile(fname,'Save file name for the processed data');  
dlmwrite(newfile,All5,'\t')
```

```
[newfile,newpath] = uiputfile(fname,'Save file name for the event times');  
SpeedS = SpeedS';  
FSpeedS = FSpeedS';  
cycle_d = cycle_d';  
outputTimes=[EventTimes2,SpeedS,FSpeedS,cycle_d,Startframe,Starttime]; %add speed data to  
output data to be saved  
dlmwrite(newfile,outputTimes,'\t')
```

```
%=====
```

```
% --- Executes during object creation, after setting all properties.
```

```
function listbox1_CreateFcn(hObject, eventdata, handles)
```

```
% hObject    handle to listbox1 (see GCBO)
```

```
% eventdata reserved - to be defined in a future version of MATLAB
```

```
% handles    empty - handles not created until after all CreateFcns called
```

```
% Hint: listbox controls usually have a white background on Windows.
```

```
%    See ISPC and COMPUTER.
```

```
if ispc
```

```
    set(hObject,'BackgroundColor','white');
```

```
else
```

```
    set(hObject,'BackgroundColor',get(0,'defaultUicontrolBackgroundColor'));
```

```
end
```

```
%=====
```

```
% --- Executes on selection change in listbox1.
```

```
function listbox1_Callback(hObject, eventdata, handles)
```

```
% hObject    handle to listbox1 (see GCBO)
```

```
% eventdata reserved - to be defined in a future version of MATLAB
```

```
% handles    structure with handles and user data (see GUIDATA)
```

```
% Hints: contents = get(hObject,'String') returns listbox1 contents as cell array
```

```
%    contents{get(hObject,'Value')} returns selected item from listbox1
```

```
%=====
```

```
% --- Executes during object creation, after setting all properties.
```

```
function edit1_CreateFcn(hObject, eventdata, handles)
```

```
% hObject    handle to edit1 (see GCBO)
```



```

% eventdata reserved - to be defined in a future version of MATLAB
% handles empty - handles not created until after all CreateFcns called

% Hint: edit controls usually have a white background on Windows.
% See ISPC and COMPUTER.
if ispc
    set(hObject,'BackgroundColor','white');
else
    set(hObject,'BackgroundColor',get(0,'defaultUicontrolBackgroundColor'));
end

```

```

function edit1_Callback(hObject, eventdata, handles)
% hObject handle to edit1 (see GCBO)
% eventdata reserved - to be defined in a future version of MATLAB
% handles structure with handles and user data (see GUIDATA)

```

```

%p = str2double(get(hObject,'String')) %returns contents of edit1 as a double

```

```

%=====
% --- Executes during object creation, after setting all properties.
function edit2_CreateFcn(hObject, eventdata, handles)
% hObject handle to edit2 (see GCBO)
% eventdata reserved - to be defined in a future version of MATLAB
% handles empty - handles not created until after all CreateFcns called

```

```

% Hint: edit controls usually have a white background on Windows.
% See ISPC and COMPUTER.
if ispc
    set(hObject,'BackgroundColor','white');
else
    set(hObject,'BackgroundColor',get(0,'defaultUicontrolBackgroundColor'));
end

```

```

function edit2_Callback(hObject, eventdata, handles)
% hObject handle to edit2 (see GCBO)
% eventdata reserved - to be defined in a future version of MATLAB
% handles structure with handles and user data (see GUIDATA)

```

```

% Hints: get(hObject,'String') returns contents of edit2 as text
% str2double(get(hObject,'String')) returns contents of edit2 as a double

```

```

%=====
% --- Executes during object creation, after setting all properties.
function Input_names_CreateFcn(hObject, eventdata, handles)
% hObject handle to Input_names (see GCBO)
% eventdata reserved - to be defined in a future version of MATLAB
% handles empty - handles not created until after all CreateFcns called

```



```

% --- Executes on button press in Input_names.
function Input_names_Callback(hObject, eventdata, handles)
% hObject    handle to Input_names (see GCBO)
% eventdata  reserved - to be defined in a future version of MATLAB
% handles    structure with handles and user data (see GUIDATA)

num_markers = handles.num_markers;
marker_names=handles.marker_names

marker_names
%h1 = errordlg(marker_names 'that are in file','Error','modal');
%waitfor(h1)

heelname=0
metaname=0

hmarker_input=get(handles.edit1,'String')
tmarker_input=get(handles.edit2,'String')

%check input names

for d = 1:num_markers;
    C = strcmp(marker_names{d},hmarker_input);
    if C == 1
        i_heel = d;
        hname = hmarker_input;
        heelname = 1;
    end
end
for d = 1:num_markers;
    C2 = strcmp(marker_names{d},tmarker_input);
    if C2 == 1
        i_meta = d;
        mname = tmarker_input;
        metaname = 1;
    end
end
if heelname ~= 1 || metaname ~= 1

    h2 = errordlg('Marker names do not match markers in TSV data file','Error','modal')
    waitfor(h2)
    %request_input_names
else
    set(handles.edit1,'String',hname);
    set(handles.edit2,'String',mname);
    handles.i_meta=i_meta;
    handles.i_heel=i_heel;
    handles.hname=hname;
    handles.mname=mname;
    handles.tmarker_input=tmarker_input;
    handles.hmarker_input=hmarker_input;

```



```

handles.output=hObject;
Guidata(hObject,handles);
%S = [marker_input;{' marker data will be used for gait event detection'}]
%h3 = msgbox(S)
%waitfor (h3)
%button = questdlg('Do you want to continue?','Continue Operation','Yes','No','Help','No');
%if strcmp(button,'Yes')
%cycle_choice
%elseif strcmp(button,'No')
% request_input_names
%elseif strcmp(button,'Help')
%disp('Sorry, no help available')
end

```

```

handles.i_meta=i_meta;
handles.i_heel=i_heel;
handles.hname=hname;
handles.mname=mname;
handles.tmarker_input=tmarker_input;
handles.hmarker_input=hmarker_input;
handles.output=hObject;
Guidata(hObject,handles);

```

```

%=====

```

```

% --- Executes when figure1 window is resized.
function figure1_ResizeFcn(hObject, eventdata, handles)
% hObject handle to figure1 (see GCBO)
% eventdata reserved - to be defined in a future version of MATLAB
% handles structure with handles and user data (see GUIDATA)

```

```

% --- Executes on button press in Plot_Graph.
function Plot_Graph_Callback(hObject, eventdata, handles)
% hObject handle to Plot_Graph (see GCBO)
% eventdata reserved - to be defined in a future version of MATLAB
% handles structure with handles and user data (see GUIDATA)

```

```

% --- Executes on button press in Event_Detection.
function Event_Detection_Callback(hObject, eventdata, handles)
% hObject handle to Event_Detection (see GCBO)
% eventdata reserved - to be defined in a future version of MATLAB
% handles structure with handles and user data (see GUIDATA)

```

```

fname=handles.fname;

```

```

message=['Event Detection in Progress'];
handles.message=message;
handles.output=hObject;
Guidata(hObject,handles);
Detection_Status_Callback(hObject, eventdata, handles);

```



```

i_heel = handles.i_heel;
i_meta = handles.i_meta;
i_sacrum = handles.i_sacrum;
freq = handles.freq;
rpeak = handles.rpeak;
peak = handles.peak;
count4 = handles.count4;
tsv_qq = handles.tsv_qq;
cycle_input=handles.cycle_input;
suffix=handles.suffix;

if get(handles.Barefoot,'Value') == (get(handles.Barefoot,'Max'));
    w=1;
else
    w=2;
end

EventTimes=[];
All5=[];

[m3,n3] = size(rpeak);
for count4 = 1: n3-1;
    if count4 == 1
        suffix = 'st';
    elseif count4 > 3
        suffix = 'th';
    elseif count4 == 3
        suffix = 'rd';
    else
        suffix = 'nd';
    end

    % S = ['Gait event times will be determined for the ',num2str(count4),suffix,' gait cycle'];
    % h3 = msgbox(S)
    % waitfor (h3)

    .

    %starting frame = i and final frame = f
    %f = end_frame;
    %i = start_frame;
    %i = 1;
    i = rpeak(count4);
    f = rpeak(count4 + 1);

    % n is the length of the matrix from first Heel Z max to the frame before the next Heel Z max
    n = f - i;
    c = n - 1;
    % Fs = sampling frequency & R = Resolution and Ts = sampling interval
    %Fs= 200;
    Ts = 1/freq;
    end_time = (f-1) * Ts;
    e = end_time;
    start_time = i * Ts;

```



```

s = start_time;

cycle_d(count4) = (f - i)/(freq); %cycle duration in sec

Frame = i:1:(n+i-1);
Time = s:Ts:e;
Time = Time';
Frame = Frame';

HeelX = tsv_qq(:,i_heel*3-2);
HeelY = tsv_qq(:,i_heel*3-1);
HeelZ = tsv_qq(:,i_heel*3);

MetaX = tsv_qq(:,i_meta*3-2);
MetaY = tsv_qq(:,i_meta*3-1);
MetaZ = tsv_qq(:,i_meta*3);

SacrumX = tsv_qq(:,i_sacrum*3-2);
SacrumY = tsv_qq(:,i_sacrum*3-1);
SacrumZ = tsv_qq(:,i_sacrum*3);

% YZ is the sagittal plane which is the plane in which the velocity for markers is used
HeelX = HeelX(i:f-1,1);
HeelY = HeelY(i:f-1,1);
HeelZ = HeelZ(i:f-1,1);

MetaX = MetaX(i:f-1,1);
MetaY = MetaY(i:f-1,1);
MetaZ = MetaZ(i:f-1,1);

SacrumX = SacrumX(i:f-1,1);
SacrumY = SacrumY(i:f-1,1);
SacrumZ = SacrumZ(i:f-1,1);

%[b,a] = butterworth filter(filter order, cut-off frequency/half sampling frequency)
b = [];
a = [];

[b,a] = butter (2,10/(freq/2));
% Each of the signals is filtered twice (2 directions)
FHeelX = filtfilt(b,a,HeelX);
FHeelY = filtfilt(b,a,HeelY);
FHeelZ = filtfilt(b,a,HeelZ);

FMetaX = filtfilt(b,a,MetaX);
FMetaY = filtfilt(b,a,MetaY);
FMetaZ = filtfilt(b,a,MetaZ);

FSacrumX = filtfilt(b,a,SacrumX);
FSacrumY = filtfilt(b,a,SacrumY);
FSacrumZ = filtfilt(b,a,SacrumZ);

```

```

%%%%%%%%%%%%%%%%%%%%%%%%%%%%%%%%%%%%%%%%%%%%%%%%%%%%%%%%

```


%The differentials are calculated usind MATLAB function diff

```
VelHX = diff(HeelX);  
VelHY = diff(HeelY);  
VelHZ = diff(HeelZ);  
VelMX = diff(MetaX);  
VelMY = diff(MetaY);  
VelMZ = diff(MetaZ);
```

```
FVelHX = diff(FHeelX);  
FVelHY = diff(FHeelY);  
FVelHZ = diff(FHeelZ);  
FVelMX = diff(FMetaX);  
FVelMY = diff(FMetaY);  
FVelMZ = diff(FMetaZ);
```

```
VelSX = diff(SacrumX);  
VelSY = diff(SacrumY);  
VelSZ = diff(SacrumZ);  
FVelSX = diff(FSacrumX);  
FVelSY = diff(FSacrumY);  
FVelSZ = diff(FSacrumZ);
```

%%%

% processing to get the velocities using $V(x_i) = \{V(x_{i+1}) - V(x_{i-1})\} / 2$

```
VelHX1 = [VelHX;0];  
VelHY1 = [VelHY;0];  
VelHZ1 = [VelHZ;0];  
VelHX2 = [0;VelHX];  
VelHY2 = [0;VelHY];  
VelHZ2 = [0;VelHZ];  
VelHX = VelHX1 + VelHX2;  
VelHX = VelHX/(2*Ts);  
VelHX = VelHX(2:c,1:1);  
VelHX = [0;VelHX;0];  
VelHY = VelHY1 + VelHY2;  
VelHY = VelHY/(2*Ts);  
VelHY = VelHY(2:c,1:1);  
VelHY = [0;VelHY;0];  
VelHZ = VelHZ1 + VelHZ2;  
VelHZ = VelHZ/(2*Ts);  
VelHZ = VelHZ(2:c,1:1);  
VelHZ = [0;VelHZ;0];
```

```
FVelHX1 = [FVelHX;0];  
FVelHY1 = [FVelHY;0];  
FVelHZ1 = [FVelHZ;0];  
FVelHX2 = [0;FVelHX];  
FVelHY2 = [0;FVelHY];  
FVelHZ2 = [0;FVelHZ];  
FVelHX = FVelHX1 + FVelHX2;  
FVelHX = FVelHX/(2*Ts);  
FVelHX = FVelHX(2:c,1:1);  
FVelHX = [0;FVelHX;0];
```


$F_{VelHY} = F_{VelHY1} + F_{VelHY2};$
 $F_{VelHY} = F_{VelHY}/(2*Ts);$
 $F_{VelHY} = F_{VelHY}(2:c,1:1);$
 $F_{VelHY} = [0;F_{VelHY};0];$
 $F_{VelHZ} = F_{VelHZ1} + F_{VelHZ2};$
 $F_{VelHZ} = F_{VelHZ}/(2*Ts);$
 $F_{VelHZ} = F_{VelHZ}(2:c,1:1);$
 $F_{VelHZ} = [0;F_{VelHZ};0];$

%%%

$VelMX1 = [VelMX;0];$
 $VelMY1 = [VelMY;0];$
 $VelMZ1 = [VelMZ;0];$
 $VelMX2 = [0;VelMX];$
 $VelMY2 = [0;VelMY];$
 $VelMZ2 = [0;VelMZ];$
 $VelMX = VelMX1 + VelMX2;$
 $VelMX = VelMX/(2*Ts);$
 $VelMX = VelMX(2:c,1:1);$
 $VelMX = [0;VelMX;0];$
 $VelMY = VelMY1 + VelMY2;$
 $VelMY = VelMY/(2*Ts);$
 $VelMY = VelMY(2:c,1:1);$
 $VelMY = [0;VelMY;0];$
 $VelMZ = VelMZ1 + VelMZ2;$
 $VelMZ = VelMZ/(2*Ts);$
 $VelMZ = VelMZ(2:c,1:1);$
 $VelMZ = [0;VelMZ;0];$

$F_{VelMX1} = [F_{VelMX};0];$
 $F_{VelMY1} = [F_{VelMY};0];$
 $F_{VelMZ1} = [F_{VelMZ};0];$
 $F_{VelMX2} = [0;F_{VelMX}];$
 $F_{VelMY2} = [0;F_{VelMY}];$
 $F_{VelMZ2} = [0;F_{VelMZ}];$
 $F_{VelMX} = F_{VelMX1} + F_{VelMX2};$
 $F_{VelMX} = F_{VelMX}/(2*Ts);$
 $F_{VelMX} = F_{VelMX}(2:c,1:1);$
 $F_{VelMX} = [0;F_{VelMX};0];$
 $F_{VelMY} = F_{VelMY1} + F_{VelMY2};$
 $F_{VelMY} = F_{VelMY}/(2*Ts);$
 $F_{VelMY} = F_{VelMY}(2:c,1:1);$
 $F_{VelMY} = [0;F_{VelMY};0];$
 $F_{VelMZ} = F_{VelMZ1} + F_{VelMZ2};$
 $F_{VelMZ} = F_{VelMZ}/(2*Ts);$
 $F_{VelMZ} = F_{VelMZ}(2:c,1:1);$
 $F_{VelMZ} = [0;F_{VelMZ};0];$

%%%

$VelSX1 = [VelSX;0];$
 $VelSY1 = [VelSY;0];$
 $VelSZ1 = [VelSZ;0];$
 $VelSX2 = [0;VelSX];$


```

VelSY2 = [0;VelSY];
VelSZ2 = [0;VelSZ];
VelSX = VelSX1 + VelSX2;
VelSX = VelSX/(2*Ts);
VelSX = VelSX(2:c,1:1);
VelSX = [0;VelSX;0];
VelSY = VelSY1 + VelSY2;
VelSY = VelSY/(2*Ts);
VelSY = VelSY(2:c,1:1);
VelSY = [0;VelSY;0];
VelSZ = VelSZ1 + VelSZ2;
VelSZ = VelSZ/(2*Ts);
VelSZ = VelSZ(2:c,1:1);
VelSZ = [0;VelSZ;0];

```

```

FVelSX1 = [FVelSX;0];
FVelSY1 = [FVelSY;0];
FVelSZ1 = [FVelSZ;0];
FVelSX2 = [0;FVelSX];
FVelSY2 = [0;FVelSY];
FVelSZ2 = [0;FVelSZ];
FVelSX = FVelSX1 + FVelSX2;
FVelSX = FVelSX/(2*Ts);
FVelSX = FVelSX(2:c,1:1);
FVelSX = [0;FVelSX;0];
FVelSY = FVelSY1 + FVelSY2;
FVelSY = FVelSY/(2*Ts);
FVelSY = FVelSY(2:c,1:1);
FVelSY = [0;FVelSY;0];
FVelSZ = FVelSZ1 + FVelSZ2;
FVelSZ = FVelSZ/(2*Ts);
FVelSZ = FVelSZ(2:c,1:1);
FVelSZ = [0;FVelSZ;0];

```

```

%%%%%%%%%%%%%%%%%%%%%%%%%%%%%%%%%%%%%%%%%%%%%%%%%%%%%%%%%%%%%%%%%%%%%%%%
VelSYZ = sqrt ((VelSX.^2) + (VelSY.^2));    %%%%%%%%% NOTE %%%%%%%%%
FVelSYZ = sqrt ((FVelSX.^2) + (FVelSY.^2));    %VELHYZ is effectively VELHXZ =
sagittal plane velocity
% same for meta marker
%just to avoid changing variable(VELHYZ) for rest of programme

```

```

%%%%%%%%%%%%%%%%%%%%%%%%%%%%%%%%%%%%%%%%%%%%%%%%%%%%%%%%%%%%%%%%%%%%%%%%
SpeedS(count4)= mean(VelSYZ);
FSpeedS(count4)= mean(FVelSYZ);

```

```

%%%%%%%%%%%%%%%%%%%%%%%%%%%%%%%%%%%%%%%%%%%%%%%%%%%%%%%%%%%%%%%%%%%%%%%%
VelHYZ = sqrt ((VelHX.^2) + (VelHZ.^2));    %%%%%%%%% NOTE %%%%%%%%%
FVelHYZ = sqrt ((FVelHX.^2) + (FVelHZ.^2));    %VELHYZ is effectively VELHXZ =
sagittal plane velocity
% same for meta marker
VelMYZ = sqrt ((VelMX.^2) + (VelMZ.^2));    %just to avoid changing variable for rest of
programme

```



```
FVelMYZ = sqrt ((FVelMX.^2) + (FVelMZ.^2));
```

```
%%%%%%%%%%%%%%%%%%%%%%%%%%%%%%%%%%%%%%%%%%%%%%%%%%%%%%%%%
```

```
%footwear = input('Enter 1 for barefoot and 2 for shod trials:');
```

```
%w = footwear;
```

```
if w < 2; % case = barefoot
```

```
    LogH = 0;
```

```
%ENCODE Velocity values according to values
```

```
%Determine event times using appropriate thresholds and coded value transitions
```

```
for t = 2:n-1
```

```
    if FVelHYZ(t,:) < 100;
```

```
        SHeel = 1;
```

```
    elseif FVelHYZ(t,:) >= 300;
```

```
        SHeel = 0;
```

```
    else SHeel = 2;
```

```
    end
```

```
    LogH = [LogH;SHeel];
```

```
end
```

```
LogH = [LogH;0];
```

```
difflogh = diff(LogH);
```

```
for t = 1:n-1
```

```
    if difflogh(t,:) > 1;
```

```
        HeelC = t+i;
```

```
        FlagHC=1;
```

```
    elseif difflogh(t,:) < 2;
```

```
        if difflogh(t,:) > 0;
```

```
            HeelR = t+i;
```

```
            FlagHR=1;
```

```
        end
```

```
    end
```

```
end
```

```
if FlagHC == 1
```

```
    HeelCtime = HeelC*Ts;
```

```
else
```

```
    HeelCtime = 0;
```

```
end
```

```
if FlagHR==1
```

```
    HeelRtime = HeelR*Ts;
```

```
else
```

```
    HeelRtime=0;
```

```
end
```

```
LogM = 0;
```

```
for t = 2:n-1
```

```
    if FVelMYZ(t,:) < 100;
```

```
        SMeta = 1;
```

```
    elseif FVelMYZ(t,:) >= 300;
```

```
        SMeta = 0;
```

```
    else SMeta = 2;
```

```
    end
```



```

    LogM = [LogM;SMeta];
end
LogM = [LogM;0];
difflogm = diff(LogM);

for t = 1:n-1
    if difflogm(t,:) >1;
        if difflogm(t,:) <3;
            MetaC = t+i;
        end
    elseif difflogm(t,:) >= 1;
        if difflogm(t,:) < 2;
            MetaR = t+i;
        end
    end
end
MetaCtime = MetaC*Ts;
MetaRtime = MetaR*Ts;
All2 = [HeelC;MetaC;HeelR;MetaR];
All3 = [HeelCtime;MetaCtime;HeelRtime;MetaRtime];
All4 = [All2,All3];

elseif w > 1;
    LogH = 0; %CASE = SHOD
    for t = 2:n-1
        if FVelHYZ(t,:) < 100;
            SHeel = 1;
        elseif FVelHYZ(t,:) >= 300;
            SHeel = 0;
        else SHeel = 2;
        end
        LogH = [LogH;SHeel];
    end

    LogH = [LogH;0];
    difflogh = diff(LogH);
    FlagMC=0;
    for t = 1:n-1
        if difflogh(t,:) > 1;
            HeelC = t+i;
            FlagHC=1;
        elseif difflogh(t,:) < 2;
            if difflogh(t,:) > 0;
                HeelR = t+i;
                FlagHR=1;
            end
        end
    end

    if FlagHC == 1
        HeelCtime = HeelC*Ts;
    else
        HeelCtime = 0;
    end
end

```



```

end
if FlagHR==1
    HeelRtime = HeelR*Ts;
else
    HeelRtime=0;
end

LogM = 0;
for t = 2:n-1
    if FVelMYZ(t,:) < 100;
        SMeta = 1;
    elseif FVelMYZ(t,:) >= 100;
        SMeta = 0;
    else SMeta = 2;
    end
    LogM = [LogM;SMeta];
end
LogM = [LogM;0];
difflogm = diff(LogM);
for t = 1:n-1
    if difflogm(t,:) <0;
        if difflogm(t,:) > -2;
            MetaC = t+i;
            FlagMC=1;
        end
    elseif difflogm(t,:) >= 1;
        if difflogm(t,:) < 2;
            MetaR = t+i;
            FlagMR=1;
        end
    end
end
end

if FlagMC==1;
    MetaCtime = MetaC*Ts;
else
    MetaC = 0;
    MetaCtime=0;
end
if FlagMR==1;
    MetaRtime = MetaR*Ts;
else
    MetaRtime=0;
end

All2 = [HeelC,MetaC,HeelR,MetaR];
All3 = [HeelCtime,MetaCtime,HeelRtime,MetaRtime];
All4 = [All2,All3];
end
All

```

=

```

[Frame,Time,HeelX,HeelY,HeelZ,MetaX,MetaY,MetaZ, VelHX, VelHY, VelHZ, VelMX, VelMY, V
elMZ,FHeelX,FHeelY,FHeelZ,FMetaX,FMetaY,FMetaZ,FVelHX,FVelHY,FVelHZ,FVelMX,FV
elMY,FVelMZ, VelHYZ, VelMYZ,FVelHYZ,FVelMYZ,LogH,LogM];

```



```

[m3,n3] = size(rpeak);

if cycle_input == 0 % if requested to analyse all cycles then output data on end of analysis
    EventTimes=[EventTimes;All4];
    %get rid of zeros at start and end frame in velocity data
    Alltemp = All;
    Alltemp(1,29) = Alltemp(2,29);
    Alltemp(1,30) = Alltemp(2,30);
    [m5,n5] = size(Alltemp);
    Alltemp(m5,29) = Alltemp(m5-1,29);
    Alltemp(m5,30) = Alltemp(m5-1,30);
    All5=[All5;Alltemp];
else
    EventTimes = All4;
    All5 = All;
    All5(1,29) = All5(2,29);
    All5(1,30) = All5(2,30);
    [m4,n4] = size(All);
    All5(m4,29) = All5(m4-1,29);
    All5(m4,30) = All5(m4-1,30);

    %outputalldata %if just one cycle analysis requested then output data
end

end
EventTimes2=EventTimes;
% Event Detection variables to be used by other functions
handles.All5=All5;
handles.EventTimes= EventTimes;
handles.SpeedS = SpeedS;
handles.FSpeedS= FSpeedS;
handles.cycle_d = cycle_d;
handles.EventTimes2=EventTimes2;
handles.output=hObject;
Guidata(hObject,handles);

message=[fname,' events determined'];
handles.message=message;
handles.output=hObject;
Guidata(hObject,handles);
Detection_Status_Callback(hObject, eventdata, handles);

button = questdlg('Do you want to Update Results Plot?','Continue Operation','Yes','No','No');
if strcmp(button,'Yes')
    DISPLAY_RESULTS_Callback(hObject, eventdata, handles)
elseif strcmp(button,'No')
end

return
%=====
% --- Executes on button press in Zoom.
function Zoom_Callback(hObject, eventdata, handles)

```



```

% hObject handle to Zoom (see GCBO)
% eventdata reserved - to be defined in a future version of MATLAB
% handles structure with handles and user data (see GUIDATA)

```

```

All5 = handles.All5;
fname = handles.fname;
EventTimes2 = handles.EventTimes2;

```

```

Time = All5(:,2);
HeelZ = All5(:,5);
ToeZ = All5(:,8);
FVelHYZ = All5(:,29);
FVelMYZ = All5(:,30);

```

```

%lined = 1:5:3000;%(max(FVelHYZ/(2))); %vector of data to be used for plotting the events
(value goes up to half of highest velocity)
%lined2= 1:5:3500;%(max(FVelHYZ/1.3));
lined = 1:5:(max(FVelHYZ/(2))); %vector of data to be used for plotting the events (value goes up
to half of highest velocity)
lined2= 1:5:(max(FVelHYZ/1.3));
% get rid of the zeros on the first and last frame of the cycle in the velocity data
%FVelHYZ(1) = FVelHYZ(2);
%FVelMYZ(1) = FVelMYZ(2);
%[m4,n4] = size(All5);

```

```

%FVelHYZ(m4) = FVelHYZ(m4-1);
%FVelMYZ(m4) = FVelMYZ(m4-1);

```

```

% get threshold values for velocities
if get(handles.Barefoot,'Value') == (get(handles.Barefoot,'Max'));
    w=1;
else
    w=2;
end

```

```

if w < 2; % case = barefoot
    HCThreshold = 300;
    HRThreshold = 100;
    TCThreshold = 100;
    TOThreshold = 100;
elseif w > 1; % case = SHOD
    HCThreshold = 300;
    HRThreshold = 100;
    TCThreshold = 100;
    TOThreshold = 100;
end

```

```

xmin = min(Time);
xmin = round(xmin);
if xmin < min(Time)
    xmin = xmin;
else

```



```

    xmin = xmin - 0.5;
end

xmax = max(Time);
xmax = round(xmax);
if xmax > max(Time);
    xmax = xmax;
else
    xmax = xmax + 0.5;
end

figure
plottedit on
plot(Time,HeelZ,Time,ToeZ,Time,FVelHYZ,'-o',Time,FVelMYZ,'-+', 'MarkerSize',3)
axis([xmin xmax 0 5500])
legend('HeelZ','MetatarsalZ','Filtered Heel Vels','Filtered Toe Vels',1);
xlabel('Time (s)');
ylabel('Sagittal velocity (mm/s)');
titlestring = [fname,' sagittal velocities of heel and toe markers and event times'];
title(titlestring);
grid on;
hold on

plot(Time,HCThreshold,Time,HRThreshold,Time,TCThreshold,Time,TOThreshold)
[m6,n6]=size(EventTimes2);
for count6=1:m6;
    plot(EventTimes2(count6,5),lined2,'-b',EventTimes2(count6,7),lined2,'-r',...
        EventTimes2(count6,6),lined,'-m',EventTimes2(count6,8),lined,'-y');
    HCtime = num2str(EventTimes2(count6,5),4);
    HRtime = num2str(EventTimes2(count6,7),4);
    TCtime = num2str(EventTimes2(count6,6),4);
    TOtime = num2str(EventTimes2(count6,8),4);
    HCstring = ['HC ',HCtime];
    HRstring = ['HR ',HRtime];
    TCstring = ['TC ',TCtime];
    TOstring = ['TO ',TOtime];
    text(EventTimes2(count6,5)-0.05,max(lined2)+50,HCstring,'FontSize',7,'BackgroundColor',[1 1
1]);
    text(EventTimes2(count6,7)-0.05,max(lined2)+125,HRstring,'FontSize',7,'BackgroundColor',[1
1 1]);
    text(EventTimes2(count6,6)-0.05,max(lined)+50,TCstring,'FontSize',7,'BackgroundColor',[1 1
1]);
    text(EventTimes2(count6,8)-0.05,max(lined)+125,TOstring,'FontSize',7,'BackgroundColor',[1 1
1]);
    hold on
end

hold off

figure
a=gca;

% Set appropriate axis limits and settings

```



```

set(gcf,'doublebuffer','on');
%% This avoids flickering when updating the axis
xmin=min(Time);
xmax=max(Time);
n=xmin+1.2;

set(a,'xlim',[xmin n]);
set(a,'ylim',[0 5500]);
% Generate constants for use in uicontrol initialization
pos=get(a,'position');
Newpos=[pos(1) pos(2)-0.1 pos(3) 0.05];
%% This will create a slider which is just underneath the axis
%% but still leaves room for the axis labels above the slider
xmin=min(Time);
xmax=max(Time);
sliderstep=[0.05 0.05];

get(gcbo,'value');
S=['set(gca,"xlim",get(gcbo,"value")+[' 0 ' num2str(1.2) '])'];
%S=['set(gca,"xmin",get(gcbo,"value")+[' 0 ' num2str(1) '])'];
%% Setting up callback string to modify XLim of axis (gca)
%% based on the position of the slider (gcbo)

% Creating Uicontrol
h=uicontrol('style','slider',...
    'units','normalized','position',Newpos,...
    'callback',S,'Sliderstep',sliderstep,'value',xmin,'min',xmin,'max',xmax-1.2);

hold on

%figure
titlestring = [fname,' HeelZ vs HeelX scatter plot'];
title(titlestring);
grid on
hold on
HeelX=All5(:,3);
%plot(HeelX,HeelZ,'-o','Markersize',3)

figure
titlestring = [fname,' A plot showing the velocity of the heel marker near heel contact time'];
title(titlestring);
grid on
hold on
HeelX=All5(:,3);
plot(Time,HeelZ,'-+',Time,(All5(:,9)),'-o',Time,(All5(:,11)),'-*',Time,(All5(:,21)),'-o',Time,(All5(:,23)),'-*',Time,(All5(:,27)),'-s',Time,(All5(:,29)),'-^')
legend('HeelZ','VelHX','VelHZ','FVelHX','FVelHZ','VelHXZ','FVelHXZ');
xlabel('Time (s)');
ylabel('Velocity (mm/s)');

a=gca;
% Set appropriate axis limits and settings
set(gcf,'doublebuffer','on');

```



```

%% This avoids flickering when updating the axis
xmin=min(Time);
xmax=max(Time);
n=xmin+0.5;
%Tick=[xmin:0.01:xmax]
%Ticklabel=[xmin:0.1:xmax]
set(a,'xlim',[xmin n]);
set(a,'ylim',[-500 500]);
%set(a,'xtick',Tick);
%set(a,'xticklabel',Ticklabel);

% Generate constants for use in uicontrol initialization
pos=get(a,'position');
Newpos=[pos(1) pos(2)-0.1 pos(3) 0.01];
%% This will create a slider which is just underneath the axis
%% but still leaves room for the axis labels above the slider
xmin=min(Time);
xmax=max(Time);
sliderstep=[0.01 0.01];

get(gcbo,'value');
S=['set(gca,"xlim",get(gcbo,"value")+[' 0 ' num2str(0.5) '])'];
%S=['set(gca,"xmin",get(gcbo,"value")+[' 0 ' num2str(1) '])'];
%% Setting up callback string to modify XLim of axis (gca)
%% based on the position of the slider (gcbo)

% Creating Uicontrol
h=uicontrol('style','slider',...
    'units','normalized','position',Newpos,...
    'callback',S,'Sliderstep',sliderstep,'value',xmin,'min',xmin,'max',xmax-0.5);

%=====
=====
% --- Executes during object creation, after setting all properties.
function listbox2_CreateFcn(hObject, eventdata, handles)
% hObject    handle to listbox2 (see GCBO)
% eventdata  reserved - to be defined in a future version of MATLAB
% handles    empty - handles not created until after all CreateFcns called

% Hint: listbox controls usually have a white background on Windows.
%    See ISPC and COMPUTER.
if ispc
    set(hObject,'BackgroundColor','white');
else
    set(hObject,'BackgroundColor',get(0,'defaultUicontrolBackgroundColor'));
end

% --- Executes on selection change in listbox2.
function listbox2_Callback(hObject, eventdata, handles)
% hObject    handle to listbox2 (see GCBO)
% eventdata  reserved - to be defined in a future version of MATLAB
% handles    structure with handles and user data (see GUIDATA)

```



```
% Hints: contents = get(hObject,'String') returns listbox2 contents as cell array
% contents{get(hObject,'Value')} returns selected item from listbox2
```

```
%=====
% --- Executes during object creation, after setting all properties.
function ignored_peaks_CreateFcn(hObject, eventdata, handles)
% hObject handle to ignored_peaks (see GCBO)
% eventdata reserved - to be defined in a future version of MATLAB
% handles empty - handles not created until after all CreateFcns called
```

```
% Hint: listbox controls usually have a white background on Windows.
% See ISPC and COMPUTER.
if ispc
    set(hObject,'BackgroundColor','white');
else
    set(hObject,'BackgroundColor',get(0,'defaultUicontrolBackgroundColor'));
end
```

```
% --- Executes on selection change in ignored_peaks.
function ignored_peaks_Callback(hObject, eventdata, handles)
% hObject handle to ignored_peaks (see GCBO)
% eventdata reserved - to be defined in a future version of MATLAB
% handles structure with handles and user data (see GUIDATA)
```

```
% Hints: contents = get(hObject,'String') returns ignored_peaks contents as cell array
```

```
ignoredpeaks=get(hObject,'String');
index_selected = get(hObject,'Value');
```

```
handles.ignoredpeaks=ignoredpeaks;
handles.index_selected=index_selected;
handles.output=hObject;
Guidata(hObject,handles);
```

```
%=====
% --- Executes on button press in peaks_Done.
function peaks_Done_Callback(hObject, eventdata, handles)
% hObject handle to peaks_Done (see GCBO)
% eventdata reserved - to be defined in a future version of MATLAB
% handles structure with handles and user data (see GUIDATA)
```

```
rpeak=handles.rpeak;
%ignoredpeaks=handles.ignoredpeaks;
%index_selected = handles.index_selected;
```

```
ignoredpeaks=get(handles.ignored_peaks,'String');
index_selected = get(handles.ignored_peaks,'Value');
```

```
for count = 1:length(index_selected);
    ipeak(count)=ignoredpeaks(index_selected(count));
```



```

end

ppeak = rpeak;

m10=length(ipeak);

for count = 1:m10;
    n = ipeak(count);
    n=str2num(n);
    ppeak(n)=0;
end

count2=1;
[m9,n9]=size(rpeak);
for count=1:n9;
    if ppeak(count) ~= 0;
        fpeak(count2)=ppeak(count);
        count2=count2+1;
    end
end

fpeak;

rpeak=fpeak;

handles.ignoredpeaks=ignoredpeaks;
handles.ipeaks=ipeak;
handles.rpeak=rpeak;
handles.output=hObject;
Guidata(hObject,handles);

tsv_qq=handles.tsv_qq;
i_heel = handles.i_heel;
freq = handles.freq;
HeelZ = tsv_qq(:,i_heel*3);

suffix = "";

%starting frame = i and final frame = f
% n is the length of the matrix from first Heel Z max to the frame before the next Heel Z max
%footwear = input('Enter 1 for barefoot and 2 for shod trials:');
[f,i] = size(HeelZ);

n = f - i;
% Fs = sampling frequency & R = Resolution and Ts = sampling interval

Ts = 1/freq;
e = f * Ts; %end time

s = i * Ts; %start time

Frame = i:1:(f);

```



```

Time = s:Ts:e;
Time = Time';
Frame = Frame';

axes(handles.axes2);
plot(Frame,HeelZ);
hold on;

lined3 = 1 :(max(HeelZ*1.3)); %vector of data to be used for plotting the events (value goes up to
half of highest velocity)

axes(handles.axes2);

[m7,n8]=size(rpeak);

xmin = rpeak(1,1) - 100;
xmax = rpeak(1,n8) + 100;
ymax= max(HeelZ)*1.5;

axis([xmin xmax 0 ymax]);

for count7=1:n8;
    axes(handles.axes2);
    plot(rpeak(1,count7),lined3,'-r');
    peaktime = num2str(round(rpeak(1,count7)));
    peakstring = [peaktime];
    text(rpeak(1,count7)-0.05,max(lined3),peakstring,'FontSize',8,'BackgroundColor',[1 1 1]);
    hold on
end

[m3,n3]=size(rpeak);
set(handles.num_cycles,'String',(n3-1));

%=====
% --- Executes during object creation, after setting all properties.
function num_cycles_CreateFcn(hObject, eventdata, handles)
% hObject    handle to num_cycles (see GCBO)
% eventdata  reserved - to be defined in a future version of MATLAB
% handles    empty - handles not created until after all CreateFcns called

% Hint: edit controls usually have a white background on Windows.
%    See ISPC and COMPUTER.
if ispc
    set(hObject,'BackgroundColor','white');
else
    set(hObject,'BackgroundColor',get(0,'defaultUicontrolBackgroundColor'));
end

function num_cycles_Callback(hObject, eventdata, handles)
% hObject    handle to num_cycles (see GCBO)
% eventdata  reserved - to be defined in a future version of MATLAB
% handles    structure with handles and user data (see GUIDATA)

```



```

% Hints: get(hObject,'String') returns contents of num_cycles as text
%      str2double(get(hObject,'String')) returns contents of num_cycles as a double

% -----
function File_Callback(hObject, eventdata, handles)
% hObject   handle to File (see GCBO)
% eventdata reserved - to be defined in a future version of MATLAB
% handles   structure with handles and user data (see GUIDATA)

% -----
function Print_Callback(hObject, eventdata, handles)
% hObject   handle to Print (see GCBO)
% eventdata reserved - to be defined in a future version of MATLAB
% handles   structure with handles and user data (see GUIDATA)

print -dsetup

% --- Executes during object creation, after setting all properties.
function Detection_Status_CreateFcn(hObject, eventdata, handles)
% hObject   handle to Detection_Status (see GCBO)
% eventdata reserved - to be defined in a future version of MATLAB
% handles   empty - handles not created until after all CreateFcns called

% Hint: edit controls usually have a white background on Windows.
%      See ISPC and COMPUTER.
if ispc
    set(hObject,'BackgroundColor','white');
else
    set(hObject,'BackgroundColor',get(0,'defaultUicontrolBackgroundColor'));
end

set(hObject,'String','Please load TSV file');

function Detection_Status_Callback(hObject, eventdata, handles)
% hObject   handle to Detection_Status (see GCBO)
% eventdata reserved - to be defined in a future version of MATLAB
% handles   structure with handles and user data (see GUIDATA)

% Hints: get(hObject,'String') returns contents of Detection_Status as text
%      str2double(get(hObject,'String')) returns contents of Detection_Status as a double

set(handles.Detection_Status,'String','');
message=handles.message;
set(handles.Detection_Status,'String',message);

return

% -----
function Tools_Callback(hObject, eventdata, handles)
% hObject   handle to Tools (see GCBO)
% eventdata reserved - to be defined in a future version of MATLAB
% handles   structure with handles and user data (see GUIDATA)

```



```

% -----
function Analyse_All_Cycles_Callback(hObject, eventdata, handles)
% hObject handle to Analyse_All_Cycles (see GCBO)
% eventdata reserved - to be defined in a future version of MATLAB
% handles structure with handles and user data (see GUIDATA)

% --- Executes on button press in Unsynchronise.
function Unsynchronise_Callback(hObject, eventdata, handles)
% hObject handle to Unsynchronise (see GCBO)
% eventdata reserved - to be defined in a future version of MATLAB
% handles structure with handles and user data (see GUIDATA)

% Hint: get(hObject,'Value') returns toggle state of Unsynchronise
if (get(hObject,'Value') == get(hObject,'Max'))
    Event_Detection_Callback(hObject, eventdata, handles)
end

% -----
function Display_after_detection_Callback(hObject, eventdata, handles)
% hObject handle to Display_after_detection (see GCBO)
% eventdata reserved - to be defined in a future version of MATLAB
% handles structure with handles and user data (see GUIDATA)

% -----
function Untitled_1_Callback(hObject, eventdata, handles)
% hObject handle to Untitled_1 (see GCBO)
% eventdata reserved - to be defined in a future version of MATLAB
% handles structure with handles and user data (see GUIDATA)

% -----
function Help_Callback(hObject, eventdata, handles)
% hObject handle to Help (see GCBO)
% eventdata reserved - to be defined in a future version of MATLAB
% handles structure with handles and user data (see GUIDATA)

end

```


Appendix B

Assembly language code running on the PIC


```

;This program runs on the PIC16C73B
; Last updated 13/05/2003
;the shank angular rate is used to detect heel contact and break of contact with the ground
;the digital output can be used to control the timing a foot drop stimulator
;Gyro input is on port A0
;the heel state is reflected on porta,2
;HEEL ON = low          HEEL OFF = high
; the way this program works is by using the CCP special event trigger
; so the interrupt is set on TIMER1 matching CCP2RH/L

```

```

;there is a routine at the end of the isr that reflects the
;sampling frequency of the program
;this can be done by looking at the change in porta,1
;duration between each transition reflects 1 cycle

```

```

;portc,0 could be used as a control for the DAC
;by connecting it to the cs pin

```

```

Processor    PIC16C73B

```

```

LIST        R=DEC, COLUMNS=120, XREF=YES, NOWRAP,LINES=0

```

```

;

```

```

include      "P16c73b.inc"

```

```

__CONFIG    _CP_OFF & _WDT_OFF & _BODEN_ON & _PWRTE_ON &

```

```

_XT_OSC

```

```

;

```

```

;Declarations

```

```

POST80      equ    0x20

```

```

POST255     equ    0x21

```

```

Compres     equ    0x22

```

```

VAR1        equ    0x23

```

```

VAR2        equ    0x24

```

```

ReadyfHO    equ    0x25

```

```

velocity    equ    0x26

```

```

previousvelocity equ    0x27

```

```

ReadyfPHO   equ    0x28

```

```

PHOCount    equ    0x29

```

```

ReadyfHC    equ    0x2A

```

```

HeelOnOff   equ    0x2B

```

```

SwPDetected equ    0x2C

```

```

StPCount    equ    0x2D

```

```

StPDetected equ    0x2E

```

```

FSTTest     equ    0x2F

```

```

FSOnOff     equ    0x30

```

```

FStepCount  equ    0x31

```

```

FStillCount equ    0x32

```

```

HeelOffCount equ    0x33

```

```

OffsetFlag  equ    0x34

```

```

OffsetSuccess equ    0x35

```

```

Offset      equ    0x36

```

```

FirstRun    equ    0x37

```

```

Vo          equ    0x38

```

```

SwPCount    equ    0x39

```



```

VelocityZero      equ    0x3A
SampleTest        equ    0x3B
Spcccontrol       equ    0x3C
Fsccontrol        equ    0x3D
Fstccontrol       equ    0x3E
Stpccontrol       equ    0x3F
Phoccontrol       equ    0x40
Hoccontrol        equ    0x41
Fstcontrol        equ    0x42
Swpccontrol       equ    0x43
temp1             equ    0x44
IDControl         equ    0x45
RSdatain         equ    0x46
Smller           equ    0x47
Lrger            equ    0x48
LEDflag          equ    0x49
temp2            equ    0x4A
Blind            equ    0x4B
BlindCount       equ    0x4C
porta            equ    PORTA
portb            equ    PORTB
portc            equ    PORTC
tmr1l           equ    TMR1L
tmr1h           equ    TMR1H
trisa           equ    TRISA
trisb           equ    TRISB
trisc           equ    TRISC
adcon0          equ    ADCON0
adcon1          equ    ADCON1
intcon          equ    INTCON
pie1            equ    PIE1
pie2            equ    PIE2
ccp2con        equ    CCP2CON
t1con           equ    T1CON
ccpr2l         equ    CCPR2L
ccpr2h         equ    CCPR2H
adres          equ    ADRES
pir2           equ    PIR2
pir1           equ    PIR1

```

```

ORG 0x00
goto Start

```

```

;=====

```

```

;Subroutines

```

```

Init

```

```

    clrf    porta
    clrf    portb
    goto    InitContinue
    goto    isr

```

```

Initsub

```

```

    bsf    STATUS,RP0    ;select bank1
    movlw  b'00011'      ;RA0 is the An input from RA1

```



```

movwf trisa
clrf trisb
clrf RSdatain ;clear Serial data in flag
movlw 0x07
movwf adcon1
bcf STATUS,RP0
clrf porta
return
InitContinue
; clrf STATUS
; bcf STATUS,5
; bcf STATUS,RP0
clrf tmr1l ;clear TIMER1
clrf tmr1h
; bsf status,5
; clrf STATUS
clrf RSdatain
call Initsub
salim1
btfss porta,1 ;Is the serial module button pressed?
goto salim
goto RSinit ;Yes: proceed to RS initialisation
salim
clrf adres
clrf Compres
clrf VAR1
clrf VAR2
clrf ReadyfHO
clrf velocity
clrf previousvelocity
clrf ReadyfPHO
clrf PHOCount
clrf ReadyfHC
bsf HeelOnOff,0
; movlw b'11110000'
; movwf portb ;*****
bcf porta,2 ;heel is on at startup
clrf SwPDetected
clrf StPCount
clrf StPDetected
clrf FSTTest
bsf FSONOff,0 ;
clrf FStepCount
clrf FStillCount
clrf HeelOffCount
clrf OffsetFlag
clrf OffsetSuccess
clrf Smller
clrf Lrger
clrf BlindCount
clrf Blind
clrf LEDflag
clrf Offset

```



```

movlw d'0'
movwf Offset
bsf   FirstRun,0
clrf  SwPCount
clrf  Vo
clrf  VelocityZero
clrf  SampleTest
bsf   STATUS,RP0
clrf  adcon1
clrf  intcon
;clrf trisc      ;PORTC is used by the CCP
movlw b'00000100'
movwf adcon1      ;analog inputs on RA0 and RA1
movlw b'11000000'
movwf intcon
;bcf  pie1,5      ;UART      RCIF disable
bsf   pie2,0      ;CCP2ie enable
movlw b'00011'
movwf trisa
;clrf trisc
;bcf  STATUS,5
bcf   STATUS,RP0      ;select bank 0
bcf   RCSTA,7        ;Disable Serial port
movlw b'01000001'
movwf adcon0      ;A/D clock Fosc/8 channel AN0 is on
movlw b'00001011' ;Compare mode - reset TIMER1
movwf ccp2con      ;special event trigger for A/D
movlw b'00000001' ;T1CON<5:4> prescalar
movwf t1con        ;T1CON<1> internal clock (Fosc/4)
movlw b'01000000' ;16 bit register to compare to
movwf ccpr2l       ;when TMR1 matches,interrupt is enabled
movlw b'00100011'
movwf ccpr2h

```

setcontrols

```

btfsc RSdatain,1 ;were paraneters set using serial port?
return           ;yes: returns to the Start sr "call Init"
movlw .4         ;No: proceed to setting them Default Values
movwf Spccontrol ;Swing Phase Count control 4
movlw .9
movwf Fsccontrol ;Foot Still Count Control 9
movlw .1
movwf Fstcontrol ;First Step Count Control 1
movlw .1
movwf Stpccontrol ;Stance Phase Count Control 1
movlw .3
movwf Phoccontrol ;Pre Heel Off Count Control 5
movlw .5
movwf Hoccontrol ;Heel Off Count Control 10
movlw .2
movwf Fstcontrol ;First Step Taken Control 2
movlw .130
movwf Swpcontrol ;Swing Phase Control 129

```



```
return ;returns to the Start sr "call Init"
```

```
RSinit
```

```
; clrf portb ;Clear PORT_B output latches
movlw b'11111111'
movwf IDControl
bsf STATUS,RP0
movlw b'00000111'
movwf adcon1
;clrf TRIS_B ;Config PORT_B as all outputs
movlw b'11000000'
movwf trisc
movlw b'00100000' ;;bit <5> RCIE rcv interrupt enabled
movwf PIE1
movlw 16h;19h ;9600 baud @4MHz
movwf SPBRG
movlw b'10100100' ;async tx 8 bit: bit <4> SYNC cleared(Async mode)
movwf TXSTA ; : bit <6> TX9 cleared(8 bit)
bcf STATUS,RP0 ; : bit <2> BRGH set(high speed)
bcf porta,4 ;Enable RS232 driver
movlw b'10010000' ;Enable continous reception
movwf RCSTA
movlw b'11000000' ;bit <7> GIE global interrupt enabled
movwf INTCON ;bit <6> PEIE peripheral interrupt enabled

return
```

```
isr ;Interrupt Service Routine
```

```
btfs pir1,5
goto isrt2
goto RScomm
```

```
=====
=====
isrt2
```

```
btfs pir2,0 ;TMR1 match occurred CPP2 int flag
retfie ;NO? return and reenale
;bcf portc,0 ;for the DAC cs pin
call Analysis
; bcf porta,4
;SamplingTest
; comf SampleTest,1
; btfs SampleTest,0
; goto SampleOn
; goto SampleOff
;SampleOff
; bcf porta,2
; goto Continue
;SampleOn
; bsf porta,2
; goto Continue
;Continue
```



```

;bcf   pir1,6           ;reset A/D int flag
;bsf   con0,2          ;start A/D conversion
;bsf   portc,0         ; for the DAC cs pin
;bsf   porta,4
bcf   pir2,0           ;reset the CCP2 int flag
retfie                ;return and enable global interrupt

```

```

;Program Start

```

```

Start

```

```

    bcf   STATUS,5
    call  Init

```

```

Main

```

```

    goto  Main

```

```

RScomm

```

```

    movlw 06h           ;Mask out unwanted bits
    andwf RCSTA,W       ;Check for errors
    btfss STATUS,Z
    goto  RcvError     ;Found error, flag it
    btfss PIR1,5       ;Check for data ready
    retfie             ;Some other interrupt, exit

```

```

Rcv1

```

```

    btfss IDControl,0
    goto  Rcv2
    bcf   IDControl,0
    movf  RCREG,W       ;Get input data
;    movwf PORT_B      ;Display on LEDs
    movfw RCREG
    movwf Hoccontrol
    retfie

```

```

Rcv2

```

```

    btfss IDControl,1
    goto  Rcv3
    bcf   IDControl,1
    movfw RCREG
;    movwf PORT_B
    movwf Phoccontrol
    retfie

```

```

Rcv3

```

```

    btfss IDControl,2
    goto  Rcv4
    bcf   IDControl,2
    movf  RCREG,W       ;Get input data
;    movwf PORT_B      ;Display on LEDs
    movfw RCREG
    movwf Stpccontrol
    retfie

```

```

Rcv4

```

```

    btfss IDControl,3
    goto  Rcv5
    bcf   IDControl,3
    movf  RCREG,W       ;Get input data
;    movwf PORT_B      ;Display on LEDs

```



```

    movfw RCREG
    movwf Fstcontrol
    retfie
Rcv5
    btfss IDControl,4
    goto Rcv6
    bcf IDControl,4
    movf RCREG,W           ;Get input data
;   movwf PORT_B         ;Display on LEDs
    movfw RCREG
    movwf Fsccontrol
    retfie
Rcv6
    btfss IDControl,5
    goto Rcv7
    bcf IDControl,5
    movf RCREG,W           ;Get input data
;   movwf PORT_B         ;Display on LEDs
    movfw RCREG
    movwf Spccontrol
    retfie
Rcv7
    btfss IDControl,6
    goto Rcv8
    bcf IDControl,6
    movf RCREG,W           ;Get input data
;   movwf PORT_B         ;Display on LEDs
    movfw RCREG
    movwf Fstcontrol
    retfie
Rcv8
    btfss IDControl,7
    goto Txmit
    bcf IDControl,7
    movf RCREG,W           ;Get input data
;   movwf PORT_B         ;Display on LEDs
    movfw RCREG
    movwf Swpcontrol
    call Txmit
    retfie
RcvError
    bcf RCSTA,4
    bsf RCSTA,4
;   movlw 0FFh           ;Light all LEDs
;   movwf PORT_B
    retfie
Delay
    movlw b'11111111'
    movwf temp2
SD
    movlw b'11111111'
    movwf temp1

```



```

SD1
    decfsz temp1
    goto SD1

SD2
    decfsz temp2
    goto SD

return

Txmit
    movfw Hoccontrol ;Heel Off Count Control
    movwf TXREG
    call Delay
    movfw Phoccontrol ;Pre Heel Off Count Control
    movwf TXREG
    call Delay
    movfw Stpccontrol ;Stance Phase Count Control
    movwf TXREG
    call Delay
    movfw Fstccontrol ;First Step Count Control
    movwf TXREG
    call Delay
    movfw Fsccontrol ;Foot Still Count Control
    movwf TXREG
    call Delay
    movfw Spccontrol ;Swing Phase Count Control
    movwf TXREG
    call Delay
    call Delay
    movfw Fstcontrol ;First Step taken control
;
    movlw .32
    movwf TXREG
    call Delay
    movfw Swpcontrol ;Swing Phase Control
    movwf TXREG
    call Delay

    bsf RSdatain,1 ;set the flag for RS data in
    goto Flashled ;flash LED to indicate end of comms

Flashled
    call Testled
    btfss porta,1
    goto salim1
    goto Flashled
;return ;return out of isr when button released

Testled
    btfss LEDflag,1
    goto LEDon
    goto LEDoff

LEDon
    bsf porta,2
    call Delay
    bsf LEDflag,1

```



```

    return
LEDoff
    bcf    porta,2
    call   Delay
    bcf    LEDflag,1
    return

```

```

;=====
;
;=====

```

```

;*****
;

```

```

Analysis
    btfsc  adcon0,2      ;is A/D conversion complete
    goto  Analysis      ;wait
PowerOnTest
    ;yes then process
    movfw adres
    movwf Vo
    btfsc  FirstRun,0   ;test to see if it's first run(set flag at start)
    goto  GetOffset    ;if not proceed to remove offset from reading
    call   RemoveOffset ;if it is then proceed with setting the offset
    call   Noise        ;REMOVE NOISE AROUND BASELINE
    call   LargeVel
    movfw velocity      ;send velocity after processing to DAC
    movwf portb
    btfss  HeelOnOff,0
    goto  HeelOFF
    goto  HeelON
HeelON
    bcf    porta,2
    goto  HeelOff
HeelOFF
    bsf    porta,2
    goto  HeelOff

    goto  HeelOff          ;GAIT EVENT DETECTION

```

```

;=====
;
;=====

```

```

GetOffset
    movlw d'127'
    movwf VAR2
    movfw Vo
    movwf VAR1
    call   Compare      ;compare Vo(voltage output at zero velocity) to 127
Test
    movlw d'127'
    movwf VAR2
    btfss  Compres,1    ;are they equal?
    goto  Different
    goto  Equal
Equal
    ;at startup offset = 0
    bcf    FirstRun,0   ;clear the first run flag
    bsf    OffsetSuccess,0 ;a flag to confirm offset measurement
    goto  Analyseend
Different
    btfss  Compres,0
    goto  Smaller
    goto  Larger

```


Smaller

```
bsf    OffsetFlag,1 ;flag to say that offset is +ve
bcf    Lrger,0
incf   Offset,1
movfw  Vo           ;Vo + offset
addwf  Offset,0    ;result is put back into w
movwf  VAR1
call   Compare
goto   Test
```

Larger

```
bsf    OffsetFlag,2 ;flag to say that offset is -ve
bcf    Smller,0
incf   Offset,1
movfw  Offset
subwf  Vo,0        ;(Vo - offset) result put in w
movwf  VAR1
call   Compare
goto   Test
```

=====

;Remove the offset after every reading from the A/D

RemoveOffset

```
btfss  OffsetFlag,2
goto   Add
goto   Substract
```

Substract

```
movfw  Vo
movwf  velocity
movfw  Offset      ;velocity = velocity - offset
subwf  velocity,1  ;remove offset and update velocity with new value
return
```

Add

```
btfss  OffsetFlag,1
goto   Done
movfw  Vo
movwf  velocity
movfw  Offset      ;velocity = velocity + offset
addwf  velocity,1  ;add offset and update velocity with new value
return
```

Done

```
btfss  OffsetSuccess,0
goto   Analyseend
movfw  Vo
movwf  velocity
return
```

=====

Noise

;Subroutine to remove noise and

```
bcf    VelocityZero,0
movlw  d'129'      ;small o/p due to minor movements
movwf  VAR1        ;zero the velocity between +/- 0.1
movfw  velocity    ;Compare with '+-0.1'(at gain=14.29)
movwf  VAR2        ;equivalent to 7 mv gyro o/p (10.4d/s)
call   Compare
btfsc  Compres,0
```



```

    goto Noise2          ;if velocity < 10.4d/s
    return
Noise2
    movlw d'125'
    movwf VAR2
    movfw velocity
    movwf VAR1
    call Compare
    btfsc Compres,0
    goto Noise3          ;if velocity > -10.4 d/s
    bcf VelocityZero,0
    return
Noise3
    movlw d'127'         ;vel = 0 if -7mv < V < 7mv
    movwf velocity
    bsf VelocityZero,0
    return
;=====
LargeVel
    movfw velocity
;    movwf VAR1          ;Swing Phase Control
;    movfw d'120'        ;Swpcontrol ;d'129' ;mov '0.2' to VAR2
;    movwf VAR2          ;0.2 equiv to 14mv gyro o/p(21d/s)
;    call Compare
;    btfss Compres,0
;    goto SwPDetect1
;    goto SwPDetect2
    sublw d'130'        ; (k) - W bit C is cleared if result is -ve
    btfss STATUS,0
    goto SwPDetect2
    goto SwPDetect1
SwPDetect1
    bcf SwPDetected,1
    return
SwPDetect2
    bsf SwPDetected,1
;    bcf HeelOnOff,0
    return

;bcf HeelOnOff,0
;    return
;=====
Compare
    clrf Compres
    movfw VAR1
    subwf VAR2,0        ;VAR2 - VAR1
    btfsc STATUS,2
    bsf Compres,1      ;sets bit 1 if equal
    btfss STATUS,0    ;C bit is clear only when reult is -ve
    bsf Compres,0     ;sets bit 0 if VAR1 is larger
    clrf VAR1
    clrf VAR2
    return

```

;Rules section for the algorithm

HeelOff

```

  btfsc VelocityZero,0
  goto FootInactive
  btfsc SwPDetected,1
  goto SwingPhaseCountTest
  btfss ReadyfHO,0 ;Precondition
  goto ReadyHeelOff ;if false goto ReadyHeelOff test
  movfw velocity ;if true test for heel off detection
  movwf VAR2 ;????????????????????????????????VAR2!!!!!!!!!!
  movfw previousvelocity
  movwf VAR1
  call Compare
  btfss Compres,0
  goto HeelOffCountClr
  goto HeelOffTest

```

HeelOffCountClr

```

  goto Analyseend

```

HeelOffTest

```

  incf HeelOffCount,1 ;inc. HeelOffCount if Velocity<previousvel
  movfw HeelOffCount
  movwf VAR1
  movfw Hoccontrol ;Heel off count control d'15' can vary this value to delay HR
  movwf VAR2
  btfss Compres,0 ;if count> 10(not necessarily consecutive)
  goto Analyseend
  bcf HeelOnOff,0 ;Outcomes:HEEL RISE
; bcf porta,4
; movlw b'00001111' ;***for demo board dbugging
; movwf portb
  bcf ReadyfHO,0
  clrf HeelOffCount
  goto Analyseend

```

ReadyHeelOff

```

  btfss ReadyfPHO,0 ;Precondition
  goto BlindBand ;if false go to heel contact test
  movfw velocity
  movwf VAR2
  movfw previousvelocity
  movwf VAR1
  call Compare
  btfss Compres,0
  goto PreHeelOffCountClr
  goto PreHeelOffCnt

```

PreHeelOffCnt

```

  incf PHOCount,1 ;if Var1<Var2 increment PHOCount
  movfw PHOCount ;this section is to confirm that Vel is dec.
  movwf VAR1 ;before applying HR criteria
  movfw Phoccontrol ;PreHeel off count control d'5' if count >3 consecutively
  movwf VAR2
  call Compare
  btfss Compres,0

```



```

    goto    Analyseend          ;SURE?          PreHeelOffCountClear
    bsf     ReadyfHO,0          ;Outcomes
    bcf     ReadyfPHO,0
    clrf   PHOCount
    goto    Analyseend
PreHeelOffCountClr
    clrf   PHOCount          ;Vel has to dec for 3 consecutive samples
    goto    Analyseend
BlindBand
    btfss  Blind,0
    goto    HeelContact
    incf   BlindCount,1
    movfw  BlindCount
    movwf  VAR1
    movlw  d'20'
    movwf  VAR2
    call   Compare
    btfss  Compres,0
    goto    Analyseend
    bcf    Blind,0
    clrf   BlindCount
    bsf    ReadyfPHO,0
    goto    Analyseend
HeelContact
    btfss  ReadyfHC,0          ;Precondition
    goto    StancePhase          ;if false goto stancephase test
    movfw  velocity
    movwf  VAR1
    movfw  previousvelocity
    movwf  VAR2
    call   Compare          ;criteria: first negative peak
    btfss  Compres,0          ;if Var1 > Var2
    goto    Analyseend
    bsf    HeelOnOff,0          ;Outcomes: Heel is ON
;    bsf    porta,4
;    movlw  b'11110000'
;    movwf  portb          ;*****
;bsf     ReadyfPHO,0
    bcf    ReadyfHC,0
    bsf    Blind,0
    goto    Analyseend
StancePhase
    btfss  SwPDetected,0          ;Precondition
    goto    FirstStepTaken          ;if false goto firststeptaken
    movfw  velocity
    movwf  VAR2
    movlw  d'126'          ;Compare with '-0.1'(at gain=14.29)
    movwf  VAR1          ;equivalent to 7 mv gyro o/p (10.4d/s)
    call   Compare
    btfss  Compres,0
    goto    FirstStepTaken          ;if Var1 > '-0.1' goto Firststeptaken
    goto    StanceTest          ;if Var1 < '-0.1' increment StPCount
StanceTest

```



```

incf StPCount,1 ;Stpccontrol Stance phase count control
movfw Stpccontrol ;d'1' ;if count > ??? delay heel contact
movwf VAR2 ;detection by increasing this value
movfw StPCount
movwf VAR1
call Compare
btfss Compres,0 ;outcome: bcf SwPDetected
goto Analyseend ;can do reward for lower vel to delay HC
bsf ReadyfHC,0 ;***if Var1 < '-0.2' incr StPCount
bsf StPDetected,0 ;***if Var1 < '-0.3' incr StPCount
bcf SwPDetected,0 ;**if Var1 < '-0.4' incr StPCount
clrf SwPCount
goto Analyseend
StanceCountclear
clrf StPCount
goto Analyseend
FirstStepTaken
btfss FSTTest,0 ;Precondition
goto PreFirstStepTaken
movfw velocity
movwf VAR1
movfw previousvelocity
addwf Fstcontrol,0 ;FirstSteptaken control d'2' ;add 0.05(G=14.29)to
previous vel = Var2
movwf VAR2 ;0.05 equiv to 3.5mv gyro o/p(5.2 d/s)
call Compare
btfss Compres,0 ;if VAR1 > VAR2 first negative peak
goto Analyseend
goto FirstStep
FirstStep
bcf HeelOnOff,0 ;Outcomes: Heel Rise
; bcf porta,4
; movlw b'00001111' ;*****
; movwf portb
bcf FSTTest,0
bcf FSONOff,0
clrf FStepCount
goto Analyseend
PreFirstStepTaken
btfss FSONOff,0 ;Precondition set on initialisation
goto FootInactive ;precondition not satisfied
movlw d'127'
movwf VAR1
movfw velocity
movwf VAR2
call Compare
btfss Compres,0 ;if velocity is -ve < '0' inc FStepCount
goto FirstStepCountClr
goto FirstStepCountTest
FirstStepCountClr
clrf FStepCount ;else clear Count
goto FootInactive ;Analyseend
FirstStepCountTest

```



```

    incf  FStepCount,1 ;if FStepCount control > 10
    movfw Fstccontrol          ;Fstccontrol d'1'
    movwf VAR2
    movfw FStepCount
FootInactive
    movwf  VAR1
    call  Compare
    btfss Compres,0
    goto  Analyseend          ;Sure????
    bsf   FSTTest,0          ;Outcomes: bsf      FSTTest
    bcf   FSONOff,0         ;bcf FSONOff
    clrf  FStillCount       ;call  FSTTest
    goto  Analyseend       ; Sure?????
FootInactive
    btfss VelocityZero,0          ;IF velocity EQ 0 or between +/- 0.1 e.g.
    goto  FootStillCountClear
    goto  FootStillCountTest ;if velocity = '0' increment FStillCount
FootStillCountClear
    clrf  FStillCount
    goto  SwingPhase
FootStillCountTest
    incf  FStillCount,1 ;Fsccontrol
    movfw Fsccontrol          ;Foot still count control d'9'
    movwf VAR2
    movfw FStillCount
    movwf VAR1
    call  Compare
    btfss Compres,0          ;If footstillcount > 10 then
    goto  Analyseend        ;if < 10 then skip
    bsf   HeelOnOff,0       ;then set heel On and
;    bsf   porta,4
;    movlw b'11110000'
;    movwf portb            ;*****
    bsf   FSONOff,0         ;set first step on
    bcf   SwPDetected,0     ;clear swing phase detected
    clrf  SwPCount
    movlw d'10'             ;stores 10 so the count doesn't overflow
    movwf FStillCount       ;in case there is no movement for a while
    goto  Analyseend
SwingPhase
    movfw velocity
    movwf VAR1              ;Swing Phase Control
    movfw Swpcontrol        ;d'129'          ;mov '0.2' to VAR2
    movwf VAR2              ;0.2 equiv to 14mv gyro o/p(21d/s)
    call  Compare
    btfss Compres,0          ;if velocity > '0.2' incr SwPCount
    goto  SwingPhaseCountClr ;else SwPCount = 0
    goto  SwingPhaseCountTest ;if velocity > '0.2' incr SwPCount
SwingPhaseCountClr
    clrf  SwPCount
    goto  Analyseend
SwingPhaseCountTest
    incf  SwPCount,1        ;Spcccontrol Swing Phase count control
    movfw Spcccontrol       ;d'4'

```



```

movwf VAR2                ;mov '4' to VAR2
movfw SwPCount
movwf VAR1
call   Compare
btfss Compres,1
goto  Analyseend         ;if count < 40
bsf   SwPDetected,0     ;if count > 40
bcf   StPDetected,0    ;Outcomes
bcf   HeelOnOff,0
; bcf   porta,4
; movlw b'00001111'
; movwf portb           ;*****
; clrf   SwPCount
clrf   StPCount
bcf   FSONOff,0
clrf   FStepCount
bcf   FSTTest,0
bcf   ReadyfHC,0
bcf   ReadyfPHO,0
bcf   ReadyfHO,0
clrf   PHOCount
clrf   HeelOffCount
clrf   FStillCount
goto  Analyseend

Analyseend
movfw velocity           ;****move velocity into prev velocity
movwf previousvelocity
return                   ;returns to the isr subroutine
END

```


Appendix C

Gyro data sheet – Microcontroller data sheet

GYROSTAR[®]: Piezoelectric Vibrating Gyroscope ENC Series

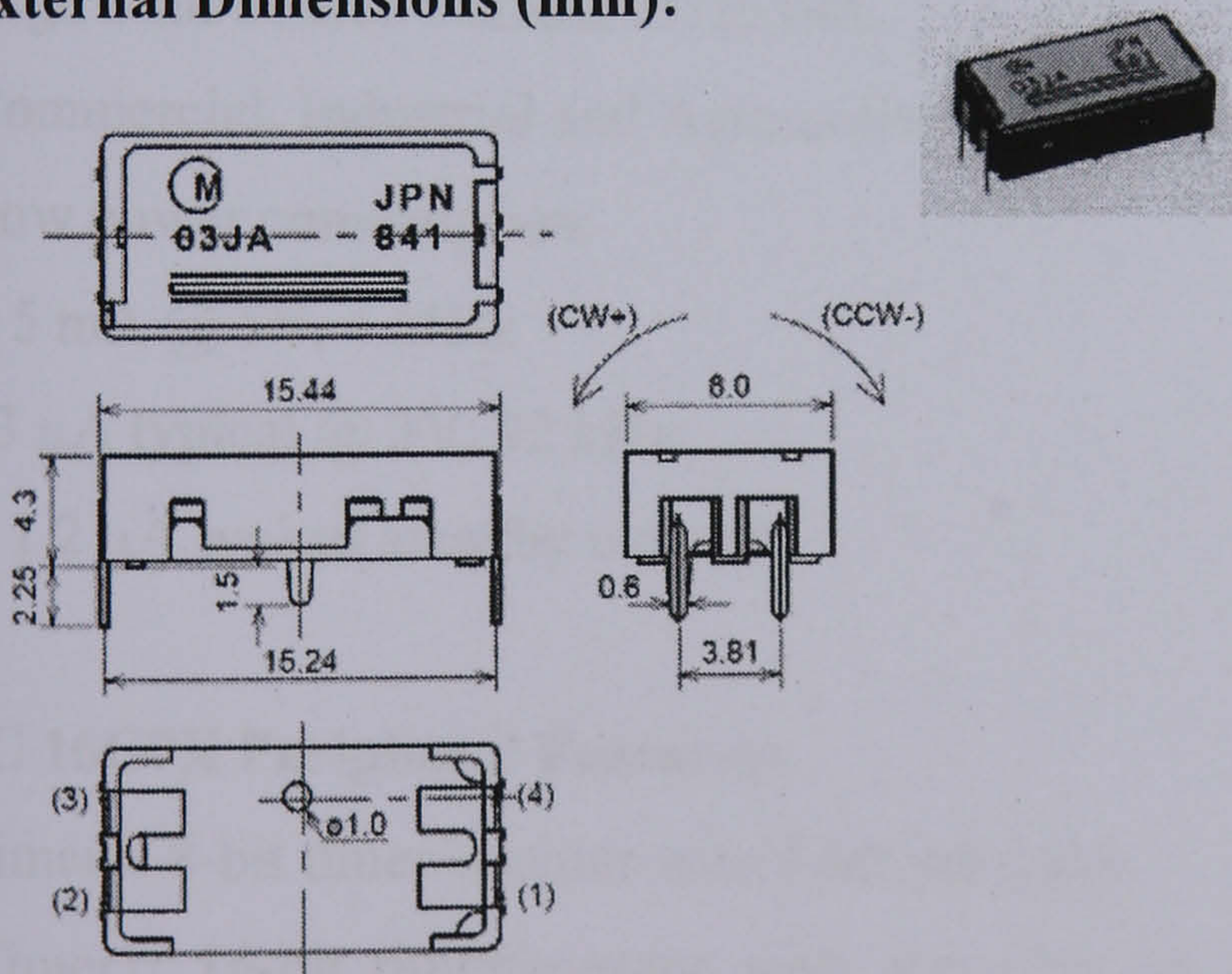
Features:

1. Ultra -Small and ultra-lightweight
2. Quick response
3. Low driving voltage; low current consumption
4. Reliable features achieved by a built-in-AGC circuit

Ratings:

Part Number	ENC-03J
Supply voltage (Vdc)	+2.7 to +5.5
Current consumption (mA max.)	5
Max. angular velocity (°/s)	±300
Output (at angular velocity=0) (Vdc)	+1.35
Scale factor (mV/°/s)	0.67
Temp. coefficient of scale factor (%)	±20
Linearity (%FS)	±5
Response (Hz max.)	50
Operating temperature range (°C)	-5 to +75
Storage temperature range (°C)	-30 to +85
Size (mm)	15.5×8.0×4.3
Weight (g max.)	1.0

External Dimensions (mm):



Terminal Descriptions:

Terminal	Descriptions
(1)	Supply voltage
(2)	Comparative voltage
(3)	Ground (GND)
(4)	Sensor output

Microcontroller: PIC16C63A/65B/73B/74B

8-Bit CMOS Microcontrollers with A/D converter

Core Features:

- High performance RISC CPU
- Only 35 single word instructions to learn
- All single cycle instructions except for program branches which are two cycle
- Operating speed: DC - 20 MHz clock input DC - 200 ns instruction cycle
- 4 K x 14 words of Program Memory, 192 x 8 bytes of Data Memory (RAM)
- Interrupt capability
- Eight-level deep hardware stack
- Direct, indirect and relative addressing modes
- Power-on Reset (POR)
- Power-up Timer (PWRT) and Oscillator Start-up Timer (OST)
- Watchdog Timer (WDT) with its own on-chip RC oscillator for reliable operation
- Programmable code protection
- Power-saving SLEEP mode
- Selectable oscillator options
- Low power, high speed CMOS EPROM technology
- Wide operating voltage range: 2.5V to 5.5V
- High Sink/Source Current 25/25 mA
- Commercial, Industrial and Automotive temperature ranges
- Low power consumption:
 - < 5 mA @ 5V, 4 MHz
 - 23 μ A typical @ 3V, 32 kHz
 - < 1.2 μ A typical standby current

PIC 16C7X Peripheral Features:

- Timer0: 8-bit timer/counter with 8-bit prescaler
- Timer1: 16-bit timer/counter with prescaler can be incremented during SLEEP via external crystal/clock
- Timer2: 8-bit timer/counter with 8-bit period register, prescaler and postscaler
- Capture, Compare, PWM modules
 - Capture is 16-bit, max. resolution is 200 ns
 - Compare is 16-bit, max. resolution is 200 ns

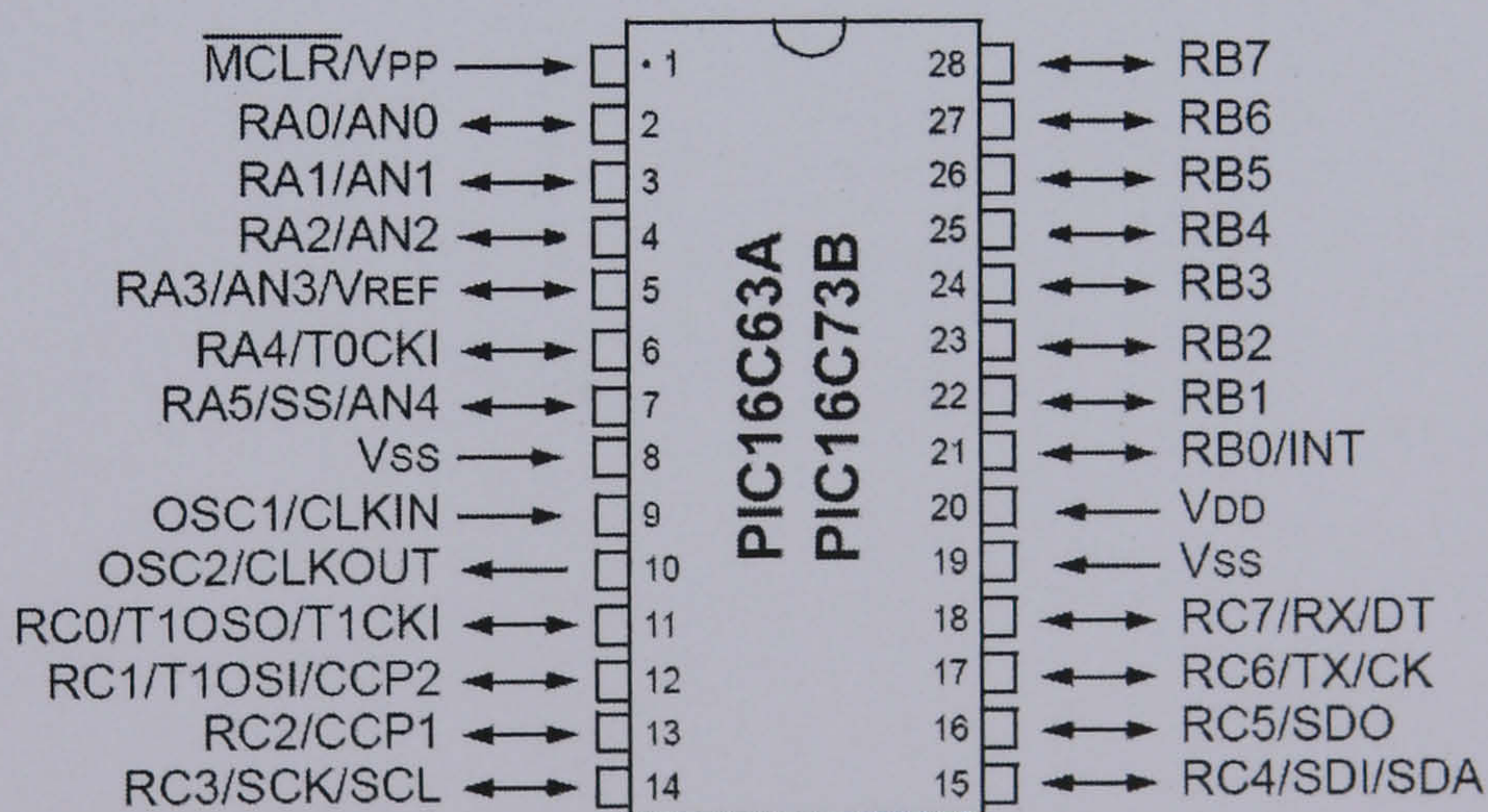
- PWM max. resolution is 10-bit
- 8-bit multichannel Analog-to-Digital converter
- Synchronous Serial Port (SSP) with SPITM and I2CTM
- Universal Synchronous Asynchronous Receiver Transmitter (USART/SCI)
- Parallel Slave Port (PSP), 8-bits wide with external RD, WR and CS controls
- Brown-out detection circuitry for Brown-out Reset (BOR)

Key Features:

Key Features PICmicro™ Mid-Range MCU Family Reference Manual (DS33023)	PIC16C63A	PIC16C65B	PIC16C73B	PIC16C74B
Program Memory (EPROM) x 14	4 K	4 K	4 K	4 K
Data Memory (Bytes) x 8	192	192	192	192
Pins	28	40	28	40
Parallel Slave Port	—	Yes	—	Yes
Capture/Compare/PWM Modules	2	2	2	2
Timer Modules	3	3	3	3
A/D Channels	—	—	5	8
Serial Communication	SPI/I2C, USART	SPI/I2C, USART	SPI/I2C, USART	SPI/I2C, USART
In-Circuit Serial Programming	Yes	Yes	Yes	Yes
Brown-out Reset	Yes	Yes	Yes	Yes
Interrupt Sources	10	11	11	12
Packages	28-pin SDIP, SOIC, SSOP, Windowed CERDIP	40-pin PDIP; 44-pin PLCC, MQFP, TQFP, Windowed CERDIP	28-pin SDIP, SOIC, SSOP, Windowed CERDIP	40-pin PDIP; 44-pin PLCC, MQFP, TQFP, Windowed CERDIP

Pin Diagram:

SDIP, SOIC, Windowed CERDIP



Appendix D

Manufacturer details

Manufacturer Addresses

<i>Manufacturer</i>	<i>Address</i>
<i>Analog Devices, Inc.</i>	Norwood, MA 02062-9106, USA
<i>BAE Systems</i>	Plymouth, Devon, England PL6 6DE
<i>BEI Technologies, Inc.</i>	Ashford, Kent, England TN25 6SX
<i>Burr-Brown Corporation</i>	Dallas, TX 75243-4136
<i>Elmetec</i>	DK8240 Risskov, Denmark
<i>ETB</i>	Codicote, Herts, England SG4 8WM
<i>Interlink Electronics, Inc.</i>	Camarillo, CA 93012, USA
<i>Intersense Inc.</i>	Burlington, MA 01803, USA
<i>Kionix, Inc.</i>	Ithaca, NY 14850, USA
<i>MATLAB – The Mathworks, Inc.</i>	Natick, MA 01760-2098, USA
<i>Maxim Integrated Products, Inc.</i>	Sunnyvale, CA 94086, USA
<i>Medtronic</i>	Minneapolis, MN 55432-5604, USA
<i>Microchip Technology, Inc.</i>	Arizona, 85224-6199, USA
<i>Microsensors – Irvine Sensors Corp.</i>	Costa Mesa, CA 92626-4526, USA
<i>Murata Manufacturing Co., Ltd.</i>	Tokyo 150-0002, Japan
<i>National Instruments</i>	Austin, TX 78759-3504, USA
<i>National Semiconductor Corporation</i>	Santa Clara, California 95052-8090, USA
<i>Neuromotion, Inc.</i>	Alberta, Canada
<i>Novel</i>	81675 Munich, Germany
<i>Panasonic</i>	Osaka 571-8501, Japan
<i>Qualisys Medical AB</i>	S-411 19 Gothenburg, Sweden
<i>RSScan International</i>	B-2250 Olen, Belgium
<i>Silicon Sensing Systems</i>	Amagasaki, Japan
<i>Tekscan, Inc.</i>	South Boston, MA 02127-1309, USA
<i>Texas Instruments</i>	Dallas, TX 75243-4136
<i>Tokin</i>	Tokyo 107-8620, Japan
<i>Watson Industries, Inc.</i>	Eau Claire, Wisconsin 54703, USA
<i>Zetex Semiconductors</i>	Oldham, England OL9 9LL

Appendix E

Contents of the compact disc

Contents of the compact disc

The enclosed compact disc has the following files stored:

1. Code

a. LabVIEW code

LabVIEW code used for data collection and serial communication with the microcontroller unit.

b. MATLAB code

MATLAB code used for gait event detection, and frequency content analysis.

Run “Event_DetectionR1.m” file. You will need to have MATLAB installed on your PC in addition to the signal processing toolbox. Use the “Test_file.TSV” for demonstration. After loading the tsv file (by clicking input TSV file. Then tick the box labelled “all cycles”. Click on “Get Event Times” next and select yes to update the results plot.

c. PIC code

Assembly language code used for heel state detection in real time.

2. Data

a. Event detection

- i. Test file: sample TSV file with marker data from the foot, that can be used to demonstrate the MATLAB code for gait event detection.
- ii. Trial image: example images of foot to floor (force plate) contact patterns one barefoot and one shod trials for a sample subject.